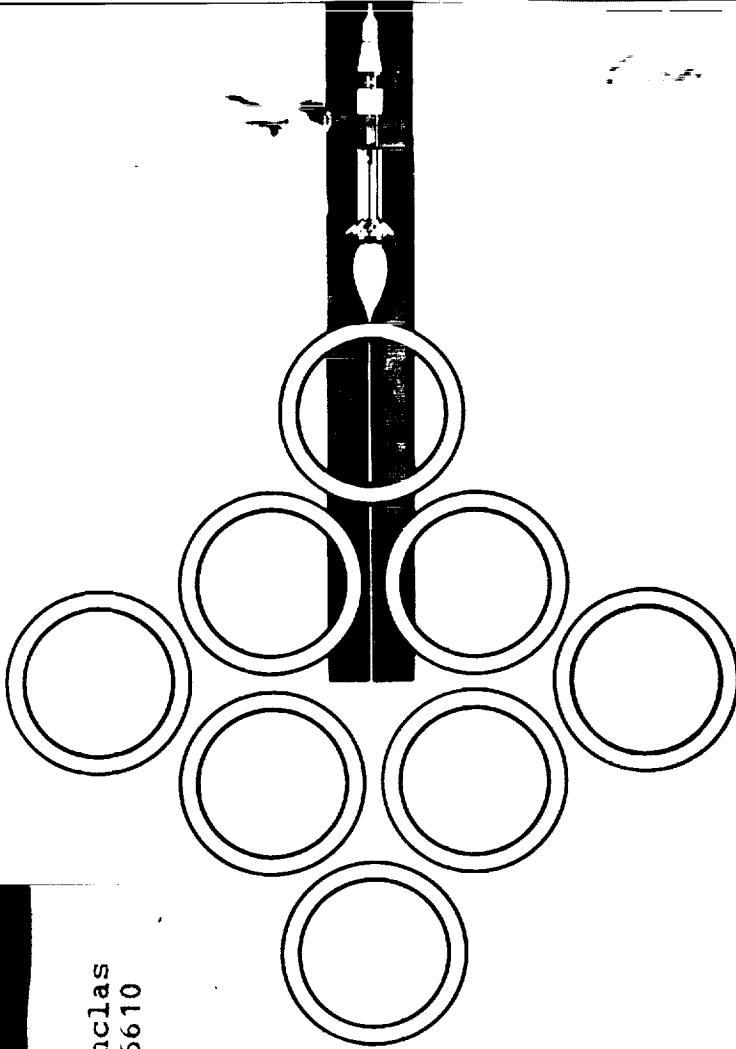


ENGINEERING DEPARTMENT
SDS-74-425
JANUARY 25, 1974



DRA

Unclas
16610
F3/30

SATURN S-IB STAGE FINAL FLIGHT REPORT

S-IB-8

(Applicable to Skylab-4, SA-208)

SATURN S-IB STAGE AND SATURN IB PROGRAM

(NASA-CR-120315) SATURN S-1B STAGE:
FINAL FLIGHT REPORT. S-1B-8 (APPLICABLE
TO SKYLAB -4, SA-208) (Chrysler Corp.)
153 p
CSCL 22C

SPACE DIVISION

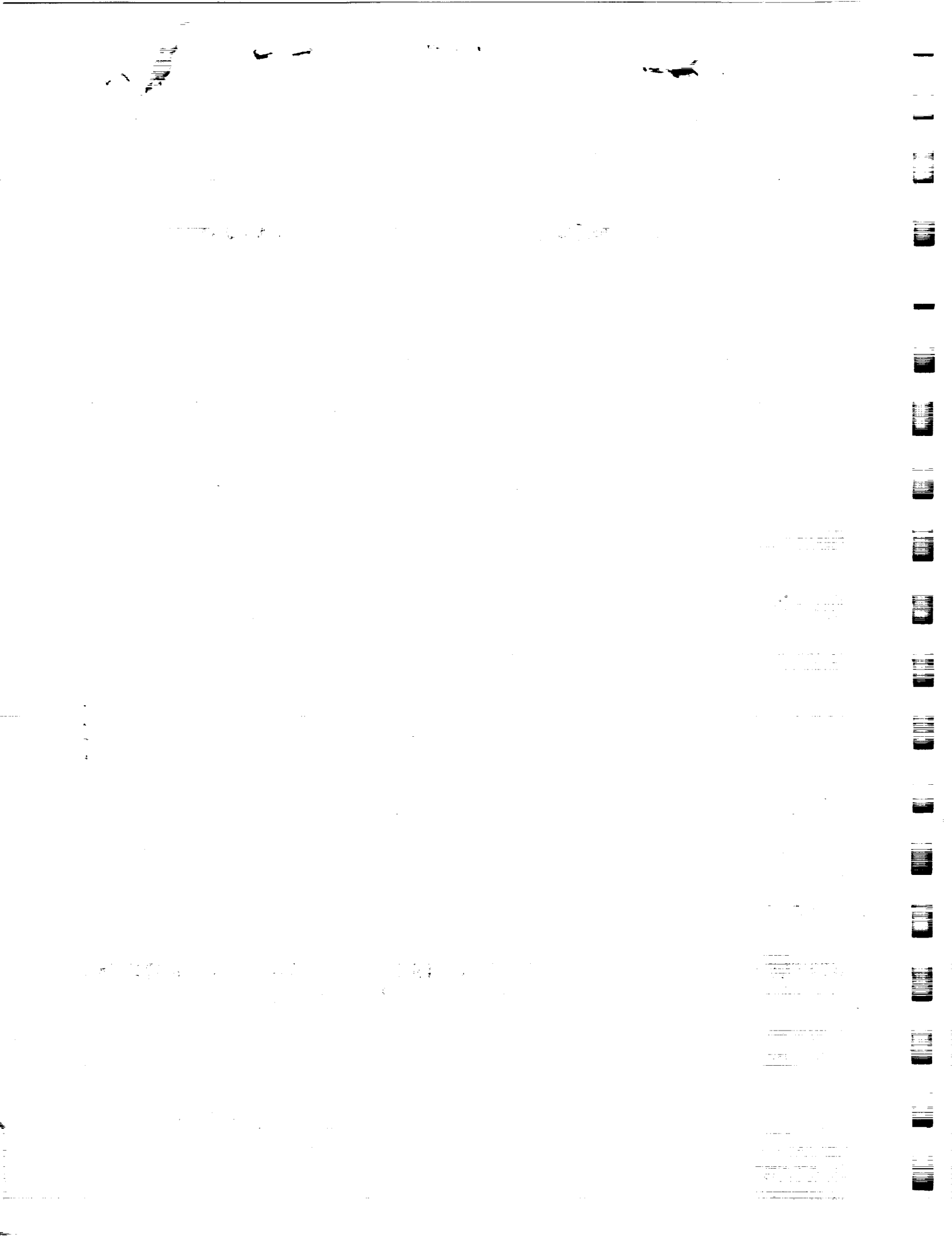


**CHRYSLER
CORPORATION**

(NASA-CR-120315) SATURN S-1B STAGE FINAL
FLIGHT REPORT S-1B-8 (APPLICABLE TO
SKYLAB-4, SA-208) (Chrysler Corp.) 153 p

N92-7043

Unclas
29/12 0083634



SATURN S-IB STAGE
FINAL FLIGHT REPORT

S-IB-8

(APPLICABLE TO SKYLAB -4, SA-208)

January 25, 1974

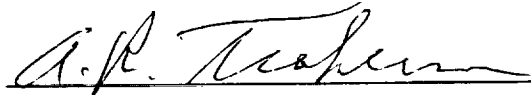
CHRYSLER CORPORATION SPACE DIVISION

CONTRACT NAS8-4016

DRL 039 LINE ITEM 12



C. A. Brakebill, Chairman
Flight Evaluation Group



A. R. Trahern, Jr.
Skylab/ASTP Project Manager

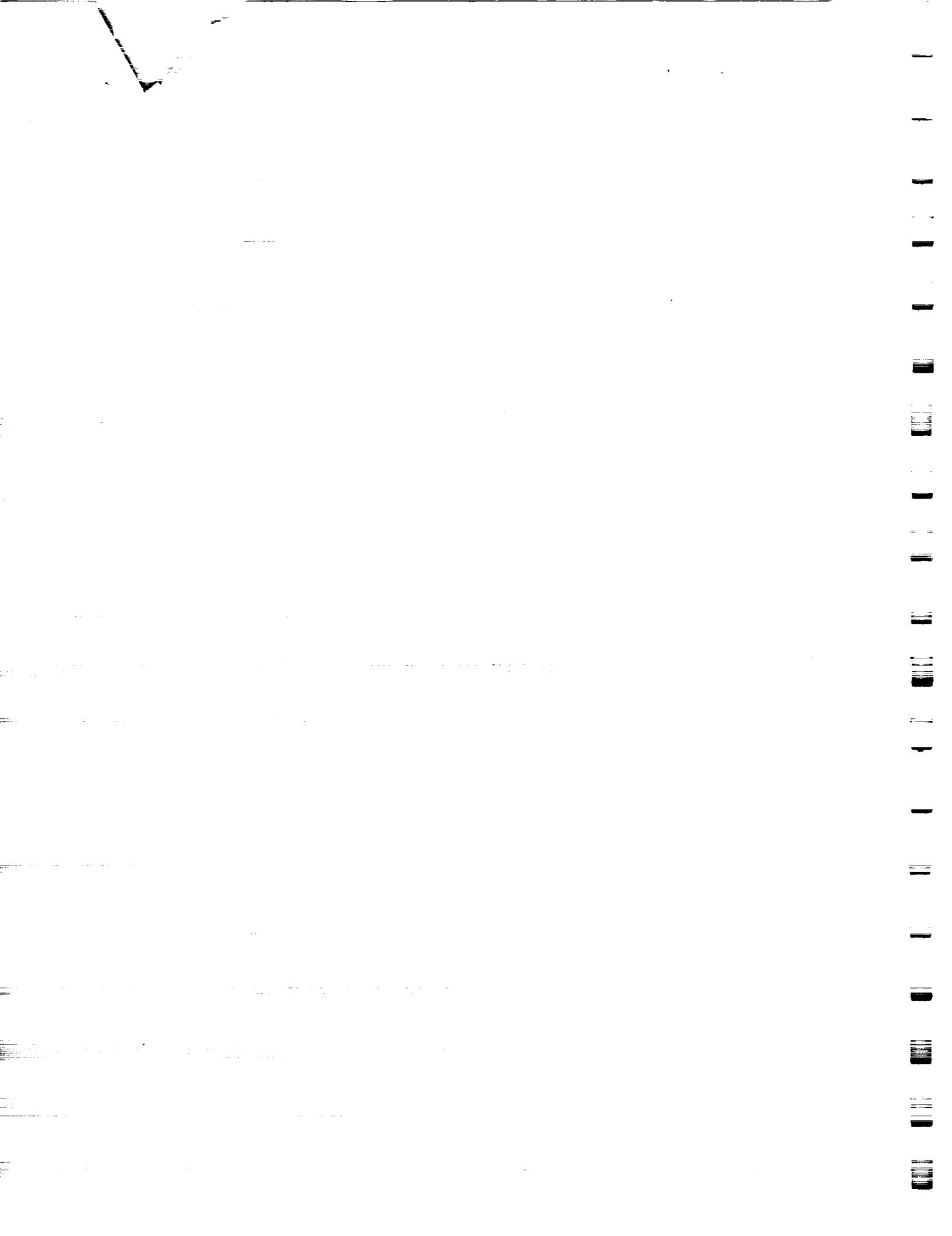


TABLE OF CONTENTS

	<u>Page</u>
ACKNOWLEDGEMENT	ix
SECTION 1 - FLIGHT SUMMARY	1-1
SECTION 2 - INTRODUCTION	
2.1 Purpose	2-1
2.2 Scope	2-1
SECTION 3 - MISSION OBJECTIVES ACCOMPLISHMENT	
3.1 Launch Vehicle Objectives	3-1
3.2 S-IB Stage Objectives	3-1
SECTION 4 - EVENT TIMES	
4.1 Summary of Events	4-1
SECTION 5 - LAUNCH OPERATIONS	
5.1 Summary	5-1
5.2 Countdown Events	5-1
5.3 S-IB Propellant Loading	5-1
5.3.1 RP-1 Loading	5-1
5.3.2 LOX Loading	5-8
SECTION 6 - MASS CHARACTERISTICS	
6.1 Summary	6-1
6.2 Predicted Mass Characteristics	6-1
SECTION 7 - PROPULSION	
7.1 Summary	7-1
7.2 S-IB Ignition Transient Performance	7-1
7.3 S-IB Mainstage Performance	7-1
7.3.1 Stage Performance	7-1
7.3.2 Individual Engine Performance	7-11
7.3.3 Stage Static Test, Engine Performance Summary	7-15
7.3.4 LOX Seal Drainline Temperature Analysis	7-19
7.4 S-IB Shutdown Transient Performance	7-19
7.5 S-IB Stage Propellant Management	7-23
7.6 S-IB Pressurization System	7-28
7.6.1 Fuel Pressurization System	7-28
7.6.2 LOX Pressurization System	7-32
7.7 Propulsion System Event Times	7-36

TABLE OF CONTENTS (Continued)

	<u>Page</u>
SECTION 8 - CONTROL PRESSURE SYSTEM	
8.1 Summary	8-1
8.2 Control Pressure System	8-1
SECTION 9 - FLIGHT CONTROL SUBSYSTEM	
9.1 Summary	9-1
9.2 S-IB Hydraulic System Performance	9-1
9.3 S-IB Actuator Performance	9-1
SECTION 10 - STRUCTURES	
10.1 Summary	10-1
10.2 Total Vehicle Structures Evaluation	10-1
10.2.1 Longitudinal Loads	10-1
10.2.2 Bending Moments	10-6
10.2.3 Combined Loads	10-6
10.2.4 Vehicle Dynamic Characteristics	10-16
10.3 Structural Assessment	10-16
10.3.1 Fuel Tank Forward Bulkhead Collapse	10-16
10.3.2 Stress Corrosion Cracking	10-16
SECTION 11 - ELECTRICAL SYSTEMS	
11.1 Summary	11-1
11.2 S-IB Electrical Systems	11-1
SECTION 12 - PRESSURE ENVIRONMENT	
12.1 Summary	12-1
12.2 S-IB Base Pressure	12-1
12.3 S-IB Base Drag	12-2
SECTION 13 - THERMAL ENVIRONMENT	
13.1 Summary	13-1
13.2 S-IB Base Heating	13-1
SECTION 14 - ENVIRONMENTAL CONTROL SYSTEM	
14.1 Summary	14-1
14.2 S-IB Environmental Control	14-1
SECTION 15 - DATA SYSTEMS	
15.1 S-IB Measurements Evaluation	15-1
15.2 Airborne VHF Telemetry Systems Evaluation	15-1
15.3 Secure Range Safety Command Systems Evaluation	15-3
SECTION 16 - MALFUNCTIONS AND DEVIATIONS	
16.1 Summary	16-1
16.2 System Failures and Anomalies	16-1
16.3 Recommendations for Corrective Action	16-1
APPENDIX A - S-IB STAGE CONFIGURATION	A-1
REFERENCES	R-1

LIST OF ILLUSTRATIONS

<u>Figure</u>	<u>Title</u>	<u>Page</u>
5-1	S-IB Fuel Temperature Density Relationship	5-5
5-2	S-IB-8 Fuel Chillo down after LOX Loading	5-6
5-3	S-IB LOX Pump Inlet Temperature During Flight	5-9
5-4	Center LOX Tank - Outboard LOX Tank Relationship	5-10
7-1	S-IB Engine Thrust Buildup	7-3
7-2	S-IB Stage Thrust Buildup	7-4
7-3	S-IB Stage Longitudinal Thrust	7-5
7-4	S-IB Stage Specific Impulse	7-6
7-5	S-IB Stage Mixture Ratio	7-7
7-6	S-IB Stage LOX Flowrate	7-8
7-7	S-IB Stage Fuel Flowrate	7-9
7-8	S-IB Total Propellant Flowrate	7-10
7-9	Thrust, Specific Impulse and Mixture Ratio Deviations (Percent Deviation from Predicted)	7-14
7-10	Sea Level Engine Thrust Comparison by Engine Position	7-16
7-11	Sea Level Specific Impulse Comparison by Engine Position	7-17
7-12	Δ Thrust History of S-IB Stages (Percent Deviation from Rocketdyne Acceptance)	7-18
7-13	LOX Seal Drainline Temperatures	7-20
7-14	S-IB Inboard Engine Total Thrust Decay	7-21
7-15	S-IB Outboard Engine Total Thrust Decay	7-22
7-16	S-IB Stage LOX Mass Above Main LOX Valve	7-25
7-17	S-IB Stage Fuel Mass Above Main Fuel Valve	7-26
7-18	S-IB Stage Fuel Pressurization System	7-29
7-19	S-IB Stage Fuel Tank Ullage Pressure (Gage)	7-30
7-20	S-IB Stage Fuel Tank Ullage Pressure (Absolute)	7-31
7-21	S-IB Stage Fuel Tank Ullage Pressure (Prelaunch)	7-33
7-22	S-IB Stage Helium Sphere Pressure	7-34
7-23	S-IB Stage LOX System	7-35
7-24	S-IB Stage Center LOX Tank Ullage Pressure (Prelaunch)	7-37
7-25	S-IB Stage Center LOX Tank Ullage Pressure	7-38
7-26	S-IB Stage GOX Flow Control Valve Position	7-39
8-1	S-IB Control Pressure System	8-2
8-2	S-IB Pneumatic Control Pressure	8-3

LIST OF ILLUSTRATIONS (Continued)

<u>Figure</u>	<u>Title</u>	<u>Page</u>
9-1	S-IB Stage Hydraulic System Characteristics	9-2
9-2	S-IB Stage Envelop Maximum Gimbal Angle	9-3
9-3	S-IB Stage Pitch Actuator Position (Engines 1 and 2)	9-5
9-4	S-IB Stage Pitch Actuator Position (Engines 3 and 4)	9-6
9-5	S-IB Stage Yaw Actuator Position (Engines 1 and 2)	9-7
9-6	S-IB Stage Yaw Actuator Position (Engines 3 and 4)	9-8
9-7	S-IB Stage Average Actuator Position	9-9
10-1	Instrumentation at Station 942	10-2
10-2	SA-208/Saturn IB Accelerometer Instrumentation	10-3
10-3	Longitudinal Acceleration during Thrust Buildup and Launch	10-4
10-4	Longitudinal Acceleration during Cutoff	10-5
10-5	Longitudinal Load from Strain Data at Station 942 vs. Time	10-7
10-6	Longitudinal Load Distribution at Time of Maximum Bending Moment and IECO	10-8
10-7	Wind Profile	10-9
10-8	Bending Moments Measured by Strain Gages	10-10
10-9	Bending Moment Distributions	10-11
10-10	Bending Moment Distributions	10-12
10-11	Bending Moment Distributions	10-13
10-12	Envelope of Combined Loads Producing Minimum Safety Margin for Saturn IB Flight	10-14
10-13	Minimum Factor of Safety During S-IB Flight	10-15
10-14	Longitudinal Acceleration and Pressure, S-IB Instrumentation	10-17
10-15	Longitudinal Acceleration and Pressure, S-IVB/IU Instrumentation	10-18
10-16	Vehicle Bending Frequencies	10-19
10-17	Vehicle Bending Amplitudes	10-20
11-1	Master Measuring Voltage Supply 9A84 (+1D81 Measuring Bus)	11-7
11-2	Master Measuring Voltage Supply 9A85 (+1D82 Measuring Bus)	11-8
11-3	Master Measuring Voltage Supply 12A38 (+1D89 Measuring Bus)	11-9
11-4	S-IB Battery Voltage (1D11)	11-10
11-5	S-IB Battery Current (1D10)	11-11
11-6	S-IB Battery Voltage (1D21)	11-12
11-7	S-IB Battery Current (1D20)	11-13
12-1	Base Region Instrumentation	12-1
12-2	S-IB Stage Heat Shield Pressure	12-3
12-3	S-IB Stage Flame Shield Pressure	12-4
12-4	S-IB Stage Heat Shield Loading	12-5
12-5	S-IB Stage Base Drag Coefficient	12-6

LIST OF ILLUSTRATIONS (Continued)

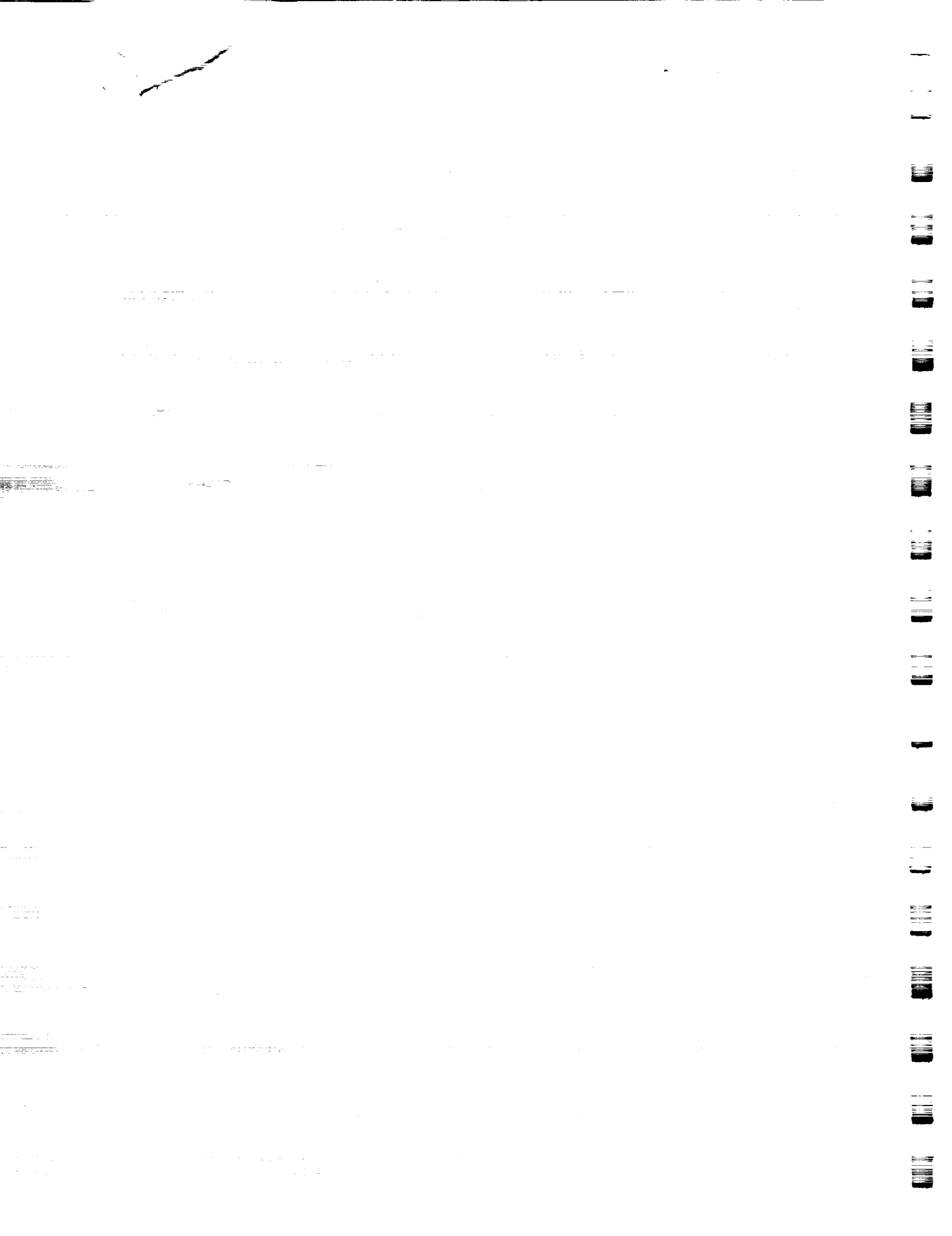
<u>Figure</u>	<u>Title</u>	<u>Page</u>
13-1	Base Region Instrumentation	13-1
13-2	S-IB Stage Heat Shield Inner Region Total Heating Rates	13-2
13-3	S-IB Stage Heat Shield Inner Region Radiation Heating Rate	13-3
13-4	S-IB Stage Heat Shield Inner Region Gas Temperature	13-4
13-5	S-IB Stage Heat Shield Outer Region Gas Temperature	13-5
13-6	S-IB Stage Flame Shield Total Heating Rate	13-7
13-8	S-IB Stage Flame Shield Radiation Heating Rate	13-9
13-7	S-IB Stage Flame Shield Gas Temperature	13-8
13-9	Comparison between Inboard Engine Thrust and Flame Shield Radiation	13-10
13-10	Comparison of Flame Shield Radiant Heating Data with Design Level	13-10
13-11	Comparison of Flame Shield Total Heating Data with Design Level	13-11
13-12	Comparison of Flame Shield Gas Temperature Data with Design Level	13-12
14-1	S-IB Engine Compartment Temperature	14-2
15-1	VHF Telemetry Systems Coverage Summary	15-2

LIST OF TABLES

<u>Table</u>	<u>Title</u>	<u>Page</u>
4-1	Significant Event Times Summary	4-2
5-1	S-IB-8 Prelaunch Milestones	5-2
5-2	S-IB-8 Propellant Weights at Ignition	5-3
5-3	RP-1 Sampling Plan Skylab SL-2, -3, -4	5-7
6-1	S-IB Stage Mass Properties	6-2
6-2	S-IB Propellant and Service Item History	6-3
7-1	S-IB Engine Start Characteristics	7-2
7-2	S-IB Propulsion Flight Performance Deviations	7-12
7-3	S-IB Individual Engine Propulsion Performance	7-13
7-4	Outboard Engine Thrust OK Pressure Switch Times at OECO	7-19
7-5	Propellant Usage	7-23
7-6	Cutoff Probe Actuation Characteristics	7-24
7-7	S-IB-8 Propellant Level Discrete Sensor Actuation Times	7-24
7-8	S-IB Propellant Mass History	7-27
7-9	S-IB Stage Propulsion System Event Times	7-40
9-1	S-IB Actuator Performance Data	9-4
11-1	S-IB Electrical System Measurements	11-2
11-2	S-IB Stage Battery Power Consumption	11-6
15-1	S-IB Measurement Summary	15-1
15-2	Flight Measurements Waived Prior to Flight	15-2
15-3	Measurement Malfunctions	15-2
15-4	S-IB Stage Telemetry Links	15-3
15-5	S-IB Stage Inflight Calibration Times	15-3
15-6	S-IB Stage Secure Command Receiver Measurements	15-3

ACKNOWLEDGEMENT

This report is the result from the combined efforts of the Engineering Department Branches of Chrysler Corporation Space Division (CCSD). Detailed evaluation and preparation of this document was performed by the CCSD Flight Evaluation Group (FEG). Launch operation information provided by the CCSD Florida Operations has been included for appropriate background.



Section 1

FLIGHT SUMMARY

Saturn IB SA-208 (Skylab-4) was launched at 9:01 am, Eastern Standard Time (EST) November 16, 1973 from Kennedy Space Center, Complex 39, Pad B. The launch vehicle successfully placed the manned spacecraft in the planned earth orbit. All S-IB-8 stage systems operated satisfactorily.

The S-IB stage objective, to boost upper stages and spacecraft through a predetermined trajectory to place them at the proper altitude and attitude with the proper velocity at S-IVB stage ignition, was successfully accomplished. The S-IB stage provided continuous thrust for 137.82 seconds until inboard engine cutoff (IECO). The four outboard engines cut off 3.47 seconds after the inboard engines. The S-IB stage separated from the S-IVB/IU/CSM at 142.9 seconds.

S-IB stage participation supported launch countdown which started November 13, 1973 and concluded November 16, 1973 with a successful launch. The launch had been re-scheduled from a November 10, 1973 date to replace all eight fins on the S-IB stage after post-CDDT inspections revealed cracks in the fin attachment fittings. During the LOX replenishing sequence, LOX was reported emanating occasionally from the vent valves; however, all S-IB stage systems operated satisfactorily during countdown.

S-IB stage mass characteristics history and predicted prelaunch data are presented for total vehicle evaluation. S-IB stage postflight analysis was not performed.

The propulsion system of the S-IB stage performed satisfactorily throughout flight. The stage longitudinal thrust and total propellant flowrate were 0.13 and 0.12 percent less than predicted, respectively. Stage mixture ratio was 0.08 percent higher than predicted. Stage specific impulse was within 0.02 percent of the prediction.

Operation of the S-IB control pressure system was satisfactory throughout prelaunch, flight and postflight intervals.

The S-IB stage flight control subsystem performed well within design capability.

Structural analysis of the S-IB stage indicates that all structural components performed satisfactorily. There was no compromise of structural integrity.

The electrical system of the S-IB stage operated satisfactorily during the flight. Battery performance, including voltages and currents, was within predicted tolerances.

Pressure and thermal measurements made in the S-IB stage base region have been compared with preflight predictions and show agreement within the design levels. The thermal radiation environment on the flame shield was similar to that experienced on SA-207, being more severe than expected from 13 to 55 seconds.

The Environmental Control System (ECS) maintained the S-IB stage engine compartment and instrument compartment at the desired temperature during prelaunch activities.

The measurement evaluation on the S-IB stage revealed that 100.00 percent of the 265 measurements active for flight performed satisfactorily. Performance of the telemetry and RF systems was satisfactory.

Evaluation of the S-IB stage data revealed that no failures or anomalies were detected.

Section 2

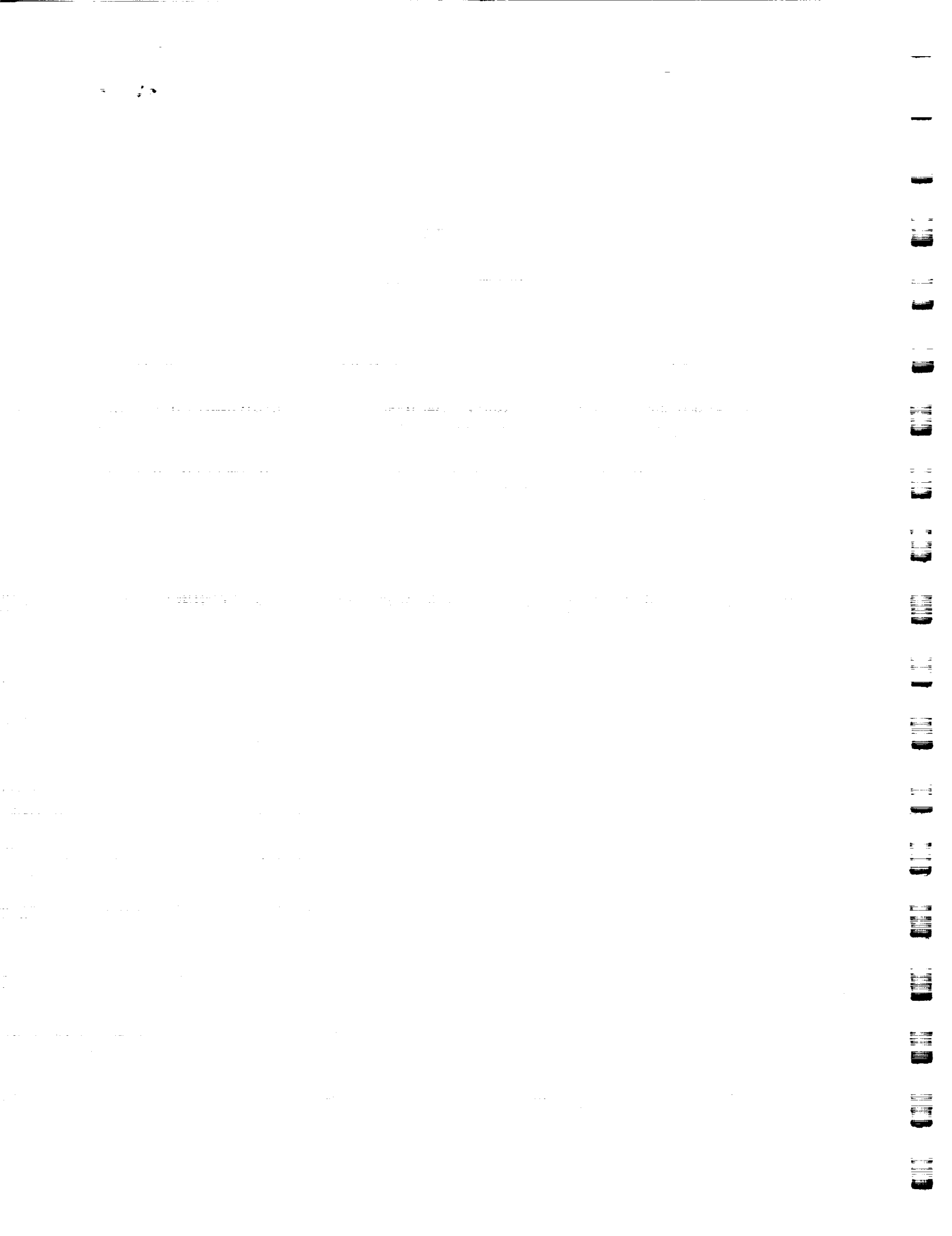
INTRODUCTION

2.1 PURPOSE

This report provides the National Aeronautics and Space Administration (NASA), Marshall Space Flight Center (MSFC), with the Saturn S-IB stage evaluation results of the SA-208 flight (Skylab-4 Mission). The basic objective of flight evaluation is to acquire, reduce, analyze, evaluate and report on flight data to the extent required to assure future mission success and vehicle reliability. To accomplish this objective, actual flight problems are identified, their causes determined, and recommendations made for appropriate corrective action.

2.2 SCOPE

This report contains the performance evaluation of the S-IB-8 stage system. Evaluation was performed by comparing actual flight events and performance with the predicted characteristics and data from previous flights.



Section 3

MISSION OBJECTIVES ACCOMPLISHMENT

3.1 LAUNCH VEHICLE OBJECTIVES

The SA-208 launch vehicle objective, to launch and insert a manned CSM into earth orbit, was successfully accomplished. Skylab-4 was targeted for a 81 x 121 n. mi. orbit during final launch countdown. The manned CSM was placed into a 80.95 x 121.19 n. mi. earth orbit from which the rendezvous with the Orbital Work Shop (OWS) was begun.

3.2 S-IB STAGE OBJECTIVES

The S-IB-8 stage objective, to boost upper stages and spacecraft through a predetermined trajectory to place them at the proper altitude and attitude with the proper velocity at S-IVB stage ignition, was successfully accomplished. The S-IB stage system performed satisfactorily throughout flight. The first stage provided continuous thrust for 137.82 seconds until inboard engine cutoff. The four outboard engines cut off 3.47 seconds after the inboard engines. The S-IB stage separated from the S-IVB/IU/CSM at 142.9 seconds.

Section 4

EVENT TIMES

4.1 SUMMARY OF EVENTS

Range zero occurred at 09:01:23 Eastern Standard Time (EST) (14:01:23 Universal Time [UT]) November 16, 1973. Range time is the elapsed time from range zero, which by definition, is the nearest whole second prior to liftoff signal, and unless otherwise noted, is the time used throughout this report. Time from base time is the elapsed time from the start of the indicated time base. Time base T_1 started with the IU umbilical disconnect sensed by LVDC; time base T_2 started with actuation of the S-IB propellant level sensors; and time base T_3 started with S-IB stage outboard engine cutoff.

A summary of significant event times for the SA-208 S-IB stage is given in table 4-1.

Table 4-1. Significant Event Times Summary

ITEM	EVENT DESCRIPTION	RANGE TIME		TIME FROM BASE	
		ACTUAL (SEC)	ACT-PRED (SEC)	ACTUAL (SEC)	ACT-PRED (SEC)
1.	S-IB Time for Ignition Command	-3.06	-	-	-
2.	Ignition Command	-3.05	-0.03	T ₁ -3.52	-0.02
3.	S-IB Start Signal Eng 5 and 7	-2.96	-0.04	T ₁ -3.43	-0.03
4.	S-IB Start Signal Eng 6 and 8	-2.86	-0.04	T ₁ -3.33	-0.03
5.	S-IB Start Signal Eng 2 and 4	-2.76	-0.04	T ₁ -3.23	-0.03
6.	S-IB Start Signal Eng 1 and 3	-2.66	-0.04	T ₁ -3.13	-0.03
7.	IU Umbilical Disconnect *	0.39	-	-	-
8.	Start T ₁ **	0.47	-	T ₁ +0	-
9.	Single Engine Cutoff Enable	3.44	-0.04	T ₁ +2.97	-0.03
10.	Multiple Engine Cutoff Enable No. 1	10.44	-0.04	T ₁ +9.97	-0.03
11.	Multiple Engine Cutoff Enable No. 2	10.54	-0.04	T ₁ +10.07	-0.03
12.	TM Cal On	20.44	-0.04	T ₁ +19.97	-0.03
13.	TM Cal Off	25.43	-0.04	T ₁ +24.96	-0.04
14.	TM Cal On	120.24	-0.04	T ₁ +119.77	-0.03
15.	TM Cal Off	125.24	-0.04	T ₁ +124.77	-0.03
16.	Propellant Level Sensors Enable	129.94	-0.04	T ₁ +129.47	-0.03
17.	Propellant Level Sensors Actuation **	134.84	-0.14	T ₁ +134.37	-0.13
18.	Start T ₂	134.84	-0.14	T ₂ +0	-
19.	Inboard Engine Cutoff (IECO)	137.82	-0.16	T ₂ +2.98	-0.02
20.	LOX Depletion Cutoff Enable	139.30	-0.18	T ₂ +4.46	-0.04
21.	Fuel Depletion Cutoff Enable	139.80	-0.18	T ₂ +4.96	-0.04
22.	S-IB Outboard Engine Cutoff (OECO)	141.29	+0.31	T ₂ +6.45	+0.45
23.	Start of T ₃	141.29	+0.31	T ₃ +0	-
24.	S-IB Switch Selector Outboard Eng Cutoff (OECO) Command	141.37	+0.29	T ₃ +0.08	-0.02
25.	S-IB/S-IVB Separation Signal On	142.55	+0.27	T ₃ +1.26	-0.04

* DEE-6

** LVDC

Section 5

LAUNCH OPERATIONS

5.1 SUMMARY

The S-IB stage systems performed satisfactorily during countdown.

A chronological summary of prelaunch milestones for the S-IB stage is contained in table 5-1.

5.2 COUNTDOWN EVENTS

S-IB stage participation supported launch countdown which started November 13, 1973 and concluded November 16, 1973 with a successful launch. The launch had been re-scheduled from a November 10, 1973 date to replace all eight fins on the S-IB stage after post-CDDT inspections revealed cracks in the fin attachment fittings. During the LOX replenishing sequence, LOX was reported emanating occasionally from the vent valves; however, all S-IB stage systems operated satisfactorily during countdown.

5.3 S-IB PROPELLANT LOADING

The propellant loading criteria for the S-IB-8 stage, presented in reference C, HSM-R19-73, "Saturn IB Vehicle Propellant Loading for Vehicle AS-208", dated August 24, 1973, were based on environmental conditions expected during November. The propellant loading table provided a LOX weight and tanking differential pressure and a nominal LOX tank ullage volume of 1.5 percent. The loading table contained fuel tanking weights and differential pressures for fuel densities from 49.735 lb/ft³ at 90.0°F to 51.211 lb/ft³ at 30.0°F.

The propellant discrete level instrumentation for this stage consisted of 3 probes in each of tanks OC, O1, O3, F1 and F3. The propellant levels in the other tanks were approximated by using data from the instrumented tanks.

The S-IB stage propellant tanking weights are shown in table 5-2. The reconstructed load is considered the best estimate of the propellants onboard at stage ignition.

5.3.1 RP-1 Loading

Fuel was initially placed onboard the S-IB stage October 23, 1973. During a normal gravity drain to the 600-inch level, the fuel ullage was subjected to a pressure 2.7 psi

Table 5-1. S-IB-8 Prelaunch Milestones

Date	Activity or Event
15 June 1973	S-IB Stage Shipped from Michoud
20 June 1973	S-IB Stage Arrived at KSC
31 July 1973	S-IB Stage Erection on Mobile Launcher
3 August 1973	LV Electrical Systems Test
4 August 1973	LV Electrical Systems Test Complete
14 August 1973	LV Moved to Pad B
28 August 1973	Crack Discovered in Channel, Upper Outrigger Assembly, Fin Position 4
4 September 1973	Repair of Crack in Channel, Upper Outrigger Assembly, Fin Position 4
5 September 1973	Flight Readiness Test (FRT)
11 October 1973	Flight Readiness Test (FRT) Repeat Complete
23 October 1973	RP-1 Loaded
23 October 1973	Fuel Tanks Inversion
25 October 1973	Fuel Tanks Reformed
1 November 1973	CDDT (Wet) Began
2 November 1973	CDDT (Wet) Complete
6 November 1973	Fin Cracks Discovered
7 November 1973	RP-1 Drain
12 November 1973	Fin Replacement Complete
14 November 1973	RP-1 Reloaded
14 November 1973	Launch Countdown Began
16 November 1973	SL-4 Launch

Table 5-2. S-IB-8 Propellant Weights at Ignition

PROPELLANT	WEIGHT REQUIREMENTS		WEIGHT INDICATIONS		WEIGHT DEVIATIONS		
	PREDICTED FOR LAUNCH LB	IGNITION LB	PTCS LB	RECONSTRUCTED (LB)	PTCS		RECONSTRUCTED
					LB	%	
LOX	632,016	632,016	632,183	632,416	+167	+0.26	+400
FUEL	279,596	280,568	280,616	280,541	+48	+0.17	-27
TOTAL	911,612	912,584	912,799	912,957	+215	+0.24	+373

- ① Predicted propellant weights are based on a nominal LOX density of 70.594 lb/ft³ and a nominal fuel density of 50.414 lb/ft³ prior to vent closure. These densities correspond to those expected for a November launch.
- ② Based upon nominal LOX density of 70.594 lb/ft³ and fuel density of 50.547 lb/ft³ determined immediately prior to launch.
- ③ Based upon PTCS data immediately prior to Terminal Countdown Sequence.
- ④ Based upon discrete probe data and Mark IV computer program reconstruction.
- ⑤ Referenced to weight requirements at ignition.

below ambient. This resulted in the partial reversal of the upper bulkheads of tanks F3 and F4. The upper bulkheads were returned to a flight-worthy configuration by applying a positive pressure to the fuel ullage. On November 7, 1973, the fuel was drained from the S-IB stage to reduce the load on the fins to allow their removal and replacement.

Fuel was again placed onboard the S-IB stage on November 14, 1973, and remained onboard until launch. A final level adjust drain sequence was accomplished just prior to launch. The desired fuel weight, obtained from the loading table, was 280,568 pounds. The PTCS number set into the computer for final level adjust was 9387. When the fuel level was raised to the overfill sensor level 8-1/2 hours prior to launch, the PTCS mass readout indicated no error in the fuel height; therefore, no error correction was made to the final PTCS number.

The fuel temperature was monitored during the launch countdown and at T-60 minutes, a final fuel temperature of 57.0°F was projected to ignition; final fuel density was obtained using the temperature projected to ignition. Actual fuel ~~TEMPERATURE~~ at ignition was 57.0°F. Figure 5-1 shows the temperature-density relationship of the fuel used for constructing the propellant loading tables. The fuel sampling plan is discussed in paragraph 5.3.1.1.

The fuel temperature chilldown from LOX loading to launch was 15.4°F; predicted chilldown was 8.4°F. This difference is partially attributable to the LOX being loaded 8 hours prior to launch rather than the 7 hours used for criteria purposes which subjected the fuel to an additional hour of chilldown time. The remainder of the difference is attributed to the 09:01 EST launch time; therefore, the major portion of the fuel chilldown time occurred during the night hours in which the chilldown rate was greater than predicted.

Individual tank and average fuel temperatures, from LOX loading through launch, shown in figure 5-2, were obtained from computer program BEO3, the Propellant Monitor Program.

5.3.1.1 Fuel (RP-1) Sampling Plan

The consignment of 255,000 gallons of RP-1 for Skylab Missions SL-2, SL-3 and SL-4 was stored at LC-39B storage facility from February 1972. Samples of fuel were collected in accordance with a specified sampling plan during March 1972 through February 1973 and subjected to analysis. An additional sample was collected on August 31, 1973, prior to SL-4 CDDT. Sample dates and representative data are given in table 5-3. Data required for S-IB-8 flight evaluation, fuel density as a function of temperature, were determined from the initial fuel sample taken March 2, 1972. The percent errors (lb/ft³) at flight temperature are -0.01 percent, March 1972 equation versus August 1973 equation; and +0.002 percent, March 1972 equation versus average equation.

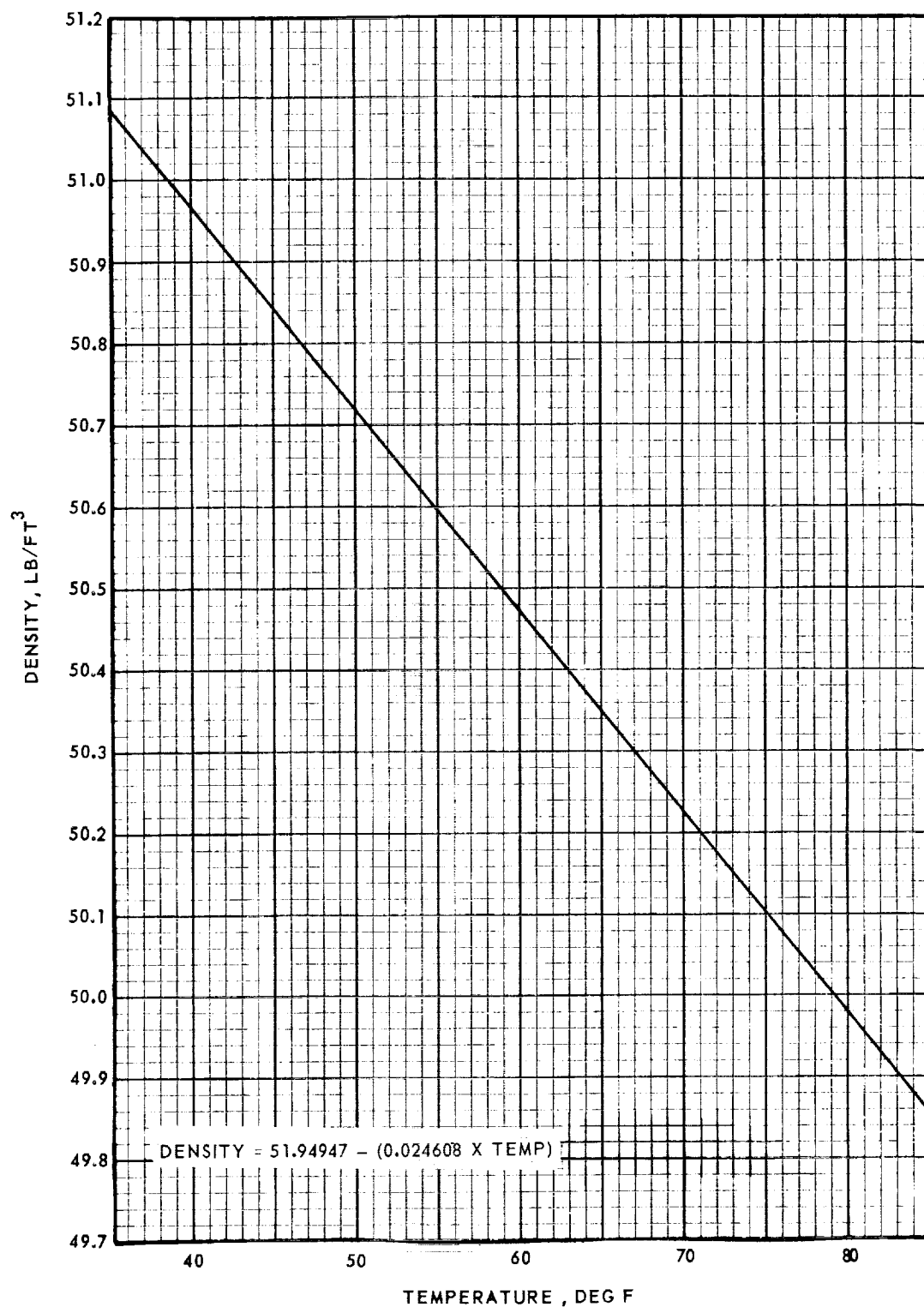


Figure 5-1. S-IB Fuel Temperature Density Relationship

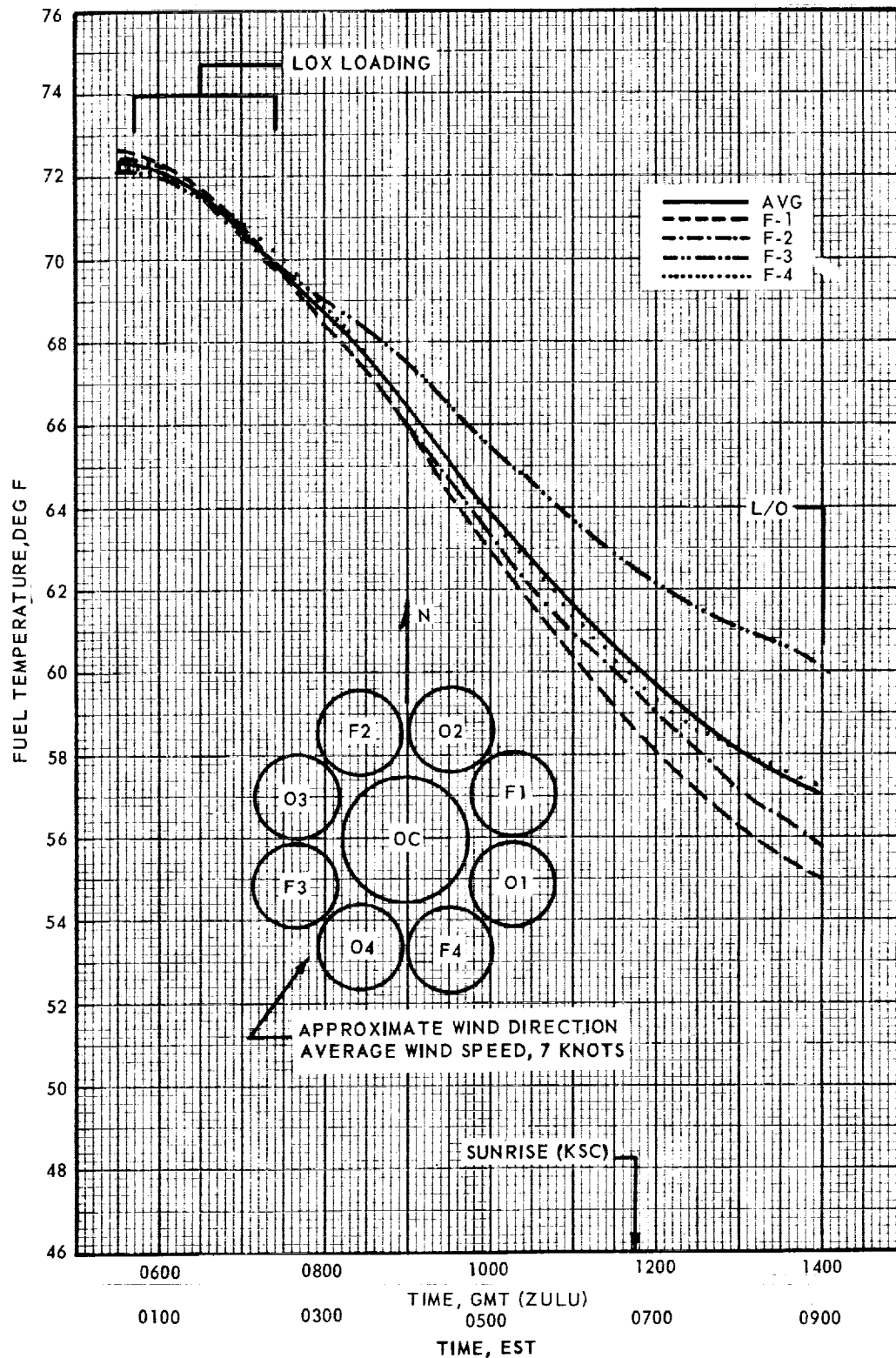


Figure 5-2. S-IB-8 Fuel Chardown After Lox Loading

Table 5-3. RP-1 Sampling Plan - Skylab SL-2, -3 and -4

SAMPLE DESCRIPTION	LABORATORY ANALYSIS DATE	SAMPLE IDENTIFICATION (LAB WORK ORDER)	CLASSIFICATION	DENSITY DATA CURVE FIT EQUATION FUEL DENSITY (LB/FT ³) VS TEMPERATURE (F)	GROSS HEATING VALUE (BTU/LB)	GROSS HEATING VALUE (BTU/LB)
Receiving Inspection 3/2/72	3/7/72	G-03276 G-03277 G-03276 A & G-03277 B	Primary Backup Density vs. Temperature	$\rho = 51.94947 - 0.024608 \times \text{Temp}$	20,027 20,027	18,719 18,719
Sampling Plan (scheduled) 6/29/72	7/13/72	G-10171 G-10173 G-10175 all (-A) samples	Primary Backup Density vs. Temperature	$\rho = 51.9636 - 0.02488 \times \text{Temp}$	20,073 20,029 19,910	18,756 18,721 18,635
Sampling Plan (scheduled) 9/15/72	9/18/72	G-14808 G-14809 G-14810, 11 & 12	Primary Backup Density vs. Temperature	$\rho = 51.9537 - 0.02467 \times \text{Temp}$	19,590 19,985	18,552 18,695
Sampling Plan (PLAST, SL-2) 2/21/73	2/26/73	G-03643 G-03644 G-03645, 46 & 47	Primary Backup Density vs. Temperature	$\rho = 51.951351 - 0.0246605 \times \text{Temp}$	19,948 19,977	18,662 18,540
Flight - SL-2 (CDDT)	No Sample taken	-	-	-	-	-
Flight-SL-3 (CDDT)	7/3/73	G-12035 G-12036 G-12037, 38&39	Primary Backup Density vs. Temperature	$\rho = 51.95614 - 0.02480 \times \text{Temp}$	19,942 19,780	18,659 18,542
Sampling Plan 8/31/73	9/5/73	G-14984 G-14985 G-14984, 85 & 86	Primary Backup Density vs. Temperature	$\rho = 51.96847 - 0.024936 \times \text{Temp}$	20,021 20,010	18,715 18,707
Flight - SL-4 11/16/73	No Sample taken	-	-	--	-	-
Average					19,948	18,663

5.3.2 LOX Loading

The reconstructed average LOX density at ignition, based on the average LOX pump inlet temperature throughout flight, was 70.600 lbm/ft³. The LOX pump inlet temperature monitored during the flight indicated that the temperature of the LOX at ignition was 0.17°F colder than predicted. The LOX pump inlet temperature, determined from the average of measurements XC0054-1 through XC0054-8, is shown in figure 5-3. The PTCS number set into the computer to tank the required load was 9900.

At 07:14Z, LOX slow fill was completed and the LOX replenish sequence commenced with 99 percent of the flight mass on board. By 08:00Z, LOX was reported emanating from the outboard LOX tank vents. The motion picture film from the east side camera, facing west, offered the best view of LOX eruptions with coverage beginning at 05:01:25Z to 11:34:48Z. This coverage included about 4 hours and 20 minutes of LOX replenish operations. This film was reviewed and 119 eruptions were counted from tank O4. Most of these eruptions were very small with 20 eruptions considered medium to large. Because of the direction of the wind (southwesterly) and camera view, the eruptions from tank O4 were clearly discernible as to their origin. Additional discharges were noted from other outboard tanks viewed from other camera positions, but were fewer in number and of smaller magnitude than O4 discharges. Reconstructed flight performance, as it pertains to the problem, showed nothing unusual. Actual LOX load was within 400 pounds of predicted, and LOX pump inlet temperature averaged, throughout flight, 0.17°F colder than predicted. Time required to prepressurize the ullage was 55 seconds, approximately the same as during the CDDT, which indicated normal ullage volume. The wind and humidity during the countdown were near normal.

Figure 5-4 depicts the relative heights of liquid in the center tank and a windward outer tank. Note that with a nominal wind speed of 9.2 knots, the windward outer tank level is approximately 2.7 inches above that of the center tank and 23.4 inches below the bottom of the vent duct. A wind increase to 34 knots (maximum expected) would cause the outer tank level to increase approximately 4 inches while the center tank level would be unchanged.

Instrumentation to detect or investigate the phenomenon is inadequate because its intended use was for flight evaluation. However, the eight LOX pump inlet temperatures (one/engine) were reviewed together with the Engine No. 1 LOX pump inlet pressure for the 8-hour period prior to launch. This period covered start of LOX loading until liftoff. Additionally, center LOX tank ullage pressure was scrutinized for any unusual fluctuations which could be related to the discharges seen on the film. None were noted during the 8-hour period. The overfill sensor, located 21 inches below the vent duct, did not indicate liquid presence during LOX loading.

Review of films taken during SA-206 and SA-207 countdowns revealed similar occurrences. Several small eruptions were also observed in reviewing the films of the SA-206, SA-207 and SA-208 Countdown Demonstration Tests (CDDT). While the cause is not known, this LOX ejection had no apparent effect on flight performance.

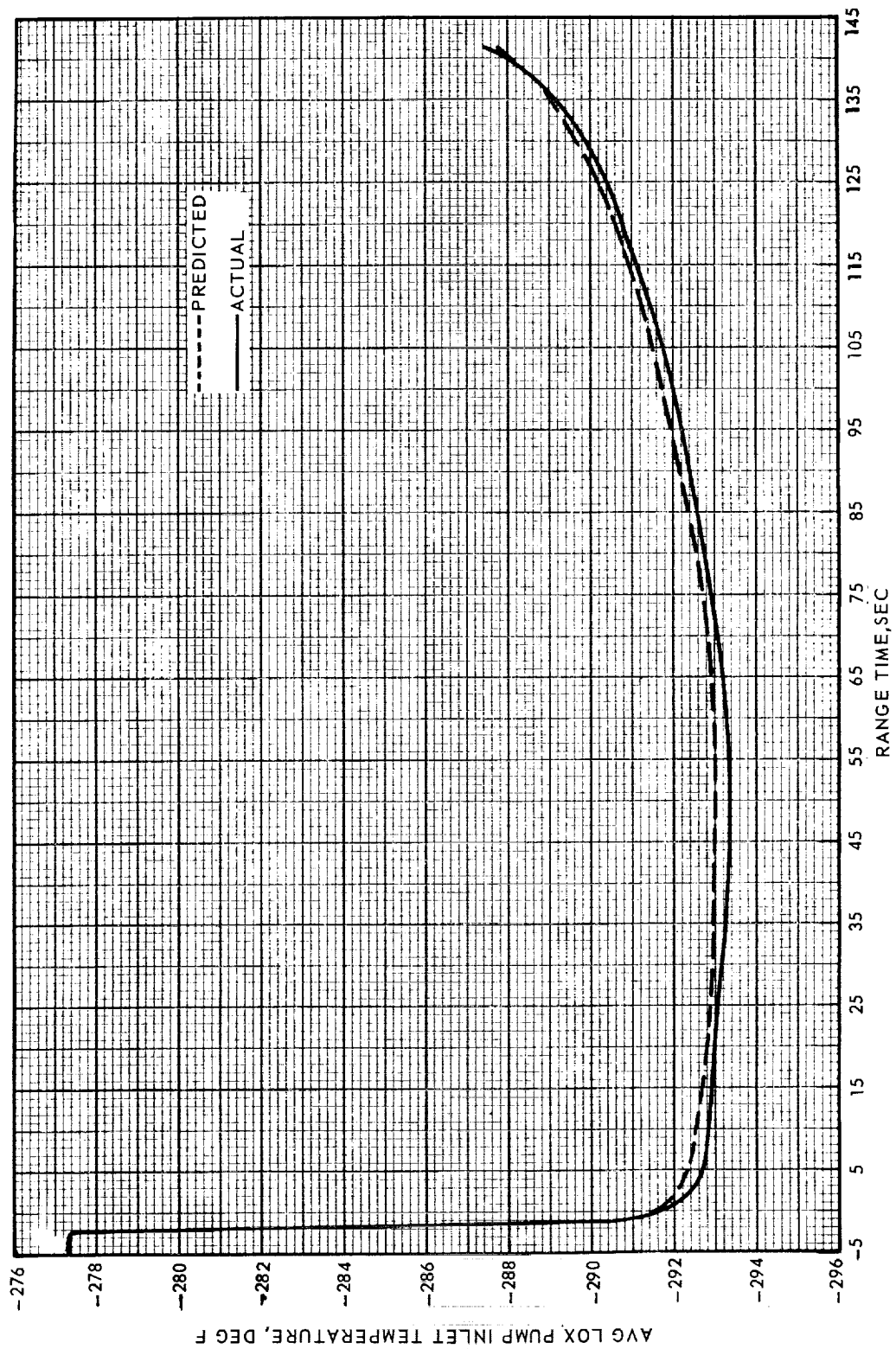


Figure 5-3. S-IB Lox Pump Inlet Temperature During Flight

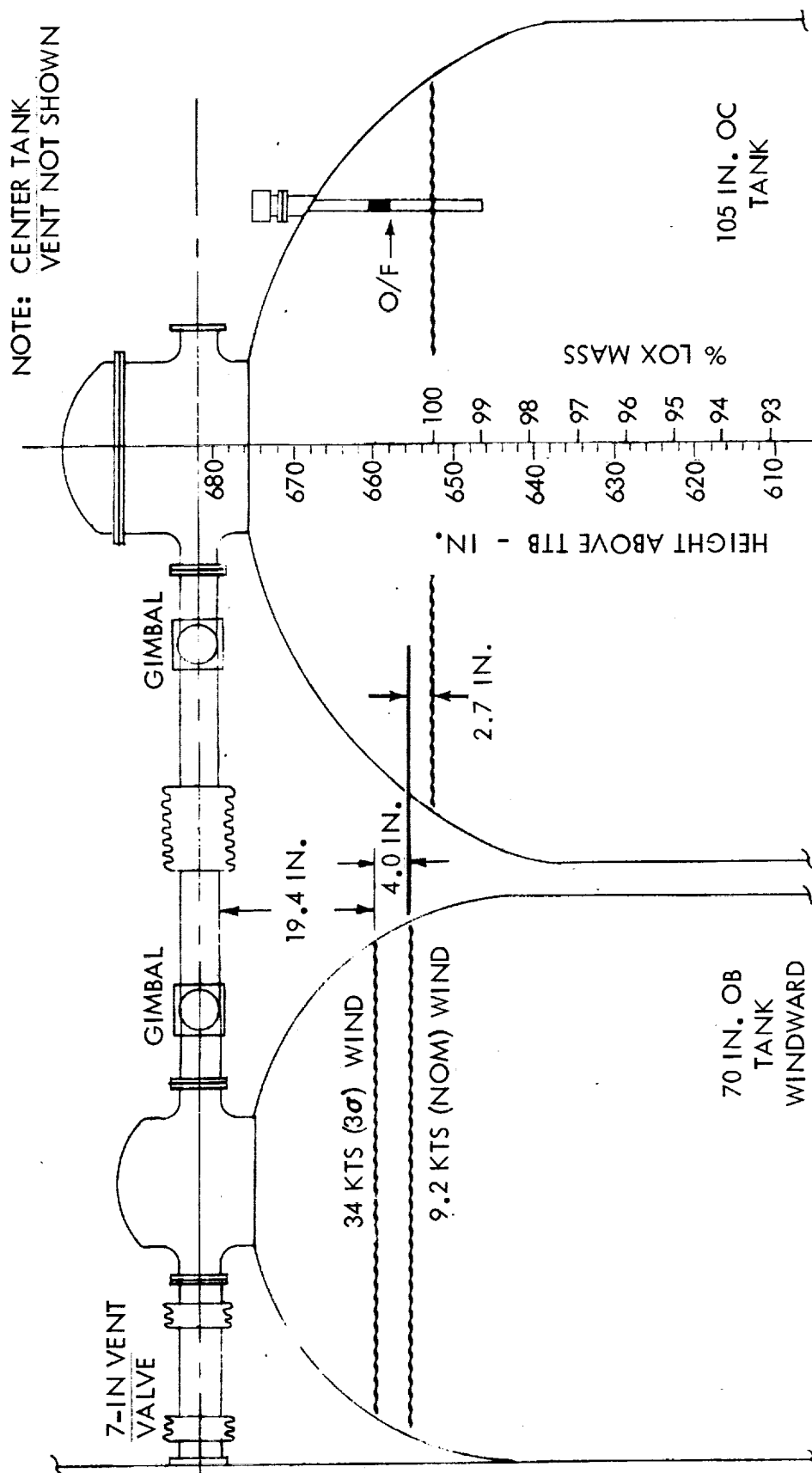


Figure 5-4. Center LOX Tank - Outboard LOX Tank Relationship

Section 6

MASS CHARACTERISTICS

6.1 SUMMARY

The S-IB stage mass characteristics history and predicted prelaunch data were provided for the vehicle evaluation. A postflight stage analysis was not performed.

6.2 PREDICTED MASS CHARACTERISTICS

The final predicted mass characteristics for the S-IB stage are presented in TN-WG-73-1-208, Revision A, dated August 17, 1973. Dry stage mass characteristics reflect the status as stated in TN-P&VE-73-73, dated August 20, 1973. These data are based on the measured weight and longitudinal center of gravity taken at the Michoud Assembly Facility, April 28, 1967, and include all changes and modifications applied to the stage from the time of weighing until August 20, 1973. Predicted stage mass properties for significant event times are compiled in table 6-1.

Propellant loading, utilization and event times were obtained from TR-P&VE-73-153, dated June 20, 1973 (reference B). These propellant data are the final predicted loading and consumption for the S-IB stage under normal conditions. A propellant weight breakdown for selected flight conditions is given in table 6-2.

Table 6-1. S-IB Stage Mass Properties

TIME (SECONDS)	STAGE CONDITION	WEIGHT (POUNDS)	CENTER OF GRAVITY (INCHES)			MASS MOMENT OF INERTIA (LB-FT-SEC ²)		
			X	Y	Z	ROLL	PITCH	YAW
-3.125	Ground Ignition	996,259	542.3	0.054	-0.006	1,460,694	10,346,460	10,327,847
0.000	Liftoff	982,032	536.4	0.054	-0.005	1,435,741	10,007,310	9,987,714
74.000	Max q	510,780	381.3	0.111	-0.019	769,722	3,118,750	3,099,408
137.704	Inboard Cutoff Signal	106,897	317.6	0.538	-0.117	200,663	2,063,814	2,044,689
140.704	Outboard Cutoff Signal	95,519	328.5	0.603	-0.135	184,497	2,028,246	2,016,543
142.004	Separation Signal	93,871	330.9	0.609	-0.136	181,545	2,018,417	2,008,853
142.083	Separation Complete	93,841	331.0	0.609	-0.137	181,457	2,017,776	2,008,244
143.204	End Thrust Decay	93,514	331.8	0.611	-0.137	180,883	2,013,754	2,004,437
	Dry Stage	83,958	339.4	0.700	-0.100	164,527	1,909,699	1,909,388

Table 6-2. S-IB Propellant and Service Item History

EVENT	TIME (SEC)	IGNITION	LIFTOFF	MAX q	INBOARD C. O. S.	OUTBOARD C. O. S.	SEP. SIGNAL	E. T. D.
LOX Onboard In Containers Below Containers		-3.125	0.000	74.00	137.704	140.704	142.004	143.204
		632,016	621,004	292,132	10,439	3,287	2,726	2,642
		624,259	612,798	283,947	2,340	0	0	0
		7,757	8,206	8,185	8,099	3,287	2,726	2,642
Fuel Onboard In Containers Below Containers		279,096	275,832	132,743	9,747	5,490	4,401	4,128
		274,347	270,150	127,061	4,065	274	0	0
		4,749	5,682	5,682	5,682	5,216	4,401	4,128
Oxidizer Pressurizing Gas In Containers		31	79	1,433	2,621	2,653	2,655	2,654
Fuel Pressurizing Gas In Containers		5	8	45	59	60	60	60
Fuel Pressurizing Gas In Spheres		79	76	39	25	24	24	24
GN ₂ For S-IB Engine Seal And Purge		15	15	12	10	10	10	10
Oronite		32	32	22	11	10	10	10
Hydraulic Oil		28	28	28	28	28	28	28
Frost		1,000	1,000	370	0	0	0	0
Total Propellants and Service Items		912,302	898,074	426,824	22,940	11,562	9,914	9,556

Section 7

PROPULSION

7.1 SUMMARY

The S-IB stage propulsion system performance was satisfactory. Stage longitudinal thrust averaged 0.13 percent lower than predicted. Stage LOX, fuel and total flow-rates averaged 0.10 percent, 0.18 percent, and 0.12 percent lower than predicted, respectively. Stage mixture ratio averaged 0.08 percent higher than predicted. Stage specific impulse was within 0.02 percent of predicted. Inboard engine cutoff (IECO) occurred 0.16 seconds earlier than predicted. Outboard engine cutoff (OECO) was initiated 3.47 seconds after IECO by engine number 1 Thrust OK Pressure Switch deactuation.

7.2 S-IB IGNITION TRANSIENT PERFORMANCE

All eight H-1 engines ignited satisfactorily. The automatic ignition sequence, which schedules the engines to start in pairs with a 100-millisecond delay between each pair, began with the time for ignition command at -3.050 seconds range time. The start sequence that occurred was close to optimum. The maximum spread in the start time (P_c prime times) of engines within a pair was 25 milliseconds and was between engines 2 and 4 (third pair of engines). The smallest interval in the planned 100-millisecond sequence between pairs was 75 milliseconds which occurred between the third pair's later engine and the fourth pair's earlier engine (specifically between engines 2 and 3).

Table 7-1 compares predicted and actual start event times. The individual engine thrust buildup curves are shown in figure 7-1. The thrust values shown are the engine chamber thrusts and do not account for cant angles or turbine exhaust thrust. Figure 7-2 shows the total thrust buildup of the stage.

7.3 S-IB MAINSTAGE PERFORMANCE

7.3.1 Stage Performance

S-IB mainstage flight performance was satisfactory. Stage longitudinal thrust, figure 7-3, averaged 2347 pounds (0.13 percent) lower than predicted. The stage specific impulse, figure 7-4, during flight was within 0.04 second of predicted. Stage mixture ratio, figure 7-5, averaged 0.0019 (0.08 percent) higher than predicted. Stage LOX and fuel flowrate, figures 7-6 and 7-7, averaged 4.3 lbm/sec (0.10 percent) and 3.4 lbm/sec (0.18 percent) lower than predicted, respectively. Total flowrate, figure 7-8, averaged 7.7 lbm/sec (0.12 percent) lower than predicted. These average deviations were taken between first motion and IECO.

Table 7-1. S-IB Engine Start Characteristics

ENGINE POSITION AND SERIAL NUMBER	TIME, IGNITION COMMAND TO ENGINE IGNITION SIGNAL (MSEC)		TIME, ENGINE IGNITION SIGNAL TO THRUST CHAMBER IGNITION (MSEC)		TIME, ENGINE IGNITION SIGNAL TO P _c PRIME (MSEC)	
	ACTUAL(1)	PROGRAMMED	ACTUAL	NOMINAL	ACTUAL	NOMINAL
5 - H-4077	102	100	548	584 (2)	833	875 (2)
7 H-4079	102	100	548		833	
6 H-4071	201	200	544		844	
8 H-4080	201	200	544		842	
2 H-7079	303	300	527		862	
4 H-7096	303	300	532		837	
1 H-7082	402	400	505		848	
3 H-7081	402	400	513		838	

(1) Values referenced to TCS event "Time for Ignition Command"

(2) Values presented are mean values S-IB-6 through S-IB-12 static test, Technical Bulletin - P&VE-65-148, Revision D. Sample means and standard deviations were: Time to thrust chamber ignition 583.7 MSEC and 18.4 MSEC; time to P_c prime 874.6 MSEC and 22.6 MSEC.

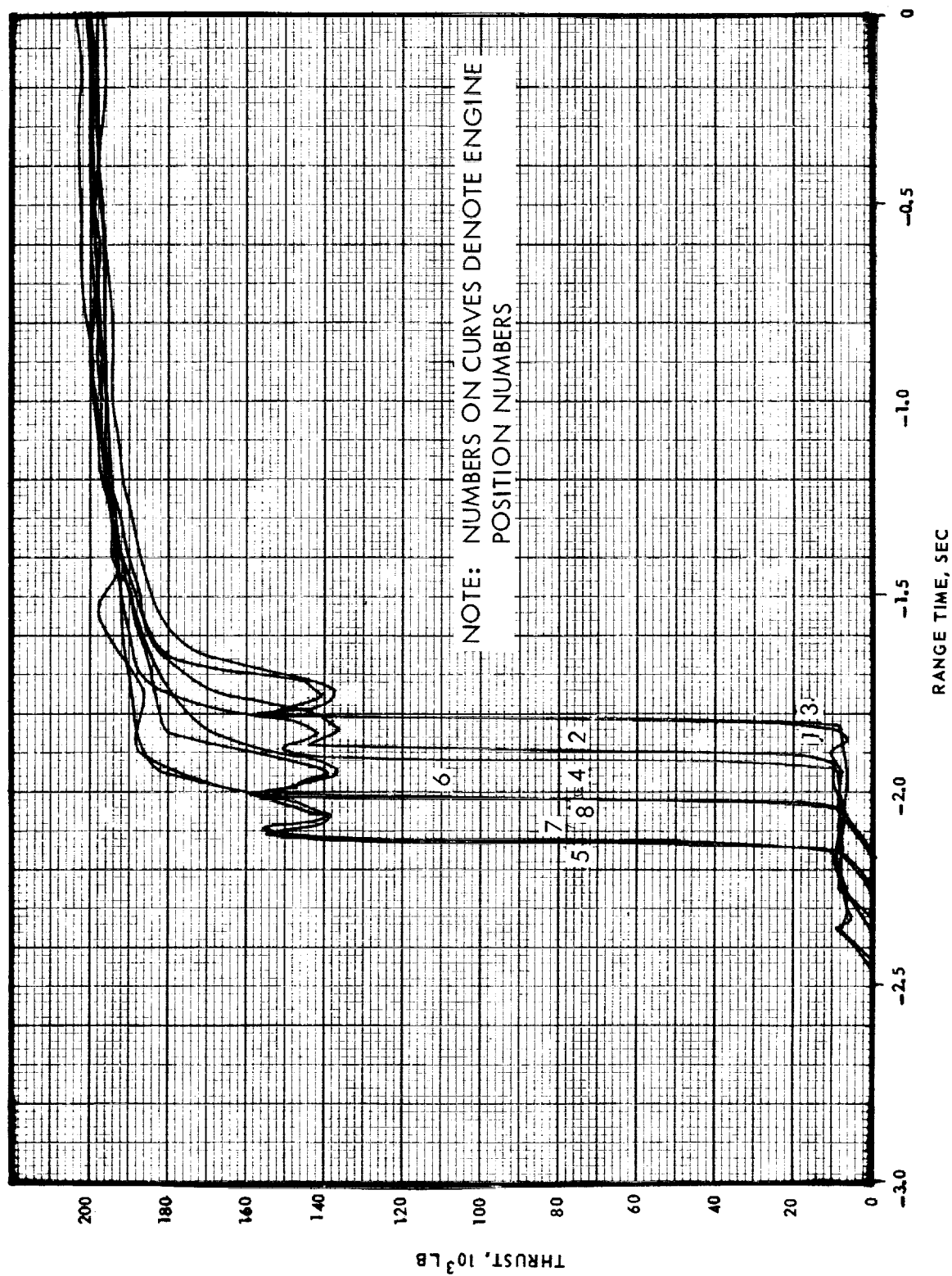


Figure 7-1. S-IB Engine Thrust Buildup



Figure 7-2. S-IB Stage Thrust Buildup

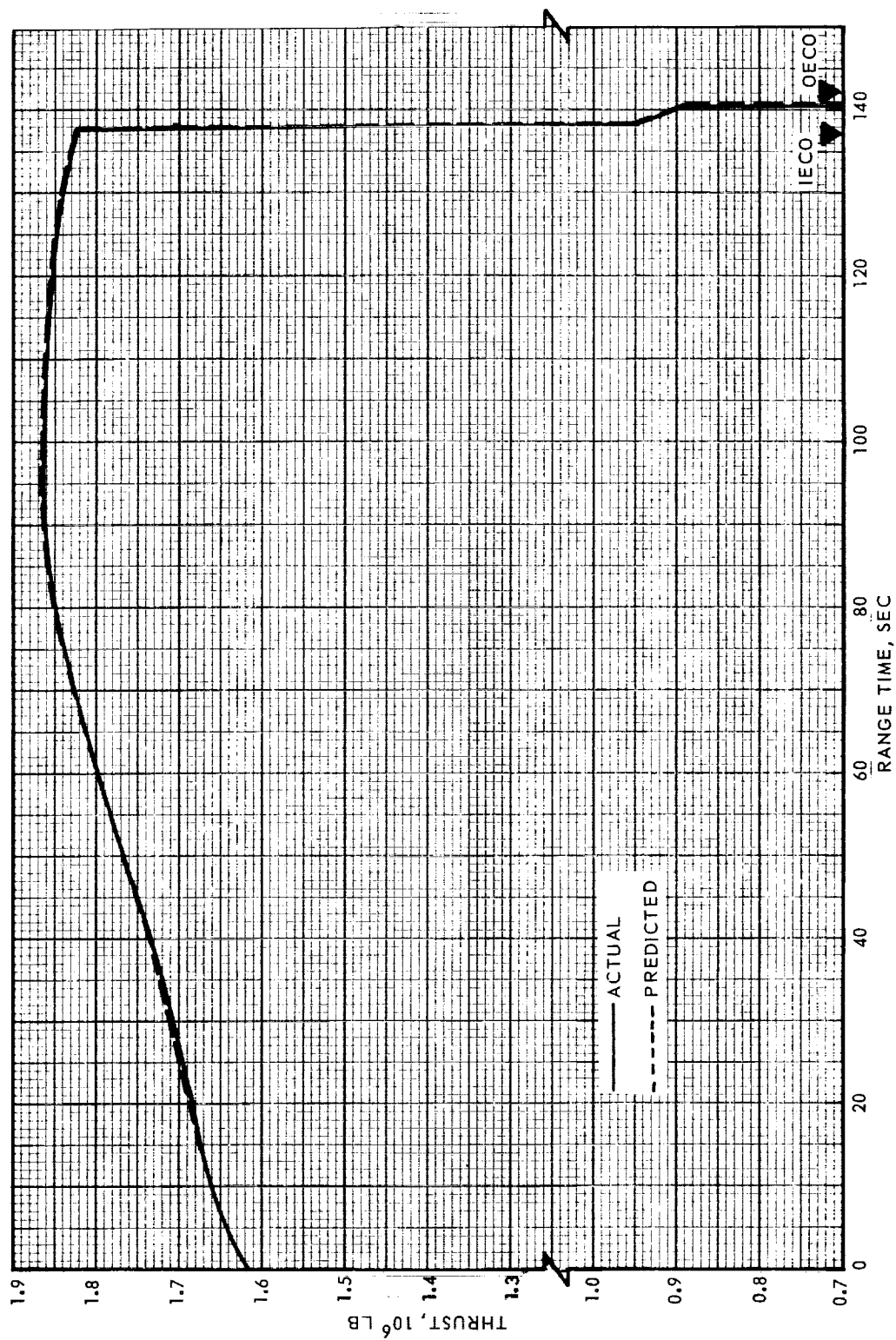


Figure 7-3. S-IB Stage Longitudinal Thrust

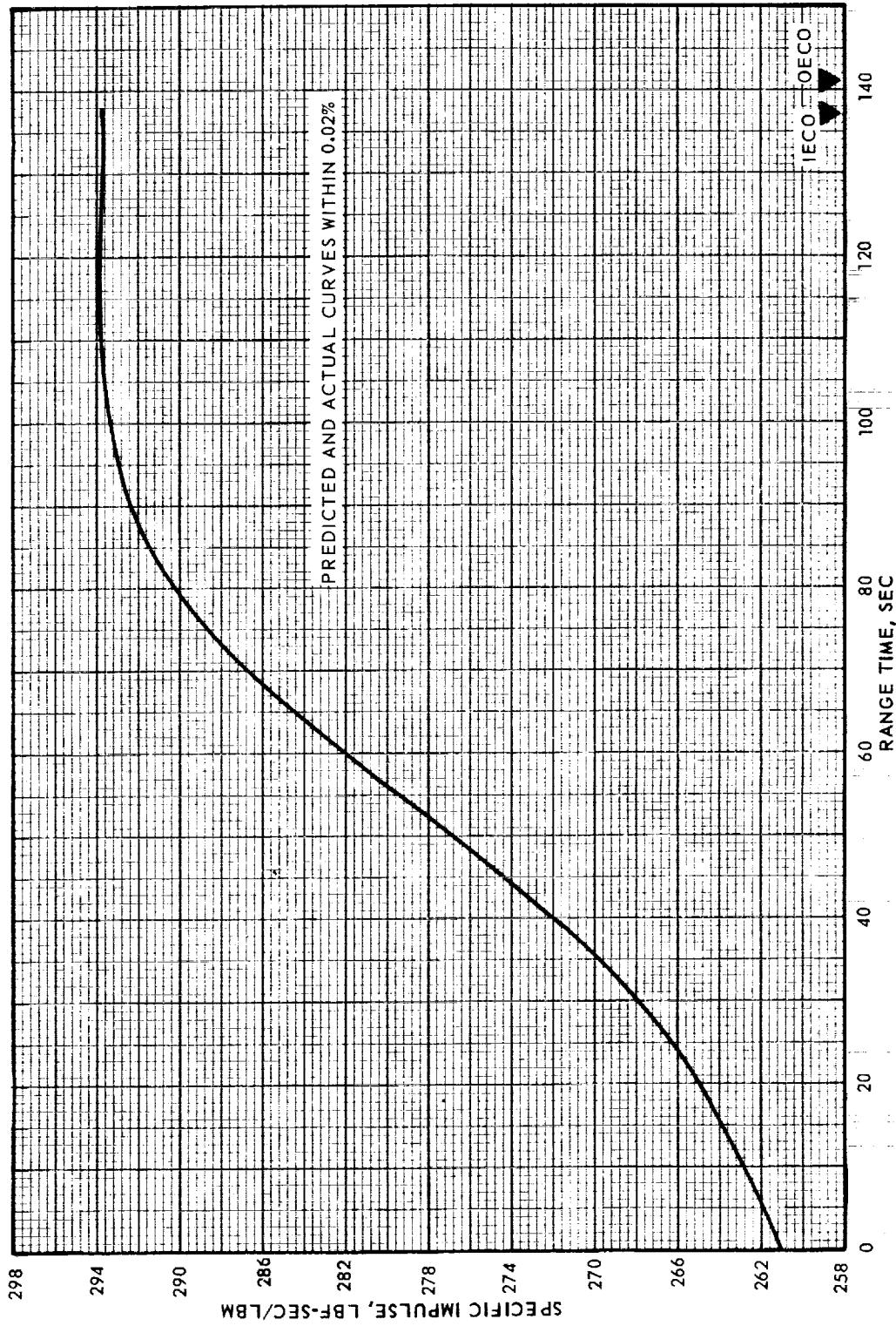


Figure 7-4. S-IB Stage Specific Impulse

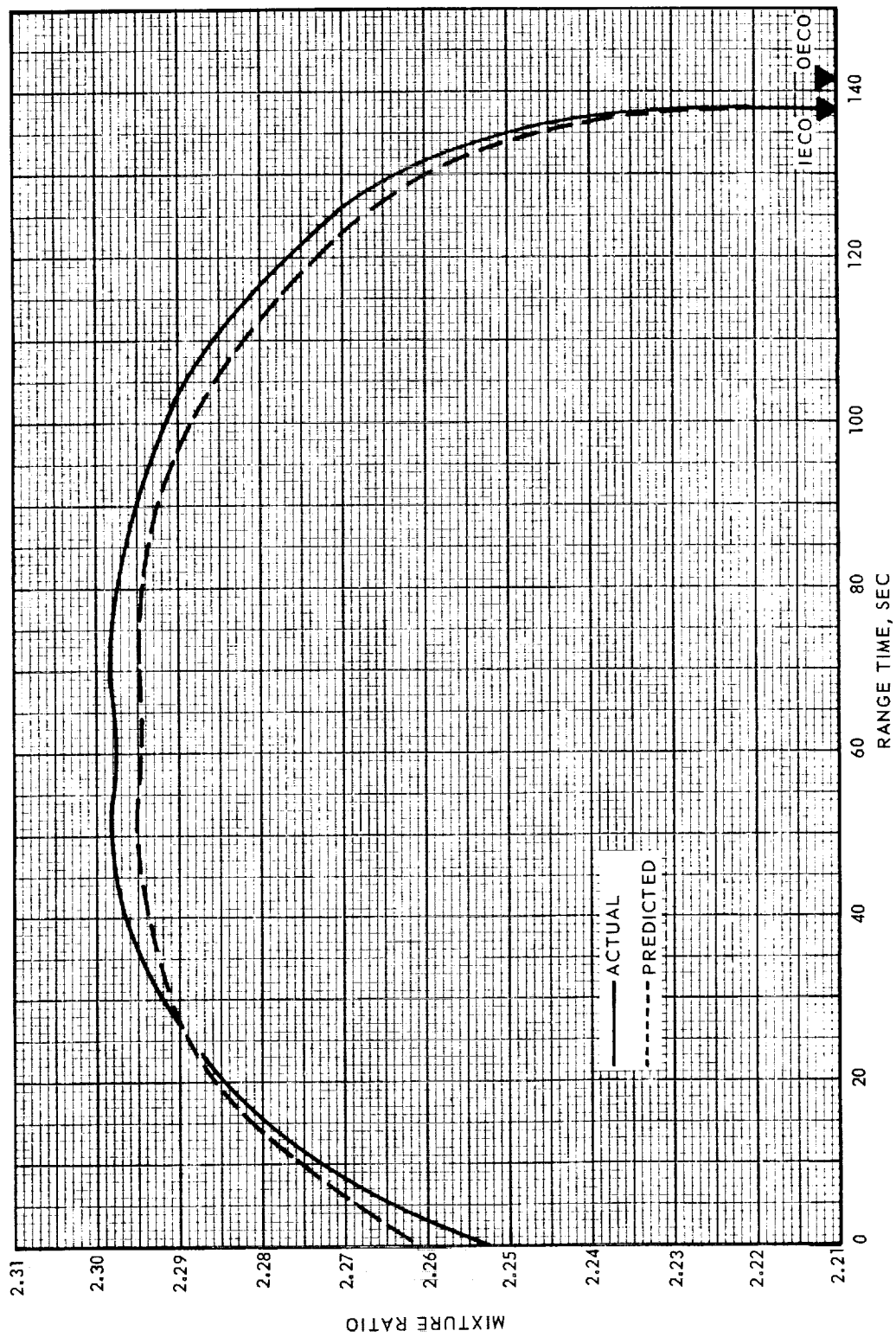


Figure 7-5. S-IB Stage Mixture Ratio

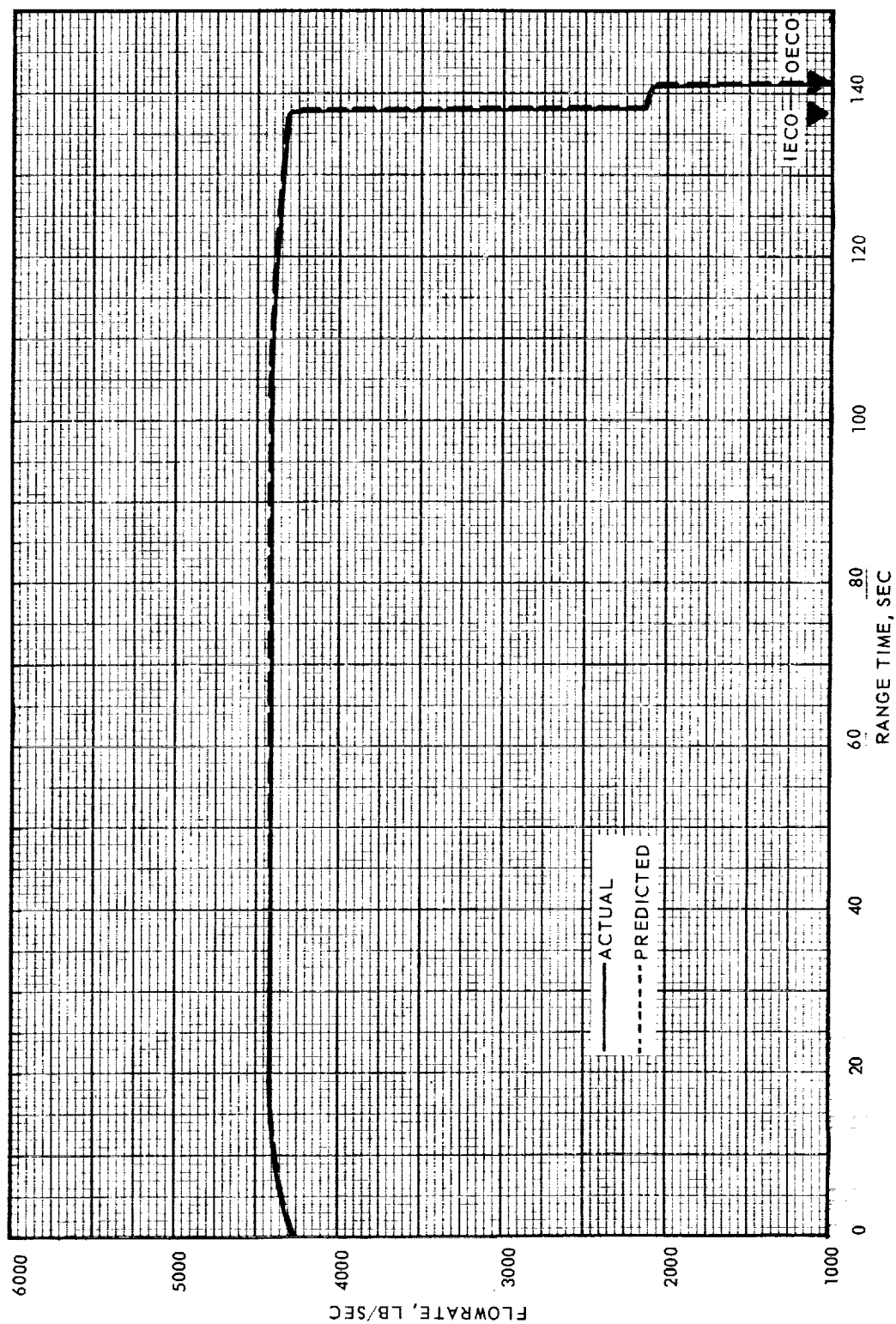


Figure 7-6. S-IB Stage LOX Flowrate

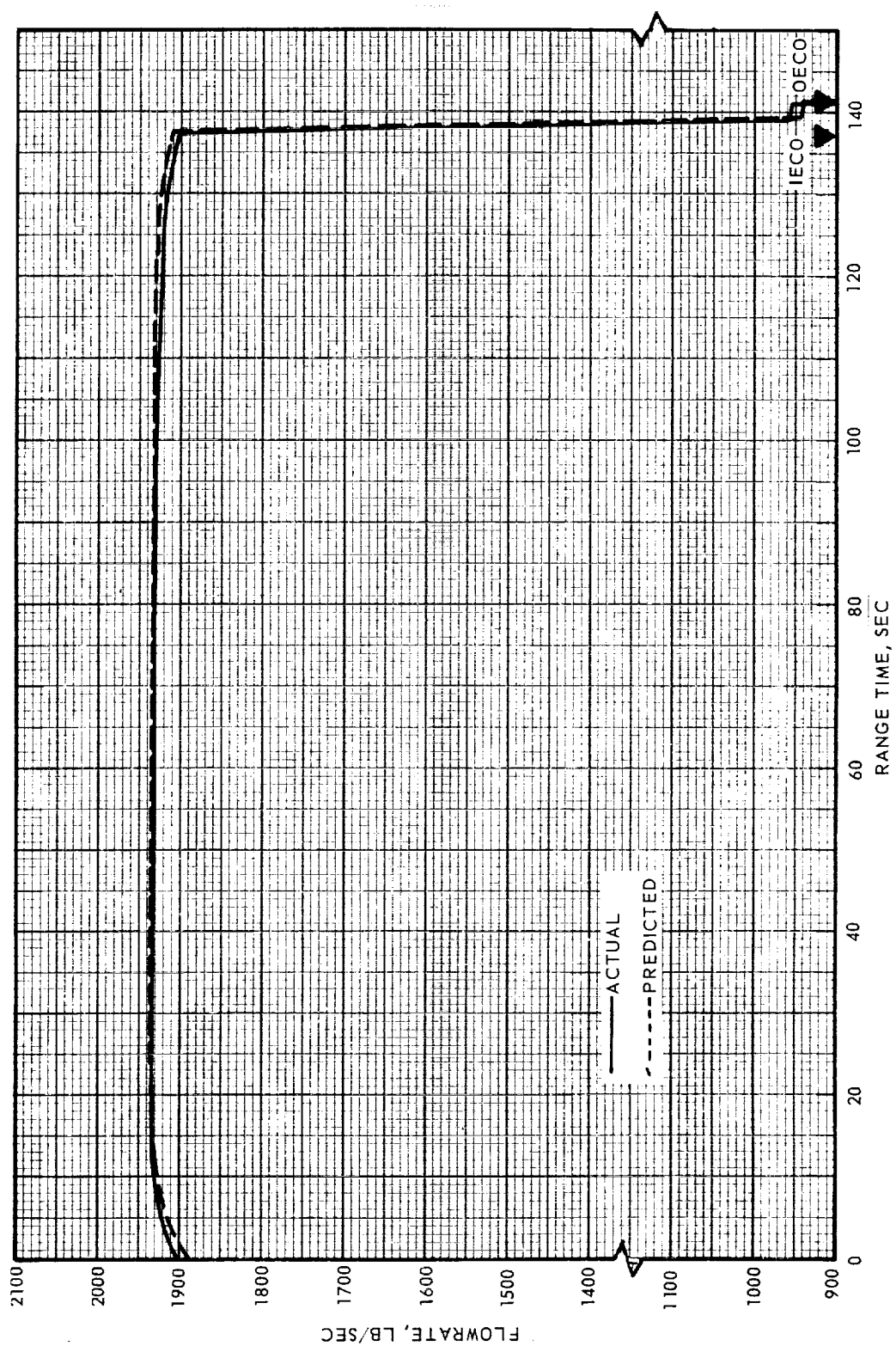


Figure 7-7. S-IB Stage Fuel Flowrate

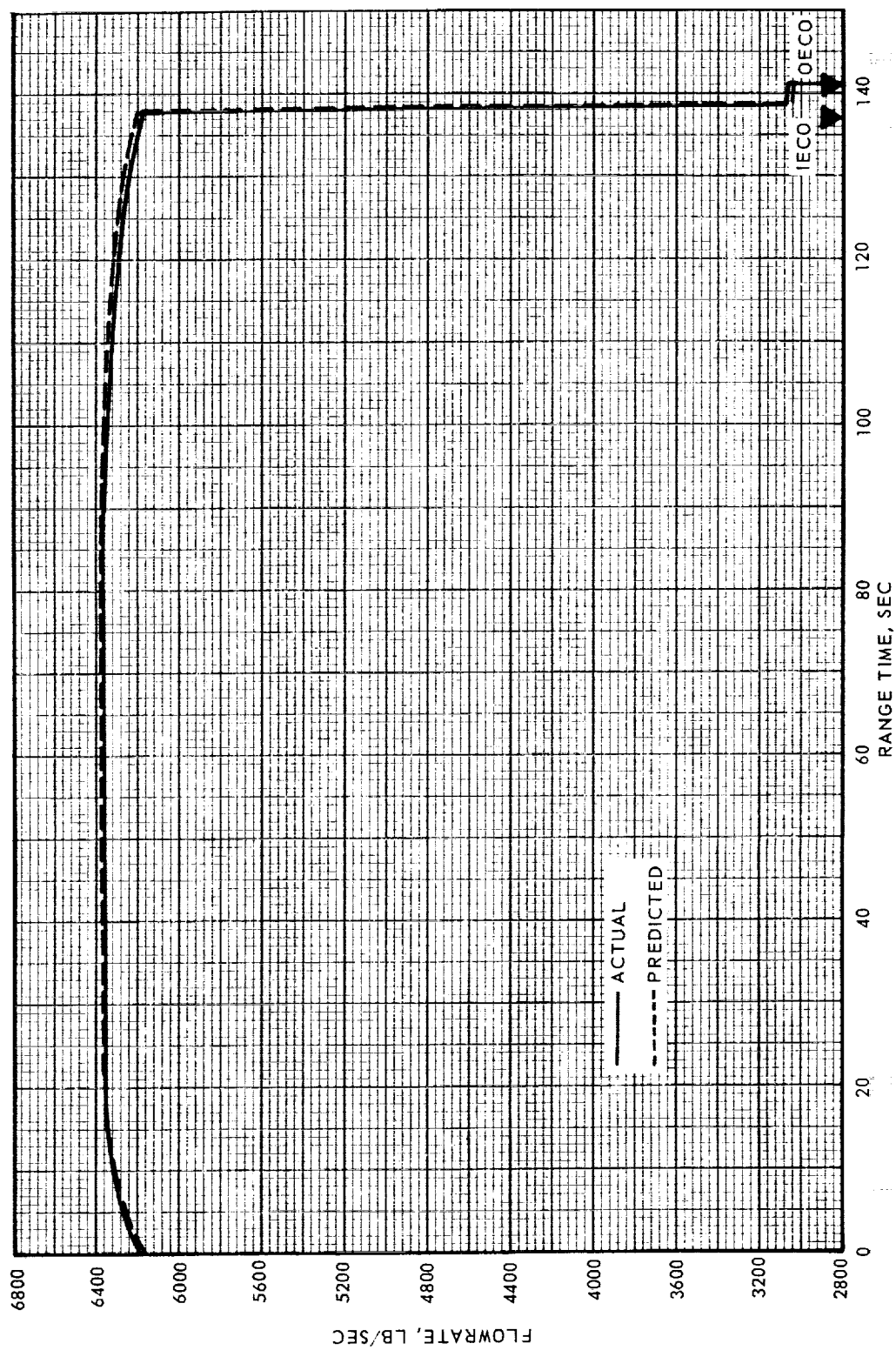


Figure 7-8. S-IB Stage Total Propellant Flowrate

The performance parameters contributing to the small deviations from predicted performance are given in table 7-2. The fuel temperature was 5.4°F lower than predicted which normally would have significantly decreased thrust and total flowrates; however, the effects of the more dense fuel were almost entirely compensated for by a slightly higher LOX tank pressure and a lower LOX temperature than predicted.

The early IECO and late OECO were primarily the result of a greater than predicted level difference between the O-2 tank which signalled level sensor actuation (ISA) and the other four tanks, particularly the center tank. The lower than predicted level in the O-2 tank caused less LOX to be consumed by the inboard engines before IECO and more LOX was available for the outboard engines before LOX depletion occurred. Another contributor to the late OECO was the 4-engine LOX starvation. The prediction incorporates a 2-engine LOX starvation OECO cutoff to provide conservatism for the other types of OECO that can occur.

The predicted performance for S-IB-6, 7 and 8 was determined before any stages with 205K thrust engines had flown. Since the flight of S-IB-6, it was expected that the fuel and LOX tank pressures would be higher, the fuel temperature lower, and the LOX level in O2 lower than predicted for S-IB-7 and S-IB-8. As the combined effects of these small deviations do not significantly affect stage performance, prediction updates were not considered necessary.

7.3.2 Individual Engine Performance

The performance of each engine was satisfactory. Individual engine propulsion performance data in table 7-3 give sea level values, which are at rated operating conditions for selected parameters obtained from Rocketdyne acceptance test data, flight prediction data and flight data at a slice time of 30 seconds.

The predicted sea level values for the S-IB-8 engines were calculated in a similar manner to the sea level values for the S-IB-7 engine prediction data. The predicted thrusts, turbine speeds and flowrate sea level data were derived by increasing the Rocketdyne acceptance test data to be consistent with the trends noted during the flights of S-IB-1 through S-IB-5 with 200K thrust engines. The 8-engine average sea level thrust, LOX flowrate, and specific impulse were within 0.1 percent of those predicted. The average sea level fuel flowrate and mixture ratio were within 0.25 percent of those predicted.

The average differences between flight and predicted thrust, specific impulse, and mixture ratio from liftoff to IECO are shown for each engine in figure 7-9. Also shown in figure 7-9 are the differences in sea level values (table 7-3) at 30 seconds for each engine.

The individual engine flight performance was determined by reconstructing the flight with the Mark IV computer program, a mathematical model of the Saturn first stage propulsion system which utilizes a table of influence coefficients to determine engine performance. The thrust levels are determined from an RPM match option of the program which uses ground test data to calculate thrust based on turbopump speeds. This method has been shown to provide better estimations of flight thrust than can be obtained with the telemetered chamber pressures.

Table 7-2. S-IB Propulsion Flight Performance Deviations

PARAMETER	AVERAGE DEVIATION	Δ THRUST (PERCENT)	Δ MIXTURE RATIO (PERCENT)	Δ SPECIFIC IMPULSE (PERCENT)	Δ LOX FLOWRATE (PERCENT)	Δ FUEL FLOWRATE (PERCENT)	Δ IEEO (SEC)	Δ OEEO (SEC)
Calibration Data	-	-0.076	+0.226	+0.004	-0.004	-0.226	+0.01	+0.01
LOX Pump Inlet Pressure	+1.4 psia	+0.240	+0.200	+0.043	+0.290	+0.060	-0.36	-0.38
Fuel Pump Inlet Pressure	+0.9 psia	-0.045	-0.099	-0.013	-0.062	+0.037	+0.08	+0.08
LOX Pump Inlet Temp.	-0.17°F	+0.110	+0.100	+0.020	+0.110	+0.020	-0.16	-0.17
Fuel Temperature	-5.4°F	-0.416	-0.338	-0.060	-0.440	-0.105	+0.59	+0.63
LOX Load	+400 lb	-	-	-	-	-	+0.10	+0.10
Fuel Load	+945 lb	-	-	-	-	-	0.00	0.00
Tank-to-tank LOX level difference at LSA	+600 lb LOX @ LSA	-	-	-	-	-	-0.15	+0.15
Lower LOX Residual	-200 lb	-	-	-	-	-	0.00	+0.12
Miscellaneous effects	-	+0.049	-0.008	-0.009	+0.096	+0.037	-0.27	-0.23
Total Effect	-	-0.132	+0.081	-0.015	-0.010	-0.177	-0.16	+0.31

NOTE: Average deviation: Flight value - predicted value

Δ: Flight value - predicted value

Percent Δ: (Δ/predicted value) x 100

Calibration data: H-1 Engine performance data at nominal pump inlet conditions (sea level data).

Table 7-3. S-IB Individual Engine Propulsion Performance

ENGINE POSITION		POSITION 1			POSITION 2			POSITION 3			POSITION 4		
ENGINE SERIAL NUMBER		H-7082			H-7079			H-7081			H-7096		
PARAMETER/DATA SOURCE		RKDN	PRED.	FLIGHT	RKDN	PRED.*	FLIGHT	RKDN	PRED.	FLIGHT	RKDN	PRED.*	FLIGHT
Engine Thrust, lb		205,417	206,629	207,309	205,351	206,562	208,650	203,964	205,167	204,381	203,586	204,787	204,917
Engine Specific Impulse, Sec		263.01	262.68	262.81	262.62	262.28	262.63	263.10	262.77	262.67	262.46	262.13	262.18
Combustion Chamber Pressure, psia		707.18	710.86	712.78	707.11	710.79	717.04	704.36	708.02	705.41	699.79	703.43	703.64
Pump Speed, rpm		6722.9	6747.8	6761.0	6683.7	6708.4	6751.4	6698.4	6723.2	6705.6	6635.7	6660.3	6662.0
Engine Mixture Ratio, O/F		2.2448	2.2593	2.2647	2.2370	2.2515	2.2577	2.2261	2.2405	2.2453	2.2195	2.2339	2.2393
Engine Oxidizer Flowrate, lb/sec		540.30	545.27	547.19	540.38	545.35	550.58	534.93	539.85	538.33	534.75	539.67	540.30
Engine Fuel Flowrate, lb/sec		240.70	241.35	241.61	241.57	242.22	243.87	240.30	240.95	239.76	240.93	241.58	241.28
Engine Total Flowrate, lb/sec		781.00	786.62	788.80	781.95	787.57	794.45	775.23	780.80	778.09	775.68	781.25	781.58
ENGINE POSITION		POSITION 5			POSITION 6			POSITION 7			POSITION 8		
ENGINE SERIAL NUMBER		H-4077			H-4071			H-4079			H-4080		
PARAMETER DATA SOURCE		RKDN	PRED.	FLIGHT	RKDN	PRED.	FLIGHT	RKDN	PRED.	FLIGHT	RKDN	PRED.	FLIGHT
Engine Thrust, lb		207,508	208,732	207,020	201,914	203,105	203,802	204,698	205,906	204,204	204,395	205,601	205,049
Engine Specific Impulse, sec		264.42	264.08	263.84	263.04	262.70	262.86	263.67	263.33	263.09	264.12	263.78	263.73
Combustion Chamber Pressure, psia		711.25	714.95	709.51	691.78	695.38	697.33	699.91	703.56	698.17	696.76	700.38	698.52
Pump Speed, rpm		6706.7	6731.5	6695.1	6639.2	6663.8	6676.9	6676.6	6701.3	6664.8	6669.5	6694.2	6681.5
Engine Mixture Ratio, O/F		2.2426	2.2572	2.2613	2.2536	2.2682	2.2739	2.2442	2.2588	2.2631	2.2394	2.2538	2.2588
Engine Oxidizer Flowrate, lb/sec		542.75	547.74	544.05	531.68	536.57	538.51	537.04	541.98	538.31	534.97	539.89	538.92
Engine Fuel Flowrate, lb/sec		242.01	242.66	240.59	235.93	236.57	236.82	239.30	239.95	237.87	238.90	239.55	238.59
Engine Total Flowrate, lb/sec		784.76	790.40	784.64	767.71	773.14	775.33	776.34	781.93	776.18	773.87	779.44	777.51

- Notes: 1. Rocketdyne data from acceptance tests using PAST 76 program Reference H)
2. Sea level data obtained at 28 to 31 second time for static stage test (simulated range time)
3. All values referenced to the following sea level conditions:
- a. Ambient pressure, 14.696 psia
 - b. Fuel pump inlet density, 50.45 lb/ft³
 - c. LOX pump inlet density, 70.79 lb/ft³
 - d. Fuel pump inlet pressure, 57 psia
 - e. LOX pump inlet pressure, 65 psia
 - f. Fuel temperature, 60°F
- Legend:
- Rocketdyne data
- Pred. Predicted sea level performance
- Flight S-IB-8 reconstructed flight performance at 30 seconds

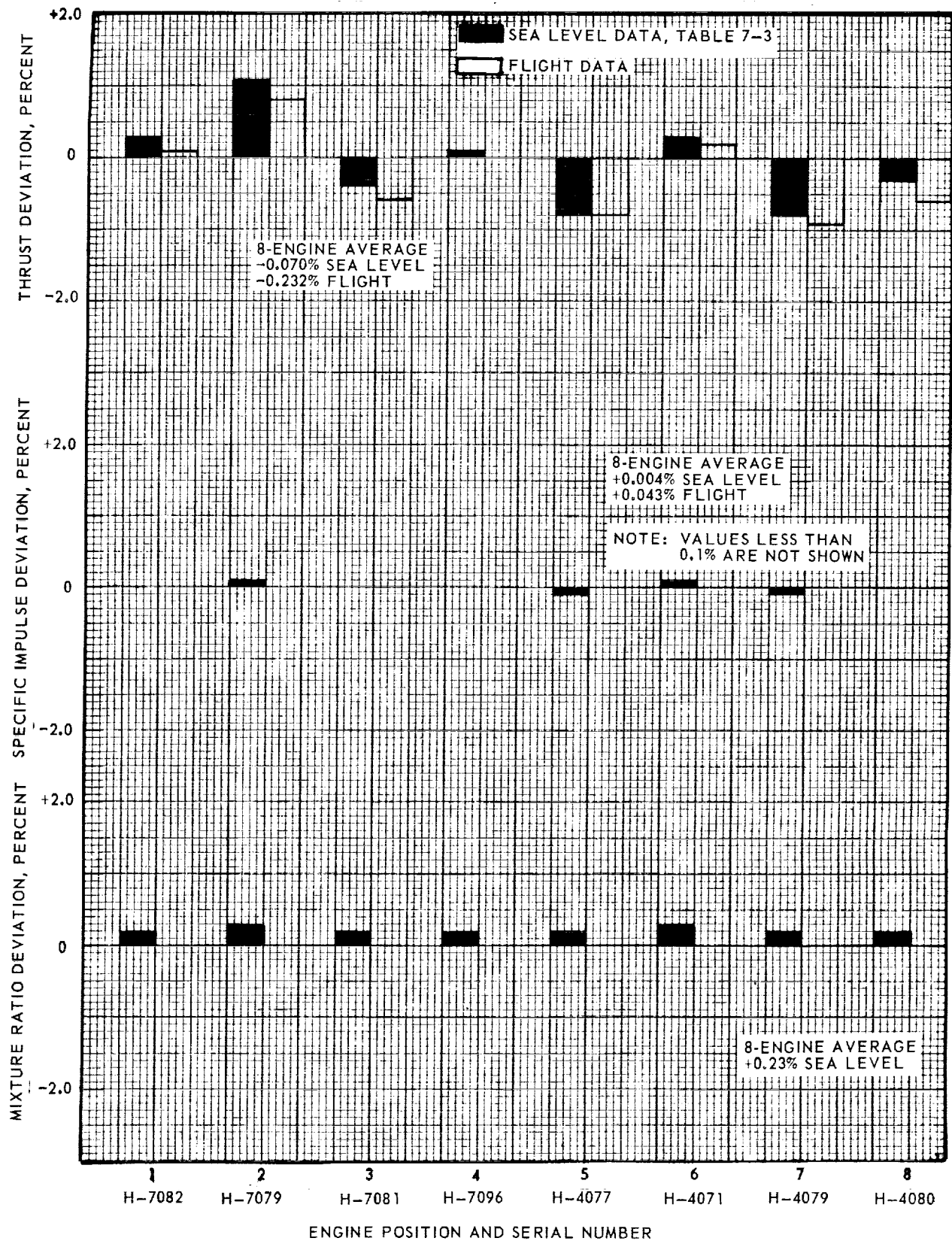


Figure 7-9. Thrust, Specific Impulse and Mixture Ratio Deviations
(Percent Deviation from Predicted)

7.3.3 Stage Static Test, Engine Performance Summary

As a result of two engine replacements and required turbine reworks, the flight configuration of the S-IB-8 propulsion system was different from the stage static test configuration. After completion of static testing, engines H-7083, H-7081, H-7085 and H-4077 (positions 2 through 5) were removed and reworked; the first stage turbine wheels were replaced and penalty acceptance tests performed prior to reinstallation on the stage. During subsequent storage, the engines in positions 2 and 4 were replaced with engines H-7079 and H-7096, respectively. Engine replacements were required because the LOX seal cavities were contaminated during storage.

Changes to the S-IB-8 propulsion system configuration post-static test were similar to changes for the S-IB-7 stage, on which three engines were replaced and one turbine reworked.

Comparisons of S-IB-8 data, Rocketdyne acceptance, stage static test and flight, are presented in figures 7-10 and 7-11. Data are shown separately for the stage static test and flight propulsion system configurations.

Information that impacts evaluation of the S-IB-8 propulsion system performance is presented in references A through U. Major revisions of engine data (acceptance and stage static test) were required as a result of fuel inlet temperature studies conducted by Rocketdyne (reference F) and the subsequent revision of H-1 engine influence coefficients (reference G). Data presented herein are from the following revised sources and supersede the original stage data published in references D and E:

<u>Test Classification</u>	<u>Test Site</u>	<u>Data Source</u>
1. H-1 Engine Acceptance	Rocketdyne, Neosho	Reference H
2. S-IB Stage Static Test	CCSD/MSFC	References I and N

Data for the long duration static test (SA-41) were evaluated by application of a reconstruction technique similar to that performed for flight analysis. The results of this analysis are presented in reference N. Propellant flowrate estimates were evaluated using information from discrete liquid level sensors, three sensors in each of tanks OC, O1, O3, F1 and F3. Estimates of engine specific impulse based upon these data are included in figure 7-11.

A comparison of S-IB stage static test and flight thrust histories relative to the Rocketdyne acceptance data is presented in figure 7-12. Flight predictions for the stages incorporating H-1 engines rated at a sea level thrust of 205K-lb (S-IB-6, S-IB-7), were made with a thrust multiplier of +0.59 percent (1.0059)*. Bias magnitudes in flight thrust for these stages are not comparable to the uniform bias observed for 5 stages incorporating 200K-lb rated H-1 engines. As shown in figure 7-12, the thrust bias observed for stage static test is representative of the flight bias.

*Two engines on S-IB-6 were predicted with no bias.

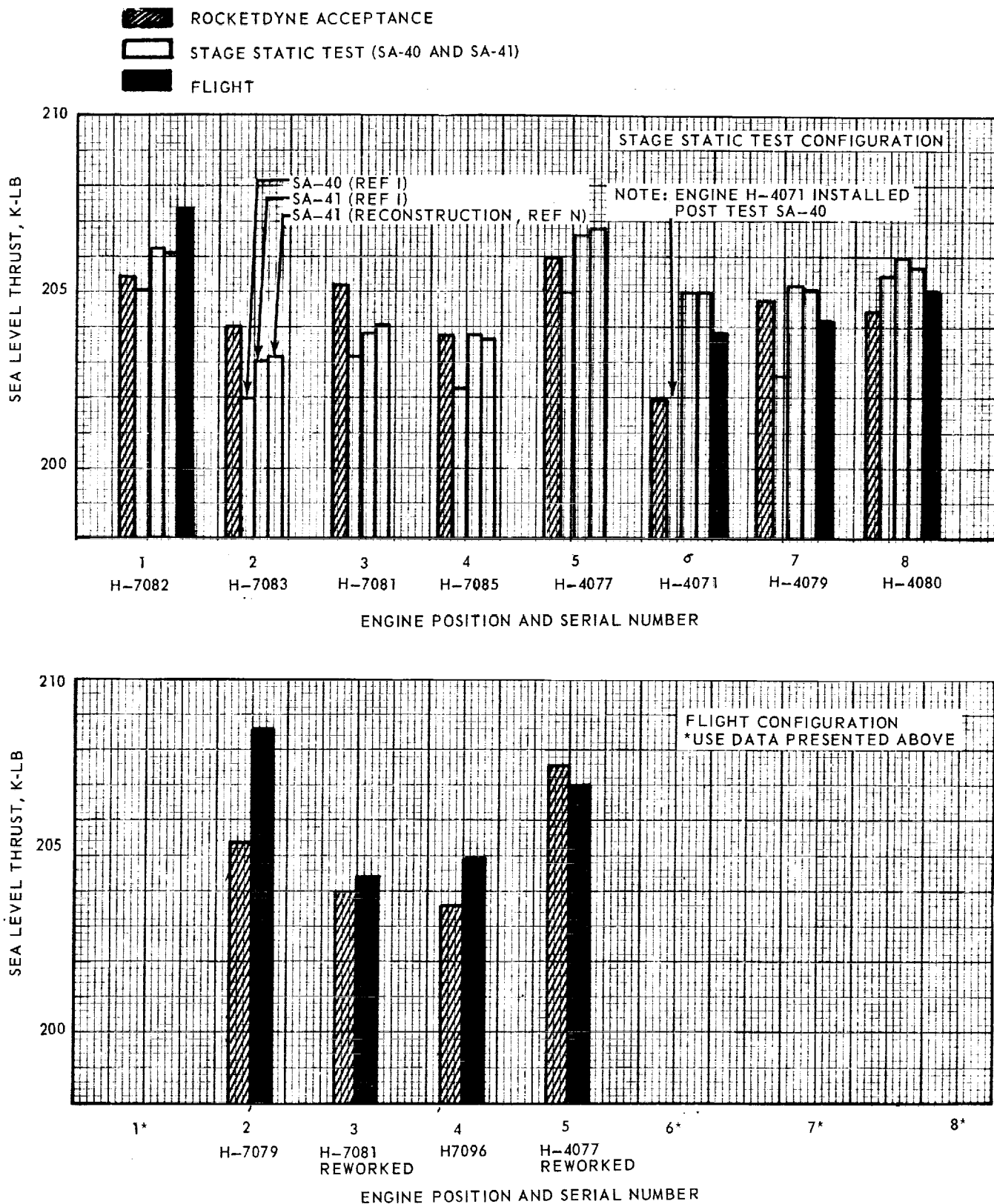


Figure 7-10. Sea Level Thrust Comparison by Engine Position

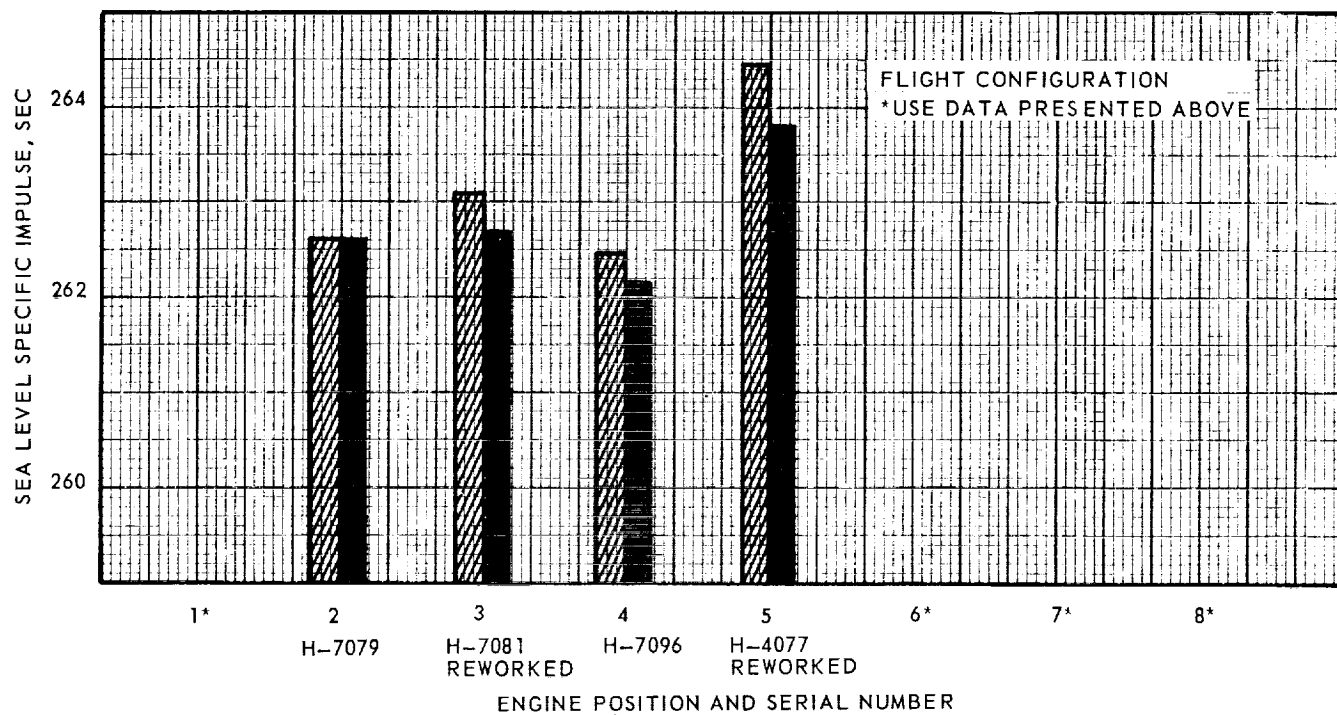
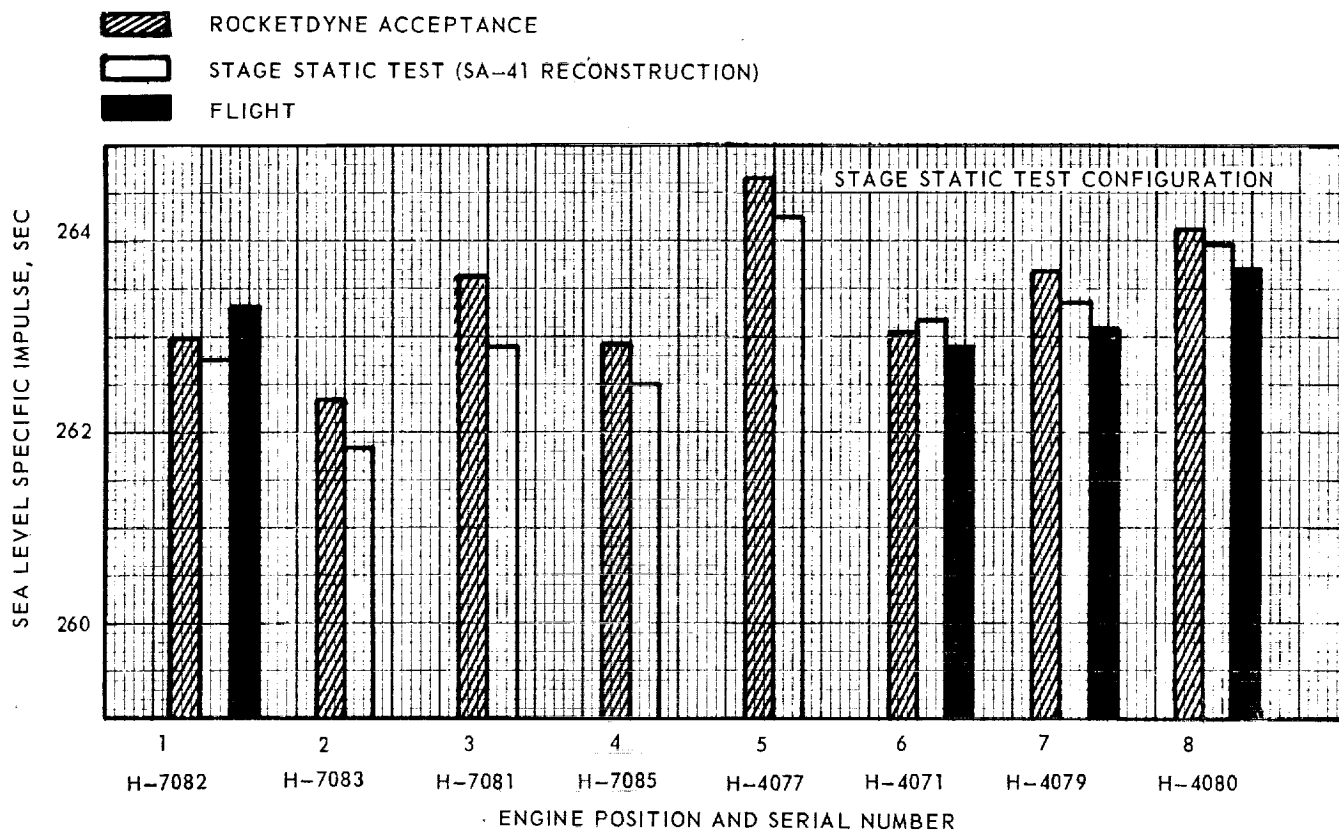


Figure 7-11. Sea Level Specific Impulse Comparison by Engine Position

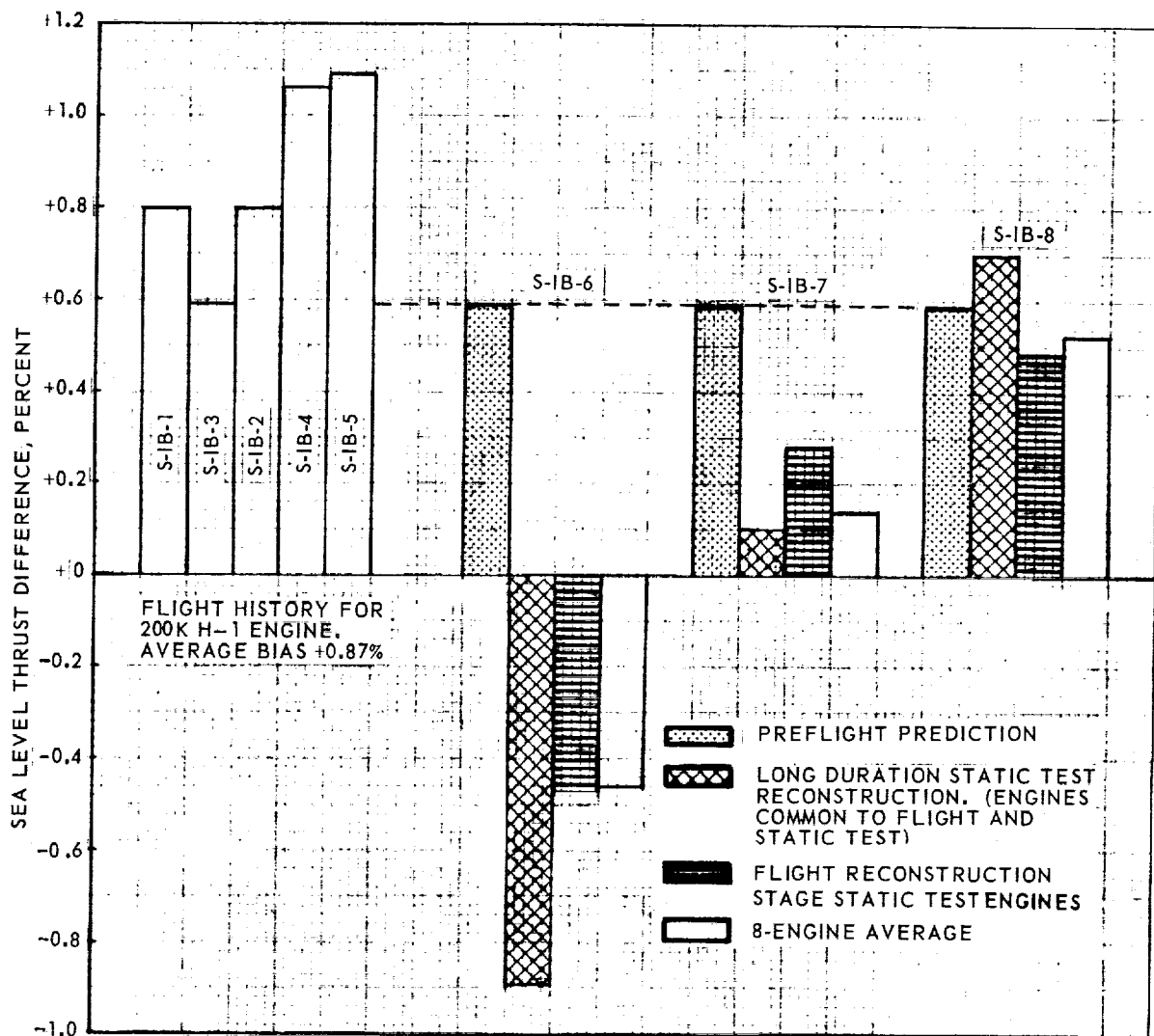


Figure 7-12. Δ Thrust History of S-IB Stages (Percent Deviation from Rocketdyne Acceptance)

7.3.4 LOX Seal Drainline Temperature Analysis

LOX seal drainline temperatures were measured with a 3-element thermocouple installed in the primary line of each engine. The secondary drainlines were not instrumented. Temperature measurements from the 3-element thermocouples are designated C540-1 through -8, C541-1 through -8 and C542-1 through -8. Representative data for each engine position are shown as a function of range time in figure 7-13.

Drainline temperatures were monitored automatically during the prelaunch countdown. Automatic cutoff occurs if the temperature for any engine is colder than -250°F (-156.6°C) based on a 2 of 3 voting logic for the 3-element thermocouple. Prior to ignition sequence, LOX drainline temperatures were in the range -141°F to -161°F (-96°C to -107°C), where values are the average of three individual measurements from the 3-element thermocouple. During the interval from ignition sequence until liftoff, the largest temperature decay was observed for engine position 1 (H-7082) with the minimum temperature -158°F (-106°C) observed approximately one second after liftoff. Relative to the pre-ignition temperature, the decrease was 13°F (7°C). No significance was assigned this event because any minimum temperature greater than -250°F (-156.6°C) is acceptable. LOX seal drainline temperature changes of approximately 25°F magnitudes were observed for engine position 2 on S-IB-5, engine position 5 on S-IB-6, and engine position 1 on S-IB-7.

7.4 S-IB SHUTDOWN TRANSIENT PERFORMANCE

The cutoff sequence of the S-IB-8 stage began at 134.84 seconds (LVDC), with the actuation of the low-level sensor in LOX tank O2. IECO was initiated 2.98 seconds later by the LVDC at 137.82 seconds. Thrust decay on each inboard engine was normal. The total IECO impulse was 251,770 lb-sec. Inboard engine total thrust decay is shown in figure 7-14.

LOX starvation occurred in the four outboard engines. Outboard engine total thrust decay is shown in figure 7-15. The total OECO impulse was 181,550 lb-sec. Each engine has three thrust OK pressure switches, and as engine performance decays during LOX starvation, the first outboard engine to lose thrust OK signal from two-out-of-three switches, will simultaneously cut off all outboard engines. Engine 1 initiated OECO which occurred at 141.29 seconds range time. Table 7-4 shows the time of thrust OK signal dropout for each switch on each outboard engine as indicated by the tabular printout from the Remote Digital Submultiplexer.

Table 7-4. Outboard Engine Thrust OK Pressure Switch Times
at OECO*

THRUST OK PRESSURE SWITCH	ENGINE 1	ENGINE 2	ENGINE 3	ENGINE 4
TOPS 1	141.3165	141.3998	141.3998	141.3998
TOPS 2	141.3165	141.3998	141.3915	141.3915
TOPS 3	141.3498	141.3498	141.3498	141.3498

*Range Time (+0, -0.083 sec)

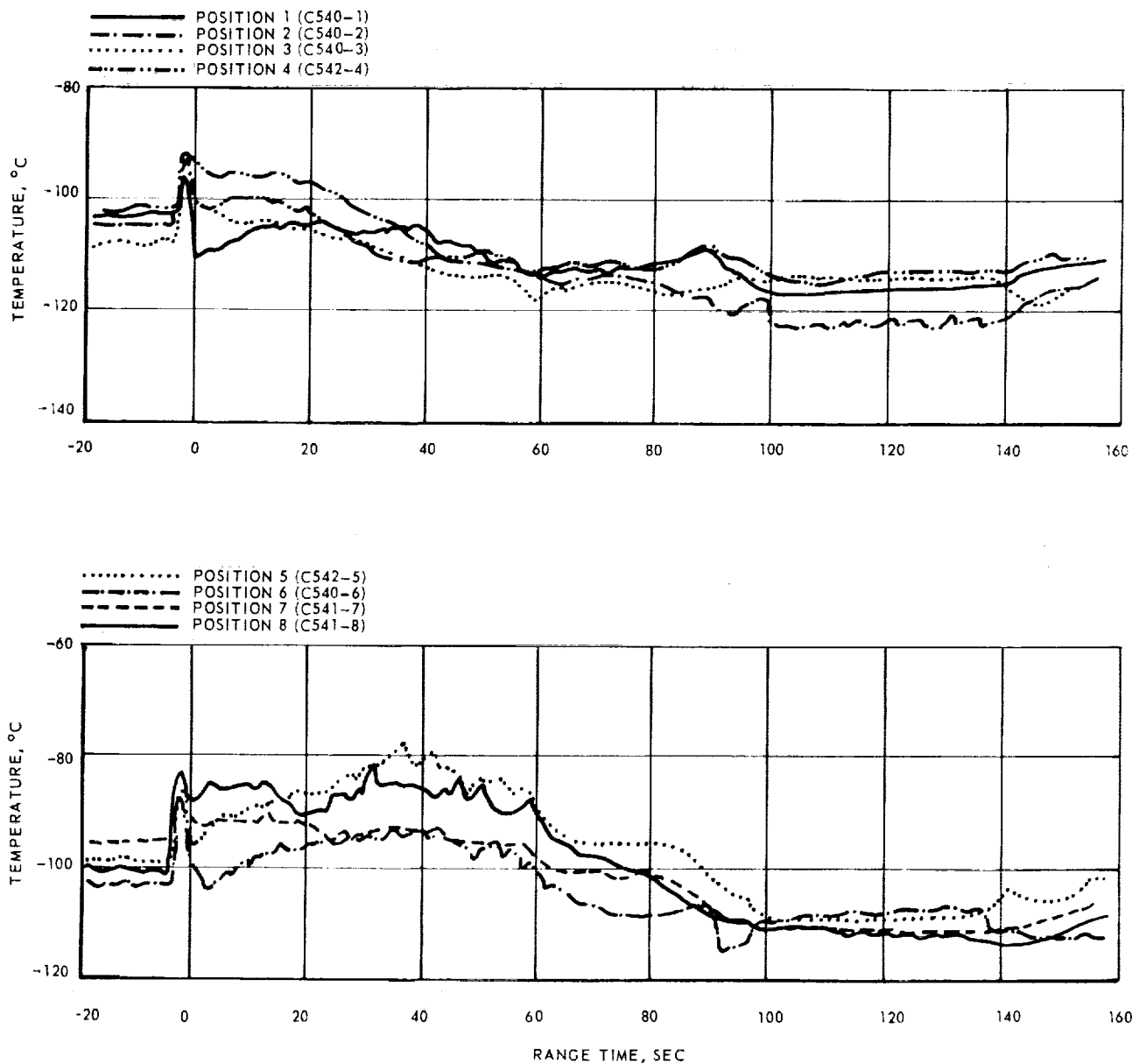


Figure 7-13. LOX Seal Drainline Temperatures

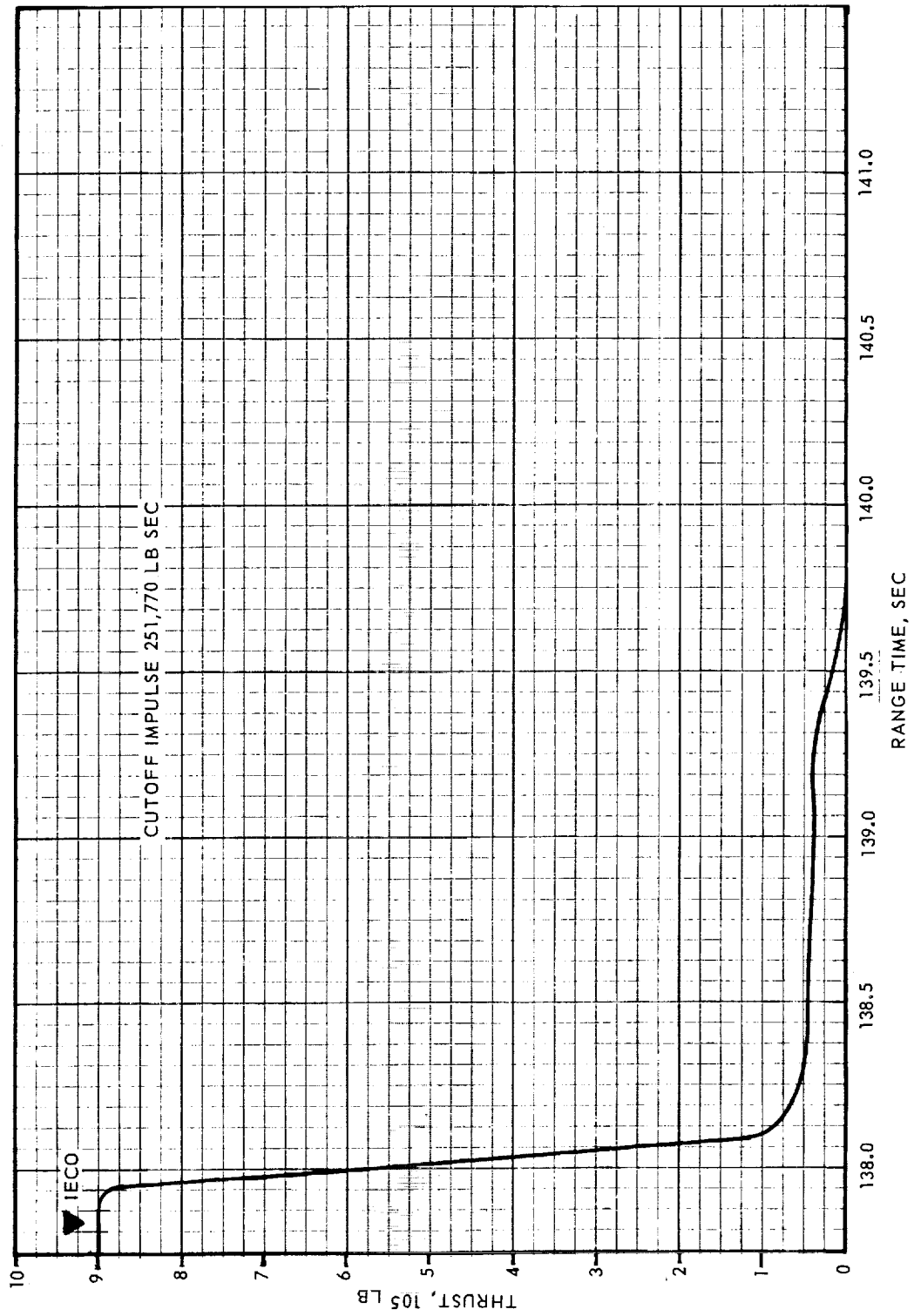


Figure 7-14. S-IB Stage Inboard Engine Total Thrust Decay

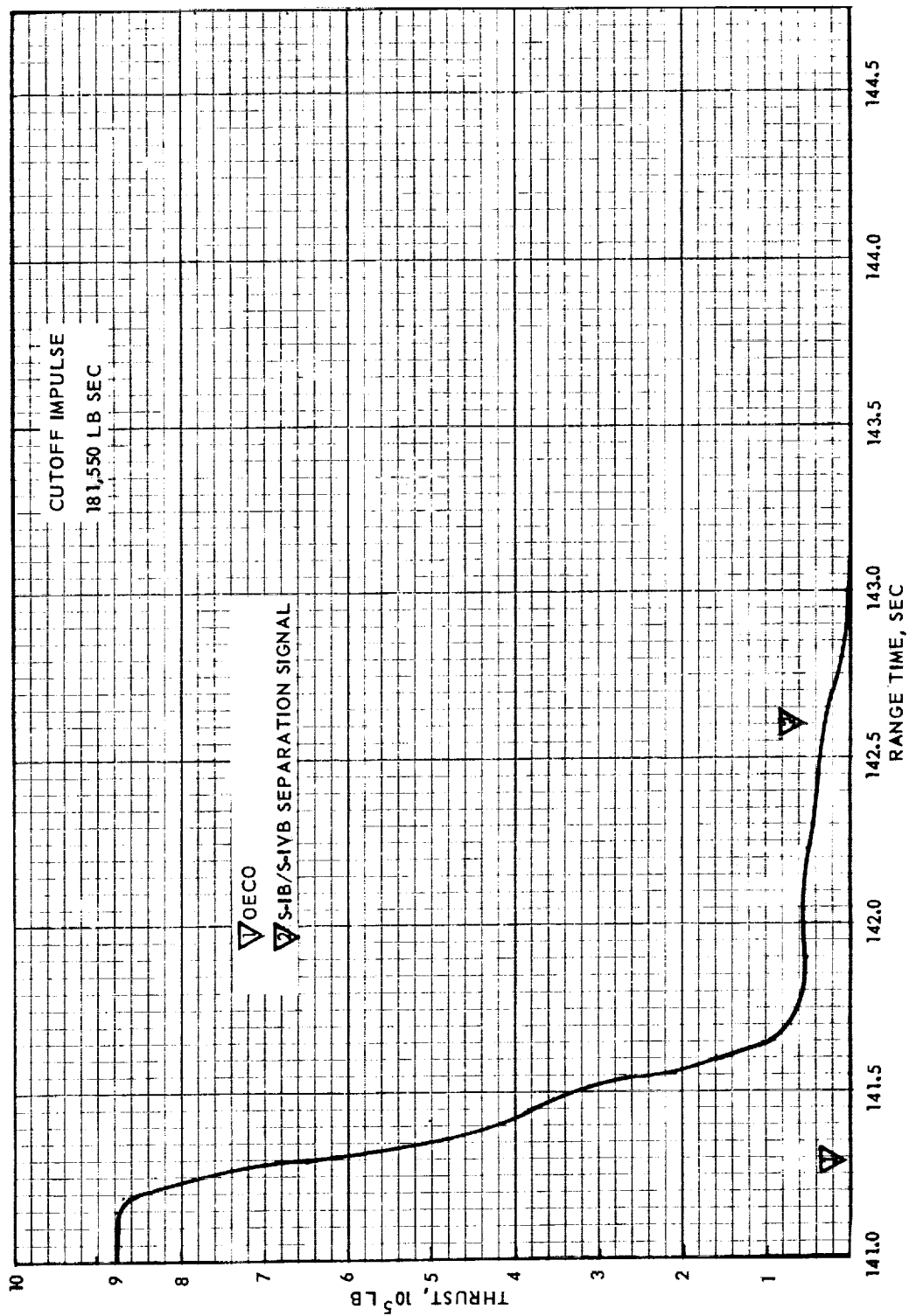


Figure 7-15. S-IB Stage Outboard Engine Total Thrust Decay

7.5 S-IB STAGE PROPELLANT MANAGEMENT

Propellant usage is the ratio of propellant consumed to propellant loaded, and is an indication of the propulsion system performance and the capability of the propellant loading system to load the proper propellant weights. The predicted and actual (reconstructed) percentages of loaded propellants utilized during the flight are shown in table 7-5.

Table 7-5. Propellant Usage

PROPELLANT	PREDICTED (%)	ACTUAL (%)
Total	99.20	99.13
Fuel	98.34	98.02
LOX	99.58	99.62

The planned mode of OECO was by LOX starvation. The LOX and fuel level cutoff sensor heights and flight sequence settings were determined for a 3.00-second time interval between cutoff sensor actuation and IECO. The planned time interval between IECO and OECO was 3.00-seconds. OECO was to be initiated by the deactuation of two of the three thrust OK pressure switches on any outboard engine as a result of LOX starvation. It was assumed that approximately 271 gallons of LOX in the outboard suction lines were unusable. The backup timer (flight sequencer) was set to initiate OECO, 13.00 seconds after level sensor actuation.

To prevent fuel starvation, fuel depletion cutoff sensors were located in the F2 and F4 container sumps. The center LOX tank sump orifice was 19.0 ± 0.005 inches in diameter, and a liquid level height differential of approximately 3.0 inches between the center and outboard LOX tanks was predicted at IECO (center tank level higher).

The fuel bias for S-IB-8 was 1550 pounds. This fuel weight, included in the predicted residual, was available for consumption to minimize propellant residual due to off-nominal conditions and is not expected to be used during a nominal flight.

Data used in evaluating the S-IB stage propellant usage consisted of two discrete probe racks of three probes each in tanks OC, O1, O3, F1 and F3; cutoff level sensors in tanks O2, O4, F2 and F4; and fuel depletion sensors in the F2 and F4 sumps.

The cutoff sequence in S-IB-8 was initiated by a signal from the cutoff level sensor in tank O2 at 134.84 seconds (LVDC). The IECO signal was received 2.98 seconds later at 137.82 seconds. OECO was initiated 3.47 seconds after IECO at 141.29 seconds by engine number 1 thrust OK pressure switch deactuation. Fuel depletion probes were not actuated prior to retrorocket ignition.

Based on discrete probe data and reconstruction analysis, liquid levels in the fuel tanks were nearly equal and approximately 24.7 inches above theoretical tank bottom at IECO. This level represents a mass of 11,619 pounds of fuel onboard. At that time 11,121

pounds of LOX remained onboard. Corresponding liquid height in the center tank was approximately 14.7 inches and average height in the outboard tanks was approximately 10.3 inches above theoretical tank bottom.

At OECO the fuel mass onboard was 6,879 pounds. The fuel height at this time was 12.2 inches above tank bottom or 23.3 inches above the fuel depletion sensor. This level corresponds to 398.4 gallons (2,692 pounds) of fuel above the fuel depletion sensor at OECO.

Propellants remaining above the main valves after outboard engine decay were 2,390 pounds of LOX and 5,550 pounds of fuel. Predicted values for these quantities were 2,642 pounds of LOX and 4,628 pounds of fuel.

Cutoff sensor signal times and setting heights from theoretical tank bottom are shown in table 7-6. Discrete probe signal times and setting heights from theoretical tank bottom are shown in table 7-7.

Table 7-6. Cutoff Sensor Actuation Characteristics

PROBE MEASUREMENT NO.	HEIGHT (INCHES)	ACTUATION TIME (SECONDS)
K15-02	27.5	134.88
K16-04	27.5	135.05
K17-F2	31.4	136.36
K18-F4	31.4	136.44

Total LOX and fuel masses above the main propellant valves beginning at ignition command are shown in figures 7-16 and 7-17. A summary of the propellants remaining at major event times is presented in table 7-8.

Table 7-7. S-IB-8 Propellant Level Discrete Sensor Actuation Times

FUEL DISCRETE NO.	TANK HEIGHT	RANGE TIME, SECONDS	
	INCHES	TANK F1	TANK F3
1	577.0	8.21	10.60
3	498.0	26.62	28.64
15	24.0	137.92	138.05

LOX DISCRETE NO.	TANK HEIGHT	RANGE TIME, SECONDS		
	INCHES	TANK OC	TANK O1	TANK O3
1	603.6	10.33	7.35	7.55
3	520.9	29.13	25.24	25.48
15	24.9	136.41	135.44	135.45

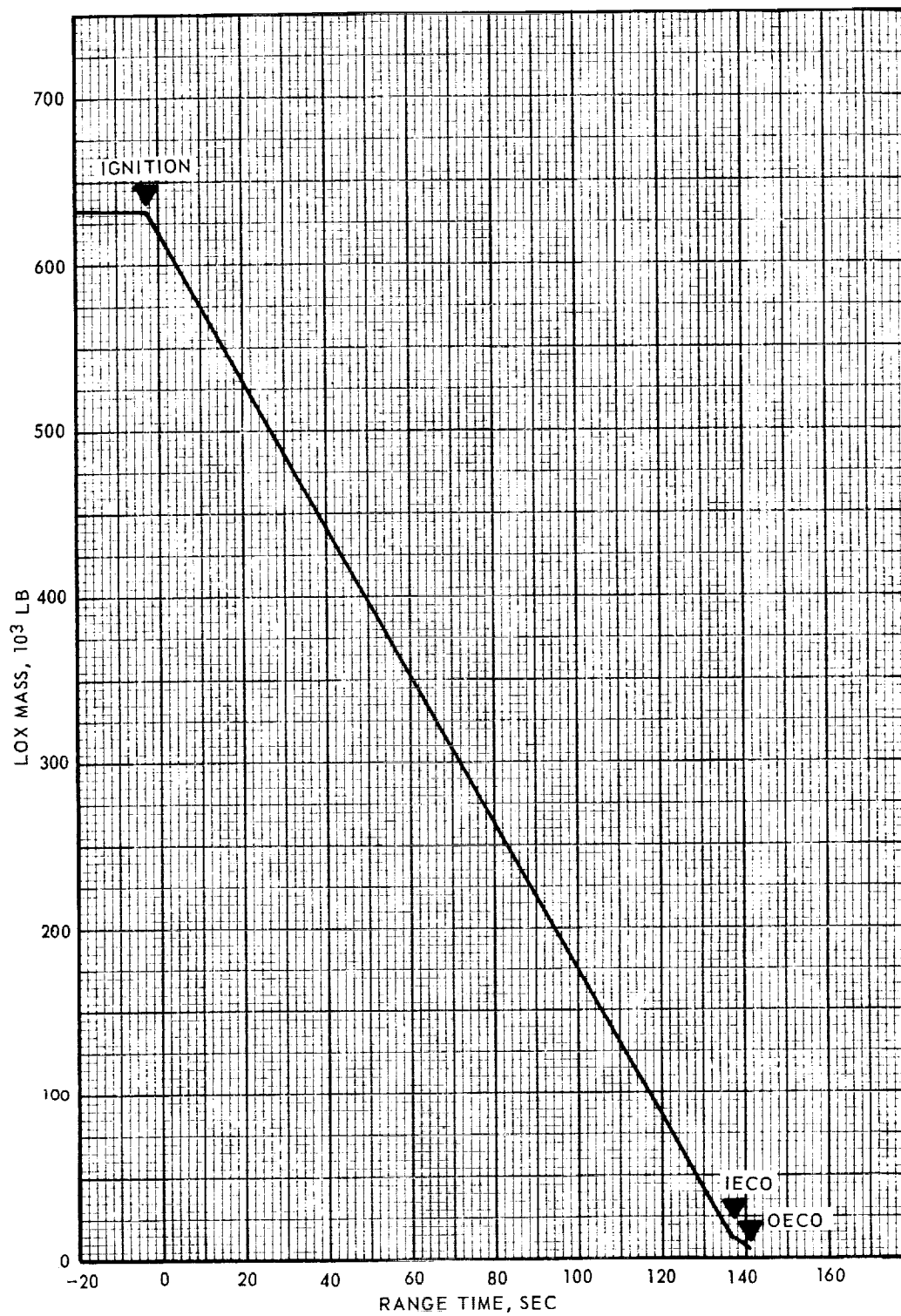


Figure 7-16. S-IB Stage LOX Mass Above Main LOX Valve

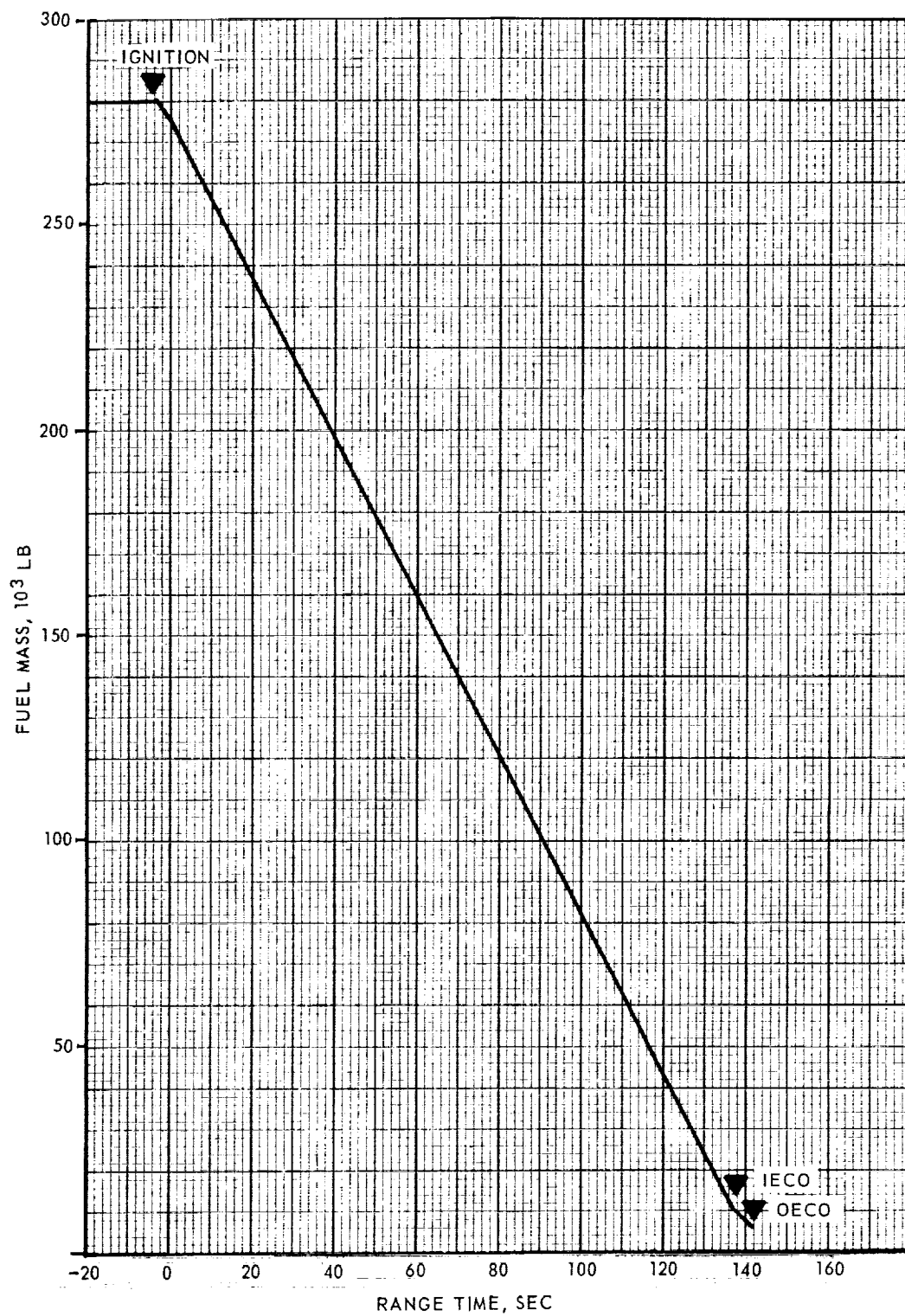


Figure 7-17. S-IB Stage Fuel Mass Above Main Fuel Valve

Table 7-8. S-IB Stage Propellant Mass History

EVENT	PREDICTED (LB)			RECONSTRUCTED (LB)		
	FUEL	LOX	TOTAL	FUEL	LOX	TOTAL
Ignition Command	279,596	632,016	911,612	280,541	632,416	912,957
IU Umbilical Disconnect	275,625	620,632	896,257	276,709	619,910	896,619
IECO	10,248	10,438	20,686	11,619	11,121	22,740
OECO	5,990	3,287	9,277	6,879	2,925	9,804
Separation	4,872	2,720	7,592	5,843	2,478	8,321
Zero Thrust	4,628	2,642	7,270	5,550	2,390	7,940

7.6 S-IB PRESSURIZATION SYSTEM

7.6.1 Fuel Pressurization System

During the flight of S-IB-8 no anomalies were observed in the performance of the helium blowdown system used to pressurize the fuel tanks. With the exception of a change in the vent valve relief pressure setting and minor changes in the vent valve sensing lines, the pressurization system was the same as on S-IB-7 and included the two 19.28 ft³ high-pressure helium spheres, lightweight tanks and fuel vent valves. Because of the accidental damage to the upper bulkheads on fuel tanks F3 and F4 (see sections 5.3.1 and 10.3.1 for discussion), the vent valves' relief pressure was lowered from the normal 21.0/21.5 psig to 19.0/19.1 psig to maintain adequate structural margin. In addition, expansion loops were added to the vent valve sensing lines on the upper bulkheads to relieve the strain on the sensing system caused by the increased bulkhead deflection. To reduce the peak pressure during tank pressurization, a pressure switch was selected which showed the lowest actuation pressure during pressure switch calibration tests. The switch installed on S-IB-8 actuated at 31.5 psia and deactuated at 30.3 psia during calibration.

Helium flow into the fuel tank ullage is metered by a sonic nozzle between the high-pressure spheres and tanks. The orifice diameter of the sonic nozzle was 0.220/0.221 inch. The pressurization system is shown schematically in figure 7-18.

Sufficient pressure must be provided by this system to meet fuel NPSH requirements at the end of flight and maintain structural integrity throughout flight. Both requirements were met. The pressures that define the operating band are 10 psig minimum for structural integrity and the minimum vent valve relief pressure is 19.0 psig. Fuel ullage pressure remained within these limits, as shown in figure 7-19. The data for figure 7-19 were generated from the absolute fuel tank ullage pressure, measurement D2-F3, and ambient pressure as a function of altitude from NASA TMX-53139, A Reference Atmosphere for Patrick AFB, Florida, Annual (1963 Revision), September 23, 1964. Because the fuel vent valves sense the fuel tank forward skirt internal pressure rather than true ambient pressure, a correction was made to the ullage gage pressure. These corrections were taken from CCSD Inter-Company Correspondence, File Code 2780/3/10/447, SL-4 Fuel Tank Forward Skirt Internal Pressure, W. B. Meinders to E. A. Rawls, October 30, 1973. This document indicates that ambient pressure as sensed by the fuel vent valve can be as much as 0.7 psi lower than true ambient thereby making the gage pressure 0.7 psi higher. Appropriate corrections were made to the ullage gage pressure from 20 seconds to 110 seconds and are reflected in figure 7-19.

A comparison of measured absolute ullage pressure and predicted ullage pressure is presented in figure 7-20. Measured ullage pressure compared favorably with predicted ullage pressure during the flight and at no time exceeded a difference of 1.0 psia from the predicted value.

The Digital Events Evaluator showed that fuel vent valves 1 and 2 closed at the beginning of the pressurization sequence and remained closed until liftoff. No vent

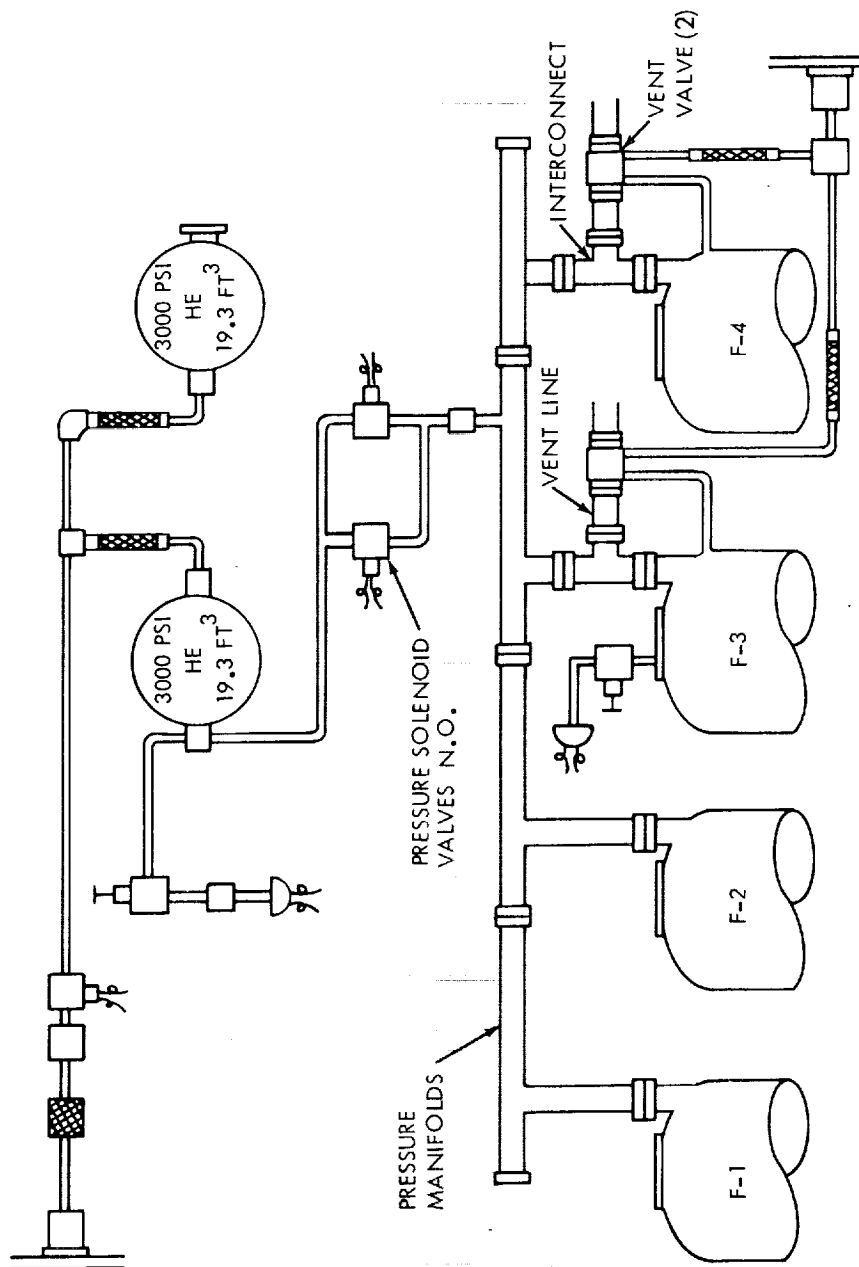


Figure 7-18. S-IB Stage Fuel Pressurization System

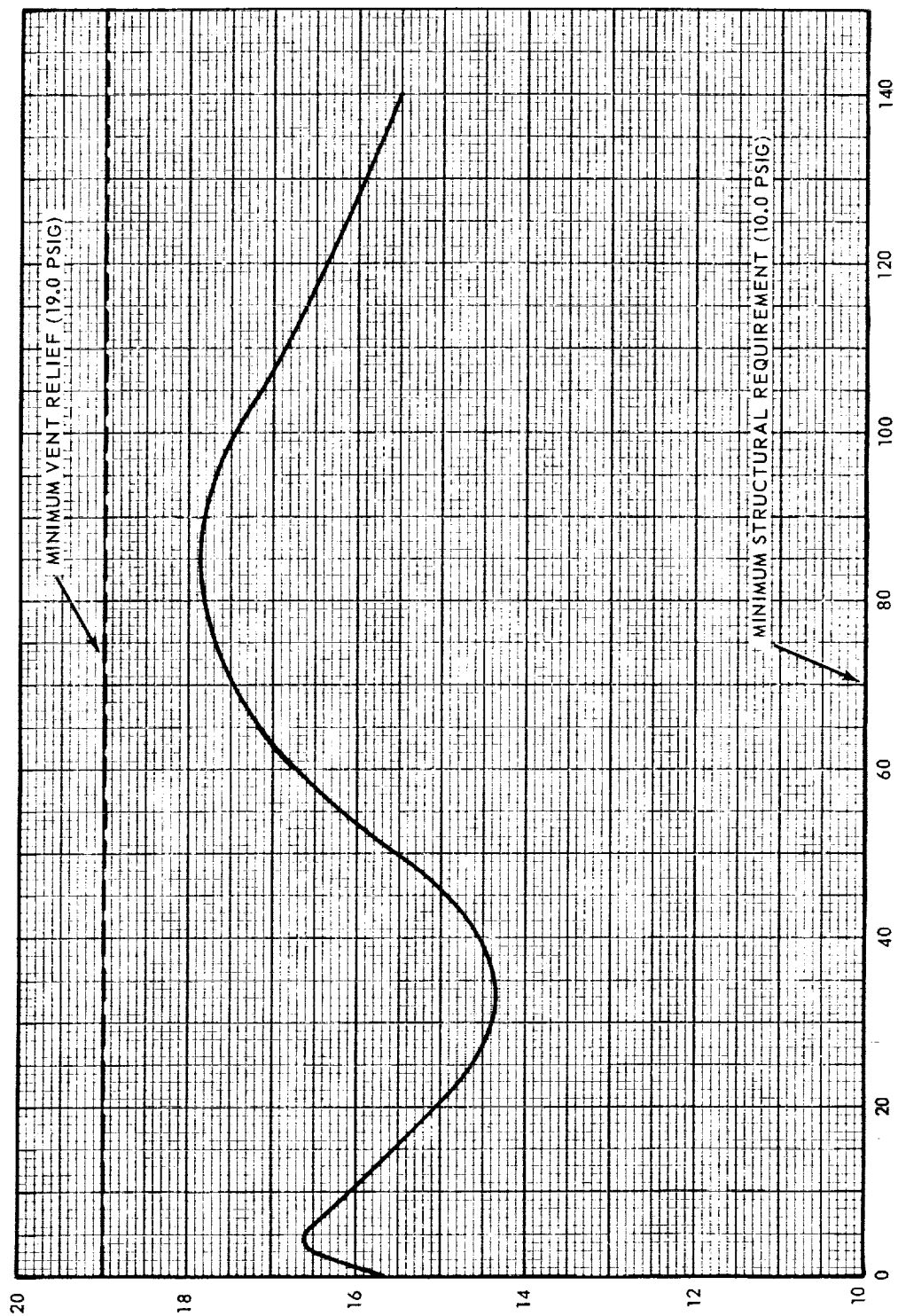


Figure 7-19. S-IB Stage Fuel Tank Ullage Pressure (Gage)

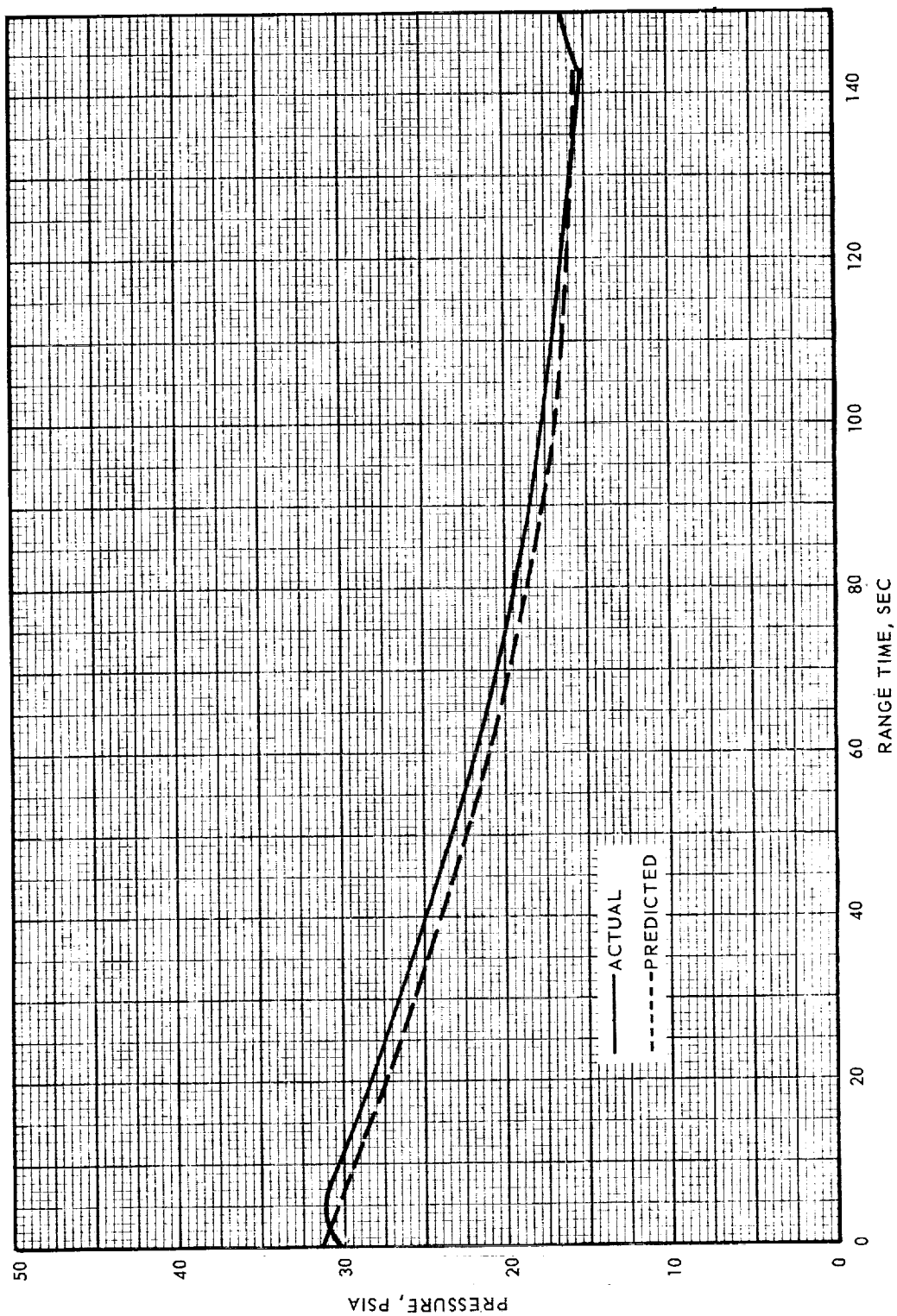


Figure 7-20. S-IB Stage Fuel Tank Ullage Pressure (Absolute)

valve position instrumentation is available during flight, but inspection of the fuel tank ullage pressure history reveals no reason to suspect that the vents opened during flight.

Tank pressurization began at T-159.86 seconds. The 1527-gallon (3.61 percent) ullage volume was pressurized to 32.2 psia in 2.43 seconds. The pressurization valves opened again at T-135.73 seconds for a period of 0.23 second to repressurize the fuel tank ullage after pressure decay due to system cooling. This is about 15 seconds earlier than in previous flights and results from the increased ullage pressure decay rate due to fuel vent and relief valve pilot valve leakage, and from the tighter operating band on the pressure switch.

S-IB-8 was the first stage to have noticeable pilot valve leakage because the pilot valve assembly is normally adjusted to provide relief action at 21.0/21.5 psig and poppet reseating at 19.0 psig. The valves used on S-IB-8 differed from the normally installed valves in that the relief setting was reduced to 19.0/19.1 psig to accommodate a lowered proof pressure for the tanks. The effect of the reduction of relief pressure was also to reduce reseat pressure to approximately 17.0 psig. Pilot valve leakage was then approximately 4000 scim per valve at a tank ullage pressure of 18.0 psig, whereas there was zero leakage at 18.0 psig for valves set to relieve at 21.0/21.5 psig.

The Digital Events Evaluator shows that the pressurizing valves opened three times to repressurize the fuel tanks. Two of these repressurization cycles occurred during the engine start sequence. Fuel tank ullage pressure from T-170 seconds to liftoff is shown in figure 7-21.

Telemetry data show helium sphere pressure to be 2903 psia at liftoff which is slightly higher than it was on S-IB-7. The sphere pressure is shown in figure 7-22.

Because the fuel temperature and ullage pressure were different in each of the tanks, the liquid levels were different. The maximum difference between tanks F1 and F3, determined from recorded discrete probe times, was 10.2 inches at T + 8.2 seconds. The levels converged to a difference of 0.6 inch at approximately T + 138.0 seconds.

7.6.2 LOX Pressurization System

The LOX tank pressurization system performed satisfactorily during the S-IB-8 flight as evidenced by measurements D3-OC, K72-9, C234-9 and D119-9. A schematic of the system is shown in figure 7-23.

Following the LOX bubbling test (OALB) at T-4 hours -8 minutes, the LOX vents were closed on three occasions prior to prepressurization during the elevator operation as a safety procedure against LOX spillage through the vents. The vents were closed at T-4 hours -2 minutes, T-2 hours -40 minutes, and T-55 minutes for durations of 129 seconds, 130 seconds and 150 seconds, respectively. The LOX tank ullage pressure rises during these periods were 3.0 psi, 2.9 psi and 3.3 psi, respectively.

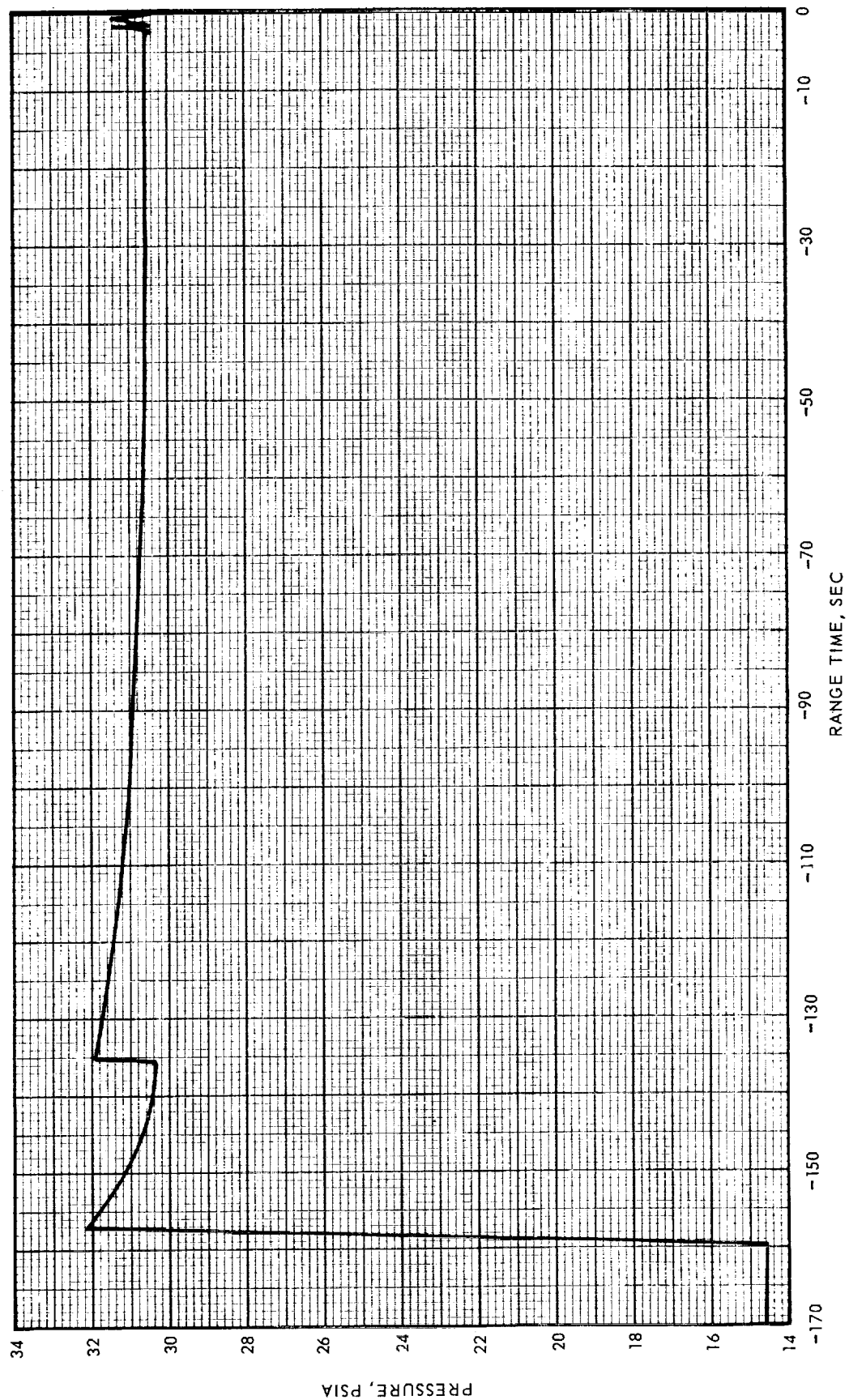


Figure 7-21. S-IB Stage Fuel Tank Ullage Pressure (Prelaunch)

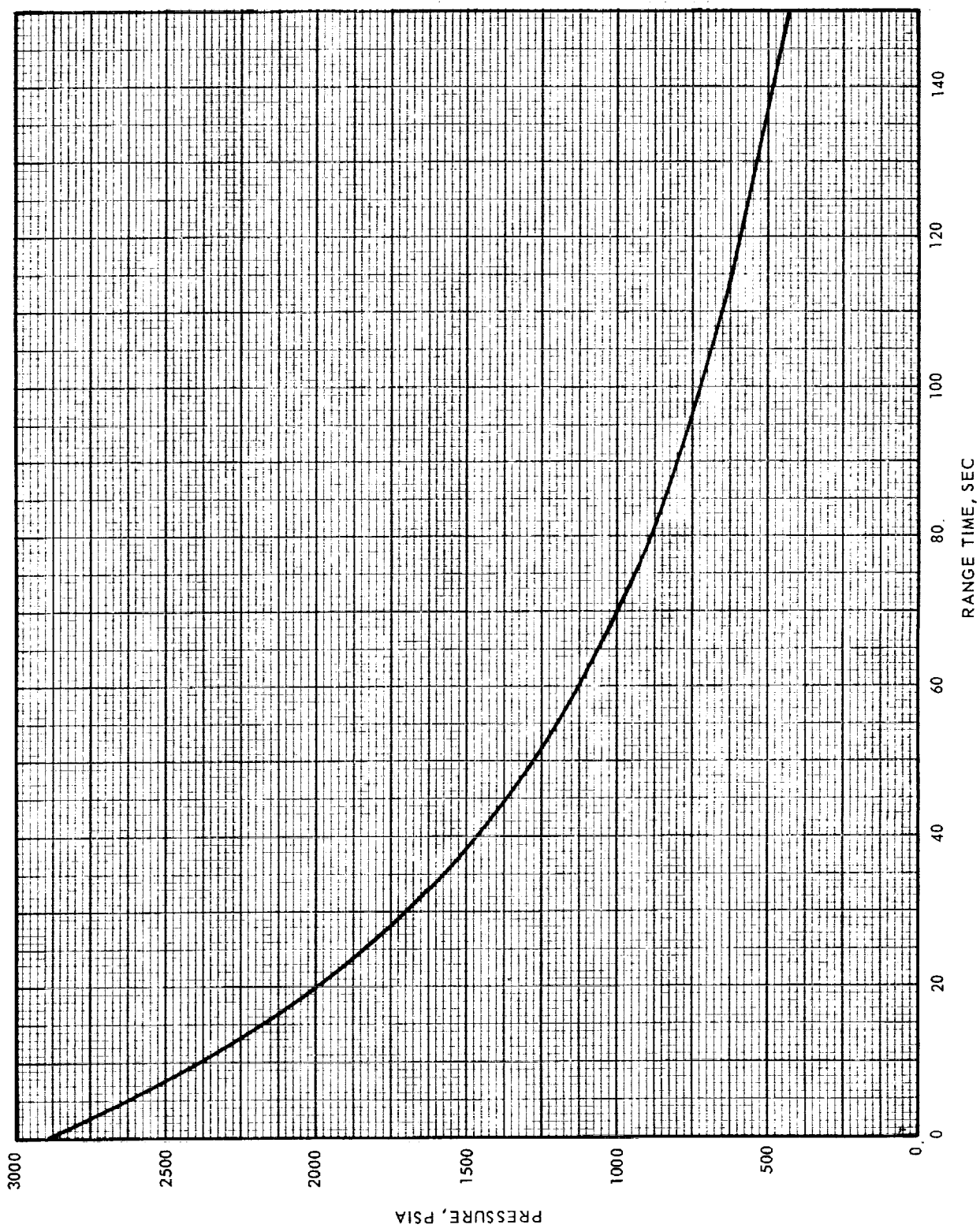


Figure 7-22. S-IB Stage Helium Sphere Pressure

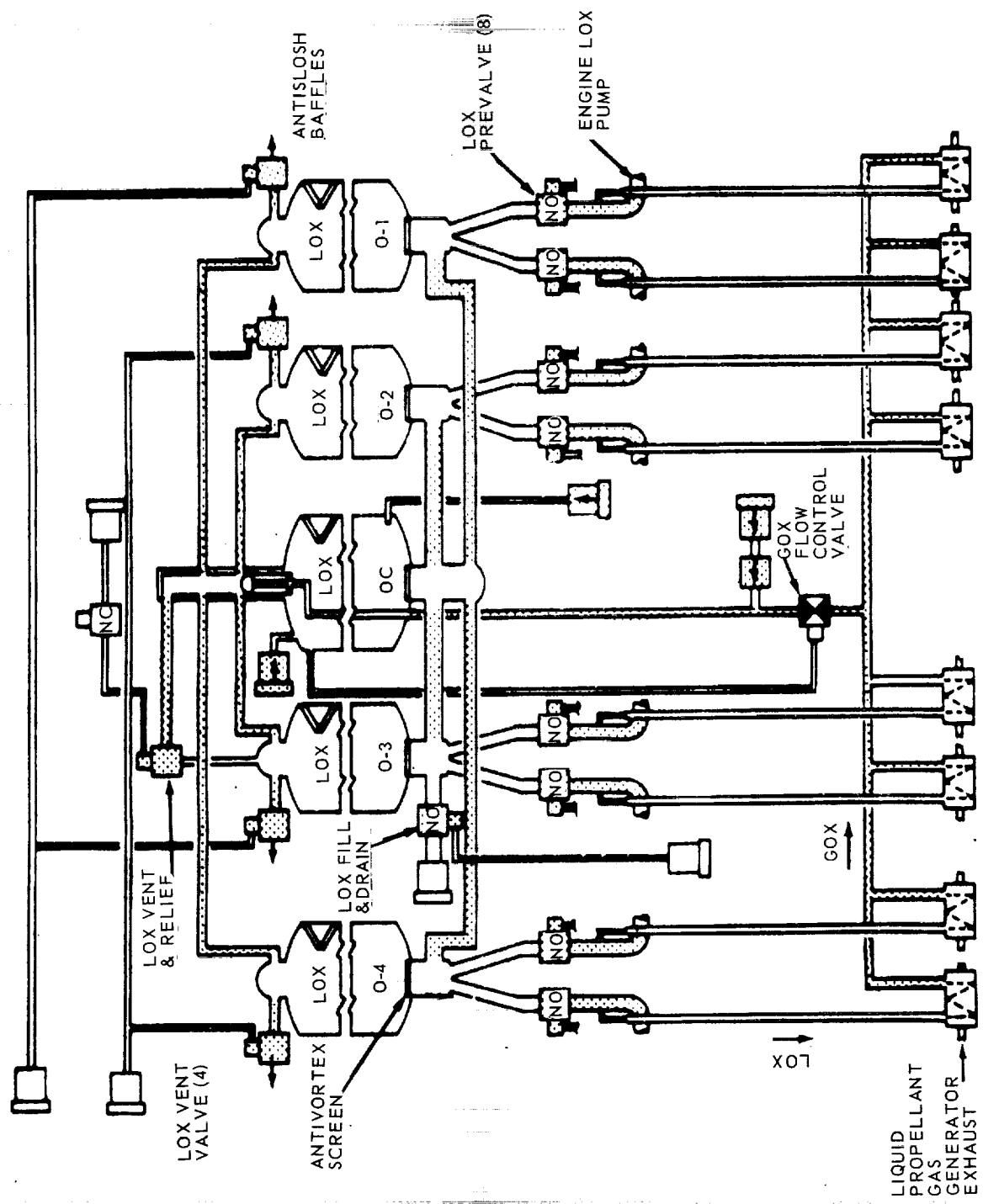


Figure 7-23. S-IB Stage LOX System

A closed-position indication for all vent valves occurred between T-159.797 and T-157.925 seconds, which resulted in the first ullage pressure rise as shown in figure 7-24. The opening of the LOX bubbling valve at T-152.921 seconds resulted in a 2-psi ullage pressure increase followed by a gradual increase for the duration of LOX bubbling as the liquid level increased until the pressurizing valve opened.

Prepressurization began with the helium pressurizing valve opening at T- 102.893 seconds and was accomplished in 55.21 seconds, compared to 73.33 seconds for S-IB-7. The faster pressurizing rate occurred because of increasing the ground pressurizing orifice diameter from 0.100 to 0.114 inch.

With the additional 18 seconds for ullage decay, the pressure switch cycled 6 times prior to ignition, which is 3 more than S-IB-7. The switch actuated at approximately 57.7 psia and deactuated at 56.2 psia, which is within the switch limits. The bypass orifice flow was initiated at T-2.387 seconds, while the pressurizing valve was open during the final cycle. The reconstructed LOX ullage volume prior to vent closure of 994 gallons (1.48 percent) was the same as that on S-IB-7.

The ullage pressure during flight is compared with the predicted pressure and presented in figure 7-25. The initial pressurization level satisfied the minimum requirement of 80 psia at the LOX pump inlet for engine start. The pressurization system is designed to provide a minimum tank pressure at OEEO of 50 ± 2.5 psia.

The minimum pressure of 47.2 psia occurred during the engine start transient and the maximum pressure of 52.7 psia occurred at T+33 seconds. The GOX flow control valve (GFCV) started to close at ignition, and after the normal hesitations during the start transient, reached the fully closed position at T+20 seconds and remained closed until T+50 seconds as shown in figure 7-26.

The GFCV moved off the minimum position at T+50 seconds, which was 22 seconds earlier than S-IB-7. The earlier opening time is attributed to a lower ullage pressure than on S-IB-7, because GFCV opened at an ullage pressure of approximately 52 psia on both flights. The GFCV continued to open gradually for the remainder of the flight to 21 percent open at IEEO, while the ullage pressure decayed to 49.5 psia.

7.7 PROPULSION SYSTEM EVENT TIMES

Event times for the S-IB-8 stage propulsion system are summarized in table 7-9. Data sources for event time measurements are included for reference.

Flight and predicted events are presented in range time, the flight values referenced to range zero of 14:01:23.000 Greenwich Mean Time. Predicted event times presented in table 7-9 are derived from values presented in reference B "Final Launch Vehicle Propulsion System Flight Performance Prediction for SA-208." The referenced values were predicted relative to vehicle first motion and have been adjusted to range time.

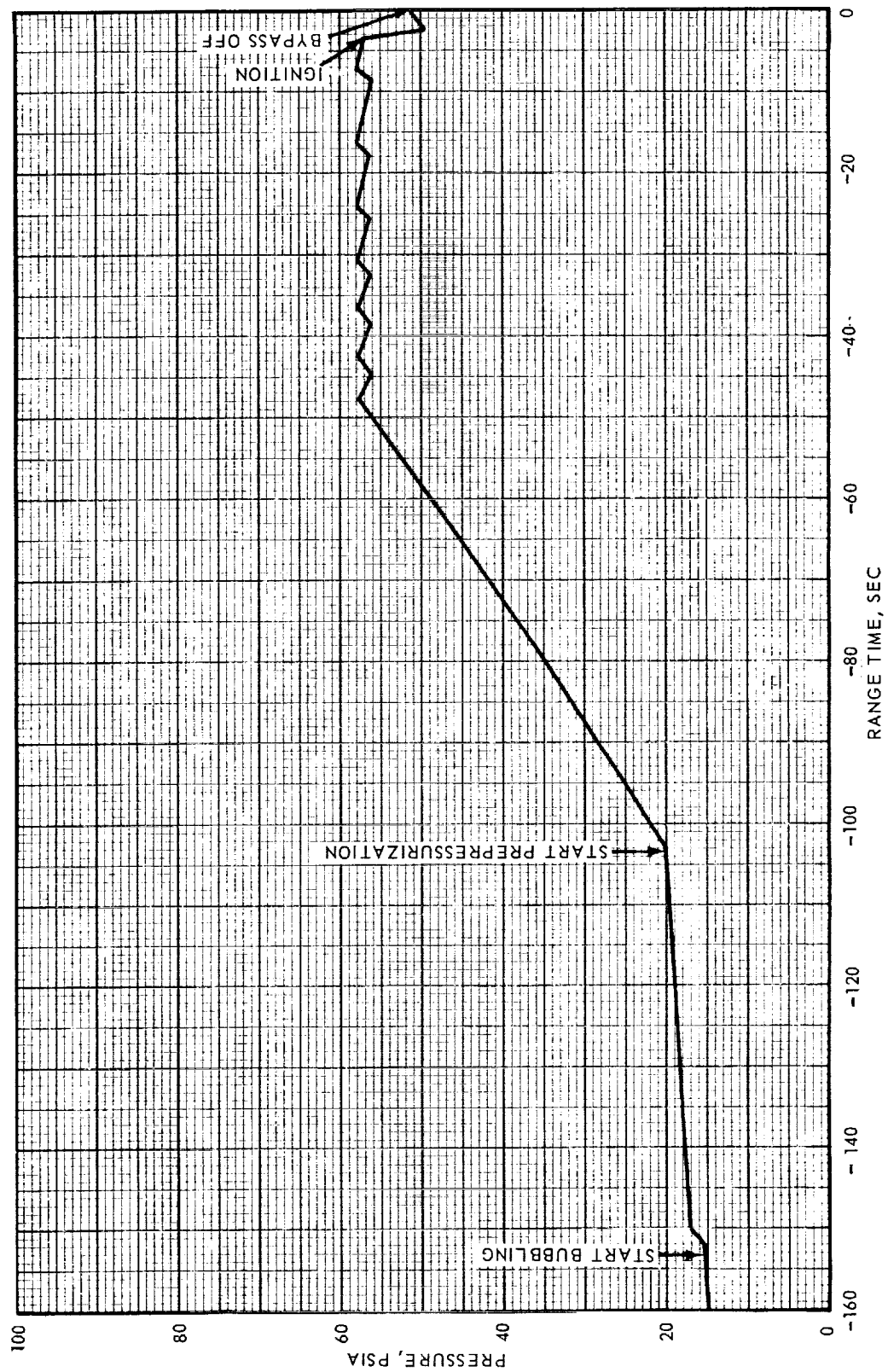


Figure 7-24. S-IB Stage Center LOX Tank Pressure (Prelaunch)

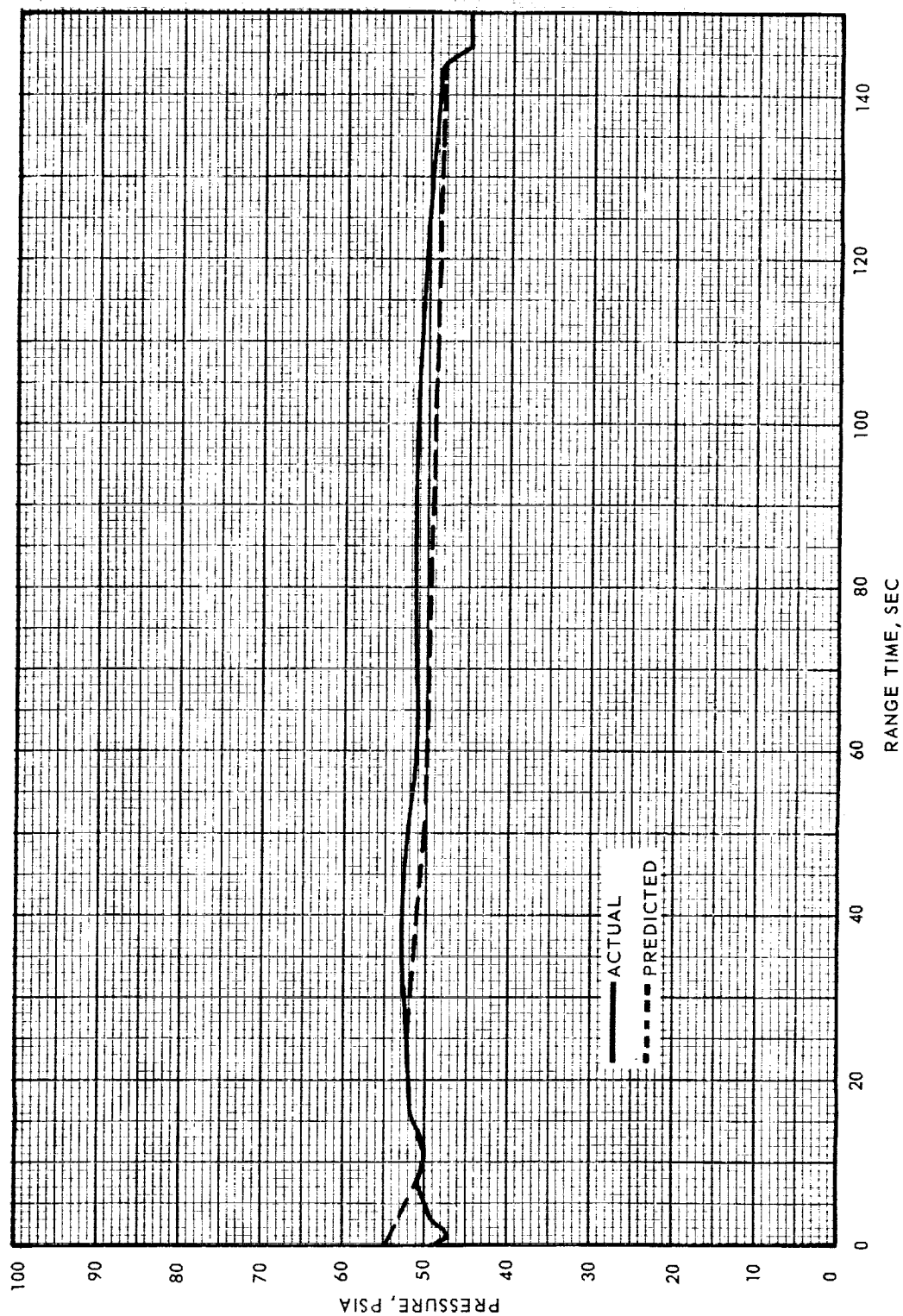


Figure 7-25. S-IB Stage Center LOX Tank Ullage Pressure

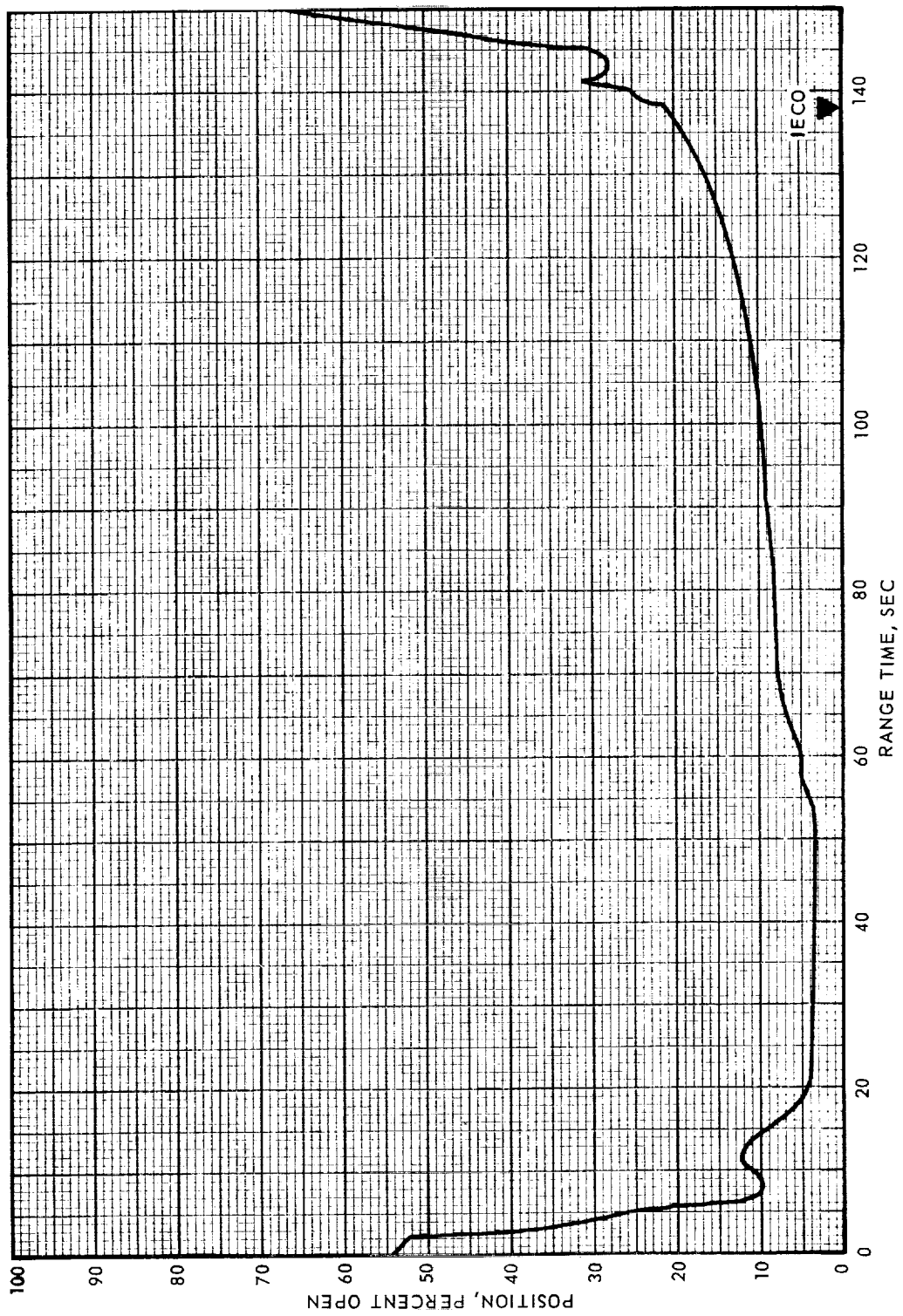


Figure 7-26. S-IB GOX Flow Control Valve Position

Table 7-9. S-IB Stage Propulsion System Event Times

MEASUREMENT OR SOURCE	EVENT	FLIGHT RANGE TIME (SEC)	PREDICTED RANGE TIME (SEC)	DIFFERENCE, FLIGHT MINUS PREDICTED (SEC)
DEE-6*	Time for Ignition Command	-3.065	-	-
DEE-6	Ignition Command	-3.050	-3.030	-0.020 (-.03)
DEE-6	Ignition Sequence No. 1 (Engines 5 and 7)	-2.963	-2.930	-0.033 (-.04)
DEE-6	Ignition Sequence No. 2 (Engines 6 and 8)	-2.864	-2.830	-0.034 (-.04)
DEE-6	Ignition Sequence No. 3 (Engines 2 and 4)	-2.762	-2.730	-0.032 (-.04)
DEE-6	Ignition Sequence No. 4 (Engines 1 and 3)	-2.663	-2.630	-0.033 (-.04)
FEWG**	First Motion	+0.27	+0.27	-
FEWG**	Liftoff (IU Umbilical Disconnect at LVDC)	+0.47	+0.47	0.00
-	Start of T2 (LVDC)	134.84	134.97	-0.13 (-.14)
K17-F2	Tank F2 LSA	136.36	-	-
K18-F4	Tank F4 LSA	136.44	-	-
K15-02	Tank O2 LSA	134.88	134.97	-0.09 (-.10)
K16-04	Tank O4 LSA	135.05	134.97	-
K1-12	IECO	137.82	137.97	-0.15 (-.16)
K3-12	OECO	141.29	140.97	+0.32 (+.31)
	OECO (Back-up Indications)			
K99, K100	OECO (Eng. 1, 2, 3, and 4)	141.29	-	-
K1-12	OECO	141.37	-	-
K1-12	S-IB/S-IVB Separation Signal	142.55	142.27	+0.28 (+.27)
K53-12	S-IB/S-IVB Separation Signal	142.60	-	-
K37-11	Retrorocket Ignition	142.60	142.27	+0.33
VK81-F2	Fuel Depletion Sensor (F2)	143.40	-	-
VK82-F4	Fuel Depletion Sensor (F4)	143.39	-	-

NOTE: Ignition command and ignition sequences 1 through 4 in the predicted column are revised values not presented in the SA-208 flight prediction.

*DEE-6: Digital Event Evaluator

**FEWG: Flight Evaluation Working Group

() Denotes difference established by FEWG predictions with first motion predicted at 0.28 seconds.

The LOX level sensor located in tank O2 initiated time base 2 (T_2) at 134.84(LVDC) while the S-IB stage indication, measurement K15-02, was recorded at 134.88 seconds range time. Indicated actuation times for fuel level sensors (measurements K17-F2 and K18-F4) were 136.36 and 136.44 seconds, respectively. Accounting for maximum sampling rate time delay of 0.083 seconds (12sps), the earliest possible fuel sensor actuation was 136.28 seconds, confirming that T_2 initiation was caused by LOX liquid level.

Inboard engine cutoff (IECO) occurred at 137.82 seconds (measurement K1-12). LOX starvation of the outboard engines produced cutoff (OECO) at 141.29 seconds. Inboard engine cutoff (IECO) was 0.16 second earlier than predicted and outboard engine cutoff (OECO) was 0.31 second later than predicted. Reasons for differences in predicted and actual burn times are discussed in paragraph 7.3.1.

The OECO sequence was as follows: Cutoff was initiated by actuation of Thrust OK Pressure Switches (TOPS) for engine position 1. Analysis of data from the Remote Digital Submultiplexer (RDSM) has shown that 2 of 3 switch voting logic was completed at 141.316 seconds. Indication of Conax valve actuation (measurement K-100) for all outboard engines was recorded at 141.292 seconds and the switch selector OECO signal (K1-12) recorded at 141.37 seconds. The RDSM data (TOPS and Conax actuation) are limited by a 12-sps data sampling rate and a corresponding maximum time delay of 0.083 second. Receipt of Conax actuation signals prior to receipt of TOPS cutoff confirmation is the direct result of scanning Conax signals ahead of TOPS information in the data sampling procedure. Paragraph 7.3 describes shutdown transient performance.

It should be noted that actuation of the fuel depletion sensors occurred after retro-rocket ignition.

Section 8

CONTROL PRESSURE SYSTEM

8.1 SUMMARY

Operation of the S-IB-8 stage control pressure system was satisfactory throughout the prelaunch, flight and postflight intervals. This system supplied GN₂ at regulated pressure within specified limits to provide pressurization of the H-1 engine turbopump gear boxes and to provide purges of the LOX and lube seal cavities and two radiation calorimeters. This regulated supply also provided closing pressure for actuation of the LOX and fuel pre valves at IECO and OECO.

8.2 CONTROL PRESSURE SYSTEM

The configuration of the control pressure system was the same as those for S-IB-6 and S-IB-7 as shown in figure 8-1. The pressure measured at the GN₂ control sphere as a function of range time is presented in figure 8-2 (measurement number XD 40-9). Prior to engine ignition, the sphere pressure was maintained within the 2800-3300 psia redline limits. During the ignition transient and flight intervals, the pressure decay was within the allowable limits.

Pressure regulation was in the range of 769-787 psia, well within the operational limits of 710-815 psia. Fluctuations in regulated pressure were observed at IECO and OECO, being consistent with the increased GN₂ demand for pre valve closure. Examinations of the 750-psig regulator discharge pressure measurements XD41-9 and XD42-9 showed normal operational characteristics.

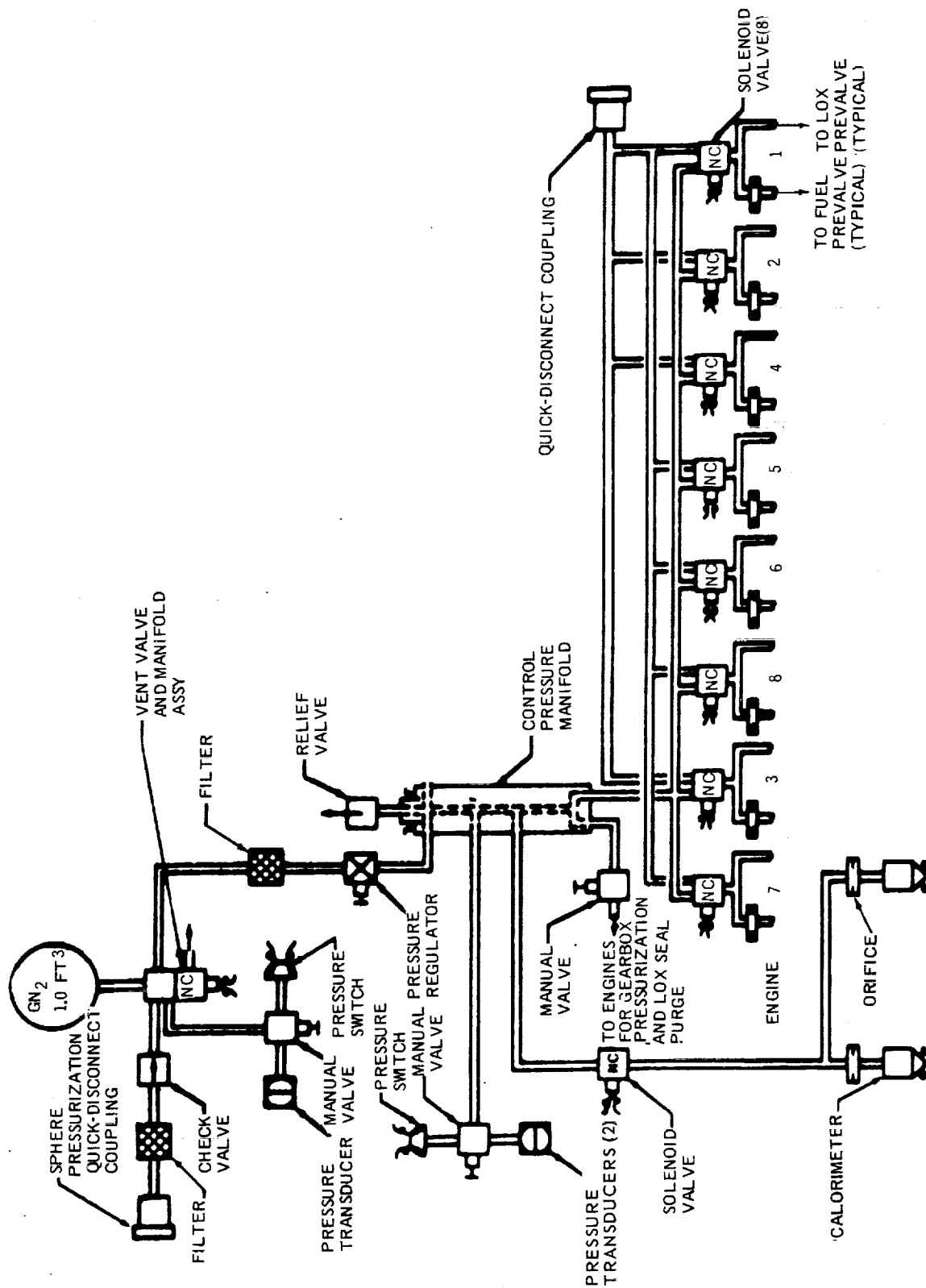


Figure 8-1. S-IB Control Pressure System

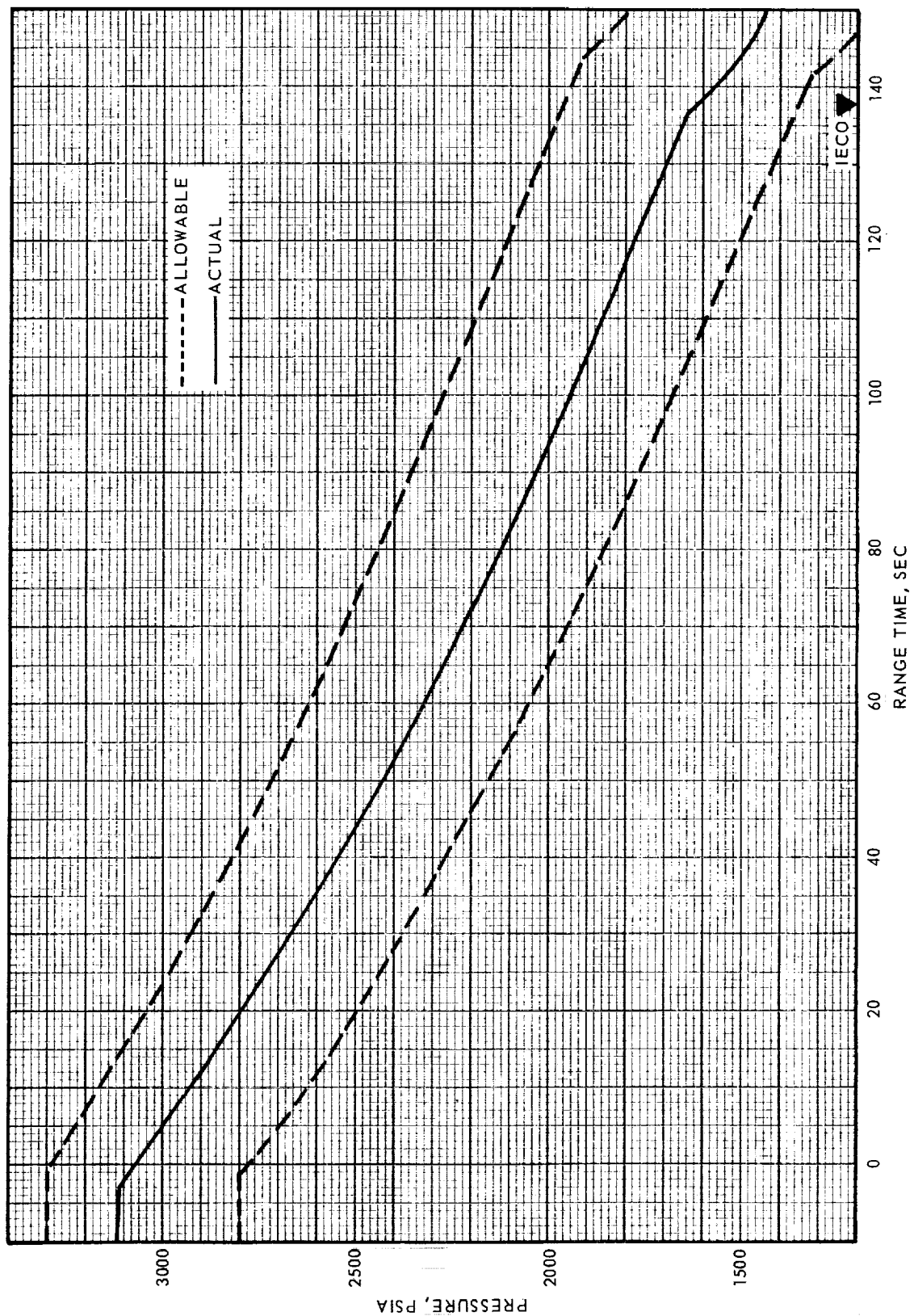


Figure 8-2. S-IB Pneumatic Control Pressure

Section 9

FLIGHT CONTROL SUBSYSTEM

9.1 SUMMARY

The S-IB stage flight control subsystem performed well within design capability. The hydraulic systems and actuator performance were satisfactory during flight and were similar to previous flights.

9.2 S-IB HYDRAULIC SYSTEM PERFORMANCE

The S-IB stage hydraulic system pressures were satisfactory during flight and were similar to those of the S-IB-7 flight. At zero seconds, the system pressures ranged from 3190 to 3250 psig. The pressure decreased approximately 50 psi on each engine during flight. This normal pressure decrease is due to the main pump temperature increase during the flight.

Reservoir oil levels were also similar to those of the S-IB-7 flight. There was a rise of approximately 2 percent in each level during flight, indicating approximately a 7°C rise in each hydraulic system's average oil temperature (not reservoir oil temperature).

The reservoir oil temperatures were satisfactory during flight. Temperature for S-IB-8 at liftoff averaged 44°C as compared to an average of 51°C for the reservoir oil temperatures of the four S-IB-7 hydraulic systems. The average temperature decrease during the flight was 7°C for S-IB-8 as compared to an average decrease of 9°C for the four S-IB-7 hydraulic systems. Figure 9-1 shows recorded values of the hydraulic oil pressure, the reservoir oil level, and the reservoir oil temperature.

9.3 S-IB ACTUATOR PERFORMANCE

All eight actuators performed smoothly during S-IB stage flight. In general, actuator activity was similar to previous flights.

The maximum pitch gimbal angle of 1.5 degrees occurred on engine No. 1 and 3 at T+58 seconds, which is approximately 19.0 percent of the maximum possible deflection. Engine No. 2 actuator represents the largest yaw gimbal angle of 1.6 degrees at T+58 seconds, or approximately 20 percent of the maximum possible deflection.

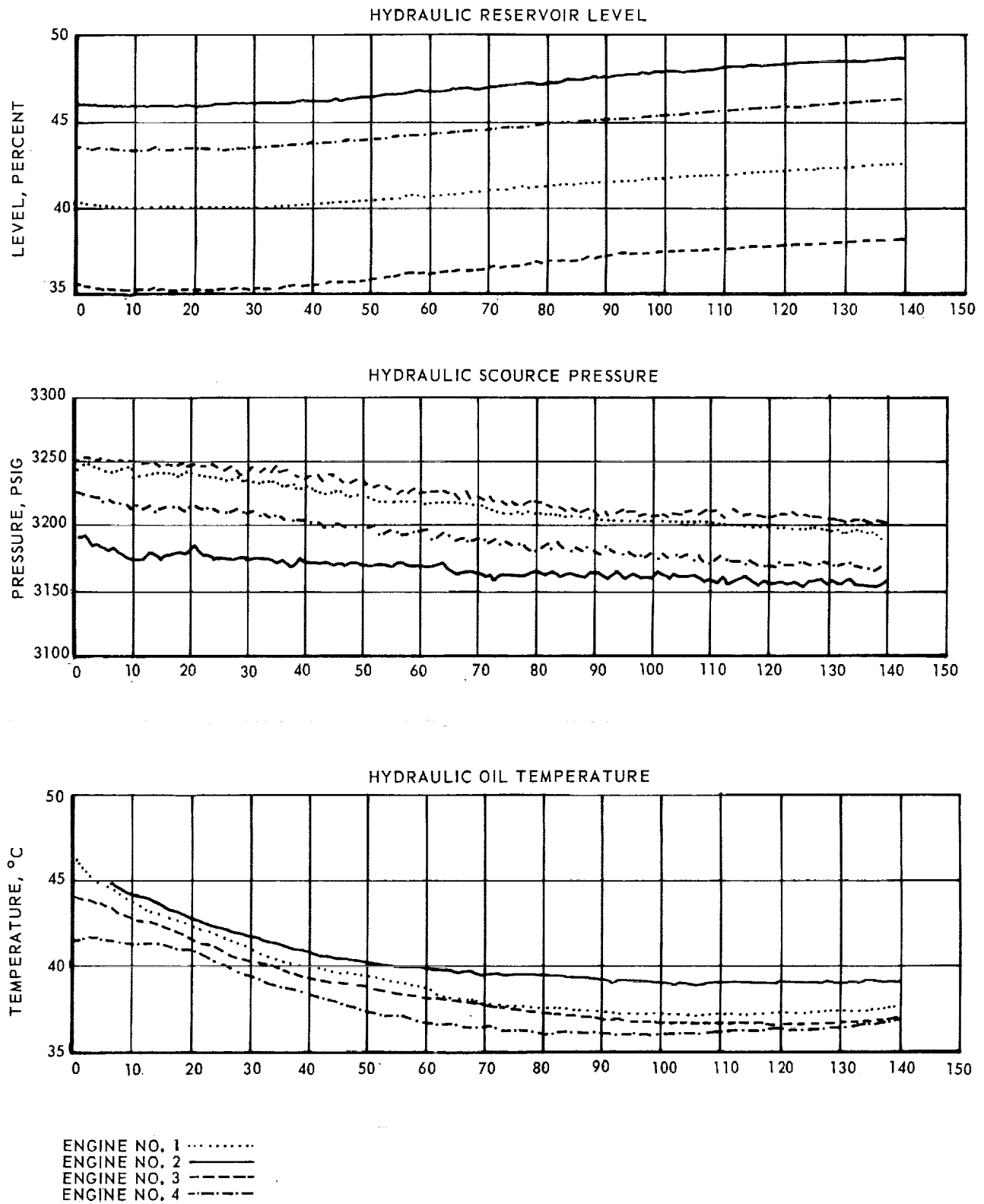


Figure 9-1. S-IB Stage Hydraulic System Characteristics

The gimbals rates observed are comparable to those experienced during previous flights. The greatest gimbal rate observed during flight was 1.7 deg/sec on engine No. 1 yaw actuator at T+58 seconds. This rate is approximately 5 percent of the actuator's maximum rate. Figure 9-2 is a comparison of gimbal angles for the S-IB flights of S-IB-1 through S-IB-8.

The differential currents to the servo valves ranged from 0 to 14 percent of rated current during S-IB stage flight. The largest differential current observed was on the engine No. 1 yaw actuator and was 1.7 ma at T+58 seconds. The maximum value of each performance parameter for each actuator during liftoff, Max q, outboard engine cutoff (OECO), and for S-IB stage flight are presented in table 9-1. It should be noted that, because of the physical mounting of the servo-actuators, the polarity of their position in degrees may not agree with the polarity of the average gimbal and angle. For example, a positive beta pitch command will produce a negative degree reading in the telemetry data for engines No. 1 and 4 and a positive readout for engines No. 2 and 3. In the yaw plane, engines No. 1 and 2 have a negative polarity for a positive beta yaw command. Figures 9-3 through 9-6 show actuator position as a function of range time. Figure 9-7 depicts the average actuator position of the four pitch actuators and the four yaw actuators during the flight of S-IB-8.

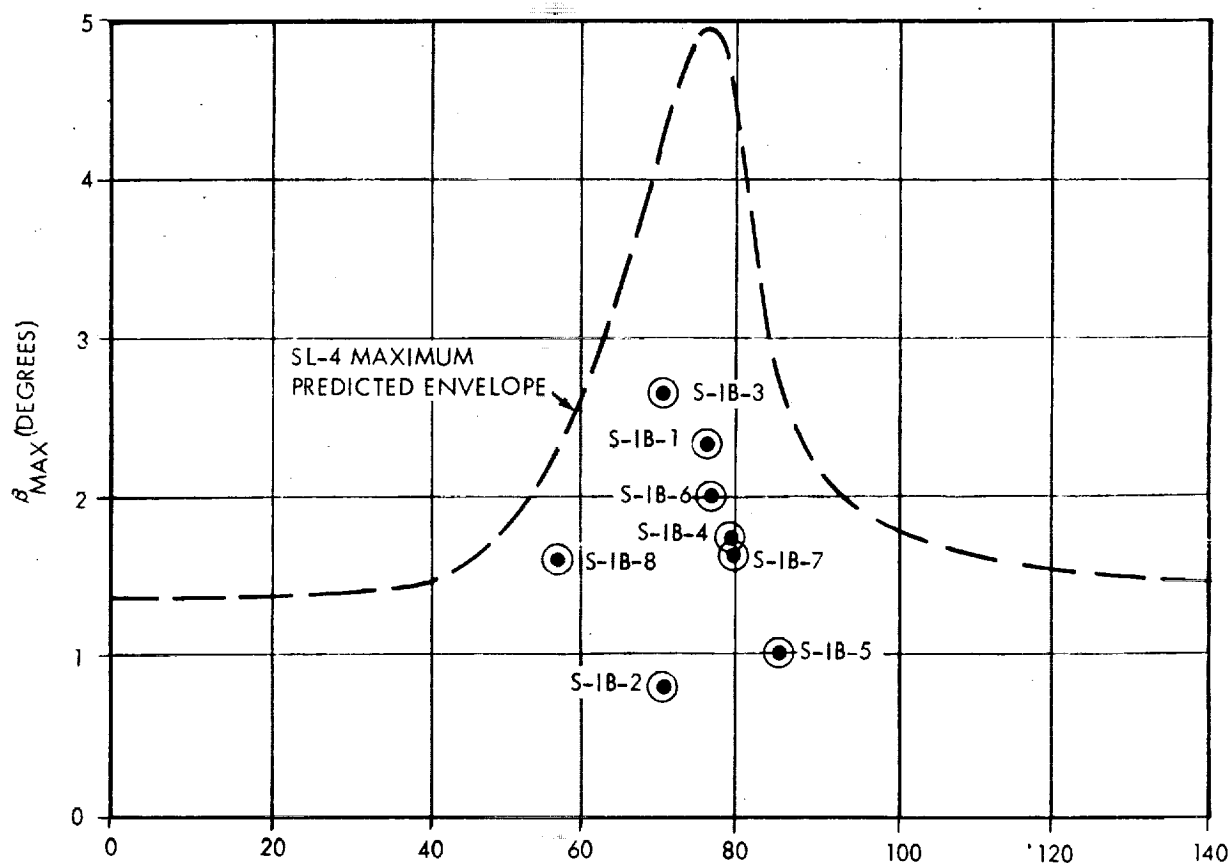
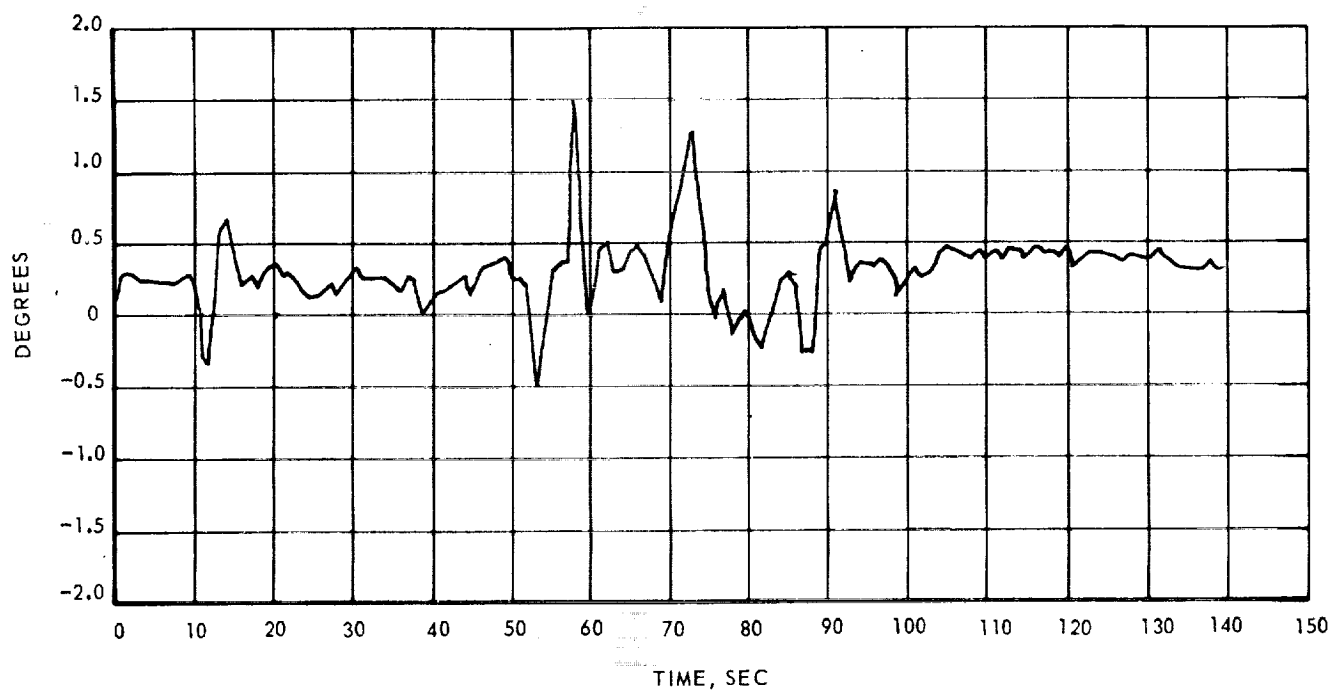


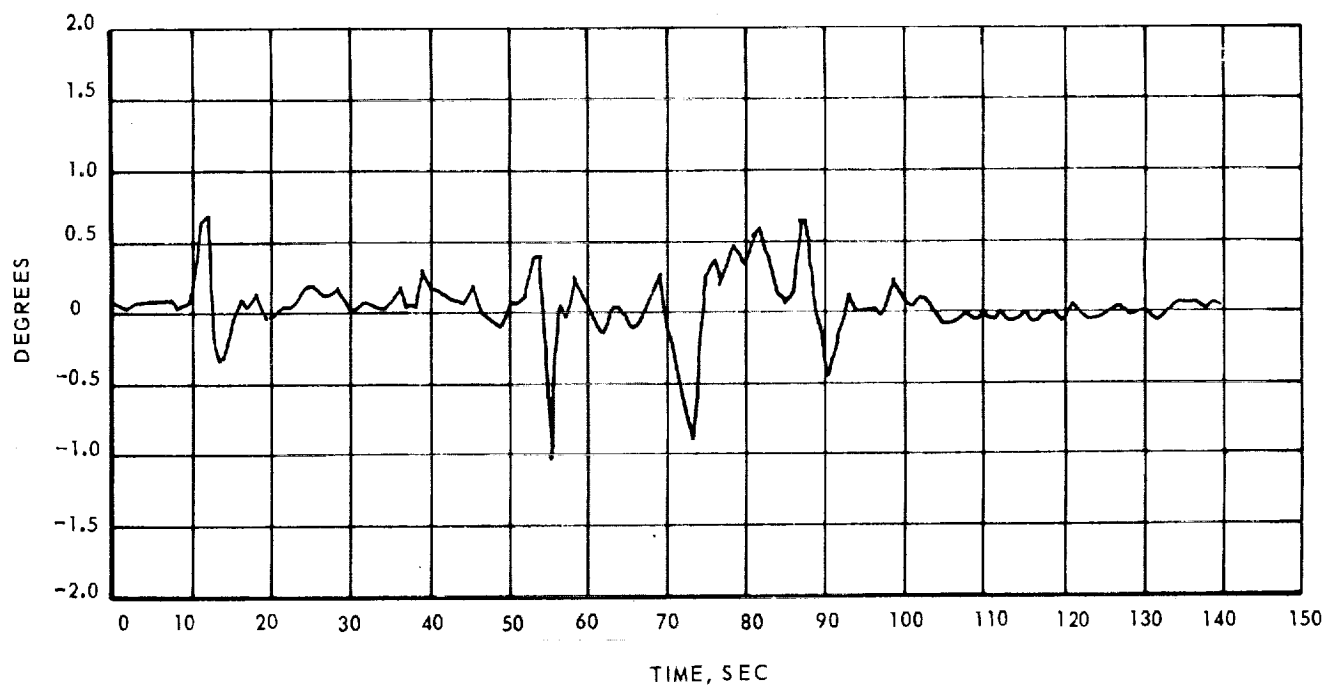
Figure 9-2 S-IB Stage Envelope Maximum Gimble Angle

Table 9-1. S-IB Actuator Performance Data

Engine 1					
Parameter	Axis	Liftoff	Max q	OECO	Flight
Gimbal Position (deg)	Pitch	0.3	1.5	0.3	1.5@58
	Yaw	0.2	1.3	0.1	1.3@58
Gimbal Rate (deg/sec)	Pitch	0.2	1.1	0.1	1.1@58
	Yaw	0.1	1.7	<-0.1	1.7@58
Valve Current (ma)	Pitch	0.2	1.7	0.2	1.7@58
	Yaw	0.3	1.6	0.2	1.6@58
Engine 2					
Gimbal Position (deg)	Pitch	0.1	0.3	0.1	0.7@12
	Yaw	0.3	.	0.4	1.6@58
Gimbal Rate (deg/sec)	Pitch	0.2	0.3	0.1	1.1@56
	Yaw	-0.1	1.6	0.1	1.6@58
Valve Current (ma)	Pitch	0.2	0.2	0.3	0.4@88
	Yaw	0.3	0.3	0.3	0.7@92
Engine 3					
Gimbal Position (deg)	Pitch	0.2	1.5	0.3	1.5@58
	Yaw	0.3	1.3	0.1	1.3@58
Gimbal Rate (deg/sec)	Pitch	0.0	1.2	0.1	1.2@58
	Yaw	0.1	0.8	<0.1	0.9@92
Valve Current (ma)	Pitch	0.2	0.2	-0.1	0.2@88
	Yaw	0.5	0.6	0.5	0.9@88
Engine 4					
Gimbal Position (deg)	Pitch	0.2	0.4	0.1	1.0@73
	Yaw	0.3	1.5	0.3	1.5@58
Gimbal Rate (deg/sec)	Pitch	0.2	0.3	-0.1	0.8@13
	Yaw	0.1	0.8	<0.1	1.2@80
Valve Current (ma)	Pitch	0.2	0.3	0.2	0.4@53
	Yaw	0.4	0.5	0.3	0.8@88

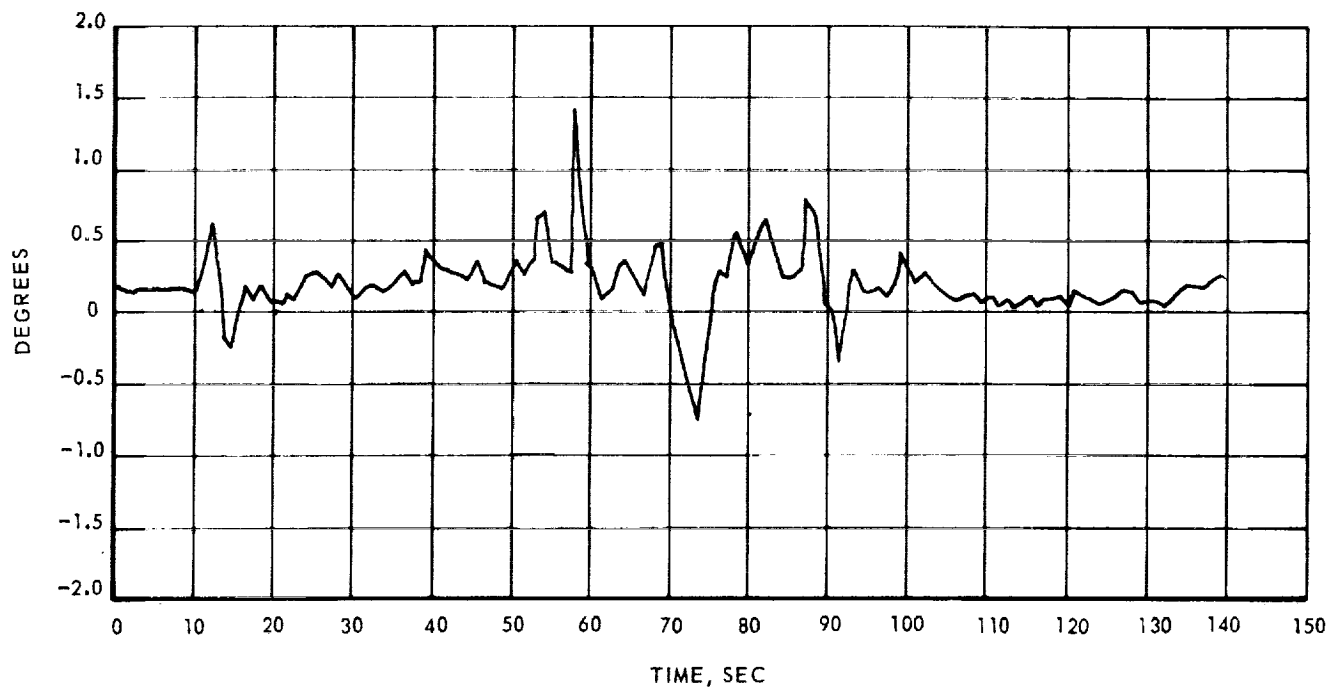


ENGINE 1

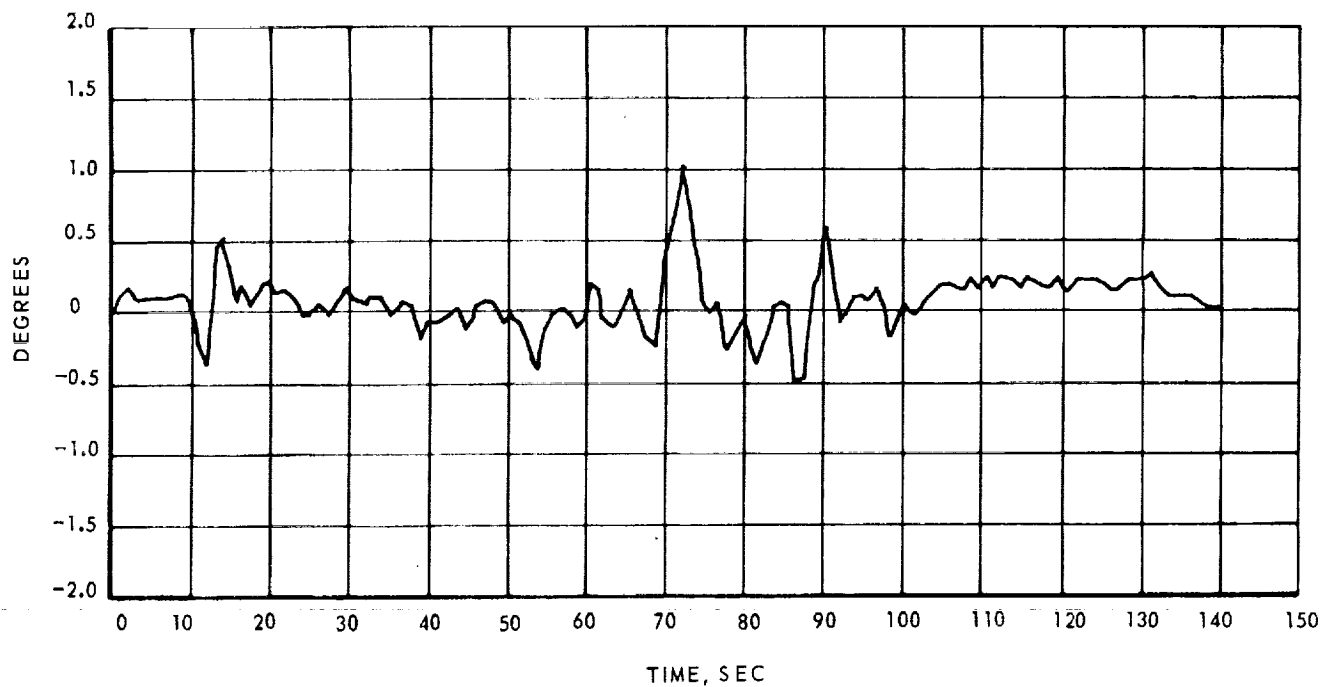


ENGINE 2

Figure 9-3. S-IB Stage Pitch Actuator Position

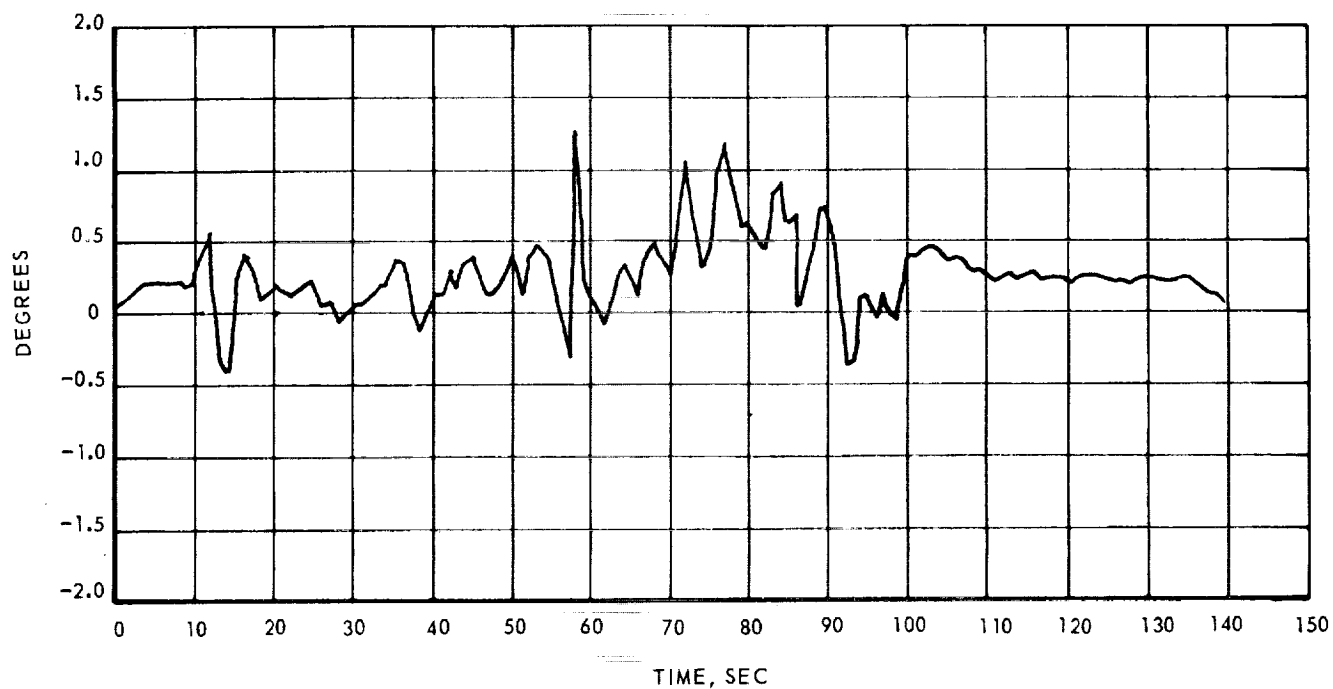


ENGINE 3

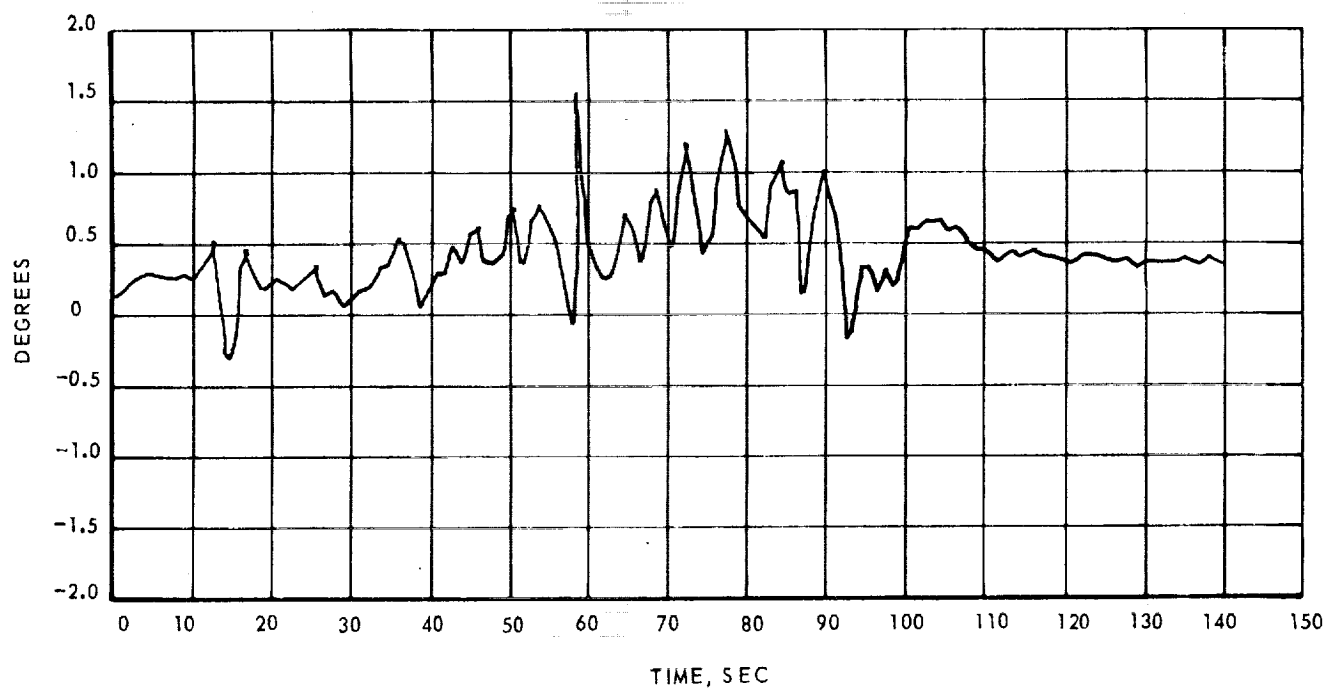


ENGINE 4

Figure 9-4. S-IB Stage Pitch Actuator Position



ENGINE 1



ENGINE 2

Figure 9-5. S-IB Stage Yaw Actuator Position

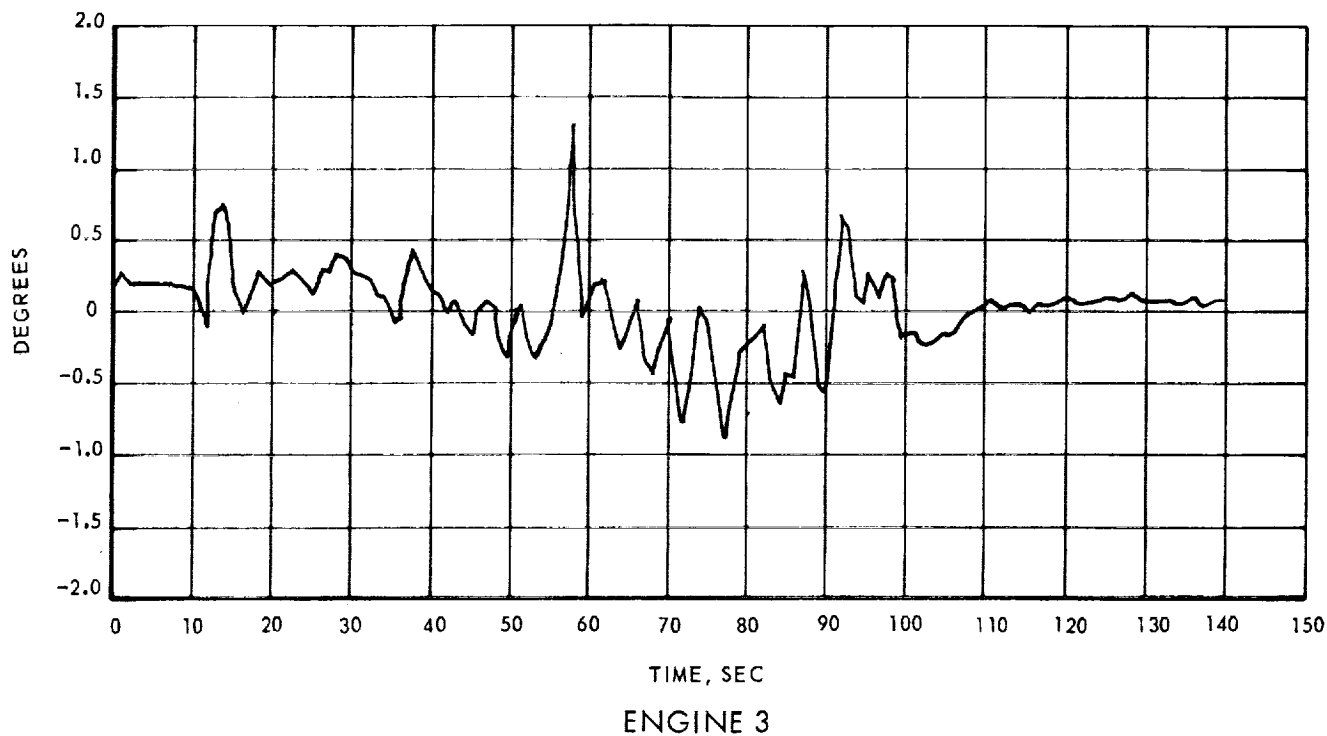


Figure 9-6. S-IB Stage Yaw Actuator Position

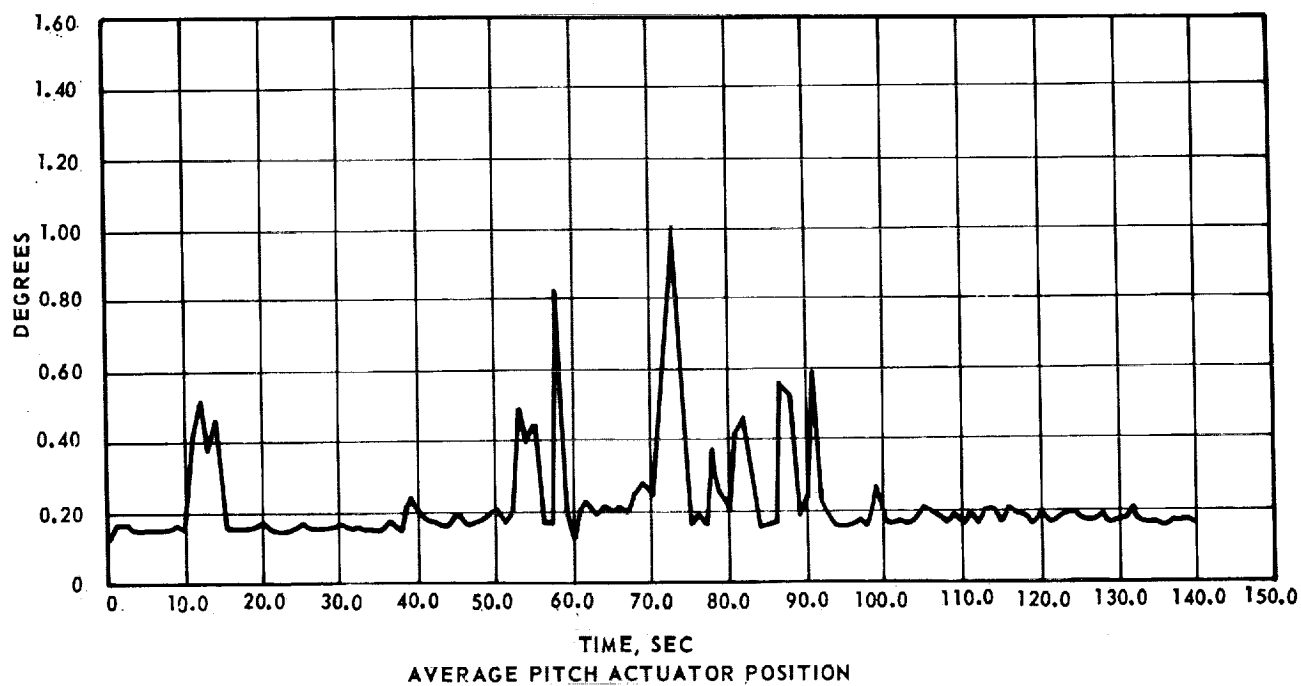
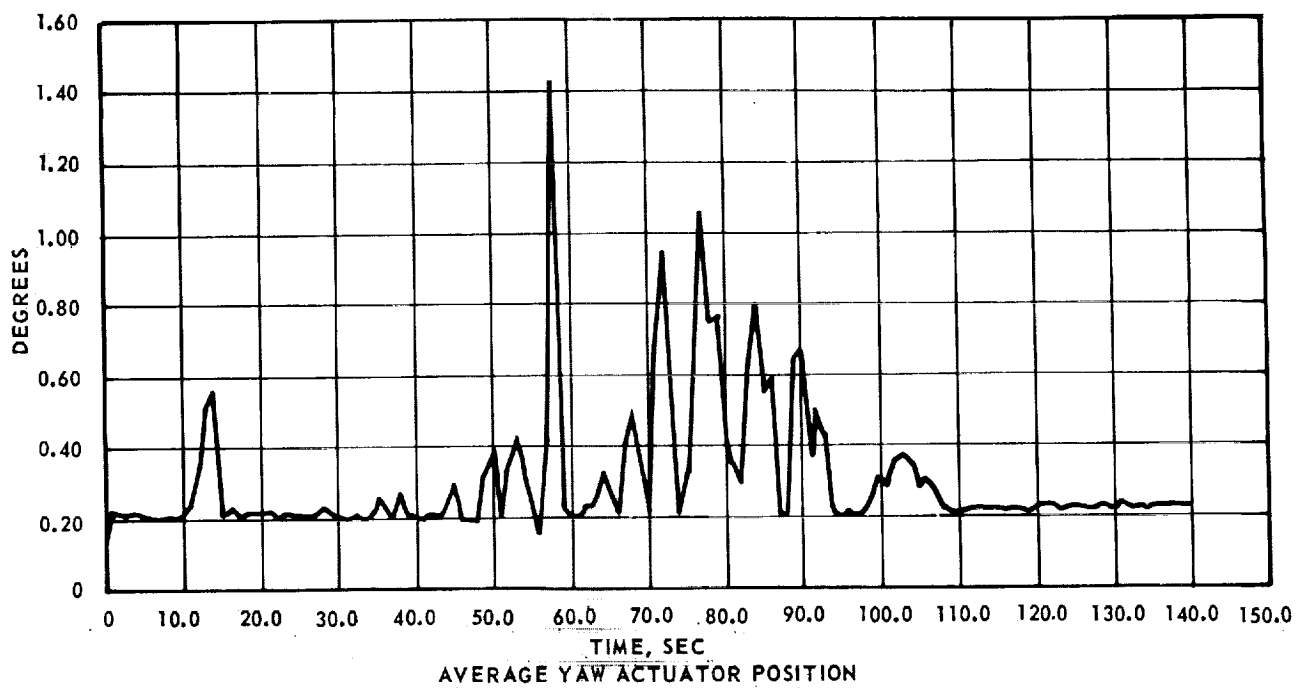


Figure 9-7. S-IB Stage Average Actuator Position

Section 10

STRUCTURES

10.1 SUMMARY

A prelaunch structural assessment of SA-208 confirmed the vehicle fully qualified to the design criteria following rework of F3 and F4 fuel tank forward bulkheads, and correction of stress corrosion cracks discovered in both the upper E-beam of the fin position 4 outrigger assembly, and all eight fin attachment fittings.

The maximum ground wind experienced by the SA-208 during the prelaunch period was 21 knots (allowable with damper, 40 knots). The ground winds at launch were 7 knots, and from the Southwest. The structural loads experienced during the S-IB boost phase were within design criteria values. The maximum bending moment was 1.06×10^6 N-m at vehicle station 942 (approximately 17 percent of design criteria bending). The maximum longitudinal dynamic responses at the instrument unit (IU) were $\pm 0.1g$ at both S-IB inboard engine cutoff (IECO) and outboard engine cutoff (OECO). The vehicle structural responses during thrust cut-off were considered normal. POGO did not occur during S-IB burn.

Strain instrumentation used to monitor the structural performance of the S-IB-8 stage consisted of eight LOX stud strain gages at Station 942 (figure 10-1). The measured pitch and yaw bending moments, as a function of range time, are presented in figure 10-8.

Longitudinal and lateral accelerations were measured with five accelerometers (figure 10-2): three on the S-IB stage, one on the IU and one on the command module. The vehicle body-bending oscillations were recorded from eight accelerometers: six on the S-IB stage and two on the command module.

10.2 TOTAL VEHICLE STRUCTURES EVALUATION

10.2.1 Longitudinal Loads

The SA-208 vehicle liftoff steady-state acceleration was 1.25g. Maximum longitudinal dynamic response measured during thrust buildup and release was $\pm 0.1g$ in the IU and ± 0.75 at the CM (figures 10-3 and 10-4). Comparable values have been recorded on previous flights.

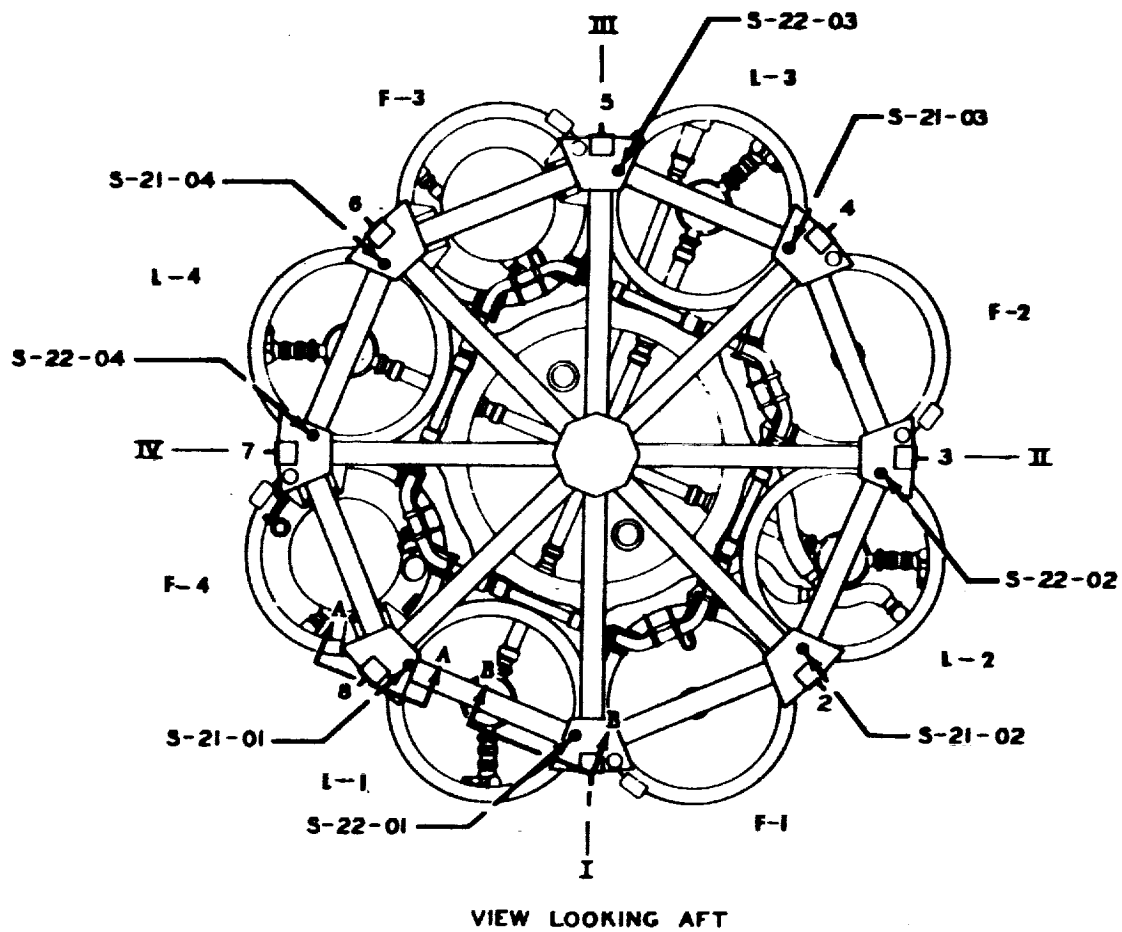


Figure 10-1. Instrumentation at Station 942

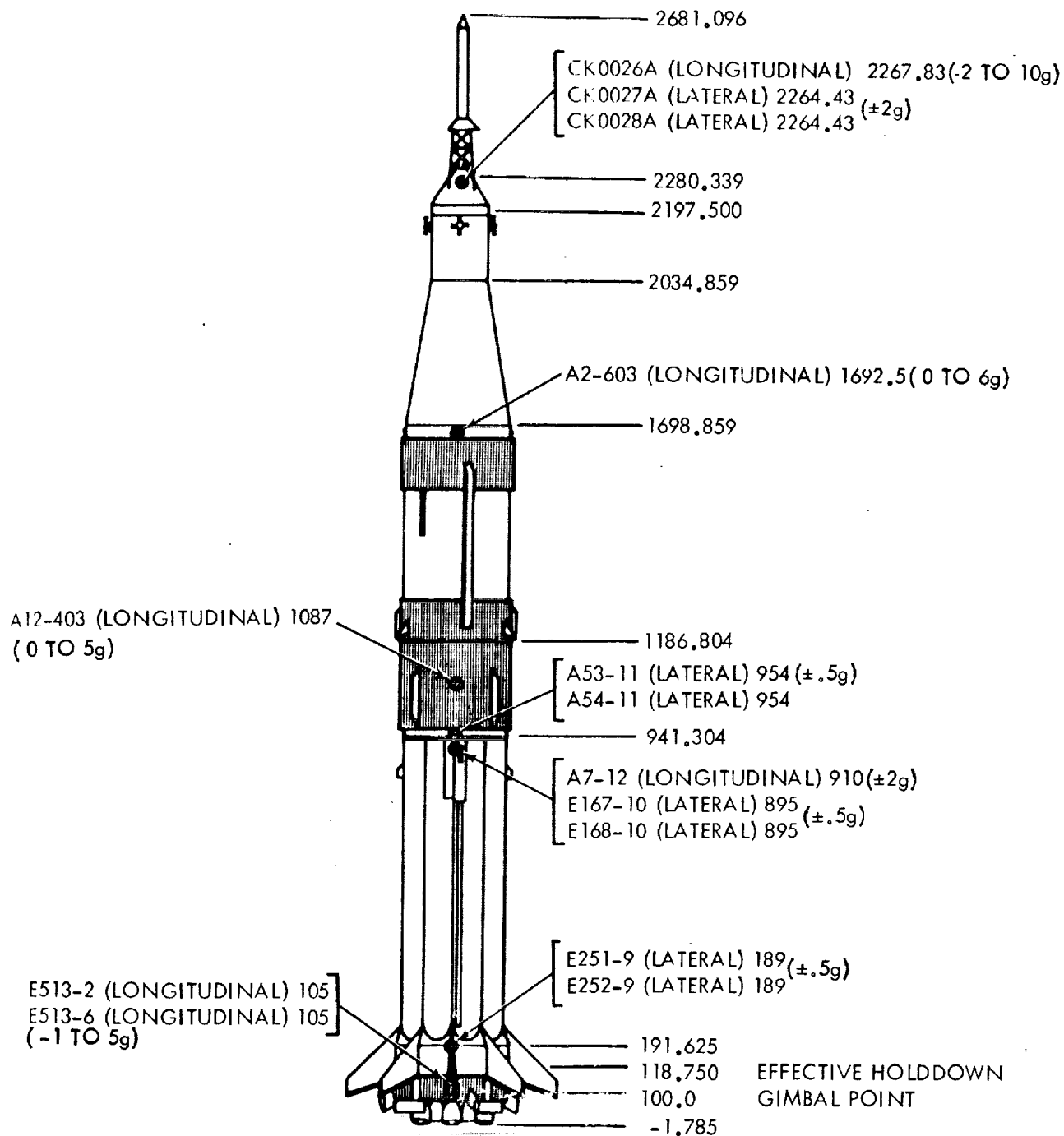


Figure 10-2. SA-208/Saturn IB Acceleration Instrumentation

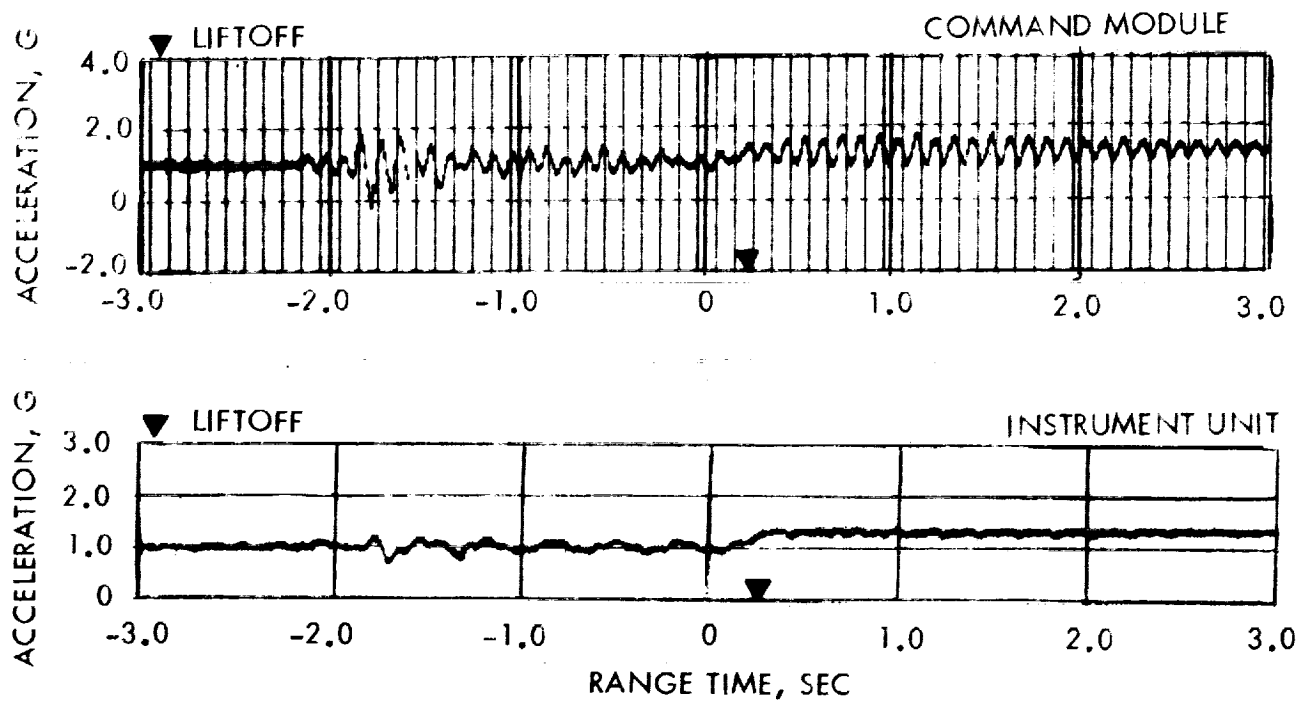


Figure 10-3. Longitudinal Acceleration During Thrust Buildup and Launch

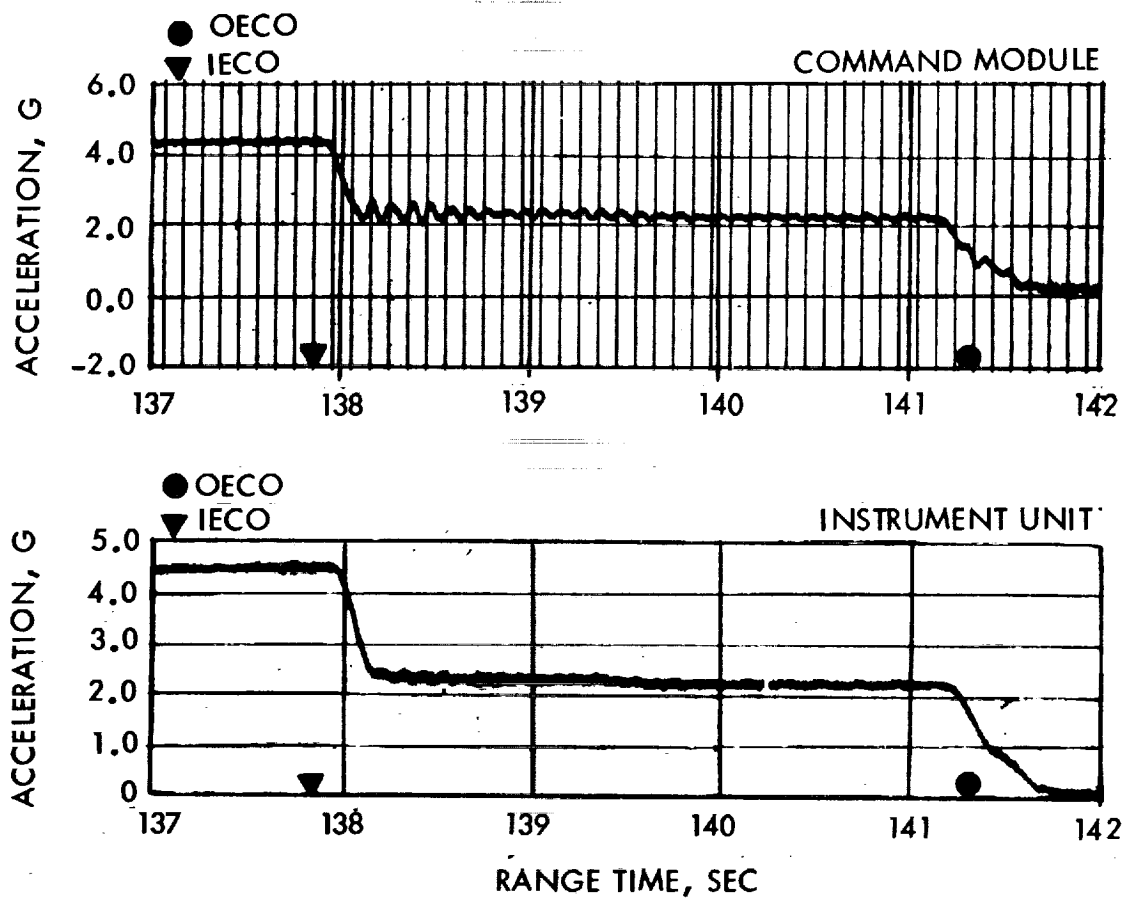


Figure 10-4. Longitudinal Acceleration During Cutoff

The SA-208 IECO and OECO transient responses were equal to or less than those of previous flights. The maximum longitudinal dynamics resulting from IECO were $\pm 0.1g$ at the IU and $\pm 0.1g$ at the IU and $\pm 0.1g$ at the IU and $\pm 0.25g$ at the CM (figure 10-4).

The total longitudinal load at station 942, based on strain data, is shown in figure 10-5 as a function of range time. The envelope of previous flights (S-IB vehicles SA-202 through -207) is shown for comparison. The maximum longitudinal load of 6.04×10^6 Newtons at time point 137.8 seconds is within design limit capability.

The longitudinal load distribution at the time of maximum bending moment (73.1 seconds) and IECO (137.8 seconds) is shown in figure 10-6. The steady-state longitudinal accelerations were 2.05g and 4.25g, respectively.

10.2.2 Bending Moments

The pitch and yaw winds-aloft profiles are shown in figure 10-7. The measured pitch and yaw bending moments, together with their times, are presented in figure 10-8. The wind velocities and vehicle bending can be correlated by comparing these figures. The maximum measured flight bending moment of 1.06×10^6 Newton meters occurred at 73.1 seconds. The measured bending moments at station 942 are the result of the 8 LOX stud strain gages, and do not include the increment carried by the 105-inch LOX tank. The strain data must be increased by approximately 10 percent (based on previous flight analyses for which 105-inch LOX strain gage data were recorded) to represent total vehicle bending moment.

The pitch, yaw, and resultant bending moments at 73.1 seconds are calculated based on post-flight vehicle mass data, trajectory and control data (figures 10-9 through 10-11). The maximum computed bending moment was 1.25×10^6 Newton meters at vehicle station 942. The bending moments in both the 105-inch tank and the 70-inch tanks were determined by the internal loads analysis so that the measured loads could be compared. The bending loads were very low compared to the design criteria 6.4×10^6 Newton meters.

10.2.3 Combined Loads

Combined compression and tension loads were computed for maximum bending moment (73.1 seconds) and engine cutoff (~137 seconds) using measured S-IVB hydrogen ullage pressure (32.0 psig). An envelope of these results plus an envelope of the allowable combined loads are presented in figure 10-12. The S-IB is not included because the clustered stage does not lend itself to this format.

The minimum safety factors are plotted versus vehicle station in figure 10-13. The minimum factor of safety of 1.54 at station 1186 was experienced at IECO. The minimum design safety factor is 1.40.

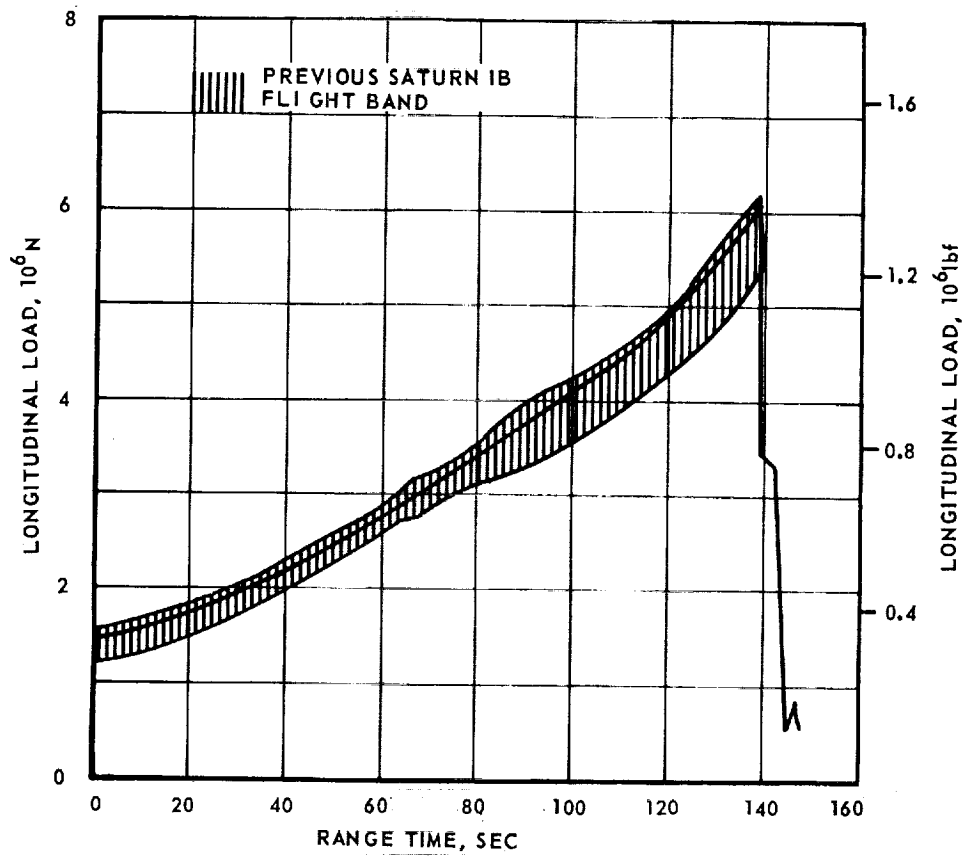


Figure 10-5. Longitudinal Load from Strain Data at Station 942 vs. Time.

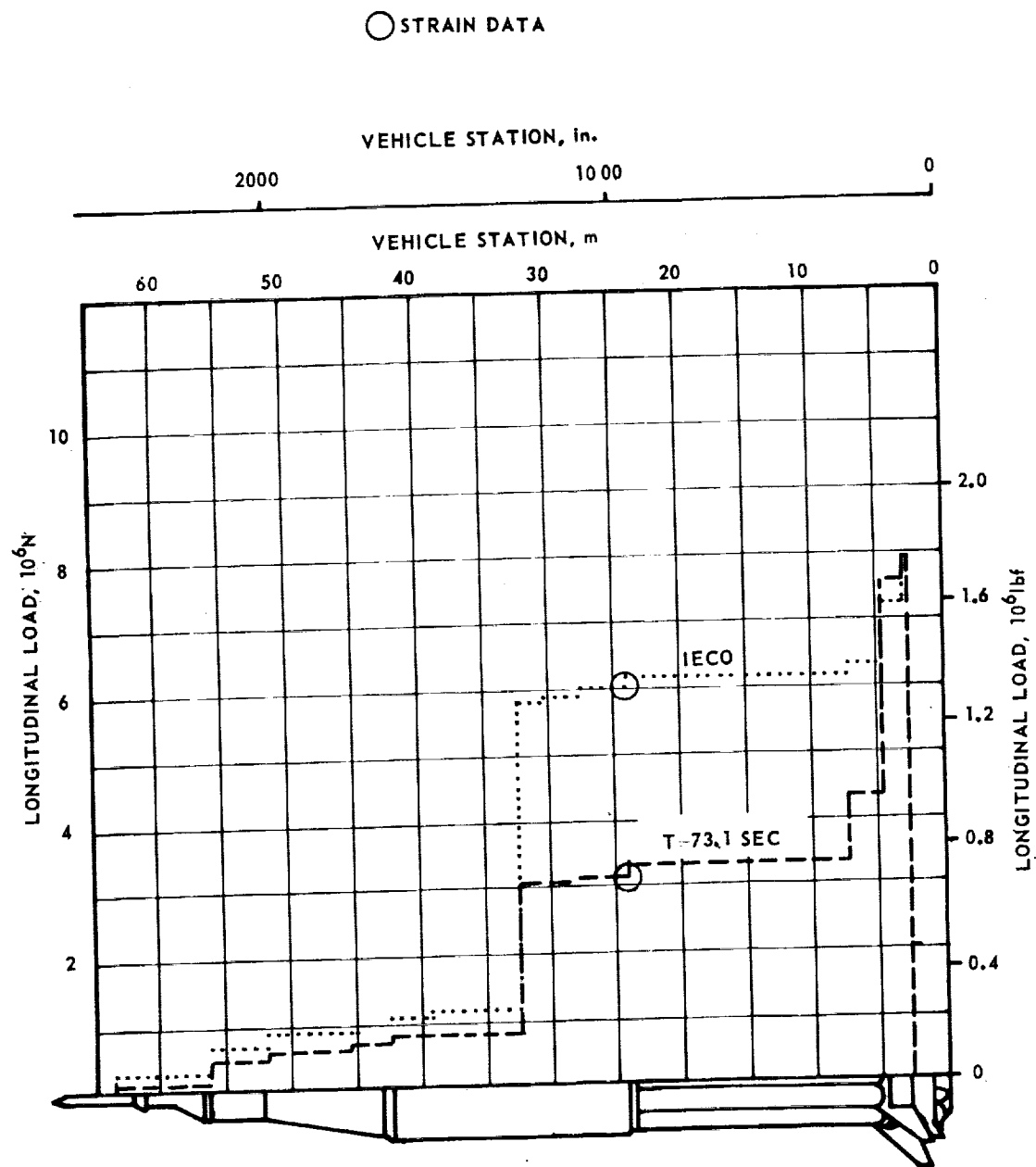


Figure 10-6. Longitudinal Load Distribution at Time of Maximum Bending Moment and IECO

MAXIMUM YAW BENDING = 77.1 SEC
 MAXIMUM RESULTANT AND PITCH BENDING = 73.1 SEC

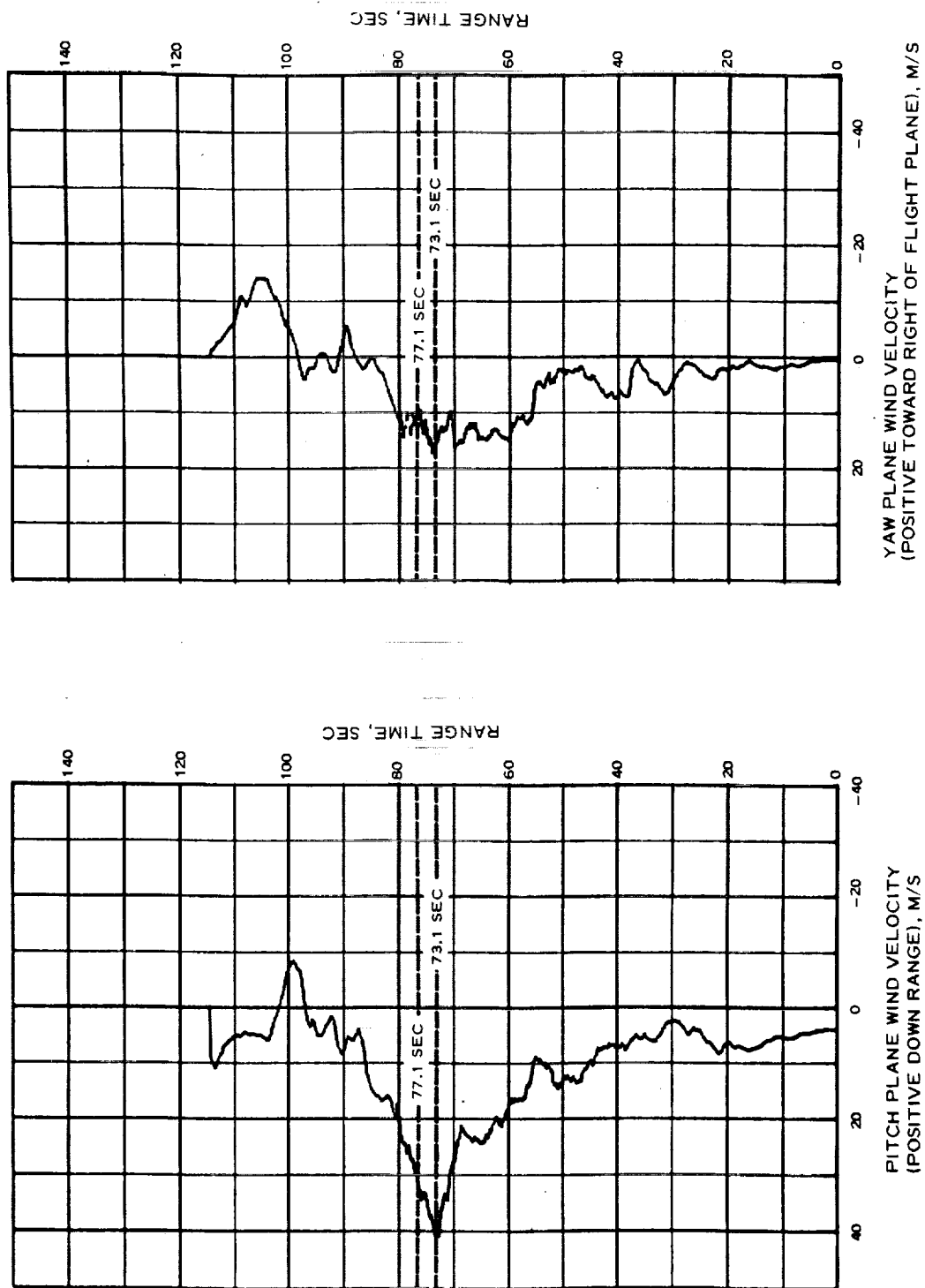


Figure 10-7. Wind Profile

MAXIMUM YAW BENDING = 77.1 SEC
 MAXIMUM RESULTANT AND PITCH BENDING = 73.1 SEC

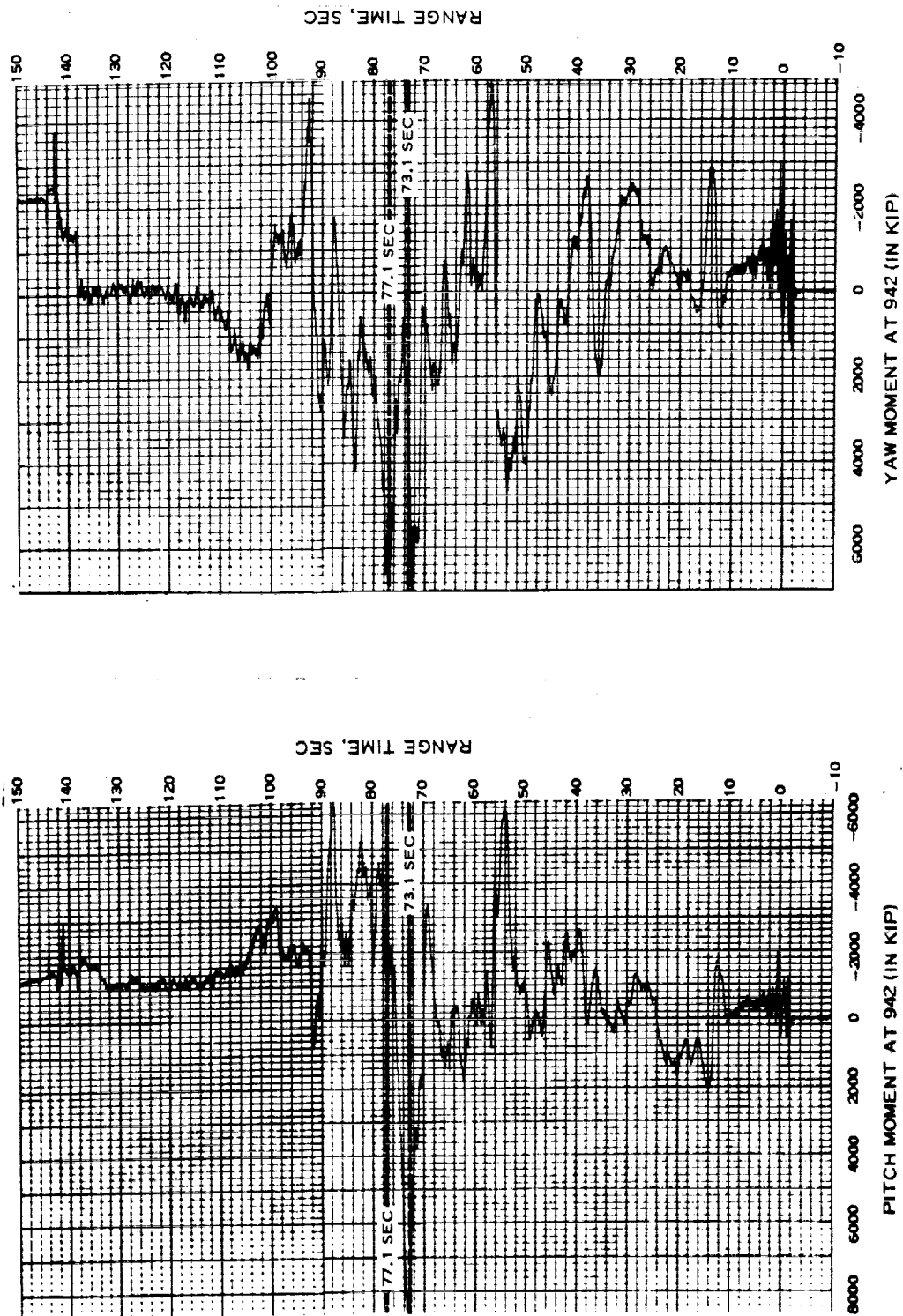


Figure 10-8. Bending Moments Measured by Strain Gages

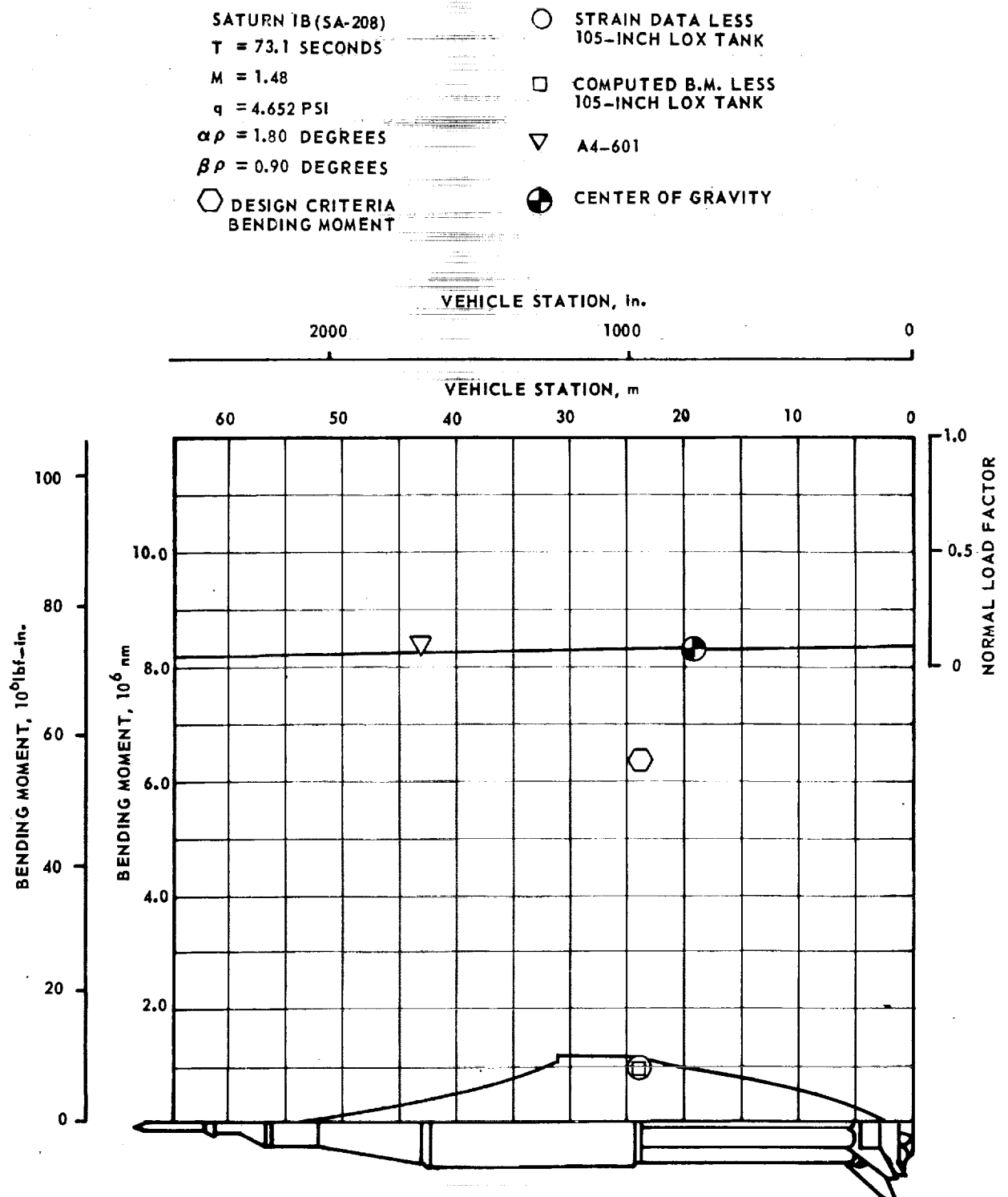


Figure 10-9. Pitch Bending Moment Distributions at Time of Maximum Resultant Moment, $T=73.1$ Seconds

SATURN IB (SA-208)
 $T = 73.1$ SECONDS
 $M = 1.48$
 $q = 4.652$ PSI
 $\alpha\gamma = 0.60$ DEGREES
 $\beta\gamma = 0.50$ DEGREES
 ○ DESIGN CRITERIA
 BENDING MOMENT

○ STRAIN DATA LESS
 105-INCH LOX TANK
 □ COMPUTED B.M. LESS
 105-INCH LOX TANK
 ▽ A5-603
 ● CENTER OF GRAVITY

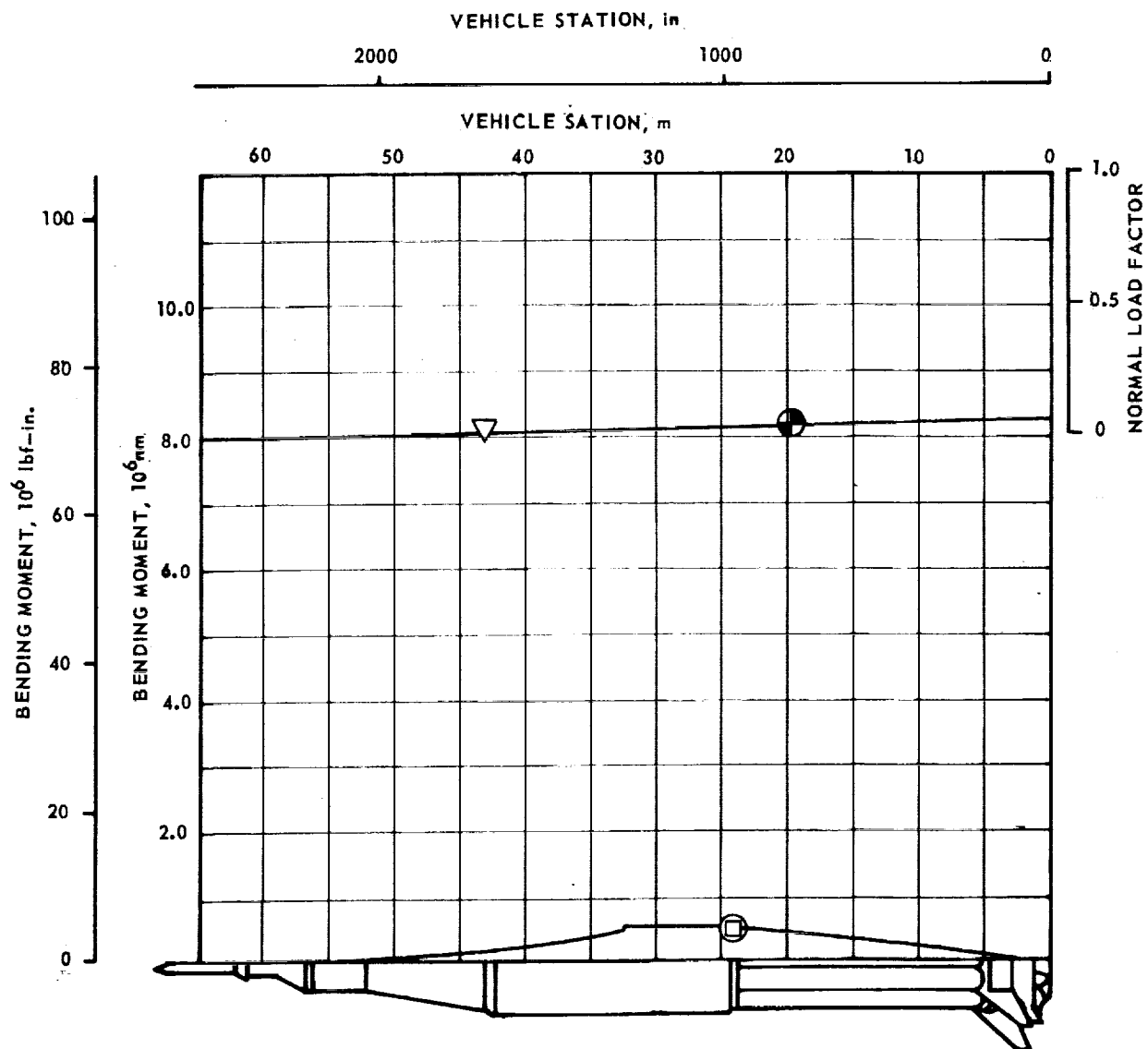


Figure 10-10. Yaw Bending Moment Distributions at Time of Maximum Resultant Moment, $T=73.1$ Seconds

SATURN IB(SA-208)

T = 73.1 SECONDS

M = 1.48

q = 4.652 PSI

α = 1.90 DEGREES

β = 1.03 DEGREES

○ STRAIN DATA LESS
105-INCH LOX TANK

□ COMPUTED B.M. LESS
105-INCH LOX TANK

⬡ DESIGN CRITERIA
BENDING MOMENT

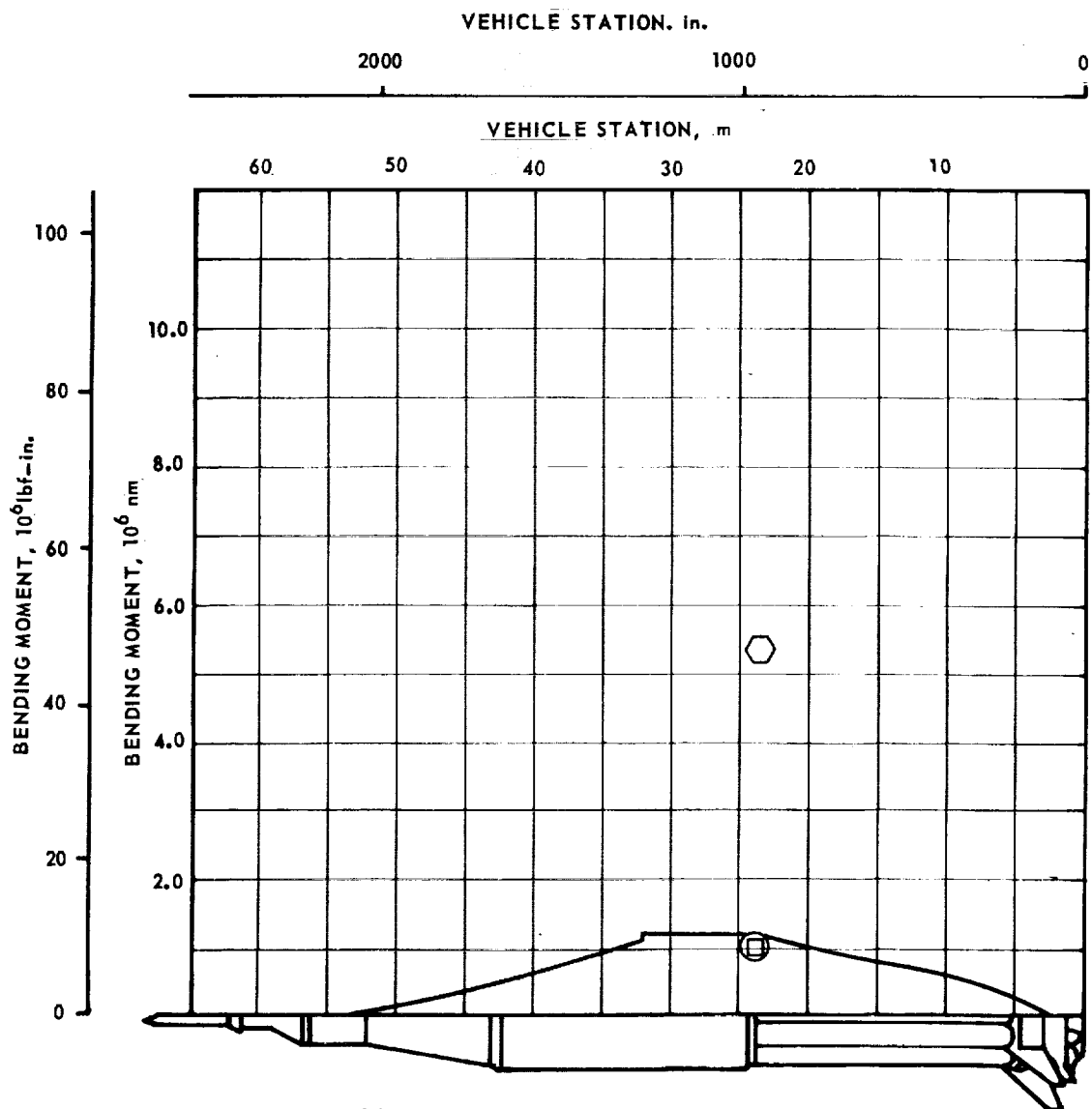


Figure 10-11. Resultant Bending Moment Distributions at Time of Maximum Resultant Moment, T=73.1 Seconds

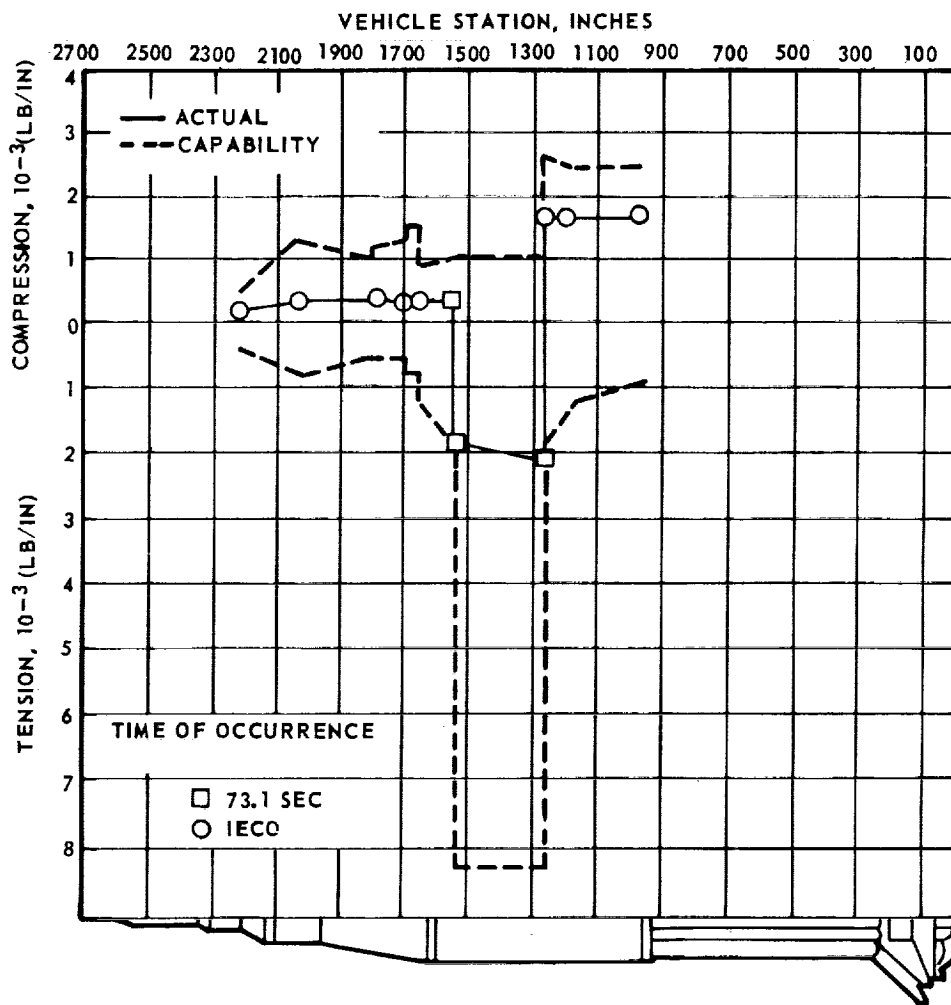


Figure 10-12. Envelope of Combined Loads Producing Minimum Safety Margin for Saturn IB Flight

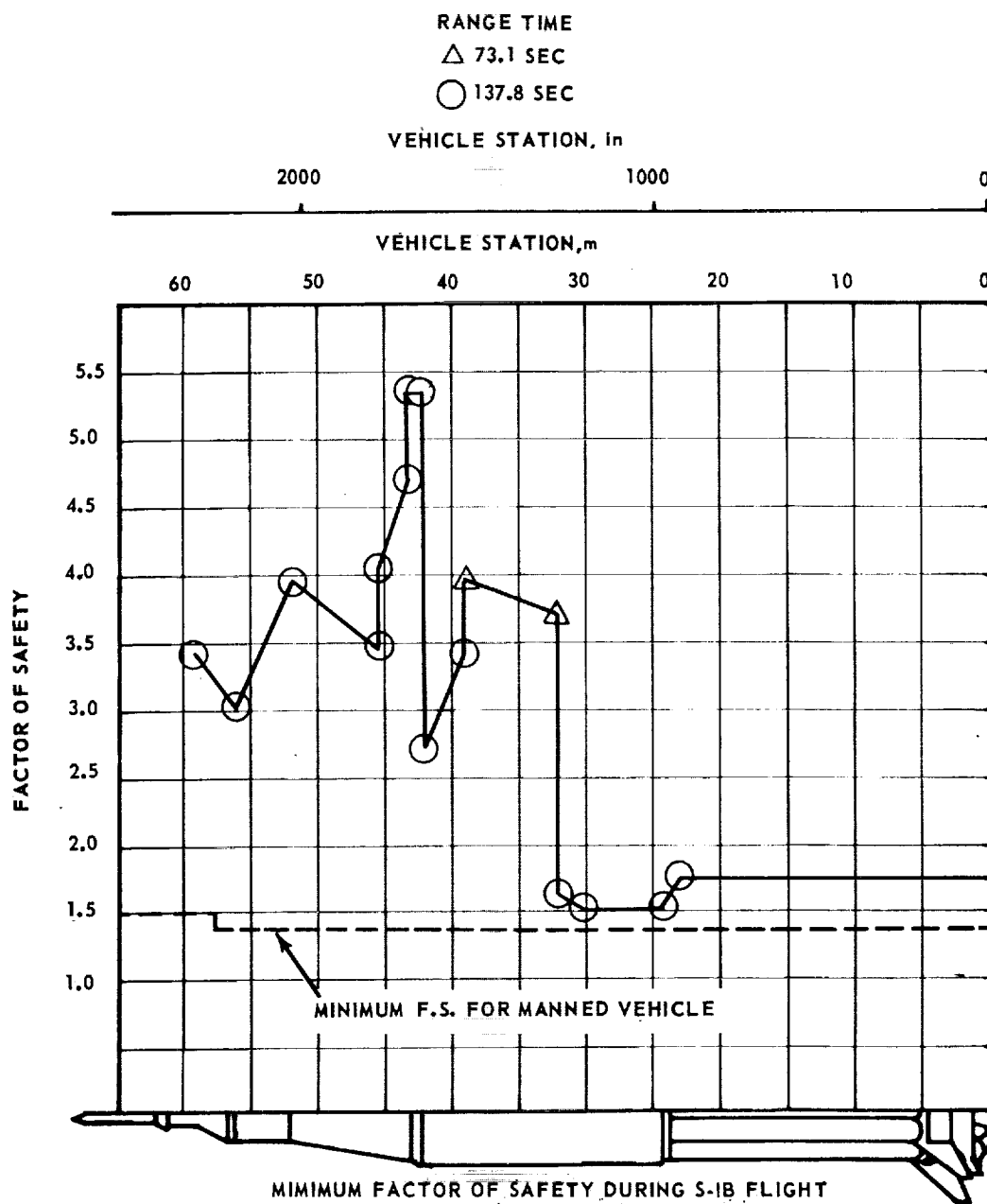


Figure 10-13. Minimum Factor of Safety During S-IB Flight

10.2.4 Vehicle Dynamic Characteristics

The longitudinal stability analysis on SA-208 has revealed all vibration and pressure fluctuation to be smooth and low with no POGO instability. Peak vibration levels accrued at liftoff, first stage cutoff and maximum dynamic pressure. Compressed time strip charts of the SA-208 vehicle POGO data are shown in figures 10-14 and 10-15.

The first, second and third bending mode frequencies are compared to the modes predicted by dynamic analysis in figure 10-16. These predominant frequencies were determined from flight data by power spectral density analysis and selected on the basis of proximity to the predicted frequencies. Response amplitudes of these frequencies as presented in figure 10-17, were low and similar to previous Saturn IB flights. In general, the pitch response amplitudes were slightly higher than the yaw. The greatest response recorded was 0.065 Grms in the pitch direction (Station 895) during the liftoff portion of flight.

10.3 STRUCTURAL ASSESSMENT

A prelaunch structural assessment of SA-208 confirmed the vehicle fully qualified to the contractually designated design criteria and the required 1.4 manned safety factor of the Skylab 4 mission. As a conservative approach, the flight envelope and ground winds were restricted, presupposing structural problems originated from stress corrosion following the last preflight inspection.

10.3.1 Fuel Tank Forward Bulkhead Collapse

The forward bulkheads of fuel tanks 3 and 4 were collapsed during an RP-1 drain operation (see paragraph 5.3.1 and 7.6.1 for additional comments). Collapse occurred because tank vent covers were not removed, causing a negative pressure on the bulkheads for which they were not designed. Tanks 3 and 4 were pressurized to restore the bulkheads to contour and then proof-pressure tested to 21.0 psig. No cracks or structural anomalies were found. Two new vent valves were installed to lower the maximum flight pressure to 19.1 psig; normal setting is 21 to 21.5 psig.

10.3.2 Stress Corrosion Cracking

During a special inspection at KSC, a crack was discovered in the upper E-beam of the outrigger assembly, fin position 4. Channel was made from stress-corrosion susceptible material 7178-T6 AL alloy forging. A 1 x 3 3/4-inch "coupon" of material was removed from the channel web and a spacer and splice-plate installed to restore the structure to the full capability of the undamaged hardware.

After the CDDT, stress-corrosion cracks were found in all eight fin assemblies, rear-spar to thrust-structure E-beam attachment fittings. Seven fins had cracks in both left and right fitting mounting bolt holes, one in only one fitting. All fins were replaced with new (no CDDT) hardware and reinforcing blocks installed about the mounting bolts at each fitting to provide an alternate loads path (a "fail-safe" feature) in the event that cracks occurred after the last preflight inspection.

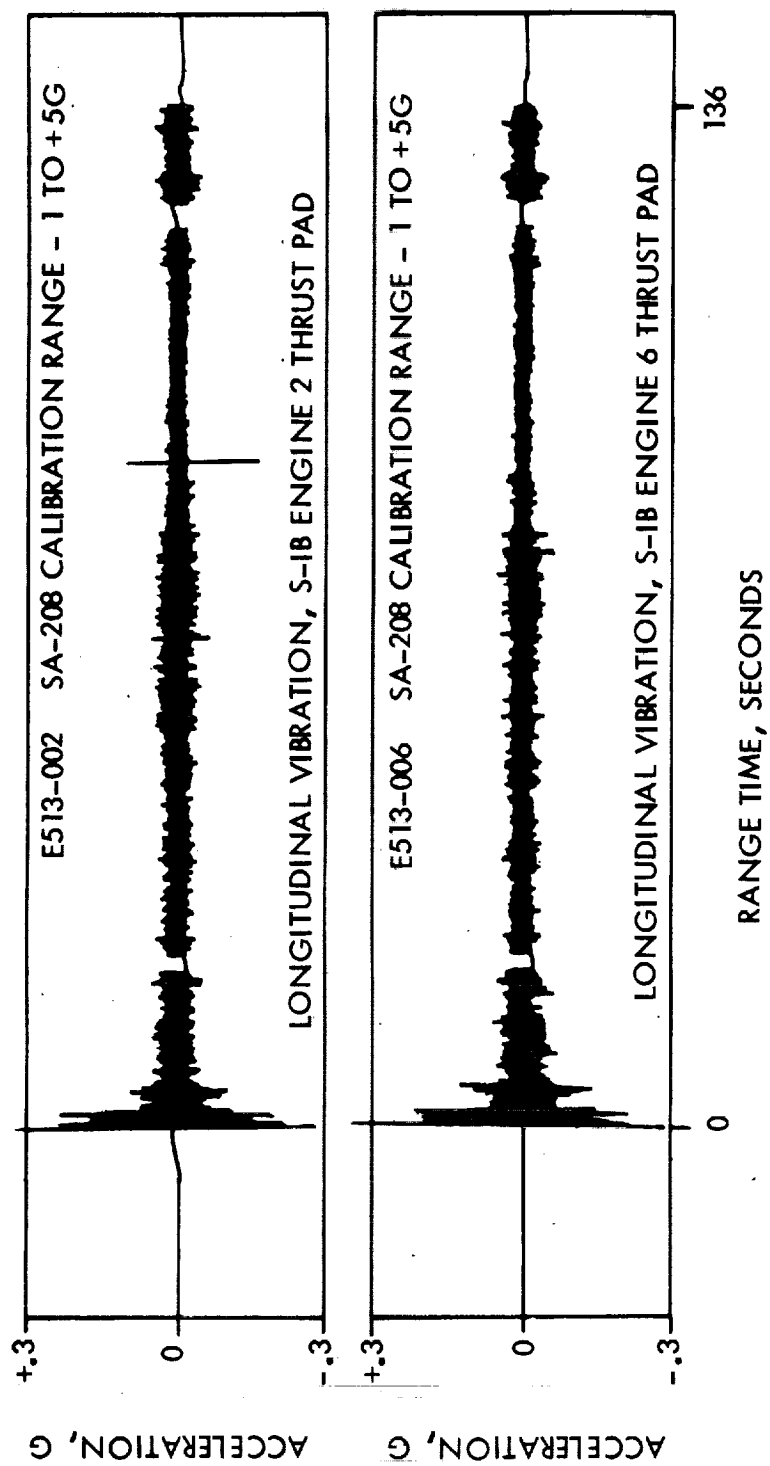


Figure 10-14. Longitudinal Acceleration, S-IB Instrumentation

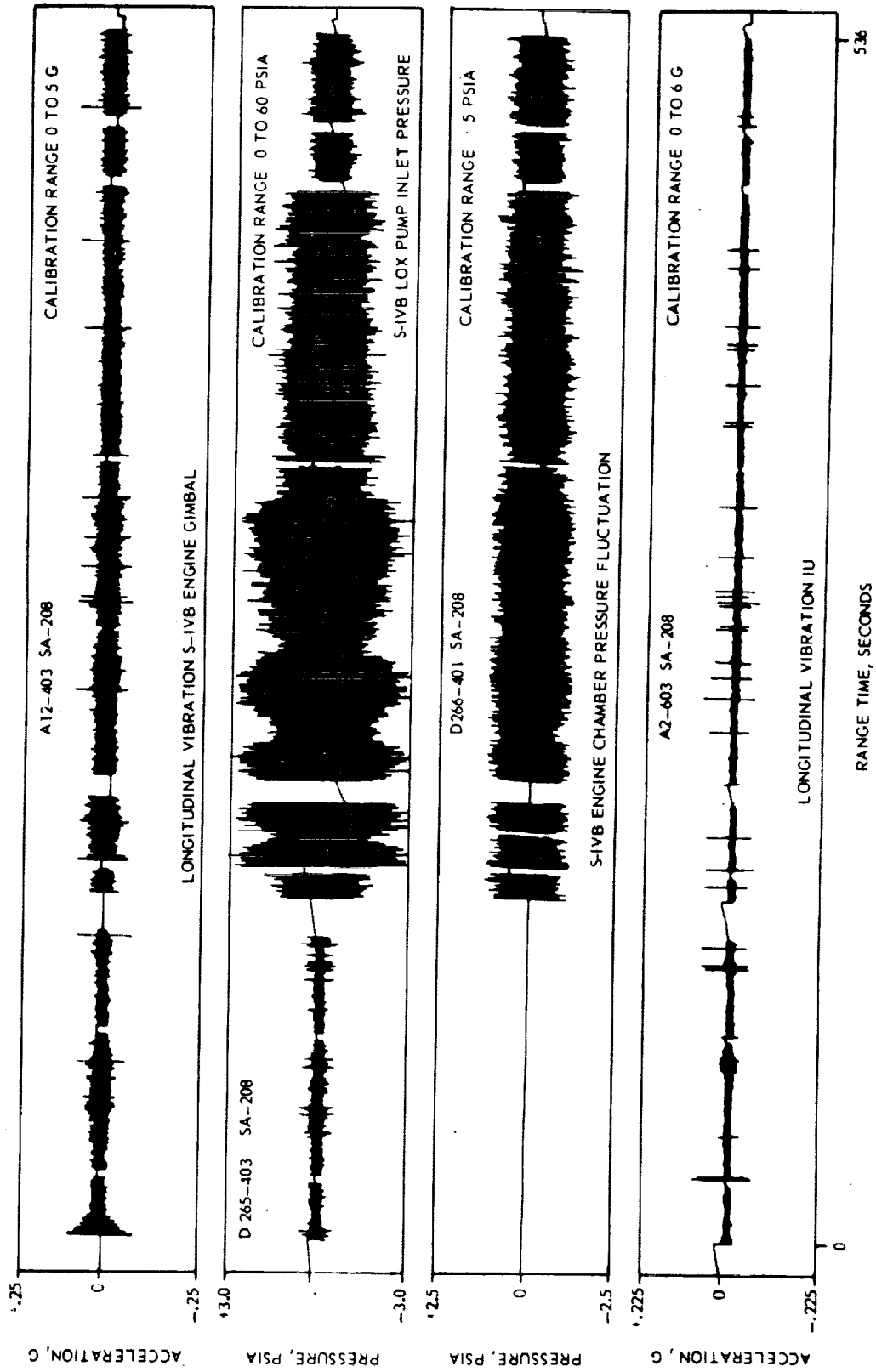


Figure 10-15. Longitudinal Acceleration and Pressure, S-IVB/IU Instrumentation

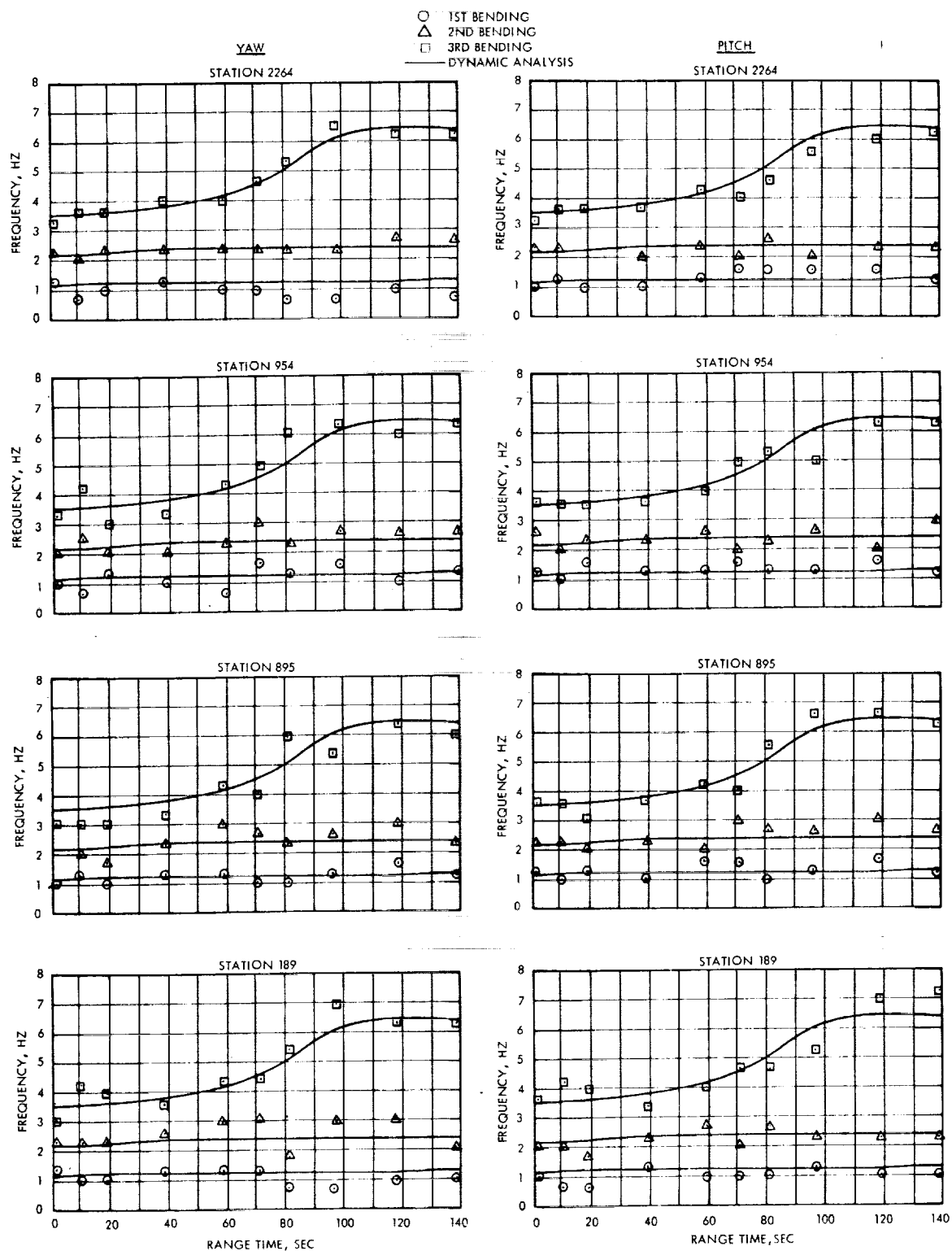


Figure 10-16. Vehicle Bending Frequencies

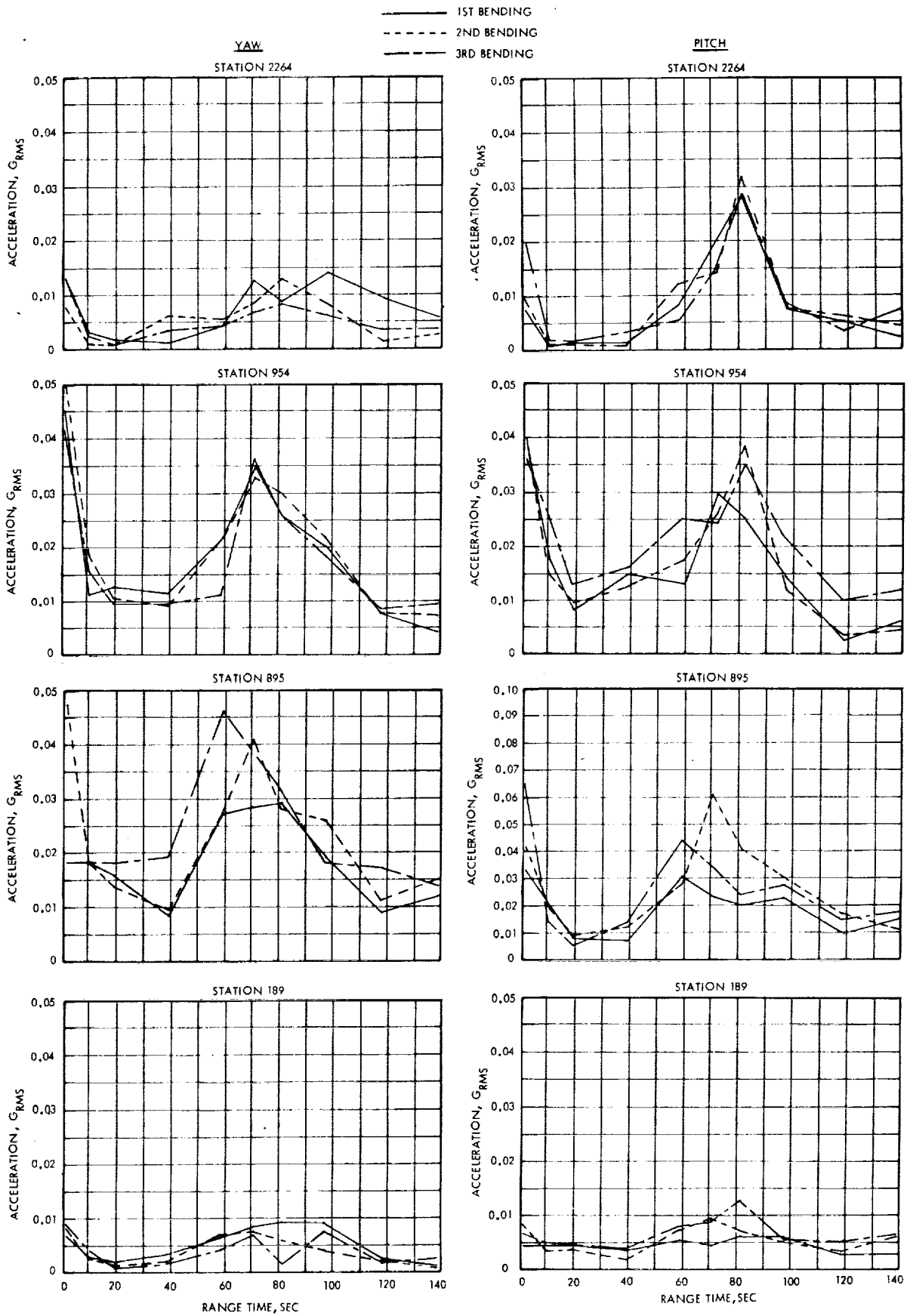


Figure 10-17. Vehicle Bending Amplitudes

Section 11

ELECTRICAL SYSTEMS

11.1 SUMMARY

The S-IB stage electrical system operated satisfactorily during the boost phase of flight and all mission requirements were met.

11.2 S-IB ELECTRICAL SYSTEMS

Inflight power for the S-IB stage is supplied by two 28-volt, zinc-silver oxide batteries, which are designated 1D10 and 1D20. Each battery is rated at a nominal 2000 ampere-minutes. The power and distribution system consists of batteries, plug type junction boxes and interconnecting circuitry. Three master measuring voltage supplies are utilized to furnish a precisely regulated reference voltage to the telemetry system. Each power supply converts 28-vdc to a regulated 5-vdc reference for use in the instrumentation measuring systems. The electrical networks for the S-IB-8 stage differed from the networks of S-IB-7 as follows:

- a. Effective with S-IB-8, all IN2150A diodes have been replaced in Propulsion System Distributor 9A1 by SIN1204A diodes. The approved vendor for IN2150A diodes had closed operations and the diodes became unavailable. SIN1204A diodes were used as an acceptable substitute.
- b. Starting with S-IB-8, the circuitry of the fire detection system has been simplified. The two plug-in type J-boxes, 9A10 and 9A11, used for interconnection of the four groups of temperature sensors, have been deleted. Interconnection is accomplished in cable 9W146 for S-IB-8.

Performance of the measurements related to the stage electrical system are given in table 11-1. A complete analysis of the performance of discrete signals monitored over the DDAS was obtained from data retrieved from the Central Instrumentation Facilities (CIF) tape. The results compared favorably with previous S-IB flight records.

All thrust OK pressure switches and EBW units functioned properly. The average charge time for the retrorocket EBW units was 0.71 seconds. The charge time for the separation EBW units was 0.675 seconds. The destruct EBW units indicated no change. The Secure Command System and Range Safety Decoder were operable during flight.

Table 11-1. S-IB Electrical System Measurements (Sheet 1 of 4)

MEASUREMENT NO.	TITLE	REMARKS/RESULTS RANGE TIME-(SEC)
K1-12	Sw Selector Output Pulses	Outputs as expected and normal
K2-12	First Motion (S-IB Liftoff)	0.42
K3-12	Cutoff Signal, Outboard	141.29
K15-02	LOX Level Cutoff	134.88 *
K16-04	LOX Level Cutoff	135.05 *
K17-F2	Fuel Level Cutoff	136.36 *
K18-F4	Fuel Level Cutoff	136.44 *
K37-11	Retro Rocket Ignition Signal (EBW)	142.60 *
K53-12	Separation Prestart S-IB to S-IVB Signal	142.60 *
K65-13	Cutoff and Destruct Indicator CDR No. 1	No Change
K66-13	Cutoff and Destruct Indicator CDR No. 2	No Change
K67-12	Cutoff Signal, Inboard	137.82
K81-F2	Fuel Depletion Sensor No. 1	143.44 *
K82-F4	Fuel Depletion Sensor No. 2	143.44 *
K99-1	Eng 1 Cutoff (+1D11)	141.37 *
K99-2	Eng 2 Cutoff (+1D11)	141.37 *
K99-3	Eng 3 Cutoff (+1D11)	141.37 *
K99-4	Eng 4 Cutoff (+1D11)	141.37 *
K99-5	Eng 5 Cutoff (+1D11)	Fired and Shorted 137.87 *
K99-6	Eng 6 Cutoff (+1D11)	137.88 * Fired and Shorted
K99-8	Eng 8 Cutoff (+1D11)	137.88 *
K100-1	Eng 1 Cutoff (+1D21)	141.29 * Fired and Shorted

*RDSM Data

Table 11-1. S-IB Electrical System Measurements (Sheet 2 of 4)

MEASUREMENT NO.	TITLE	REMARKS/RESULTS RANGE TIME-(SEC)	
K100-2	Eng 2 Cutoff (+1D21)	141.29 *	
K100-3	Eng 3 Cutoff (+1D21)	Fired and Shorted 141.29 *	
K100-4	Eng 4 Cutoff (+1D21)	141.29 *	
K100-5	Eng 5 Cutoff (+1D21)	137.87 * Fired and Shorted	
K100-6	Eng 6 Cutoff (+1D21)	Fired and Shorted 137.88*	
K100-7	Eng 7 Cutoff (+1D21)	Fired and Shorted 137.97*	
K100-8	Eng 8 Cutoff (+1D21)	Fired and Shorted <u>Closed</u> <u>Opened</u>	
K138-1	Eng 1 Thrust Press. Sw 1 Thrust OK	-1.59*	141.32*
K139-1	Eng 1 Thrust Press. Sw 2 Thrust OK	-1.59*	141.32*
K140-2	Eng 2 Thrust Press. Sw 1 Thrust OK	-1.67*	141.40*
K141-2	Eng 2 Thrust Press. Sw 2 Thrust OK	-1.67*	141.40*
K142-3	Eng 3 Thrust Press. Sw 1 Thrust OK	-1.59*	141.40*
K143-3	Eng 3 Thrust Press. Sw 2 Thrust OK	-1.60*	141.39*
K144-4	Eng 4 Thrust Press. Sw 1 Thrust OK	-1.76*	141.40*
K145-4	Eng 4 Thrust Press. Sw 2 Thrust OK	-1.68*	141.39*
K146.5	Eng 5 Thrust Press. Sw 1 Thrust OK	-1.92*	138.07*
K147-5	Eng 5 Thrust Press. Sw 2 Thrust OK	-1.93*	138.06*
K148-6	Eng 6 Thrust Press. Sw 1 Thrust OK	-1.84*	138.07*

*RDSM Data

Table 11-1. S-IB Electrical System Measurements (Sheet 3 of 4)

MEASUREMENT NO.	TITLE	REMARKS/RESULTS RANGE TIME-(SEC)		
		<u>Closed</u>	<u>Opened</u>	
K149-6	Eng 6 Thrust Press. Sw 2 Thrust OK	-1.85*	138.06*	
K150-7	Eng 7 Thrust Press. Sw 1 Thrust OK	-1.92*	138.07*	
K151-7	Eng 7 Thrust Press. Sw 2 Thrust OK	-1.93*	138.06*	
K152-8	Eng 8 Thrust Press. Sw 1 Thrust OK	-1.84*	138.07*	
K153-8	Eng 8 Thrust Press. Sw 2 Thrust OK	-1.86*	138.05*	
K171-1	Eng 1 Thrust Press. Sw 3 Thrust OK	-1.64*	141.35*	
K172-2	Eng 2 Thrust Press. Sw 3 Thrust OK	-1.72*	141.35*	
K173-3	Eng 3 Thrust Press. Sw 3 Thrust OK	-1.56*	141.35*	
K174-4	Eng 4 Thrust Press. Sw 3 Thrust OK	-1.72*	141.35*	
K175-5	Eng 5 Thrust Press. Sw 3 Thrust OK	-1.97*	138.10*	
K176-6	Eng 6 Thrust Press. Sw 3 Thrust OK	-1.81*	138.10*	
K177-7	Eng 7 Thrust Press. Sw 3 Thrust OK	-1.89*	138.10*	
K178-8	Eng 8 Thrust Press. Sw 3 Thrust OK	-1.81*	138.10*	
K205-9	Eng 1 or 2 or 3 or 4 Prevalve Cutoff Relay Control		141.31*	
K206-9	Eng 5 or 6 or 7 or 8 Prevalve Cutoff Relay Control		137.89*	
K207-9	Eng 1 or 2 or 3 or 4 +1D11 Tops Lock-up	<u>On</u> -0.10*	<u>Off</u> 0.49*	<u>On</u> 3.49*
K208-9	Eng 5 or 6 or 7 or 8 +1D11 Tops Lock-up	<u>On</u> -0.10*	<u>Off</u> 0.49*	<u>On</u> 3.49*

*RDSM Data

Table 11-1. S-IB Electrical System Measurements (Sheet 4 of 4)

MEAS NO.	TITLE	REMARKS/RESULTS RANGE TIME-(SEC)					
K211-12	+1D11 IECO	137.91*					
K212-12	+1D21 IECO	137.91*					
K213-12	+1D11 OECO	141.32*					
K214-12	+1D21 OECO	141.32*					
K215-12	+1D11 RSCR Cutoff	Normal					
K216-12	+1D21 RSCR Cutoff	Normal					
M1-9	Meas Volt No. 1 (+1D81 Ind)	Normal					
M2-9	Meas Volt No. 2 (+1D82 Ind)	Normal					
M9-12	Meas Volt (+1D89 Ind)	Normal					
M16-12	D21 Bus Voltage	Within expected range					
M17-12	D11 Bus Voltage	Within expected range					
M18-12	D10 Battery Current	Battery currents are approximately as predicted					
M19-12	D20 Battery Current	Battery currents are approximately as predicted					
		Start	Finish	Δt	%	Fire	DC Volt
M42-400	EBW No. 1 Volt(Retro No. 1)	134.9	135.55	0.65	86.5	142.6	2378
M43-400	EBW No. 2 Volt(Retro No. 1)	135.1	135.9	0.8	86.0	142.6	2365
M44-400	EBW No. 1 Volt(Retro No. 2)	134.9	135.7	0.8	86.0	142.6	2365
M45-400	EBW No. 2 Volt(Retro No. 2)	135.0	135.7	0.7	86.5	142.6	2378
M46-400	EBW No. 1 Volt(Retro No. 3)	134.9	135.5	0.6	86.0	142.6	2365
M47-400	EBW No. 2 Volt(Retro No. 3)	135.0	135.7	0.7	87.0	142.6	2392
M48-400	EBW No. 1 Volt(Retro No. 4)	134.9	135.6	0.7	86.0	142.7	2365
M49-400	EBW No. 2 Volt(Retro No. 4)	135.1	135.85	0.75	87.5	142.7	2406
M63-11	Destruct EBW Voltage No. 1	No Change					
M64-11	Destruct EBW Voltage No. 2	No Change					
M68-400	EBW Volt No. 1(Separation)	134.9	135.55	0.65	86.5	142.6	2378
M69-400	EBW Volt No. 2(Separation)	135.1	135.8	0.70	86.5	142.6	2378

*RDSM Data

Evaluation of the EBW firing unit response indicated that all EBW firing units charged and discharged. All firing units operated similarly, discharging to approximately 125v or less, then decaying as expected.

The ramp generator, used to produce a ramp output measurement at liftoff (K2-12), IECO (K67-12) and OECO (K3-12), showed a ramp output five times during the flight. The first ramp output (K2-12) occurred at approximately 0.42 seconds. This compares favorably with the ESE DEE-6 output. The second and third ramp outputs were not desired events, because they were triggered as a result of the switch selector command signals, TM Cal Off at 25.43 seconds; and again TM Cal Off, at 125.24 seconds. Both undesired ramps were triggered unintentionally, although not totally unexpectedly, and had no effect either upon the operation of the stage networks or on data retrieval. These extraneous ramp output pulses were easily correlated to the actual flight events occurring in the Flight Sequence Program. The forth and fifth ramp outputs, IECO and OECO, occurred when normally expected.

The data on measuring voltage 1D81, 1D82 and 1D89 (figures 11-1 through 11-3) showed satisfactory performance of the voltage supplies. The voltage deviation for the three power supplies did not exceed 10 millivolts, which was less than one-fifth of one percent of the supply voltage, and well within the tolerance of ± 12 millivolts.

The performance of the two batteries was very close to predicted and is shown in figures 11-4 through 11-7. The battery power consumption from activation to loss of signal (LOS) at 382 seconds is tabulated in table 11-2 for each battery.

Table 11-2. S-IB Stage Battery Power Consumption

BATTERY	POWER CONSUMPTION						
	ACTIVATION		FLIGHT	SEP TO LOS		TOTAL	
1D10	%	7.2	% 1.5	%	4.1	%	12.8
	A-M	144	A-M30.8	A-M	81.2	A-M	256
1D20	%	8.0	% 3.1	%	4.1	%	15.2
	A-M	159	A-M63.3	A-M	81.4	A-M	303.7

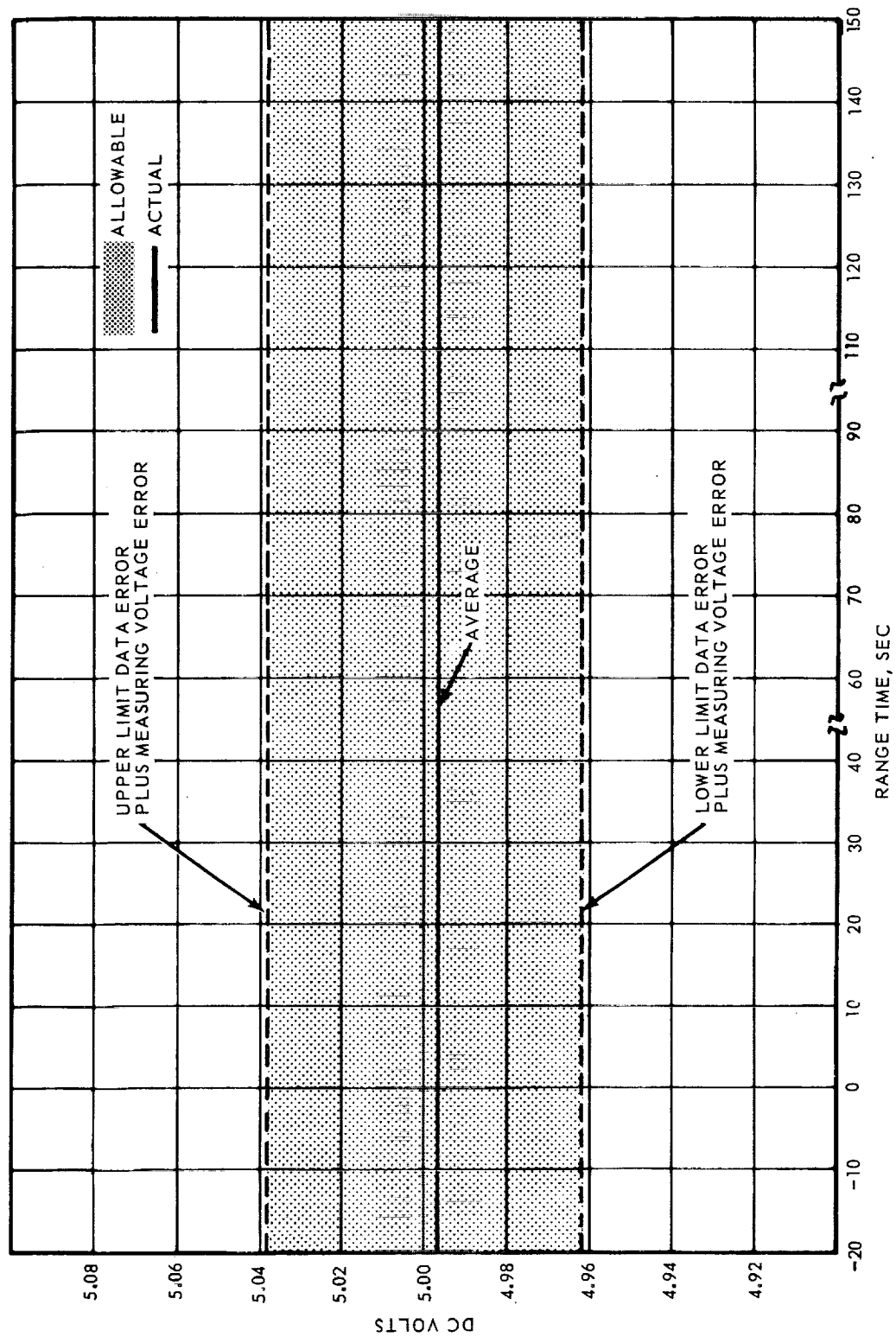


Figure 11-1. Master Measuring Voltage Supply 9A84 (+1D81 Measuring Bus)

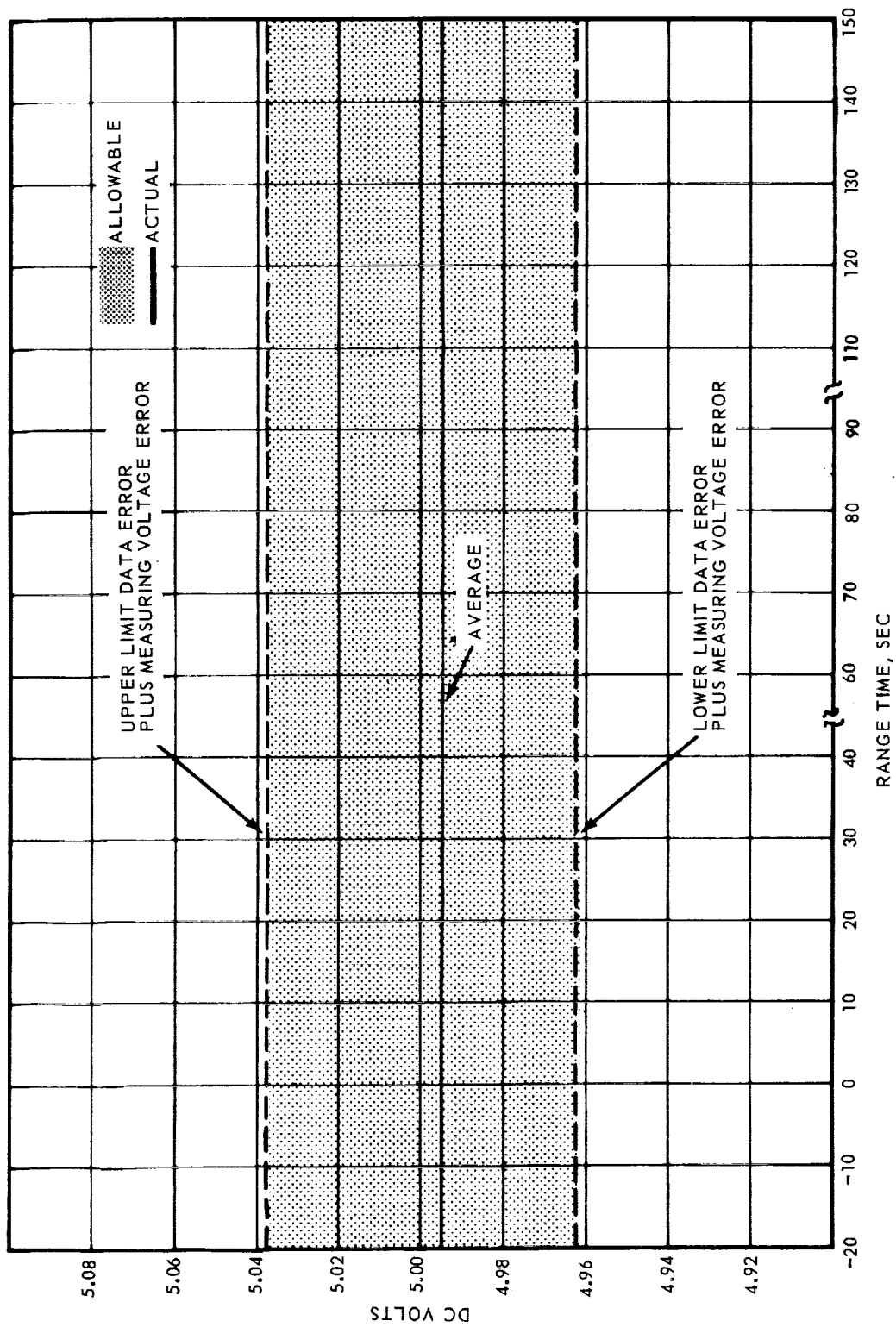


Figure 11-2. Master Measuring Voltage Supply 9A85 ($\pm 1D82$ Measuring Bus)

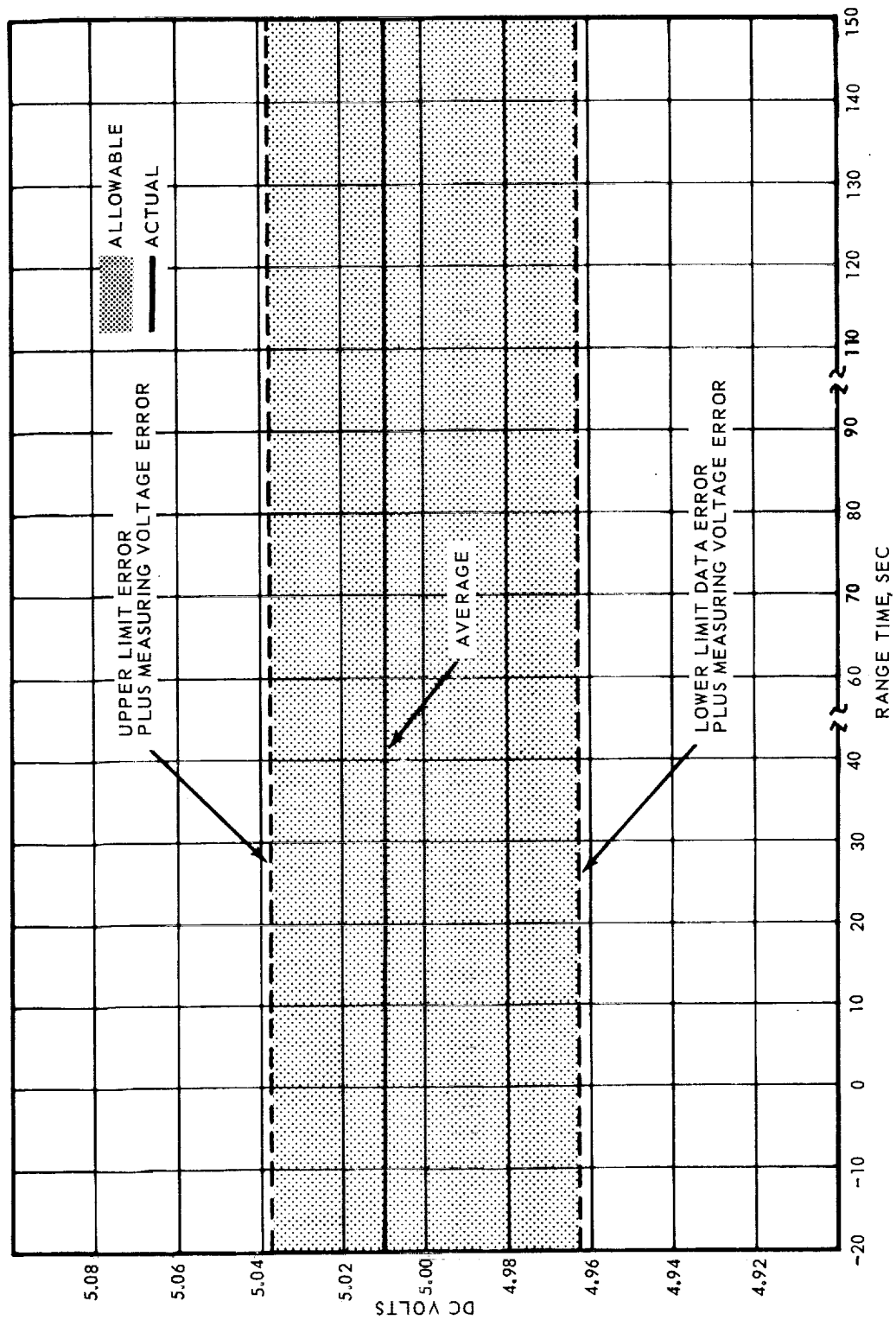


Figure 11-3. Master Measuring Voltage Supply 12A38 (+1D89 Measuring Bus)

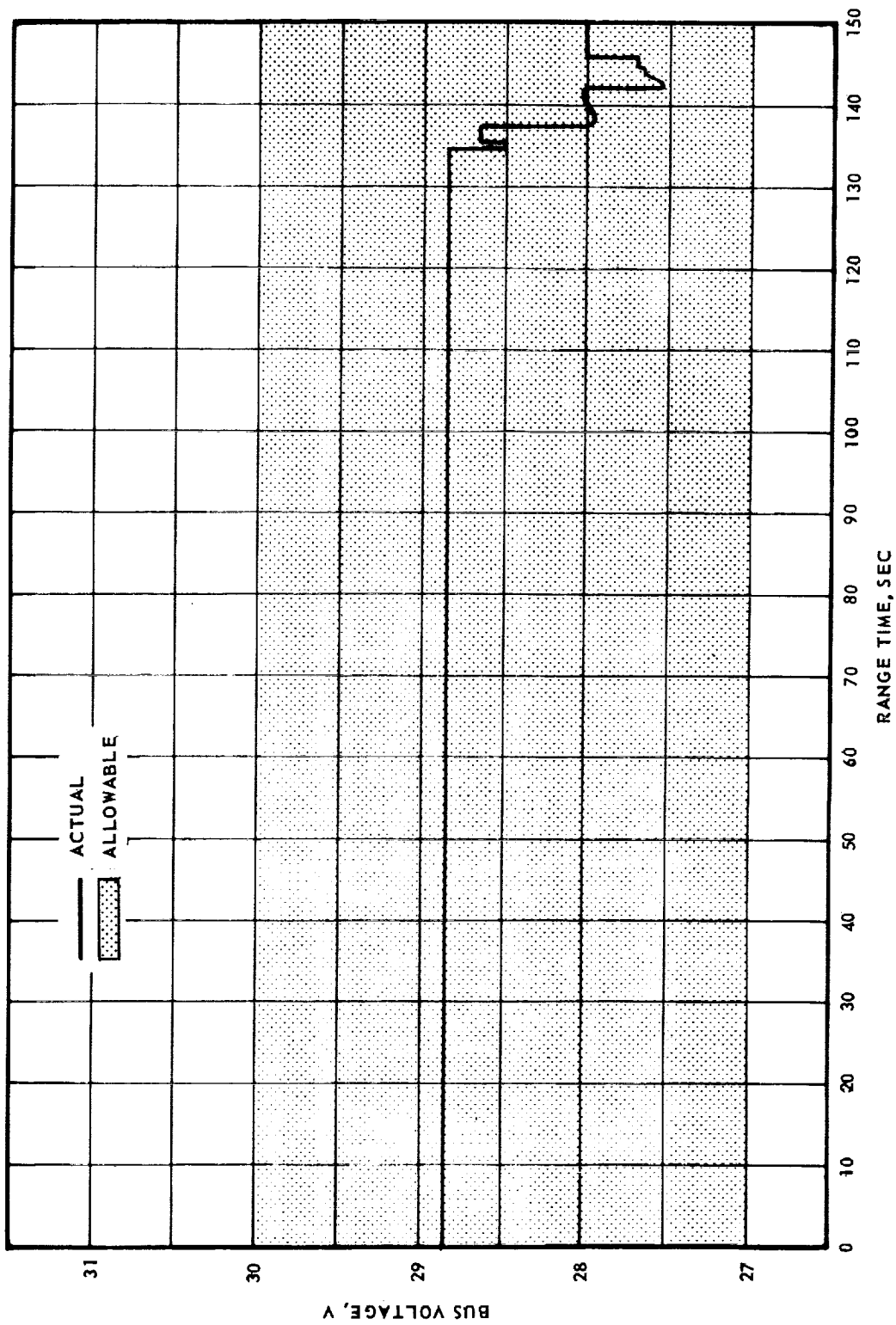


Figure 11-4. S-IB Battery Voltage (1D11)

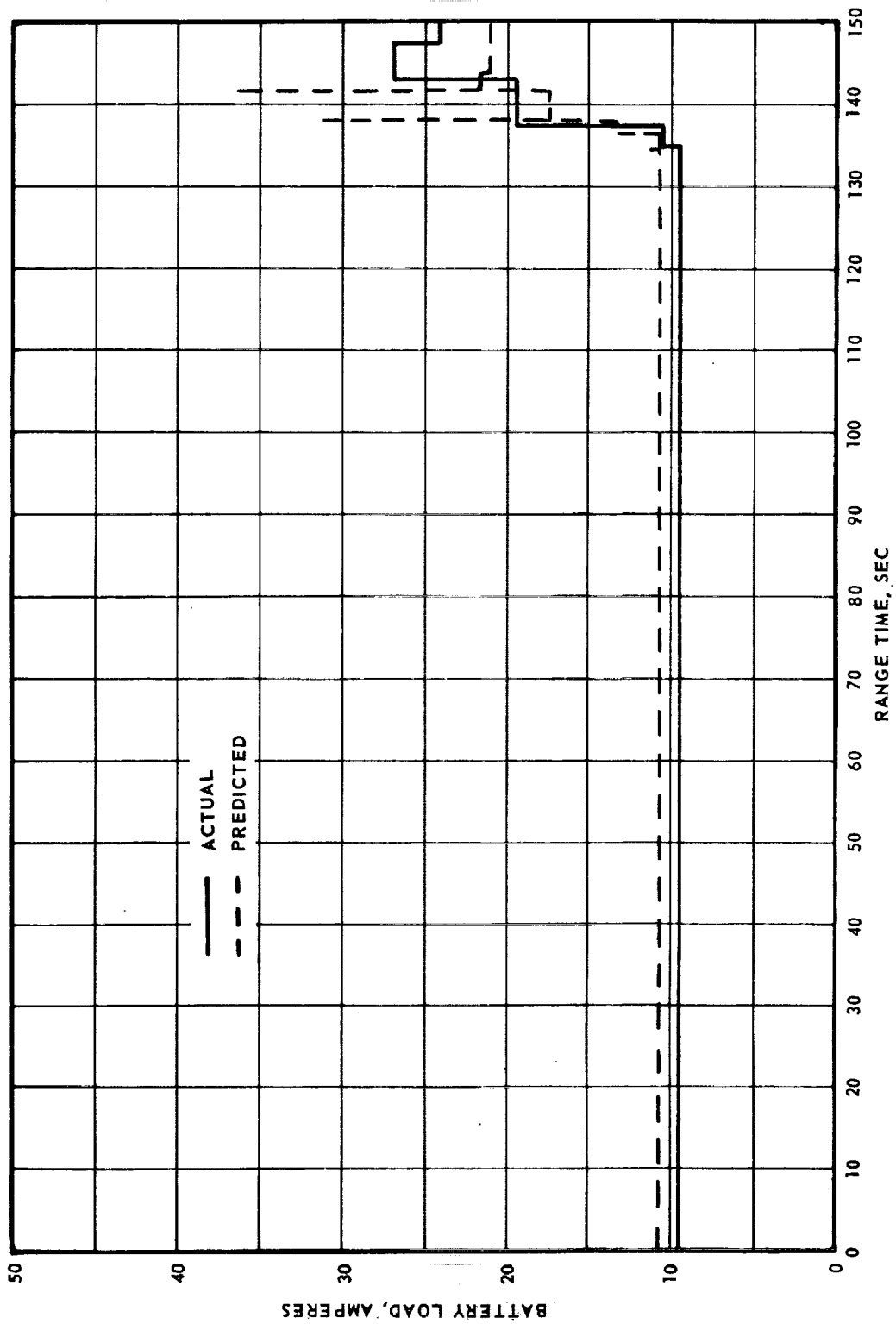


Figure 11-5. S-IB Battery Current (1D10)

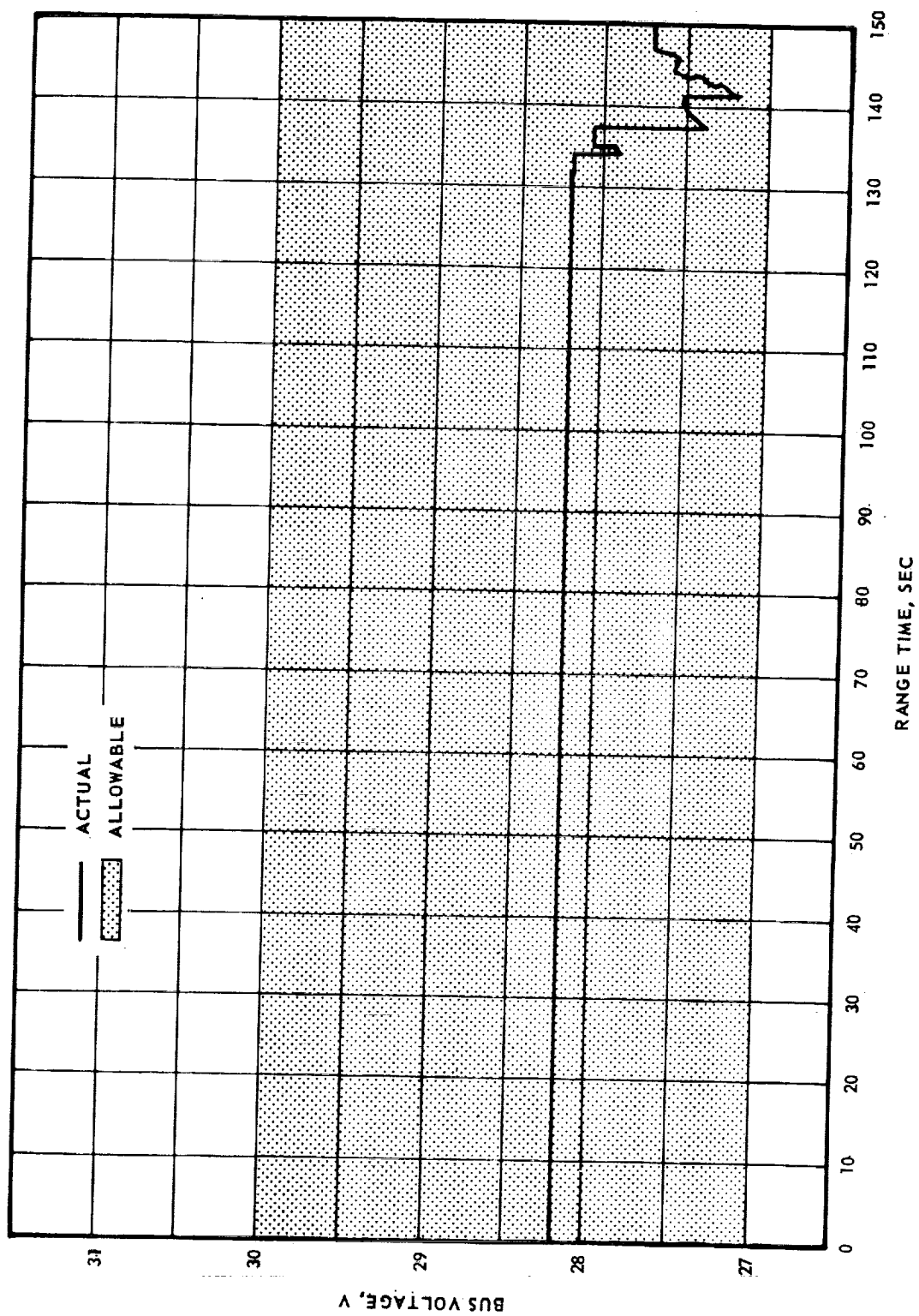


Figure 11-6. S-IB Battery Voltage (1D21)

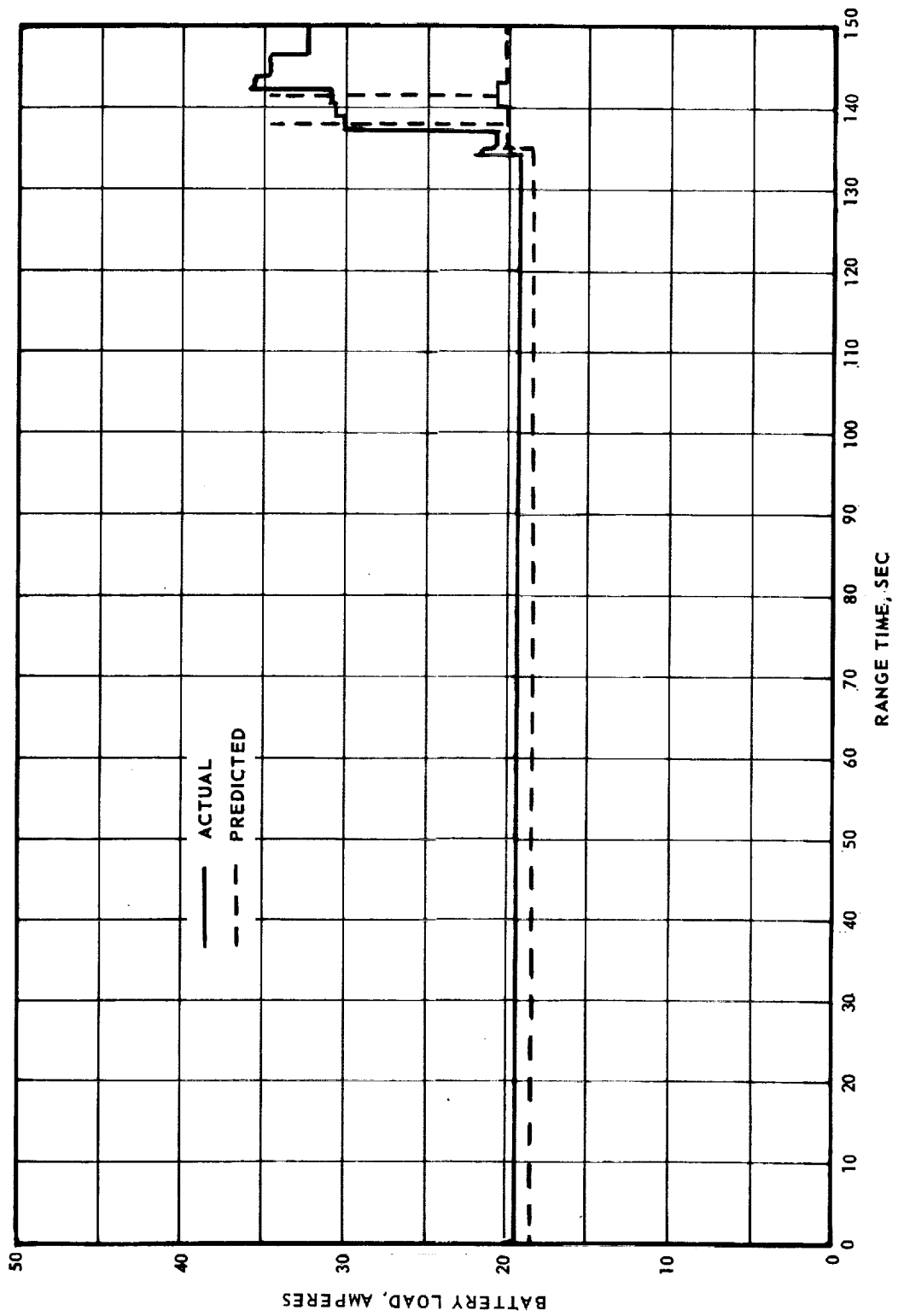


Figure 11-7. S-IB Battery Current (1D20)

Section 12

PRESSURE ENVIRONMENT

12.1 SUMMARY

Base pressure data obtained from SA-208 have been compared with preflight predictions and/or previous flight data and show good agreement. Base drag coefficients were also calculated using the measured pressures and actual flight trajectory parameters.

There were three base pressure measurements made in the S-IB base region; two on the heat shield and one on the flame shield. One measurement on the heat shield was a differential pressure across the shield, whereas the other two measurements were of absolute pressures. The approximate position and instrument number designation of these three measurements are shown in figure 12-1.

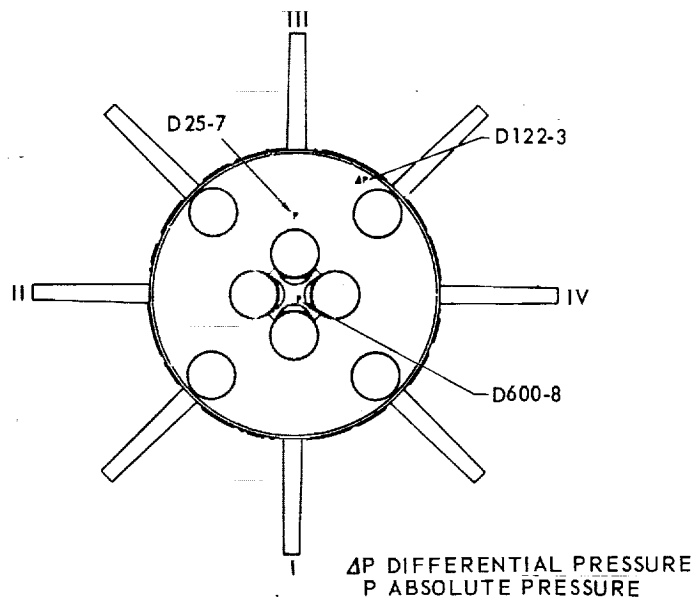


Figure 12-1. S-IB Base Region Pressure Instrumentation

12.2 S-IB BASE PRESSURE

Results of the heat shield and flame shield absolute pressure measurements are shown in figures 12-2 and 12-3, respectively. These data are presented as the difference between measured base pressures and ambient pressure. Values are compared with

the band of data obtained from previous S-IB flights of similar vehicle base configuration and show good agreement. Both the heat shield and flame shield pressure measurements were almost identical to the data from SA-206 and SA-207 flights. The data indicate that during the first 70 seconds of flight (6 N Mi.) the H-1 engine exhausts were aspirating the heat shield region, resulting in base pressures below ambient pressures. In the flame shield area, the aspirating effect was terminated by an altitude of 4 nautical miles. Above these altitudes the reversal of engine exhaust products, due to plume expansion, resulted in base pressures above ambient.

Pressure loading measured near the outer perimeter of the SA-208 heat shield is compared with data from previous flights in figure 12-4. The SA-208 data remained on the lower side of the data band during the first 7 nautical miles of flight. This also occurred on the SA-206 and SA-207 flights and the agreement is very good.

Also shown on the figure are the predicted ΔP deviations for the heat shield. The flight values are well within these limits during the entire flight. Above 15 nautical miles altitude, the SA-208 flight data return to near zero indicating the engine compartment has vented to near base pressure. This is normal and has occurred on all previous flights except SA-205.

12.3 S-IB BASE DRAG

Base drag coefficients calculated from the SA-208 data are compared to the data band from previous flights in figure 12-5. The comparison is very good considering the drag coefficients were determined from measurements taken at only two locations on the base. However, they are representative of average base pressures.

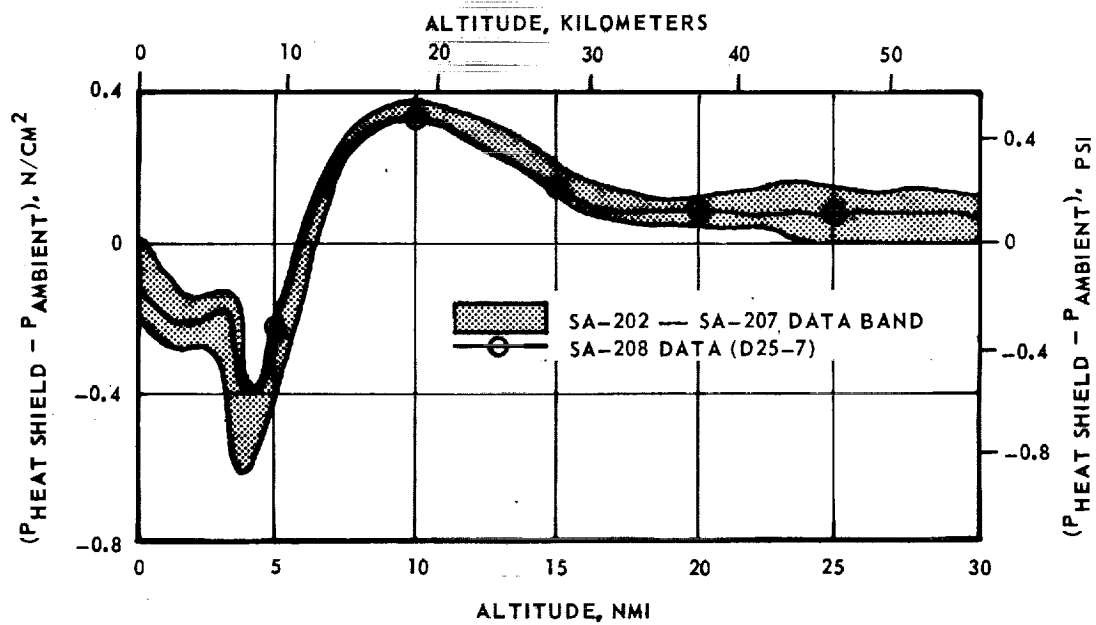
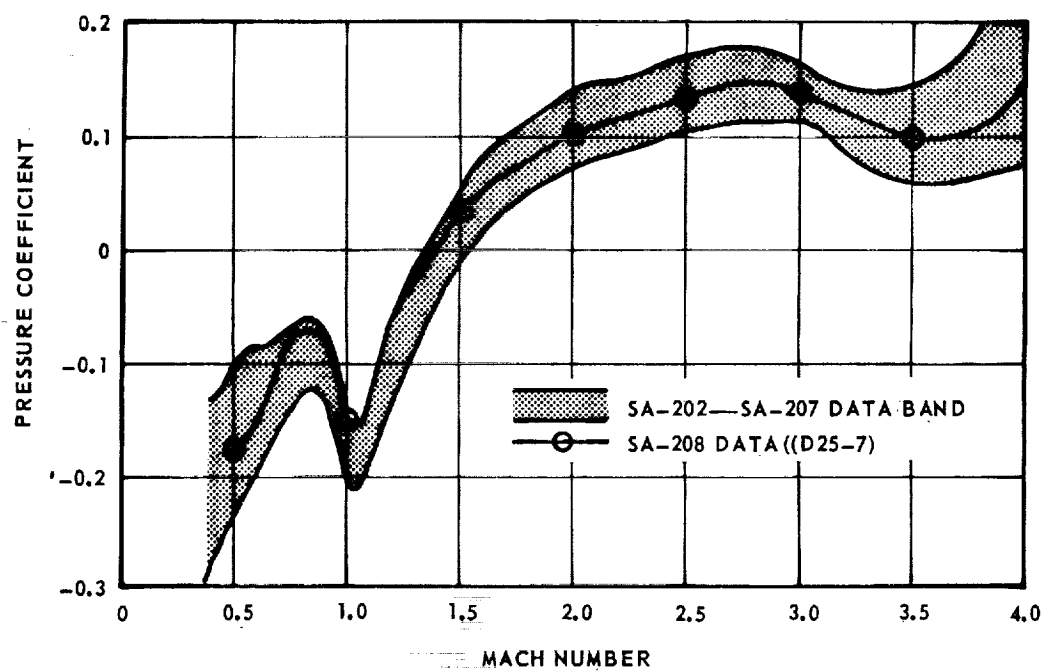


Figure 12-2. S-IB Heat Shield Pressure

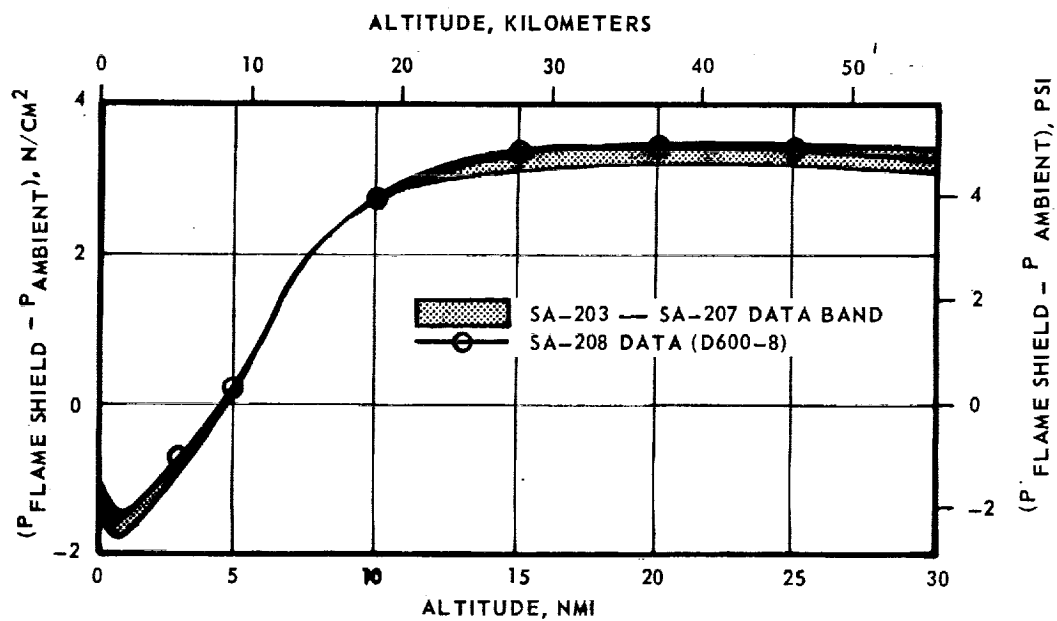
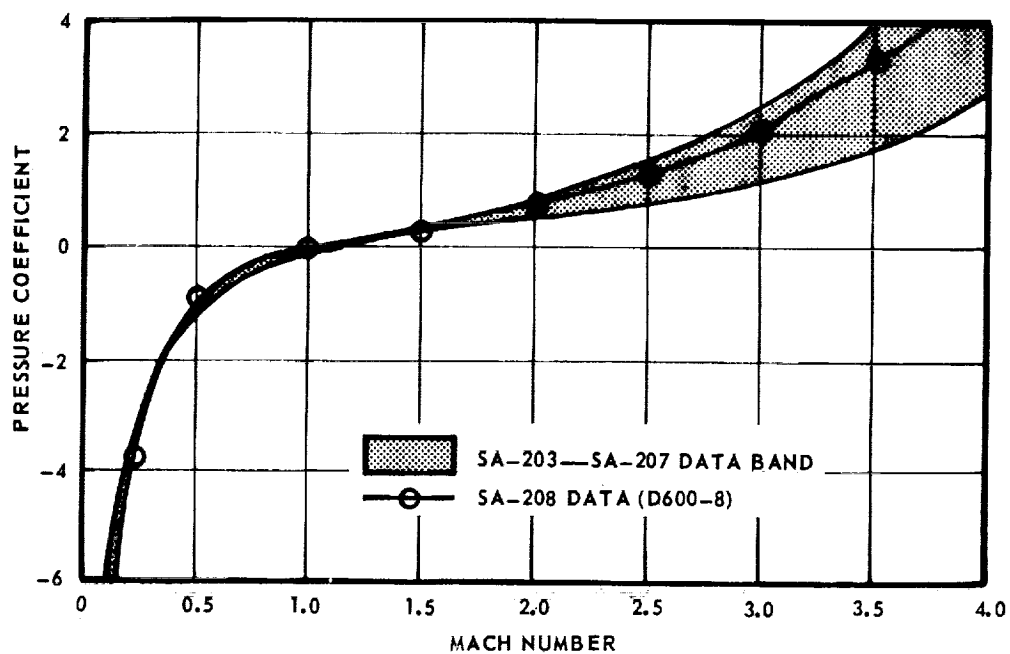


Figure 12-3. S-IB Flame Shield Pressure

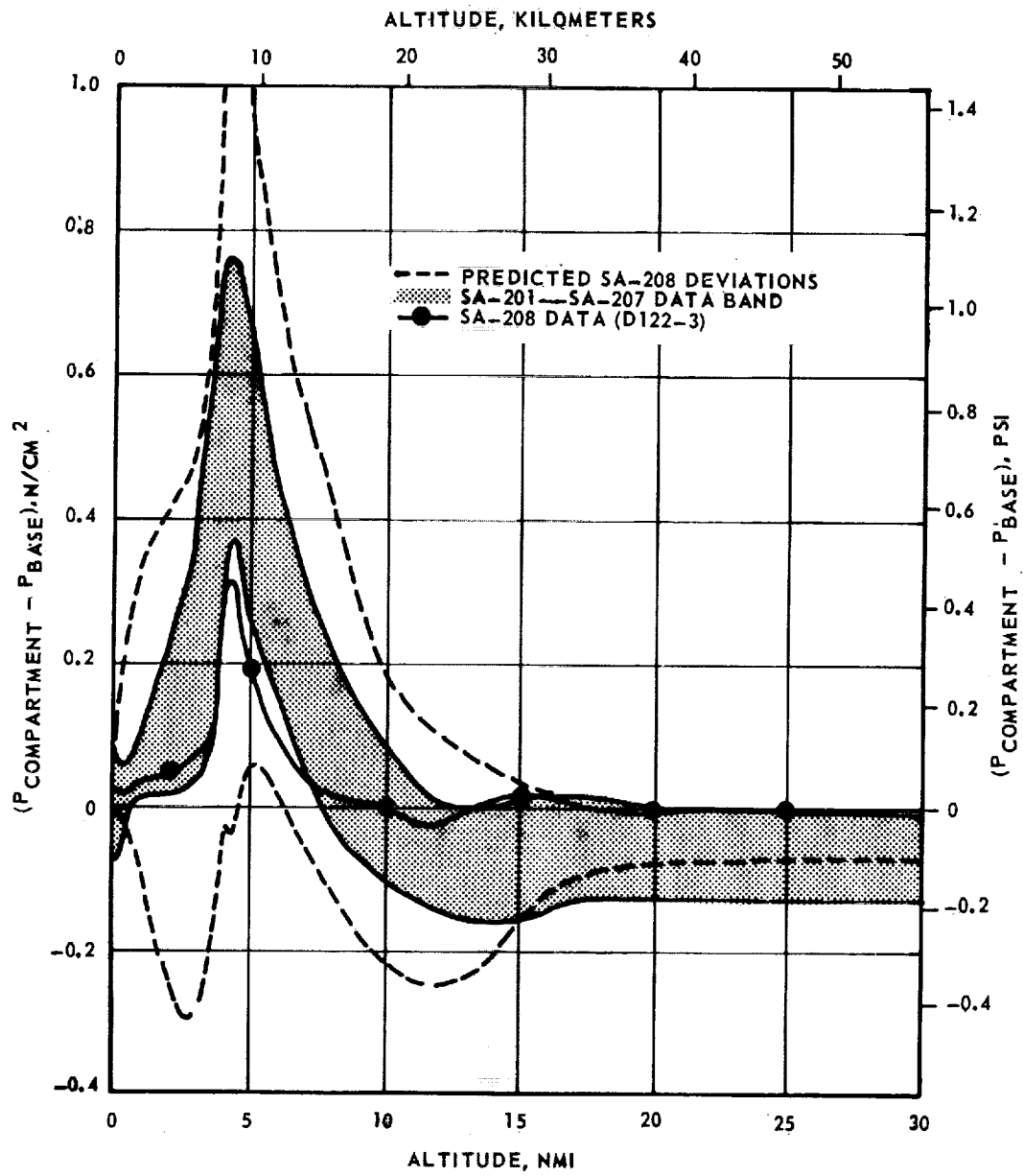


Figure 12-4. S-IB Heat Shield Loading

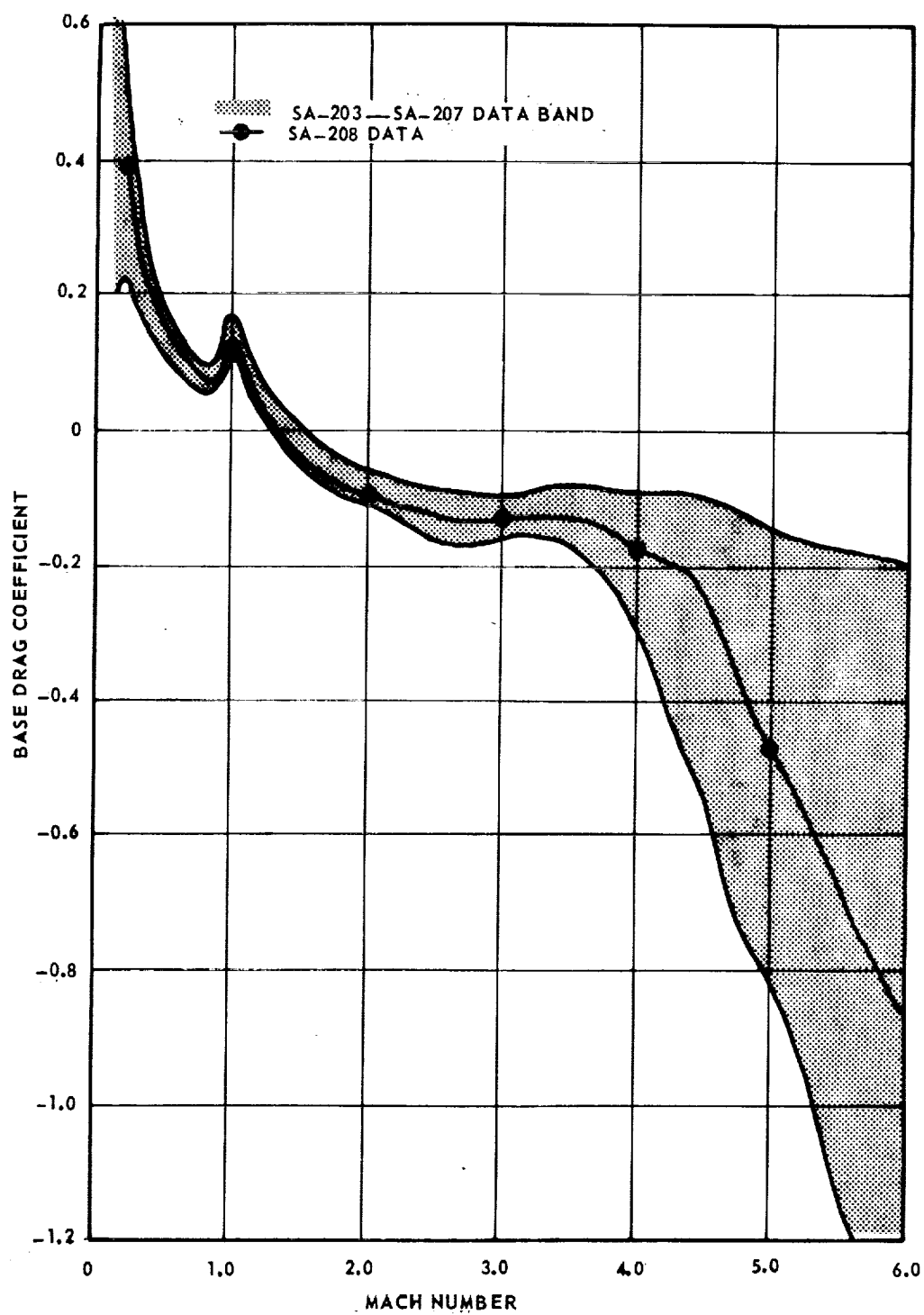


Figure 12-5. S-IB Base Drag Coefficient

Section 13

THERMAL ENVIRONMENT

13.1 SUMMARY

Data traces from the seven SA-208 S-IB stage base thermal measurements have been compared with corresponding data from the flights of SA-203 through SA-207. These comparisons indicate an SA-208 base region thermal environment of comparable magnitude, with the flame shield radiant data trend being similar to that recorded on SA-207. All measured thermal environment data were well below S-IB stage design levels.

The S-IB stage base region thermal environment of SA-208 was recorded by three gas temperature thermocouples and four heat flux calorimeters. The positioning of each of these seven thermal measurements in the heat shield and flame shield areas is shown in figure 13-1. Data from these SA-208 measurements are compared with bands formed by the maximum and minimum data extremes recorded by comparable instrumentation on previous flights.

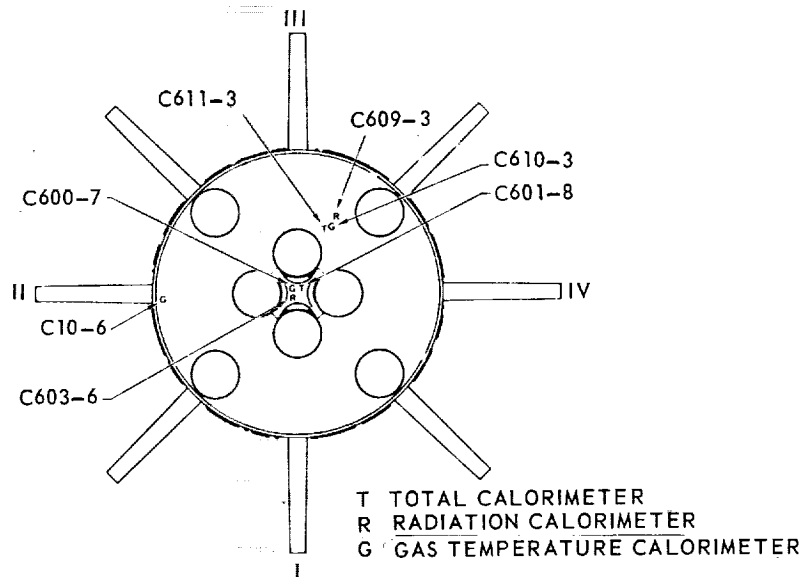


Figure 13-1. S-IB Base Region Thermal Instrumentation

13.2 S-IB BASE HEATING

Heat shield thermal environment data are presented as a function of vehicle altitude in figures 13-2 through 13-5. As indicated by these comparison plots, the SA-208 heat shield thermal environment was nominal. Data trends were consistent with those established on previous flights and deviations from previous data extremes were minor.

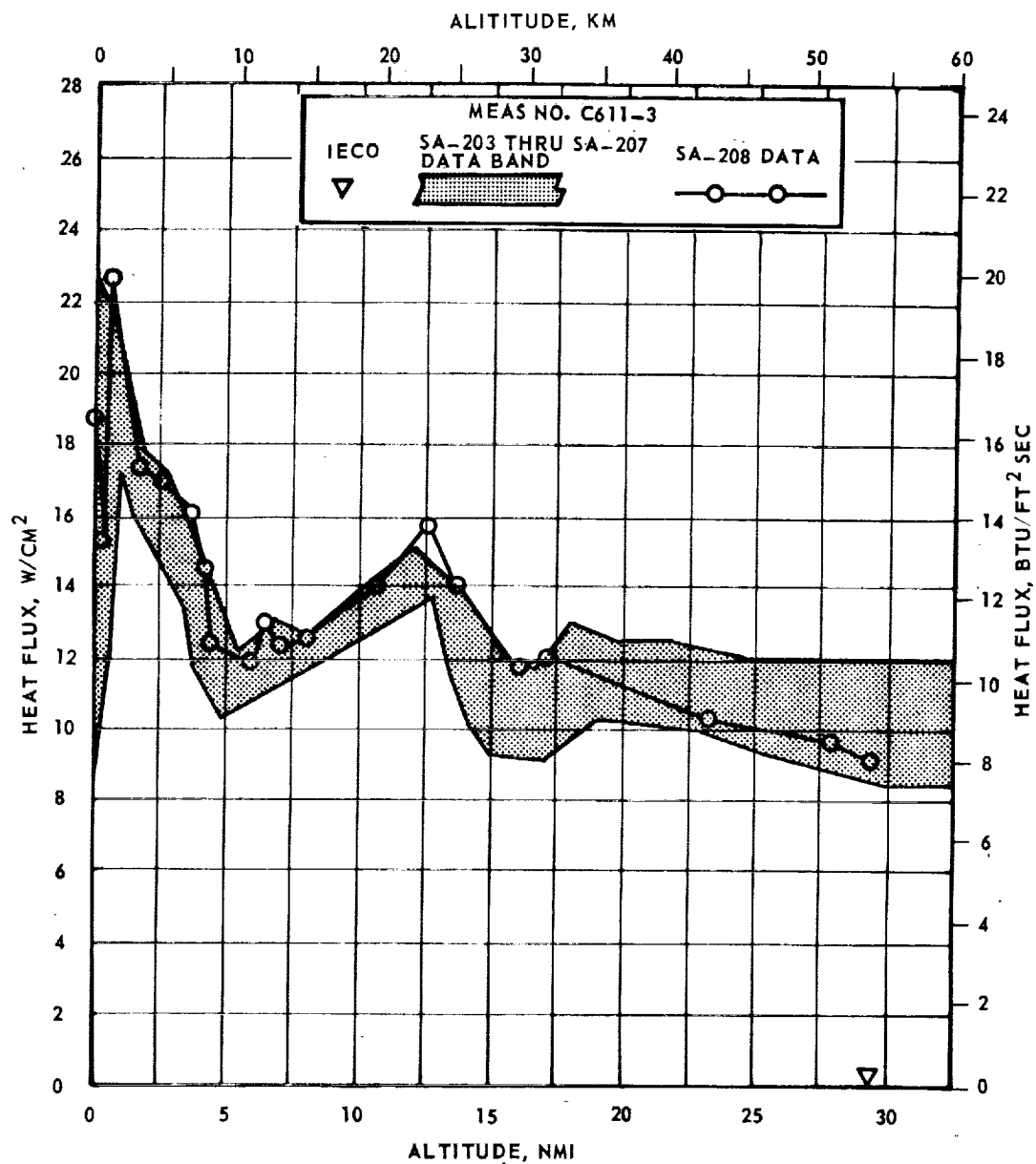


Figure 13-2. Heat Shield Inner Region Total Heating Rate

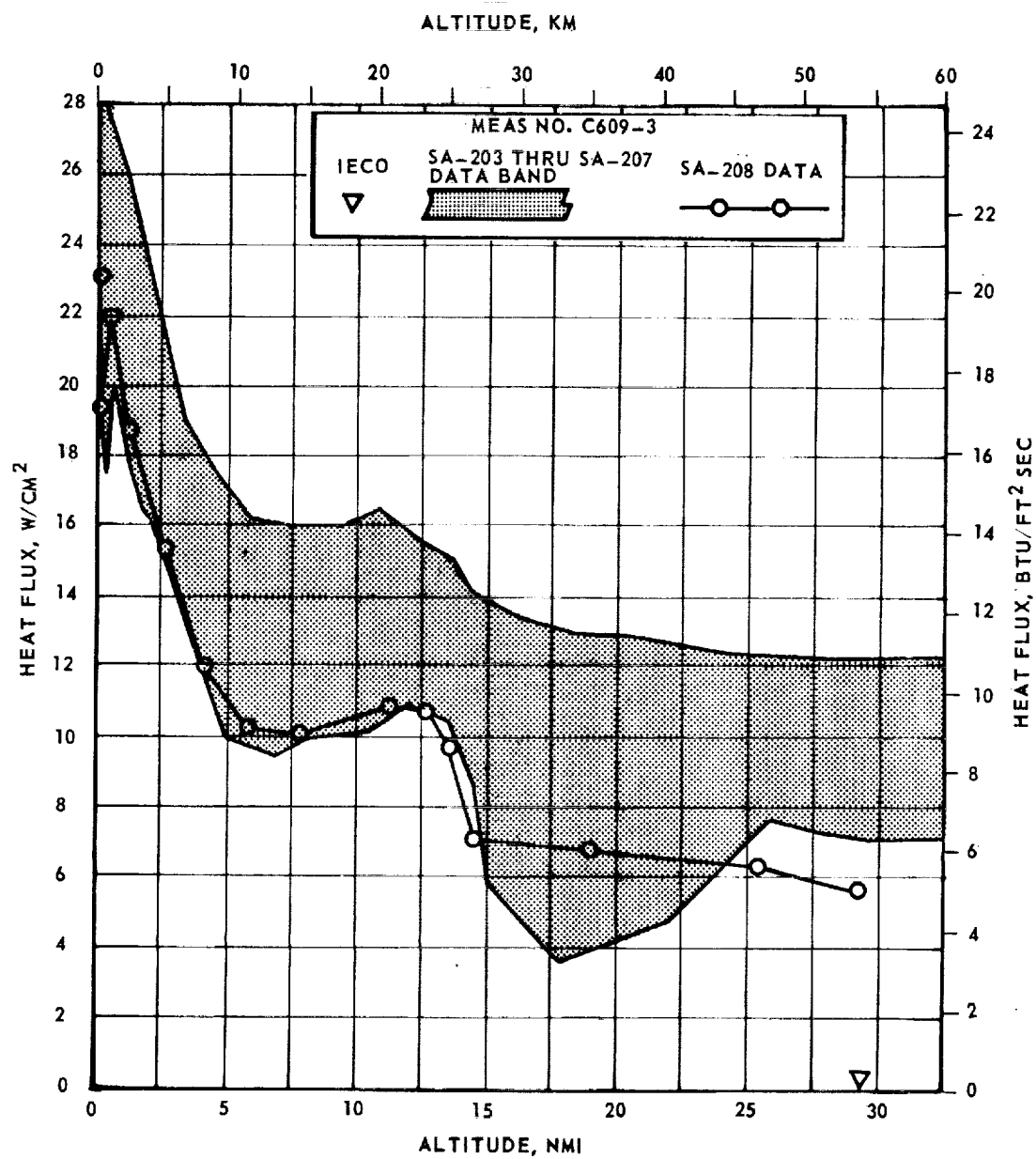


Figure 13-3. Heat Shield Inner Region Radiation Heating Rate

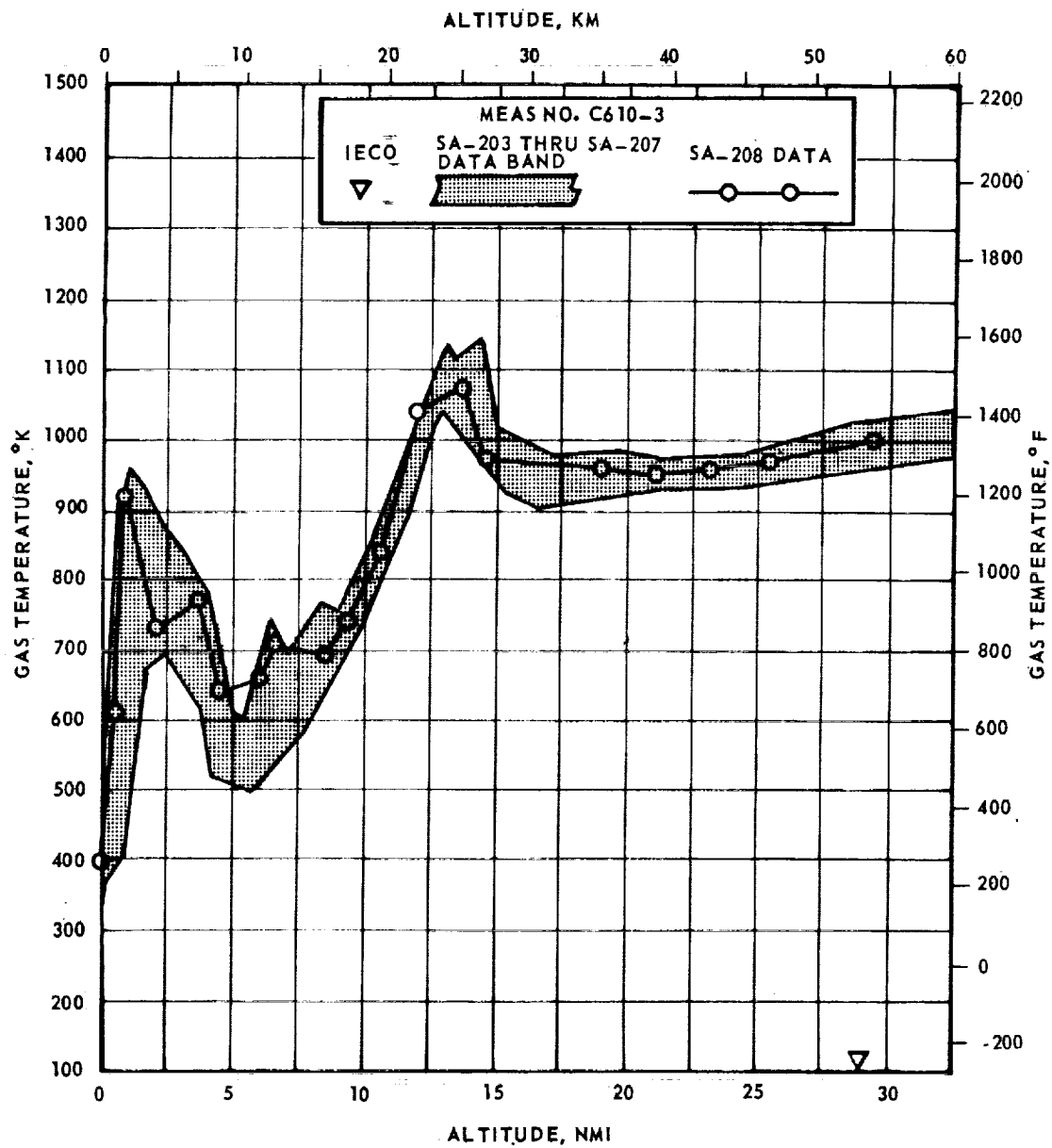


Figure 13-4. Heat Shield Inner Region Gas Temperature

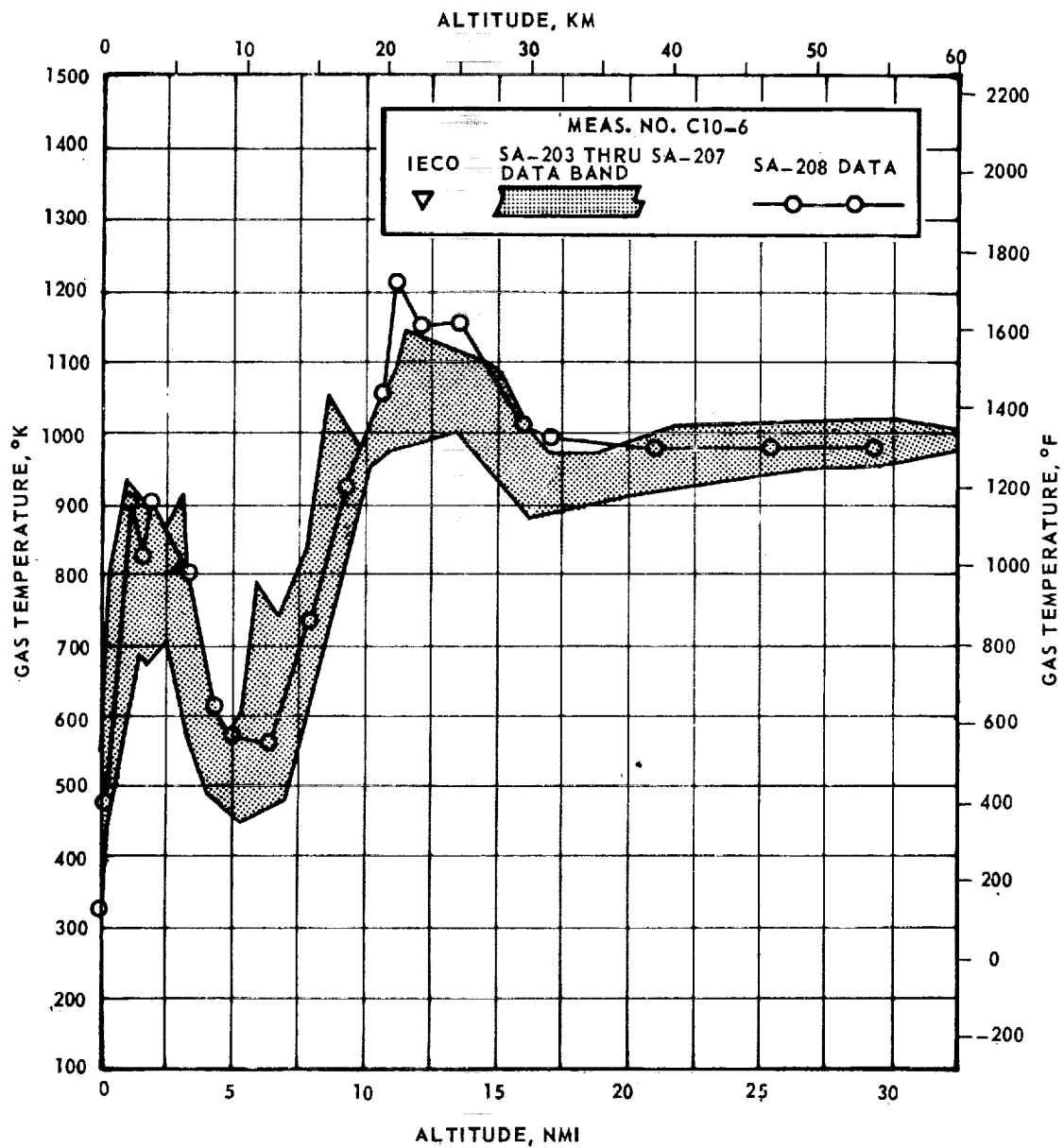


Figure 13-5. Heat Shield Outer Region Gas Temperature

In the flame shield area the recorded SA-208 thermal environment was similar to that experienced on SA-207. Total heating rate and gas temperature data were generally in the upper portion of the previous data bands through the first 55 seconds of flight; i.e., to a vehicle altitude of approximately 3.35 n mi. These data are presented vs. vehicle altitude in figures 13-6 and 13-7, respectively. During this same period, the SA-208 flame shield radiation data (presented in figure 13-8) were generally above the data trend established through the flight of SA-206, but slightly below that of SA-207. At an altitude of approximately 4.5 n mi, the flame shield thermal environment leveled off to a steady nominal level. At this altitude the inboard engine exhaust plumes had expanded sufficiently to interact and cause a sustained flow reversal of exhaust gases onto the flame shield. This reversal held the relatively cool (800°K) and opaque inboard engine turbine exhaust gases near the flame shield surface, and resulted in a substantial reduction in the magnitude of the flame shield thermal environment.

Because of the similarity of the SA-208 and SA-207 data, possible causes of the flame shield radiant heating deviations were again investigated and still no definite conclusion was reached as to why the data differed from the trend established during the previous four flights. The data appear to be valid. The flame shield and turbine exhaust duct configurations were essentially unchanged from previous vehicles since SA-203.

Three explanations for more radiation reaching the flame shield radiometer have been offered:

- a. A reduction in opacity of the turbine exhaust gases.
- b. Sustained local afterburning of the turbine exhaust gases.
- c. A variation in incident radiation correlated to the variation in inboard engine thrust level.

A possible correlation between inboard engine thrust and flame shield radiation has been investigated and a comparison of the data for flights SA-203 to SA-208 is shown in figure 13-9. The apparent correlation suggests a mechanism whereby the increased thrust level of the inboard engines may be responsible for the decreased opacity of the turbine exhaust gases, but analytical confirmation is not possible within the state of the art.

Although available data will not support a final conclusion as to the cause of the increased flame shield radiant heat level, the flame shield because of its high thermal design capability, is not in jeopardy as shown in figures 13-10, 11 and 12. Since the reroute of the inboard engine turbine exhaust duct, effective on SA-203, the recorded flame shield radiant heat load through the first 55 seconds of flight has not exceeded 50 percent of the design level; beyond 55 seconds of flight (above an altitude of 4 n mi) recorded data have been below 15 percent of the radiation design level. No further action is contemplated.

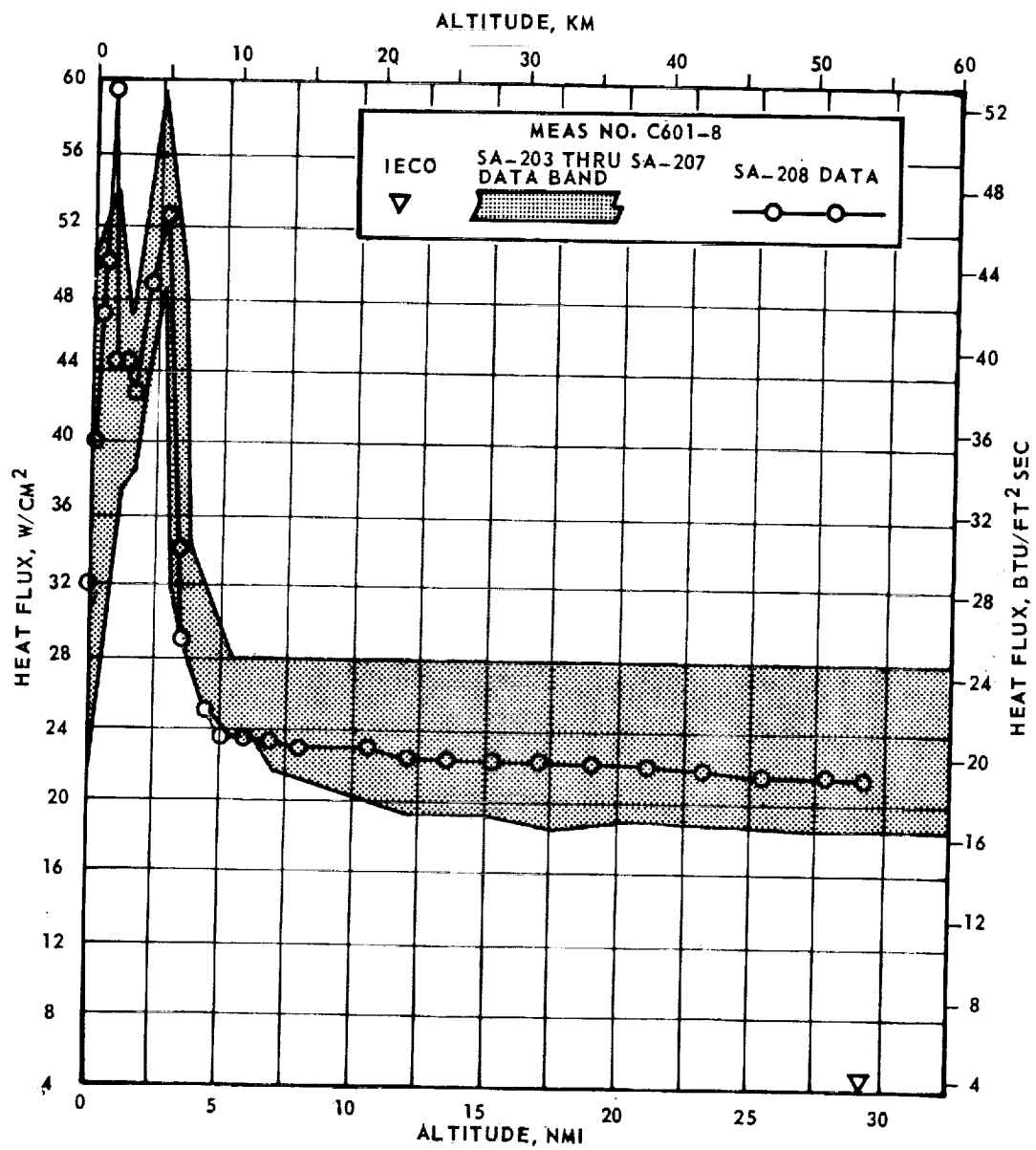


Figure 13-6. Flame Shield Total Heating Rate

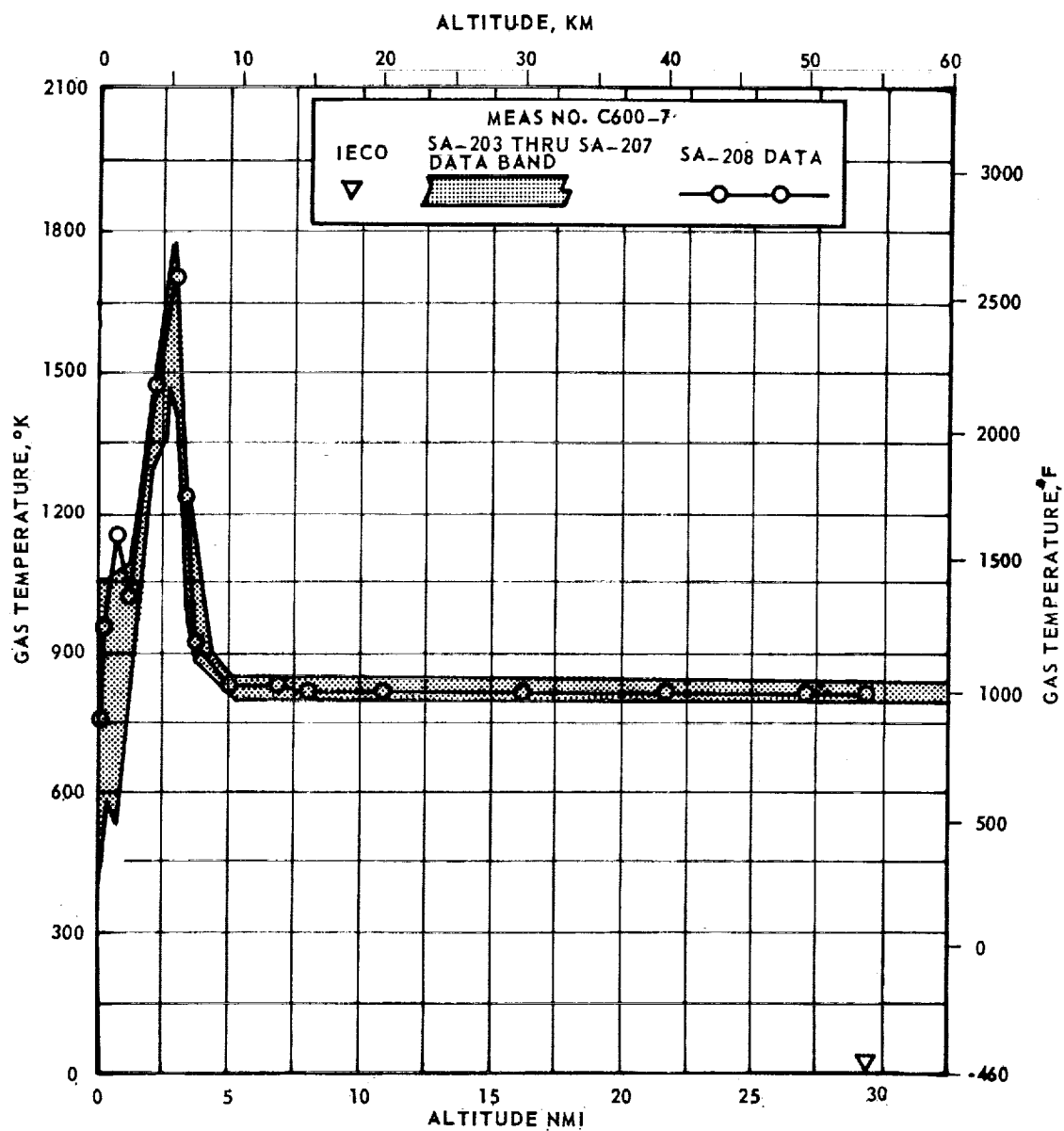


Figure 13-7. S-IB Stage Flame Shield Gas Temperature

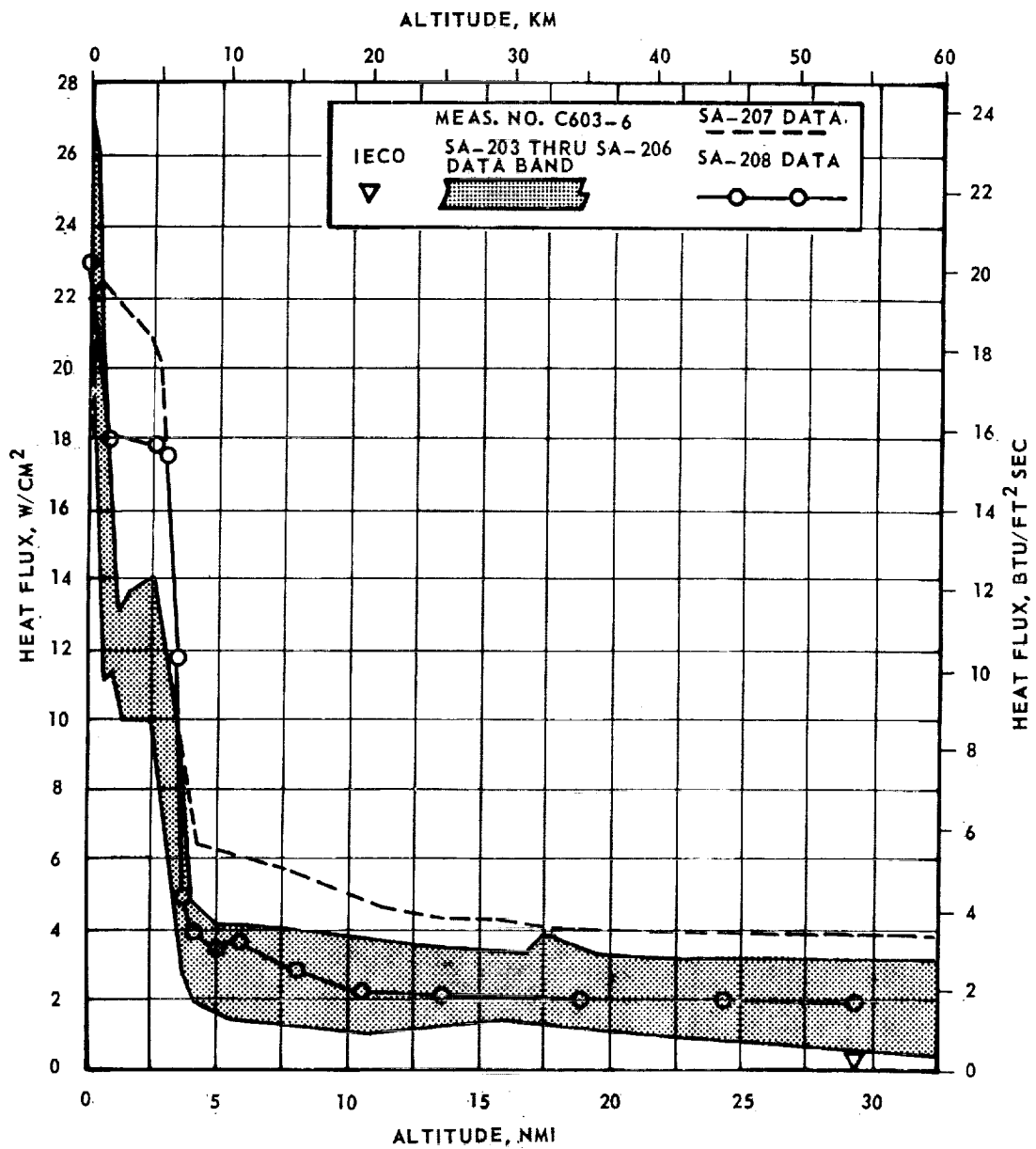


Figure 13-8. S-IB Stage Flame Shield Radiation Heating Rate

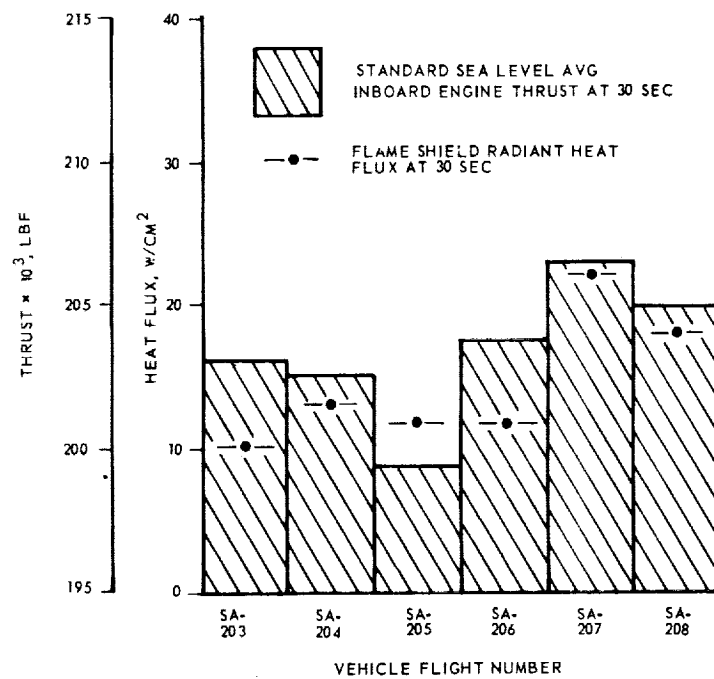


Figure 13-9. Comparison Between Inboard Engine Thrust and Flame Shield Radiation

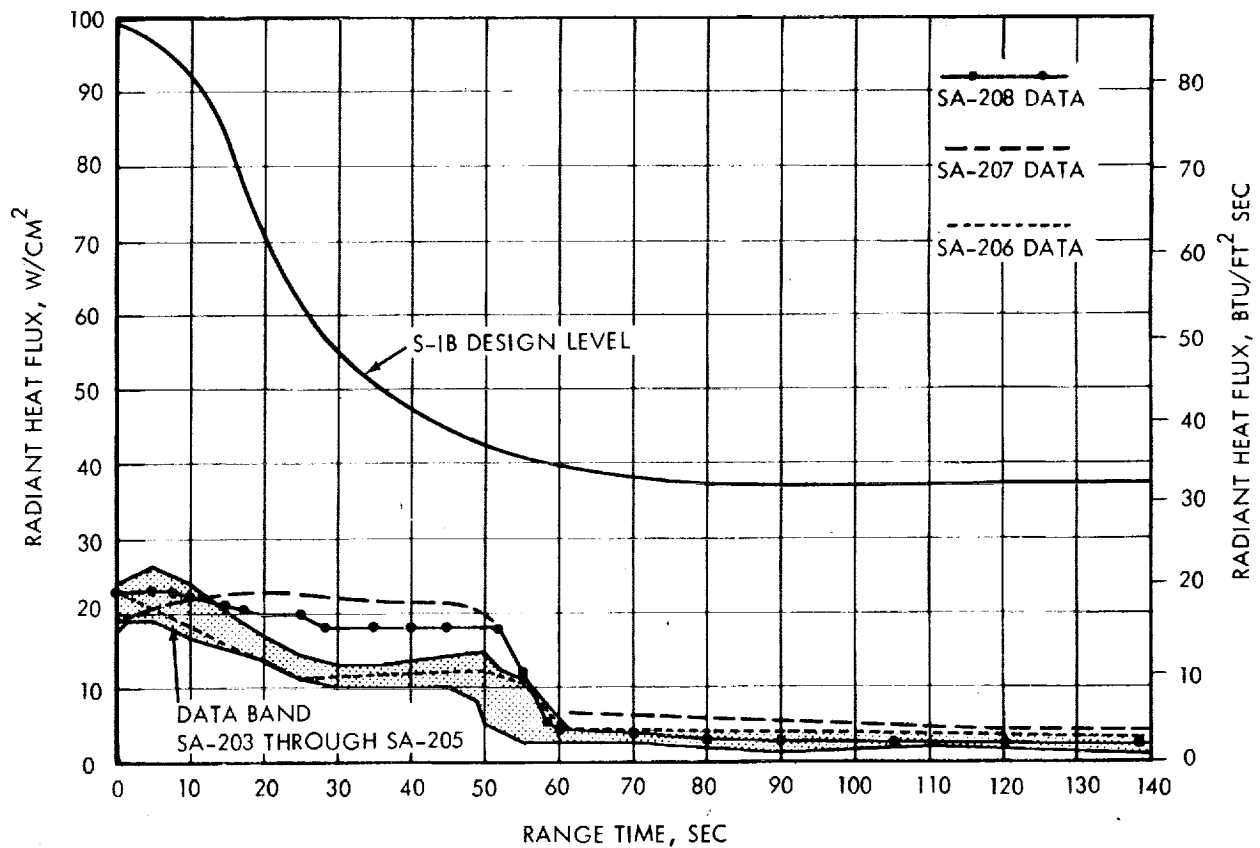


Figure 13-10. Comparison of Flame Shield Radiant Heating Data with Design Level

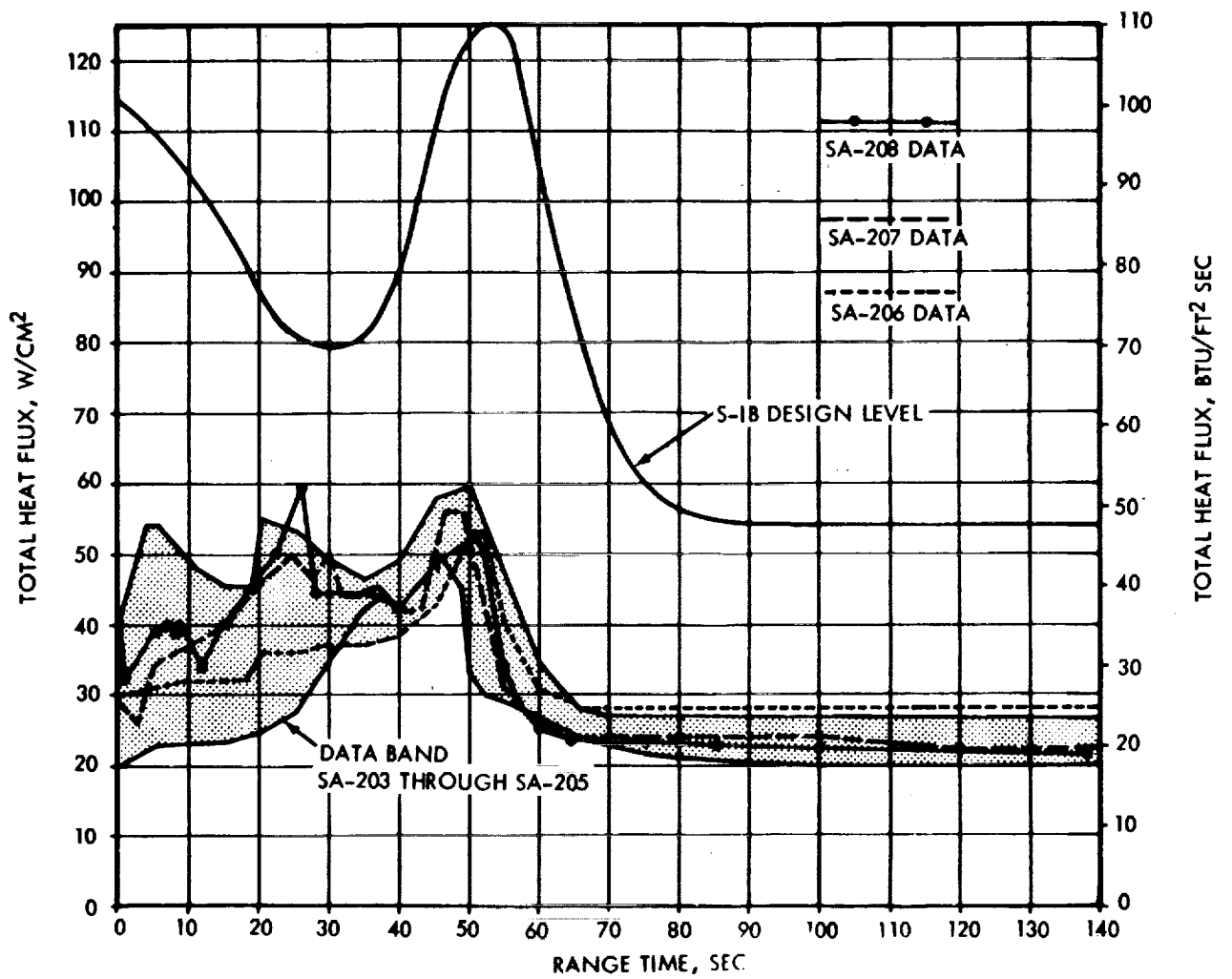


Figure 13-11. Comparison of Flame Shield Total Heating Data with Design Level

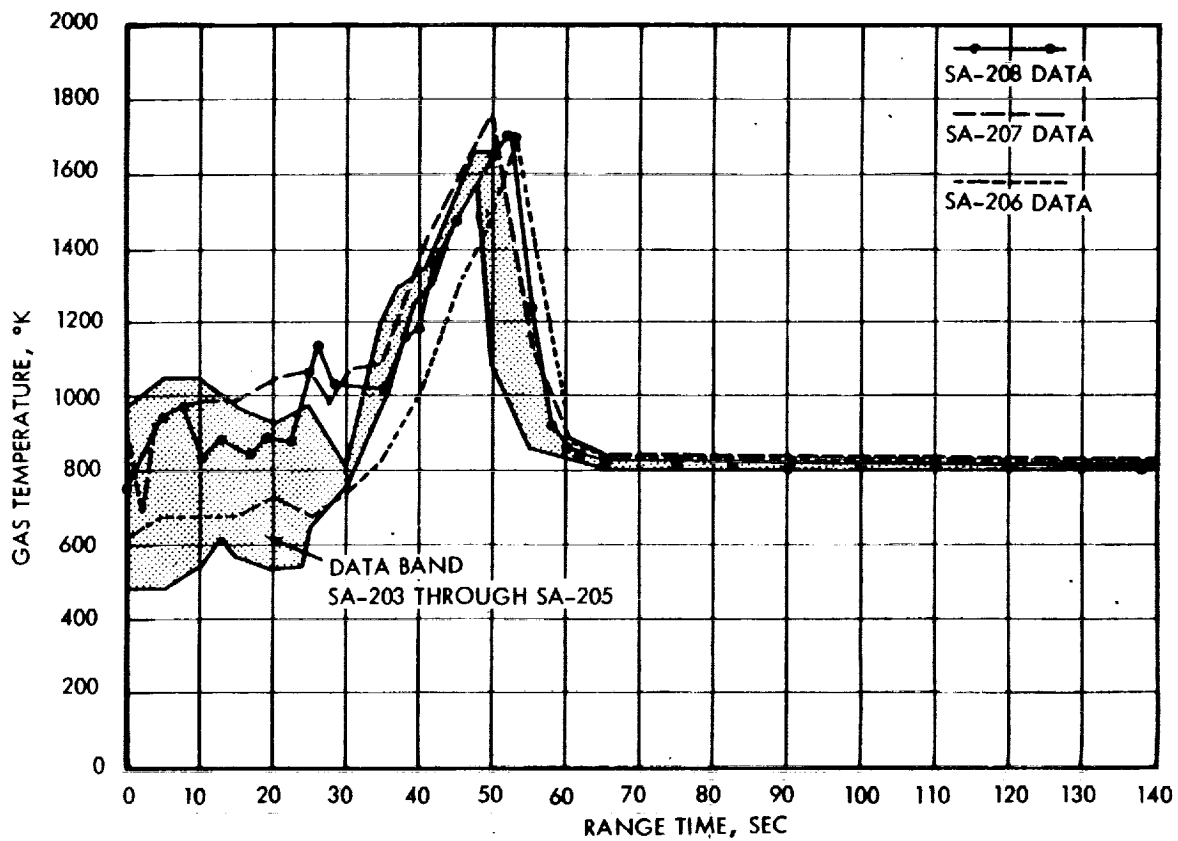


Figure 13-12. Comparison of Flame Shield Gas Temperature Data with Design Level

Section 14

ENVIRONMENTAL CONTROL SYSTEM

14.1 SUMMARY

Thermal conditioning of the S-IB stage forward and aft compartments was satisfactory during prelaunch operations. Critical component temperatures in the instrument and engine compartments were maintained well within their qualification limits.

14.2 S-IB ENVIRONMENTAL CONTROL

During prelaunch operations, measurement 12K22 was monitored to assess ECS flow and supply temperature requirements for maintaining the engine compartment temperature within the specified limits of 53 and 75°F. For SA-208 this measurement indicated that the aft compartment was maintained at approximately 60°F for 7 hours prior to liftoff. In maintaining this temperature, the ECS flow to the compartment was nominal, with GN₂ being supplied at 300 lbm/min with a measured interface temperature of 131°F.

As shown by the data presented in figure 14-1, the S-IB stage engine compartment flight thermocouples (measurements XC61-1 through XC61-4) recorded prelaunch temperatures below the 60°F indicated by 12K22. This was due primarily to the positioning of the four flight instruments, and in part to their data recording accuracy.

Within the S-IB stage instrument compartment, two battery case temperature measurements were taken prior to liftoff. Recorded data from these measurements, WXC528-12 and WXC529-12, indicate the battery temperatures remained at approximately 74°F throughout countdown. This temperature was maintained by a GN₂ conditioning mass flow of 45 lbm/min at a recorded compartment interface temperature of 77°F.

It was concluded that the critical components in the engine and instrument compartments were well within their qualification limits.

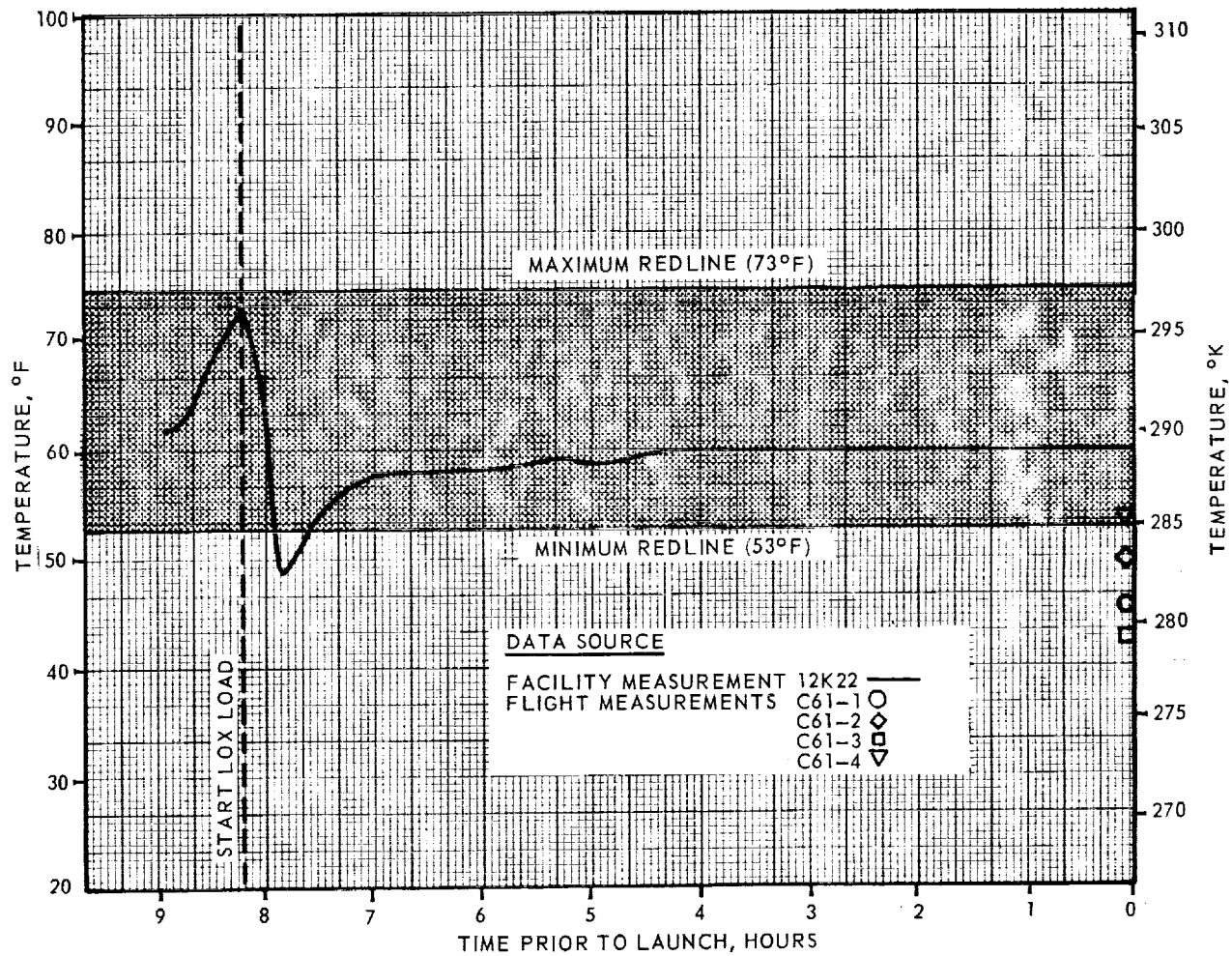


Figure 14-1. S-IB Engine Compartment Temperature

Section 15

DATA SYSTEMS

15.1 S-IB MEASUREMENTS EVALUATION

Performance of the flight measuring system on the S-IB stage was satisfactory, resulting in an overall measurement system reliability of 100 percent. The stage had 266 measurements scheduled for flight; one measurement was waived prior to start of the automatic countdown sequence; and two measurements experienced partial failures during flight. These measurement problems had no significant impact on postflight evaluation.

A summary of S-IB stage measurement reliability is presented in table 15-1. The waived measurement and partially failed measurements are listed in tables 15-2 and 15-3.

Table 15-1. S-IB Measurement Summary

MEASUREMENT CATEGORY	S-IB STAGE
Scheduled	266
Waived	1
Failed	0
Partial Failed	2
Questionable	0
Reliability Percent	100

15.2 AIRBORNE VHF TELEMETRY SYSTEMS EVALUATION

Performance of the two VHF telemetry links provided good data from liftoff until the vehicle exceeded each subsystem's limitation, well beyond the requirements of the S-IB stage as shown in table 15-4. The GP-1 and GF-1 signals terminated at MILA at 397 seconds, and at CIF at 382 seconds as indicated in figure 15-1.

No loss of GP-1 (PCM) synchronization occurred in the CIF ground stations. CIF receiving stations received a disturbance during the first 10 seconds of flight but did not lose synchronization. Analysis of the signal strength oscillograms indicates that bursts of electrical noise are apparent from T-0 to approximately T + 10 seconds. The signal strength data indicate a varying signal strength was experienced during the first 13 seconds of flight. The high electrical noise environment and varying signal strength are normal for the first few seconds of flight.

Table 15-2. Flight Measurements Waived Prior to Flight

MEASUREMENT NUMBER	MEASUREMENT TITLE	NATURE OF FAILURE	REMARKS
L0501-0F1	Fuel Level Discrete	Intermittent output from probe No. 3 (sensor 15) photoelectric cell	Access to probe located inside fuel tank No. 1 is not feasible. Measurement has no LMR classification; (reference Deviation Waiver 1-C-208-1). Valid data received during flight.

Table 15-3. Measurement Malfunctions

MEASUREMENT NUMBER	MEASUREMENT TITLE	NATURE OF FAILURE	TIME OF FAILURE (RANGE TIME)	DURATION SATISFACTORY OPERATION	REMARKS
XC0089-001	Temperature Gear Case Lubricant	Measurement dropped to zero and remained there.	116 sec	116 sec	Probably caused by either transducer, amplifier or wiring failure.
D0013-002	Pressure LOX Pump Inlet	Recorded value decreased and became noisy. Returned to normal 80 sec later	20 sec to 100 sec	62 sec [0 to 20 sec; 100 to 142 sec.]	Failure indicative of wiper lifting from potentiometer.

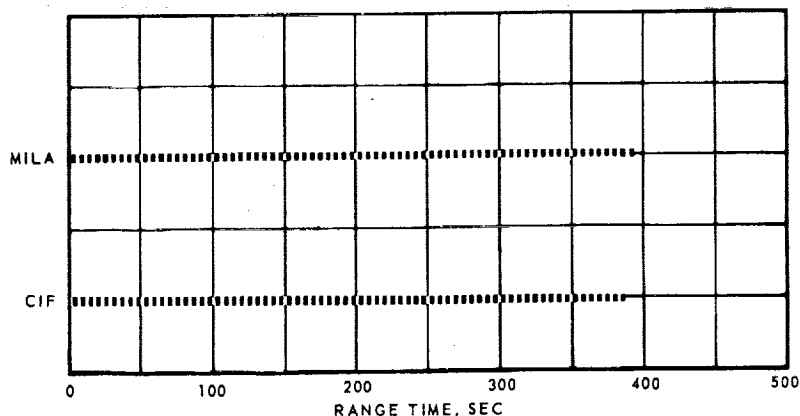


Figure 15-1. VHF Telemetry Systems Coverage Summary

Table 15-4. S-IB Stage Telemetry Links

LINK	FREQUENCY (MH _z)	MODULATION	STAGE	FLIGHT PERIOD (RANGE TIME, SEC)	PERFORMANCE SUMMARY
GF-1	240.2	FM/FM	S-IB	0 to 142.1	Satisfactory
GP-1	256.2	PCM/FM	S-IB	0 to 142.1	Satisfactory

At OEEO(141.2665 through 141.3165 seconds) the RDSM indicated 7 unexpected functions on channels monitoring flight data. By 140.4332 seconds all unexpected function indications had returned to normal. The expected functions occurred normally during the time period. All data are recoverable; analysis indicates that at OEEO, 12 of the engines' thrust OK relays deenergized normally, causing a transient which was picked up by the RDSM

The S-IB stage inflight calibration times were sequenced as programmed (table 15.5).

Table 15-5. S-IB Stage Inflight Calibration Times

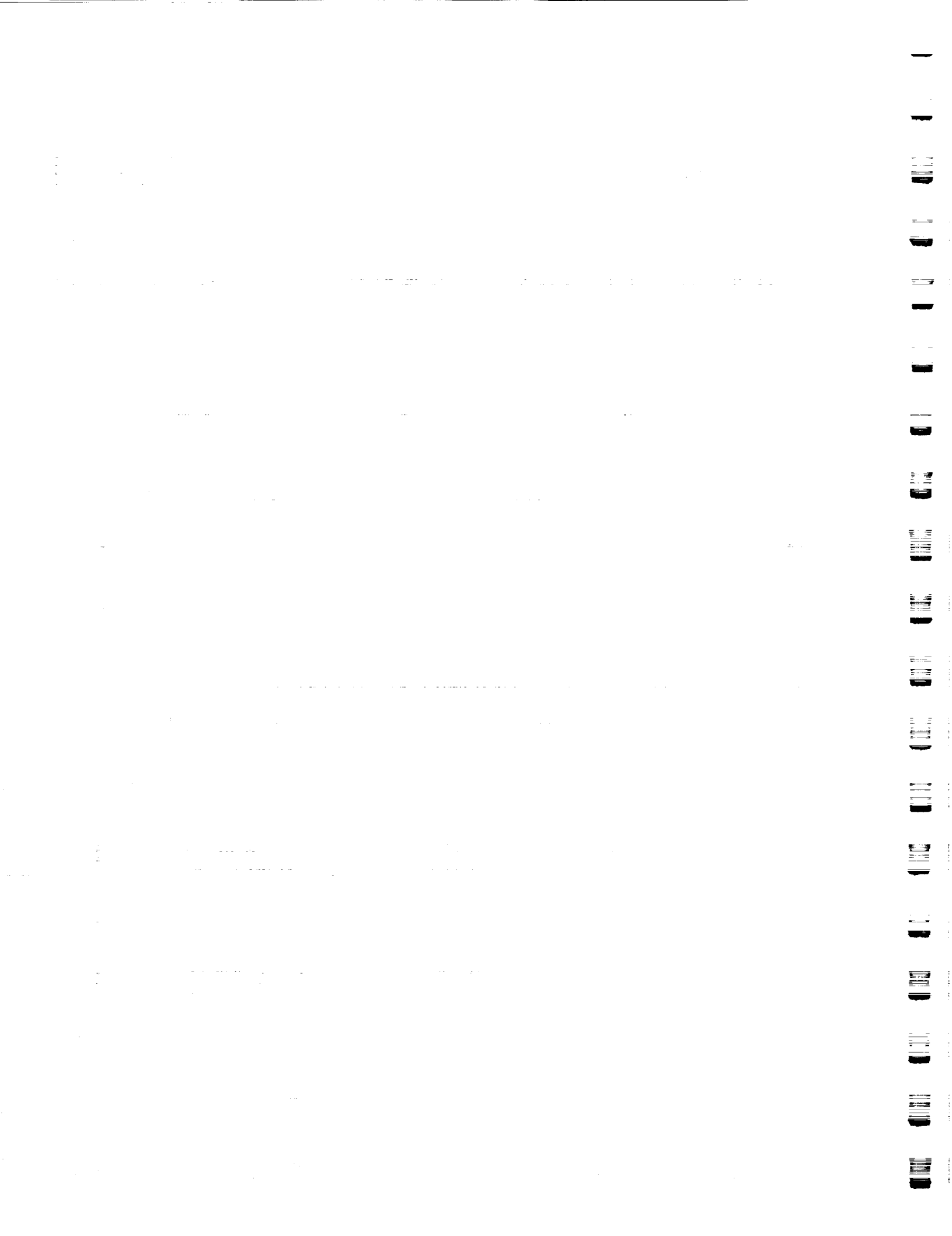
LINE	FIRST CALIBRATION (SEC)	SECOND CALIBRATION (SEC)
GP1 AO Multiplexer	21.27	121.14
GP1 BO Multiplexer	21.93	121.76
GF1/FM Link	22.6	122.4

15.3 SECURE RANGE SAFETY COMMAND SYSTEMS EVALUATION

The low-level field measurements for the S-IB stage Command Receivers (CDR) 1 and 2 indicated that both receivers generally had maximum signal strength throughout the flight as shown in table 15-6.

Table 15-6. S-IB Secure Command Receiver Measurements

MEASUREMENT NO.	MEASUREMENT NAME	REMARKS
M505-13	CDR No. 1 Low Level Field	3.55 volts (max. signal)
M508-13	CDR No. 2 Low Level Field	3.60 volts (max. signal)
K65-13	CDR No. 1 Cutoff and Destruct	1.2 volts (normal meas.)
K66-13	CDR No. 2 Cutoff and Destruct	1.15 volts (normal meas.)



Section 16

FAILURES AND ANOMALIES

16.1 SUMMARY

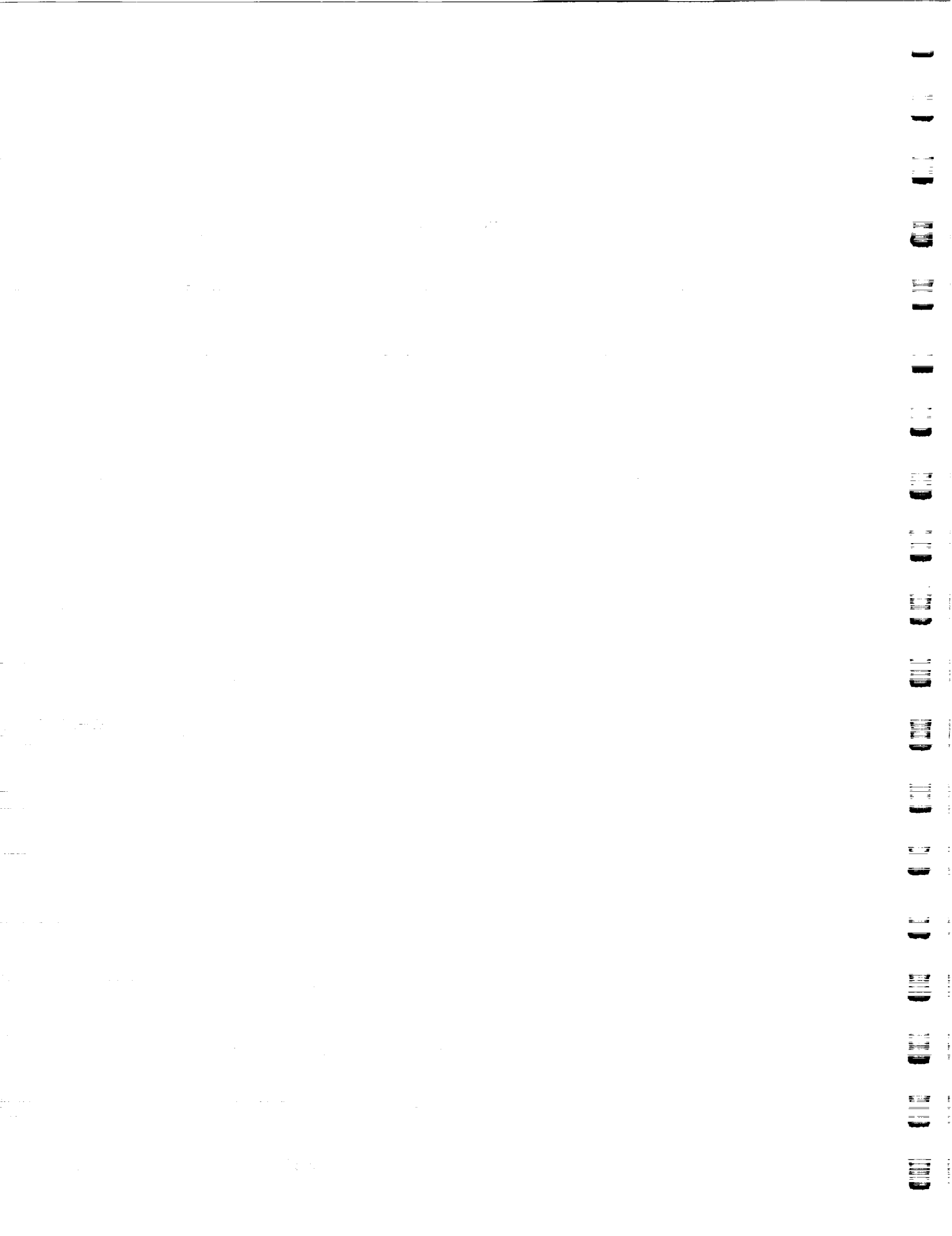
Evaluation of the S-IB stage data revealed no failures, anomalies or significant anomalies detected.

16.2 SYSTEM FAILURES AND ANOMALIES

There were no significant S-IB stage system failures or anomalies.

16.3 RECOMMENDATIONS FOR CORRECTIVE ACTION

There are no recommendations or corrective actions necessary due to the satisfactory performance of the S-IB-8 stage.



Appendix A

S-IB STAGE CONFIGURATION

VEHICLE PROFILE

The 2-stage, liquid-propellant Saturn IB launch vehicle is utilized in the Skylab program to transport the 3-man crews to the Saturn Workshop (SWS) in earth orbit.

In figure A-1, a profile of the Saturn IB vehicle, the cutaway portions identify the first powered stage (S-IB), the second powered stage (S-IVB), the instrument unit (IU), and the major features of these stages.

S-IB STAGE

The function of the S-IB stage is to boost the upper stages and spacecraft through a predetermined trajectory that will place them at the proper altitude and attitude, with the proper velocity at S-IVB stage ignition. The major S-IB stage assemblies, figures A-2 through A-4, are the tail unit with eight fins and eight H-1 engines, the nine propellant tanks, the second stage adapter (spider beam unit), and associated mechanical and electrical hardware discussed under specific systems in this section. For a summary of S-IB stage data, see table A-1.

STRUCTURE

Figure A-2 shows the primary load-carrying structural subassemblies of the S-IB stage combined with its tail unit heat and flame shields, engine flame curtains, LOX and fuel tank firewalls, and second stage adapter seal plate. Separate figures show the unique design details of the tail unit heat shield, and also the spider beam and LOX fitting reinforcements employed as a result of qualification testing. The stage structure was designed to provide a safety factor of 1.10 on yield and 1.40 on ultimate, with a dry stage weight of 85,745 lbm. The adequacy of the 1.40 safety factor (ultimate) has been demonstrated by all load-carrying structural subassemblies. From a reliability point of view, the stage structure is a simple, passive system, and its reliability prediction is based solely on whether or not strength will exceed load. The 1.40 ultimate safety factor (a conservative compilation of 2-sigma and 3-sigma loads and allowables) plus the complete analysis and test program, demonstrates a reliability assessment several times greater than the reliabilities of the other stage systems. Thus, with respect to the rest of the onboard systems, the structure has been assumed to be 100 percent reliable within the performance limits established by the CEI specification, and is considered so for purposes of calculating total stage reliability. The principal functional requirement of the stage structure is to provide adequate tankage and frame-

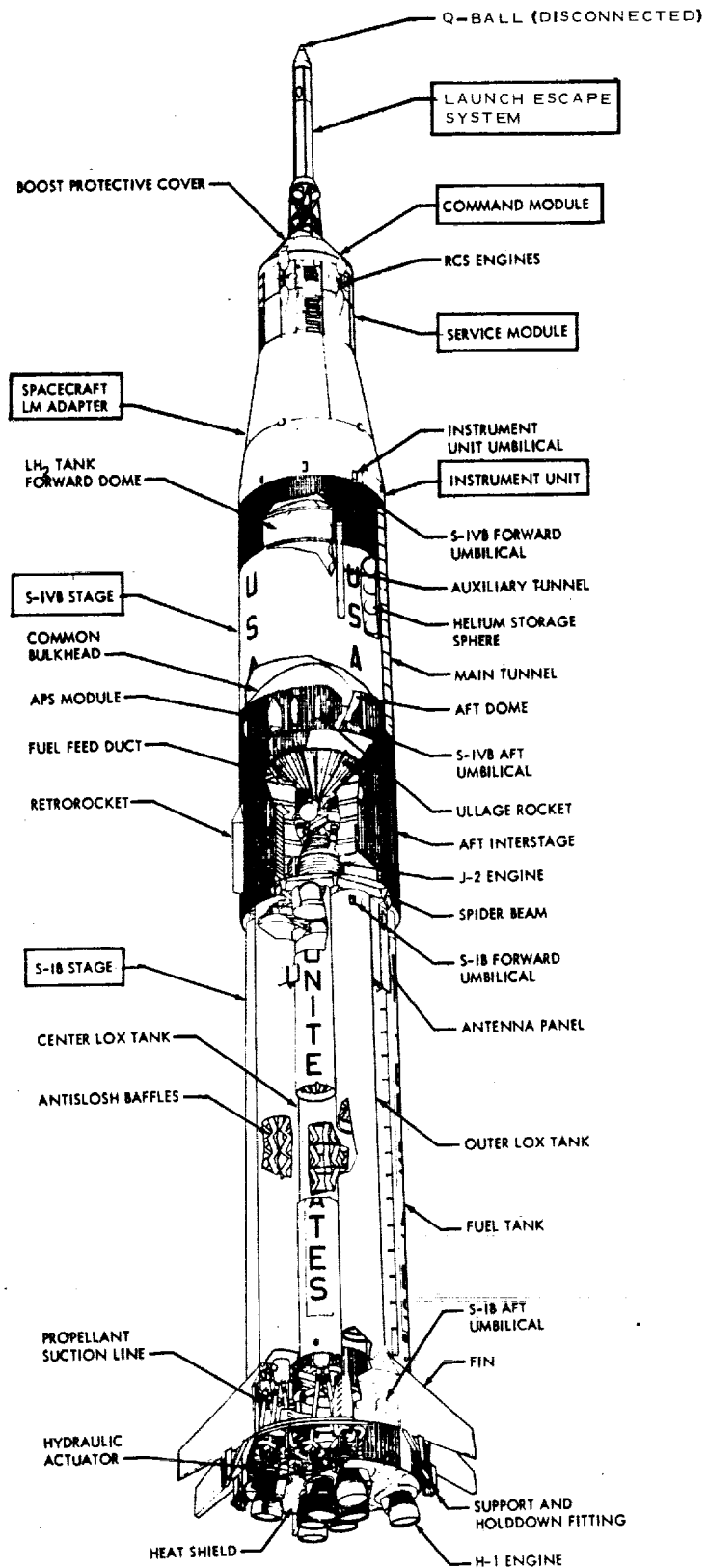


Figure A-1. Saturn IB Cutaway

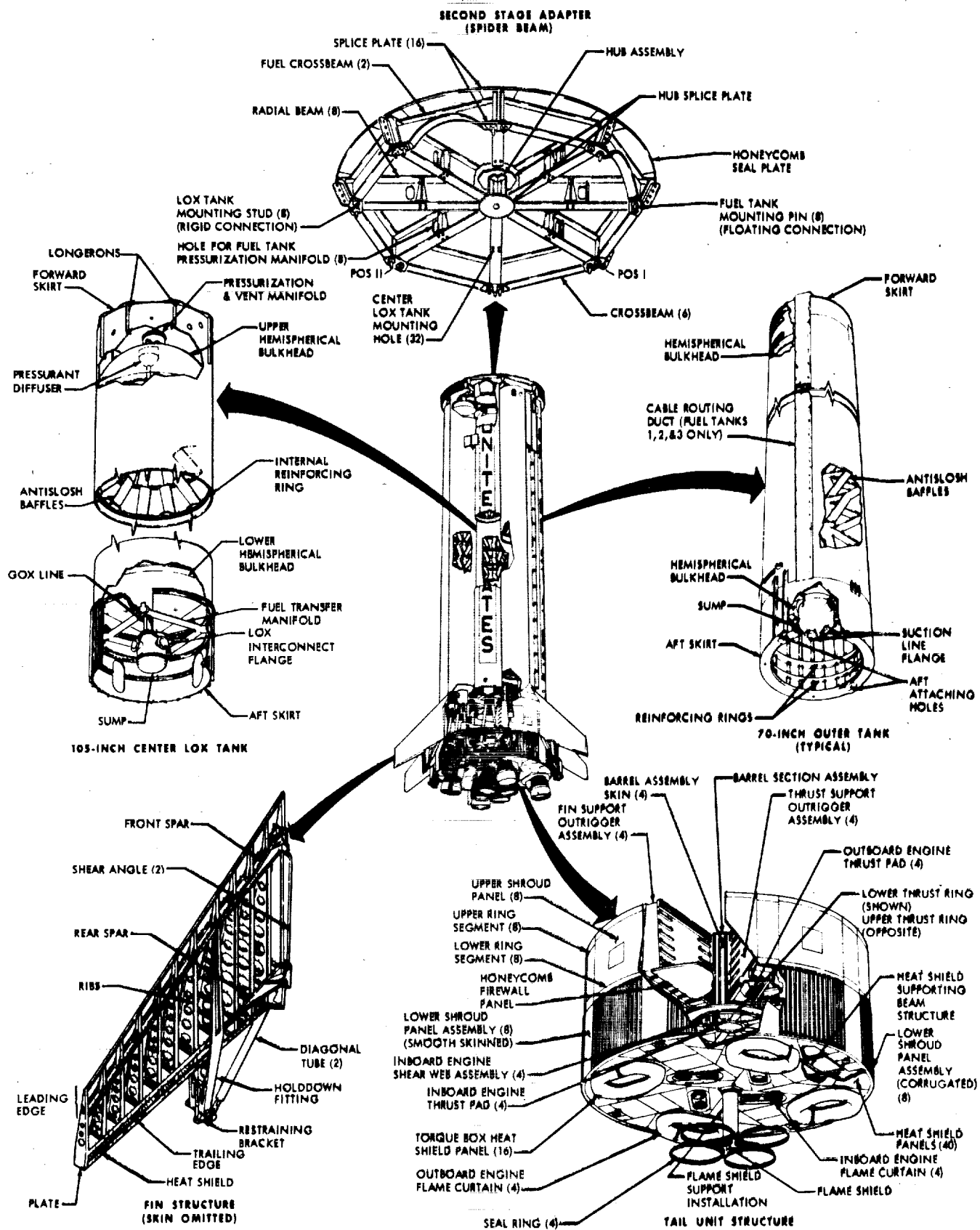


Figure A-2. S-IB Stage Structure

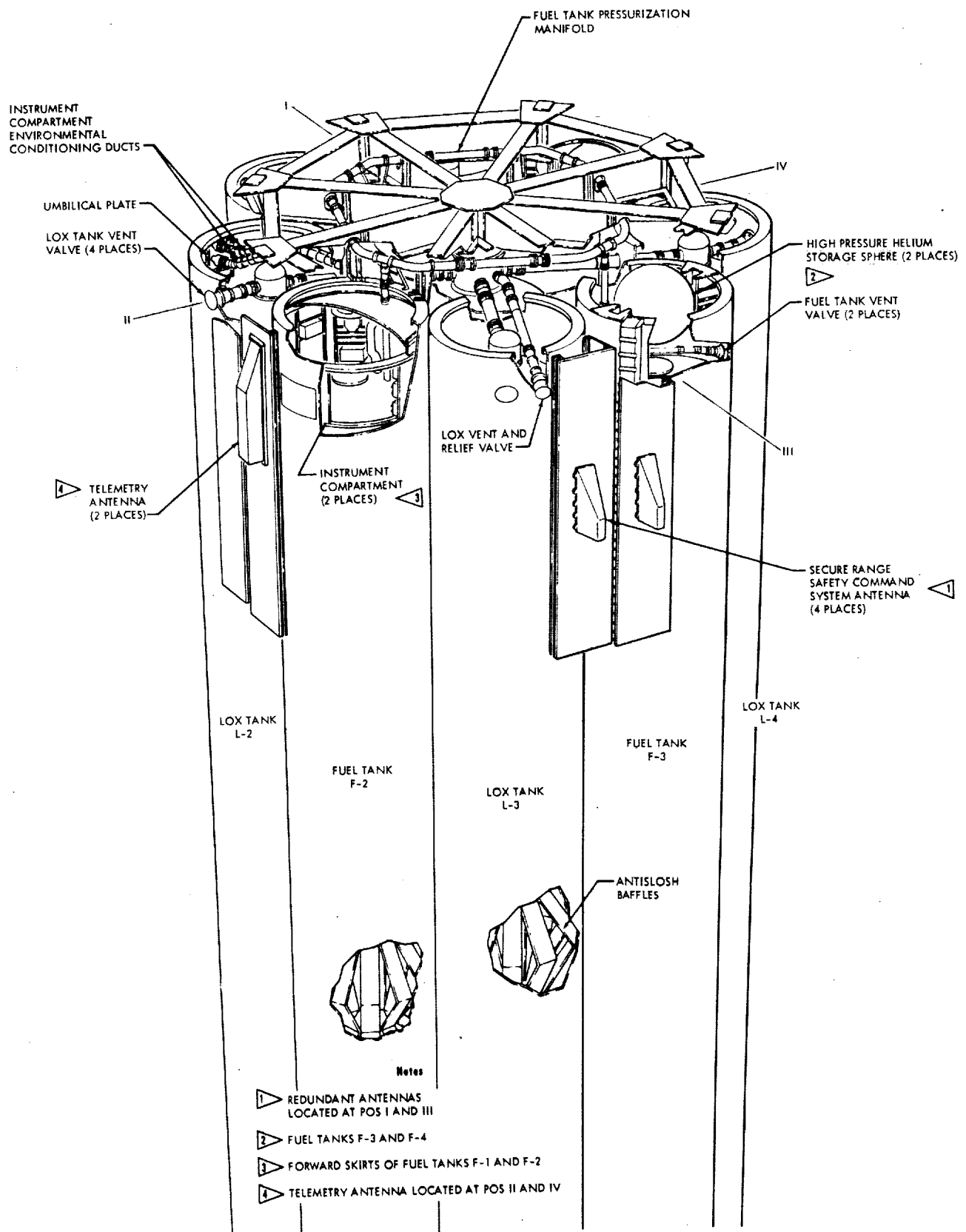


Figure A-3. S-IB Stage Forward Detail

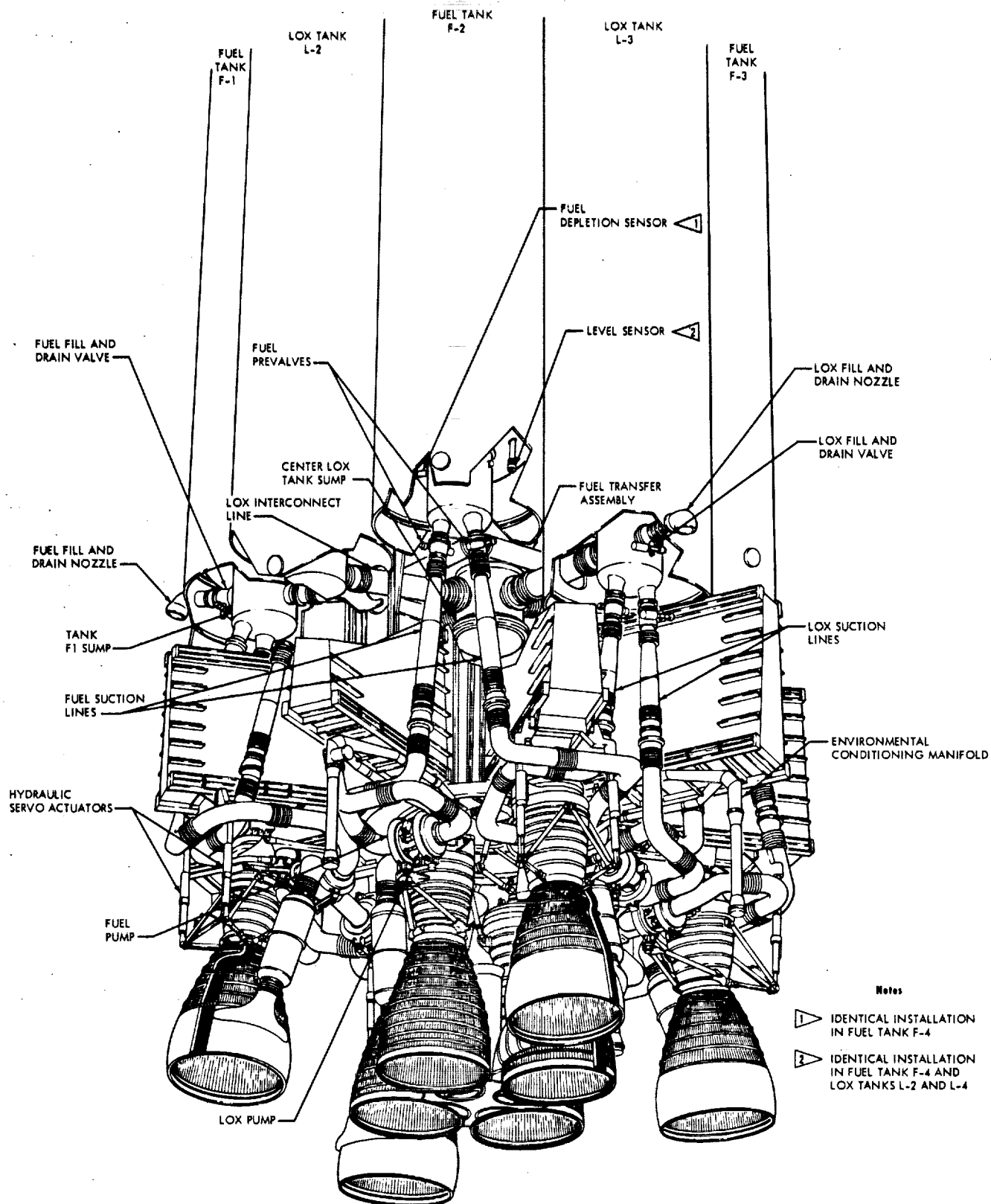


Figure A-4. S-IB Stage Aft Detail

Table A-1. Summary of S-IB Stage Data

DIMENSIONS		HYDRAULIC SYSTEM	
LENGTH	80.2 FT	ACTUATORS (OUTBOARD ONLY)	2 PER ENGINE
DIAMETER		GIMBAL ANGLE	+ 8 DEG SQUARE PATTERN
AT PROPELLANT TANKS	21.4 FT	GIMBAL RATE	15 DEG/SEC IN EACH PLANE
AT TAIL UNIT ASSEMBLY	22.8 FT	GIMBAL ACCELERATION	1776 DEG/SEC ²
AT FINS	40.7 FT		
FIN AREA	53.3 FT ² EACH OF 8 FINS	PRESSURIZATION SYSTEM	
MASS		OXIDIZER CONTAINER	INITIAL HELIUM FROM GROUND SOURCE
DRY STAGE	84,521 LB _m	FUEL CONTAINER	S-IB BURN, GOX
LOADED STAGE	997,127 LB _m	OXIDIZER PRESSURE	HELIUM
AT SEPARATION	95,159 LB _m	PREFLIGHT	58 psia
ENGINES, DRY, LESS INSTRUMENTATION		INFLIGHT	50 psia
INBOARD, PLUS TURNBUCKLES	2,003LB _m EACH	FUEL PRESSURE	
OUTBOARD, LESS HYDRAULICS	1980 LB _m EACH	PREFLIGHT	17 psig
PROPELLANT LOAD	912,606 LB _m (408,000 KG)	INFLIGHT	15 TO 17 psig
ENGINES		ULLAGE	
BURN TIME	141 SEC (APPROX)	OXIDIZER	1.5%
TOTAL THRUST (SEA LEVEL)	1.64 MLB _f	FUEL	2.0%
PROPELLANTS	LOX AND RP-1	ENVIRONMENTAL CONTROL SYSTEM	
MIXTURE RATIO	2.23:1 + 2%	PREFLIGHT AIR CONDITIONING	AFT COMPARTMENT & INSTRUMENT COMPARTMENTS F1 & F2
EXPANSION RATIO	8:1	PREFLIGHT GN ₂ PURGE	AFT COMPARTMENT & INSTRUMENT COMPARTMENTS F1 & F2
CHAMBER PRESSURE	702 psia	ASTRONICS SYSTEMS	
OXIDIZER NPSH (MINIMUM)	35 FT OF LOX OR 65 psia	GUIDANCE	PITCH, ROLL, AND YAW PROGRAM THRU THE IU DURING S-IB BURN
FUEL NPSH (MINIMUM)	35 FT OF RP-1 OR 57 psia	TELEMETRY LINKS	FM/FM, 240.2 MHz; PCM/FM, 256.2 MHz
GAS TURBINE PROPELLANTS	LOX AND RP-1	ELECTRICAL	BATTERIES, 28 Vdc (2 ZINC-SILVER OXIDE); MASTER MEASURING VOLTAGE SUPPLY, 28 Vdc TO 5 Vdc.
TURBOPUMP SPEED	6680 RMP	RANGE SAFETY SYSTEM	PARALLEL ELECTRONICS, REDUNDANT ORDNANCE CONNECTIONS.
ENGINE MOUNTING			
INBOARD	32 IN. RADIUS, 3 DEG CANT ANGLE		
OUTBOARD	95 IN. RADIUS 6 DEG CANT ANGLE		

Notes ALL MASSES ARE APPROXIMATE.

work to support the other flight systems and to provide adequate support of the upper stages, both on the pad and in flight. The evolutionary structural changes resulting from design analyses, test results, static firings, and flight performance data are summarized separately in the discussion pertaining to the individual structural elements.

PROPELLANT TANKS

The nine propellant tanks that cluster to form the main body of the stage are modifications of proven designs from the Redstone and Jupiter vehicles and have performed successfully on all Saturn I and IB flights. The individual tanks are constructed of cylindrical sections built up of mechanically milled, butt welded, aluminum alloy skin segments that are internally reinforced with rings to form a monocoque-type of construction. The material used to construct the tanks is the readily weldable 5456 aluminum alloy in the H343 temper. The use of this alloy allows for considerable

tank weight reduction over the 5086 and 5052 alloys used to construct the Jupiter and Redstone tanks, respectively. Tank wall thickness varies from top to bottom in relation to stress distributions. Hemispherical bulkheads are welded to the forward and aft end of the cylindrical sections, and a sump is welded to the aft bulkhead. A pressurization and vent manifold is fastened to the forward bulkhead of each of the LOX tanks. A cylindrical skirt reinforced with longerons is attached to the forward and aft bulkheads to complete a basic tank. The eight outer tanks are 70 inches in diameter and contain LOX and fuel alternately. The center tank is 105 inches in diameter and contains LOX. The center LOX tank is bolted to the spider beam and is attached to the tail barrel with Huck bolts. Ball-and-socket fittings attach the aft ends of the 70-inch LOX tanks to the tail unit. Banjo fittings and studs rigidly secure the forward ends of the LOX tank to the spider beam. The fuel tanks are supported by ball-and-socket fittings at the tail unit. During shipment, banjo fittings rigidly secure the fuel tanks to the tail unit; however, they are removed before flight. The forward ends of the fuel tanks are mounted to the spider beam unit by sliding pin connections, allowing the LOX tanks to shorten due to thermal contraction when loaded. In summary, the major structural improvements incorporated into the propellant tanks are revised skin gages and reduced bulkhead and frame gages to agree more closely with stress levels, inversion of the aft dome manhole cover in the center tank, and the addition of GOX interconnect domes (with the related forward skirt cut-outs) and a GOX pressurant diffuser. Also, the fuel tanks on SA-206 and subsequent vehicles are painted white instead of black for thermal reasons.

TAIL UNIT

Primarily, the tail unit rigidly supports the aft ends of the propellant tank cluster and the vehicle on the launcher; mounts the eight engines and fins; and provides the thrust structure between the engine thrust pads and the propellant tanks. Other functions of the tail unit are to support the lower shroud panels, LOX and fuel bay firewalls, heat shield support beam and panel assemblies, engine flame curtains, and the engine flame shield support installation. Unlike the propellant tank units, the tail unit is constructed with higher strength aluminum alloys of the 7000 series that are heat-treated to the T-6 or the T-73 condition.

The 7000-series aluminum alloys used in the tail unit assembly are not recommended for welded applications because of low welding efficiencies. These alloys are used in unpressurized areas where the assembling is done with mechanical fasteners. The tail unit thrust structure configuration lends itself to this definition; and high-strength, heat-treatable 7000-series aluminum alloy forgings, extrusions, plates and sheets are fabricated into components that are joined with mechanical fasteners to construct the tail unit assembly.

Because of the susceptibility of the high strength aluminum alloys to stress corrosion cracking, methods have been employed in the design and manufacture of the tail unit assembly which minimize the danger of failure due to stress corrosion cracking. Methods employed are: heat treatment to the T-73 condition, heat treatment after heavy machining operations, the use of closed-die forgings, and the use of adequate final protective finishes.

The tail unit consists of a barrel assembly, 105 inches in diameter, that directly supports the center propellant tank, encloses the inboard engine thrust beams, and acts as the hub for the four thrust support outriggers and the four fin support outriggers. The four thrust support outriggers also act as fin support outriggers. The fin support outriggers are similar to the thrust support outriggers but differ mainly in that they have no thrust support beam or actuator support beam. The outer ends of the outriggers are spanned by upper and lower ring segments and eight upper shroud panels to form the basic thrust structure. Eight smooth and eight corrugated lower shroud panels are attached to the aft end of the thrust structure to form a compartment for the eight H-1 engines. LOX and fuel bay firewall panels are installed to cover the space between the outrigger assemblies and the space over the aft end of the barrel assembly.

A reinforcing beam structure is fitted into the aft end of the lower engine shroud assembly. The heat shield panels, engine flame curtains, and flame shield support installation are attached to the beam structure. The heat shield honeycomb composite, unlike most other honeycomb composites used in the vehicle utilizing phenolic cores that are adhesively bonded to face sheets and are limited by the upper and lower temperature constraints on the adhesive system, consists of both corrosion-resistant steel foil cores and thin face sheets that are joined by a brazing process. The 0.25-inch square-cell core is brazed to both the inner and outer face sheets, has a layer thickness of 1.00 inch and acts as the chief structural core member of the composite. The 0.50-inch square-cell core is brazed to only the outer face sheet, has a layer thickness of 0.25 inch, and acts as the thermal insulation retaining member of the composite structure. M-31 insulation is trowled into the retaining core cells. Laboratory tests have generally demonstrated that, compared with adhesively bonded honeycomb composites, brazed honeycomb composites are over 100 percent greater in tensile strength, over 75 percent greater in core shear strength, over 20 percent greater in edgewise compression strength, and equal in flatwise compression strength. This heat shield design provides a lighter panel with increased stiffness which greatly improves the retention of the M-31 insulation material. Successful results of laboratory testing and static tests of the S-I-10 and S-IB-3 through S-IB-7 stages have fully qualified this heat shield panel design. In addition to the heat shield assembly, the tail unit of the S-IB incorporates fin attachment fittings, gage reduction of sheet-metal and framing, and removal of the engine skirts from the lower shroud assembly.

FINS

The eight fins of semi-monocoque construction, provide aerodynamic stability in the mid-region of first stage flight and support the vehicle on the launch pad prior to ignition and during the holddown period after ignition. A fin is fastened mechanically to each of the four thrust support outriggers and the four fin support outriggers. A heat shield is attached to the trailing edge to protect the fin from engine exhaust, and a plate is fastened to the tip of the fin between the leading edge and the heat shield. Skin panels are riveted to the ribs and spars, completing the structure and forming a smooth aerodynamic surface. The fins used on the S-IB stage are identical, replacing the arrangement of four large-fins and four stub-fins used on the S-I stages.

SPIDER BEAM UNIT

The spider beam unit holds the propellant tank cluster together at the forward end and attaches the S-IB stage to the S-IVB aft interstage. The five LOX tank units are rigidly attached to the spider beam while the fuel tank units are attached with sliding pin connections. Structurally, the spider beam consists of a hub assembly, to which eight radial beams are joined with upper and lower splice plates by mechanical fasteners. The outer ends of the radial beams are spanned by crossbeams and joined with upper and lower splice plates by mechanical fasteners. Like the tail unit thrust structure, the spider beam is constructed of extrusions and fittings made of high-strength, heat treatable aluminum alloys of the 7000-series that are heat-treated to the T6 condition. To form an aft closure for the S-IVB stage engine compartment, 24 honeycomb composite seal plate segments of approximately 0.05 inch thickness are fastened to the forward side of the spider beam. The seal plate honeycomb composite consists of 5052 aluminum alloy foil core material adhesively bonded to 7075-6 aluminum alloy face sheets to form thinner and lighter panels than those used on the S-I stages. During qualification testing of the S-IB stage spider beam, a failure of the LOX tank fitting occurred. A radial beam reinforcing angle and bracket, cross-beam web stiffening brackets and a reinforced mounting stud flange were incorporated to fix each of the eight LOX tank fittings. Other changes incorporated into the spider beam design for the S-IB stages are the reduction of beam gages and the removal of retrorockets, 45-degree fairing, and radial beam tips. This unit is qualified and has performed successfully on all Saturn IB flights.

PROPULSION

The S-IB stage propulsion system consists of an 8-engine cluster of H-1 engines that burn LOX and RP-1 fuel to propel the Saturn IB vehicle during the first boost phase of powered flight. Propellant from the LOX and fuel tanks feeds the H-1 engines under tank pressure to ensure the NPSH necessary for satisfactory engine operation. Boosters S-IB-1 through S-IB-5 used engines developing 2000,000 lbf of thrust for a total stage thrust of 1,600,000 lbf. Boosters S-IB-6 and subsequent use engines developing 205,000 lbf of thrust for a total stage thrust of 1,640,000 lbf. Four inboard engines are mounted 90 degrees apart (at vehicle positions I, II, III, and IV) on a 32-inch radius from the vehicle longitudinal axis, and are canted 3 degrees outboard from the vehicle centerline. Four outboard engines are gimbal-mounted 90 degrees apart (at fin lines 2, 4, 6 and 8) on a 95-inch radius from the vehicle longitudinal axis. The engines cant outboard 6 degrees from the vehicle centerline. Each of the eight engines is attached by a gimbal assembly to its thrust pad on the tail unit thrust structure. Inboard engine thrust pads are on the barrel assembly and outboard engine thrust pads are on the thrust support outriggers. Although the inboard engines do not gimbal for vehicle control, the gimbal assemblies permit alignment of the engines to the thrust structure; two turnbuckles used on each inboard engine, with the gimbal assembly, align and secure the engine in place. Two hydraulic actuators and a gimbal assembly secure each outboard engine to the thrust structure. The actuators attach to an actuator support beam, which is part of the thrust support outrigger. The actuators, one mounted in the pitch plane and one in the yaw plane, gimbal the engine for vehicle attitude control. The engine gimbal centerline for both

outboard and inboard engines lies in a plane perpendicular to the vehicle longitudinal axis at vehicle station 100 (figure 5). Canting the engines provides stability by directing the thrust vectors to common points on the vehicle longitudinal axis. The outboard engine thrust vectors intersect the longitudinal axis at vehicle station 1004, while the inboard engine thrust vectors intersect the longitudinal axis at vehicle station 711. The difference in cant angles and radii from vehicle centerline account for the two different intersect points. Directing the thrust vectors to the vehicle longitudinal axis reduces the possibility of excessive loading of the vehicle structure in the event of engine(s) failure during flight.

S-IB-8 CONFIGURATION DIFFERENCES

The significant configuration differences between S-IB-8 and S-IB-7 are listed in table A-2.

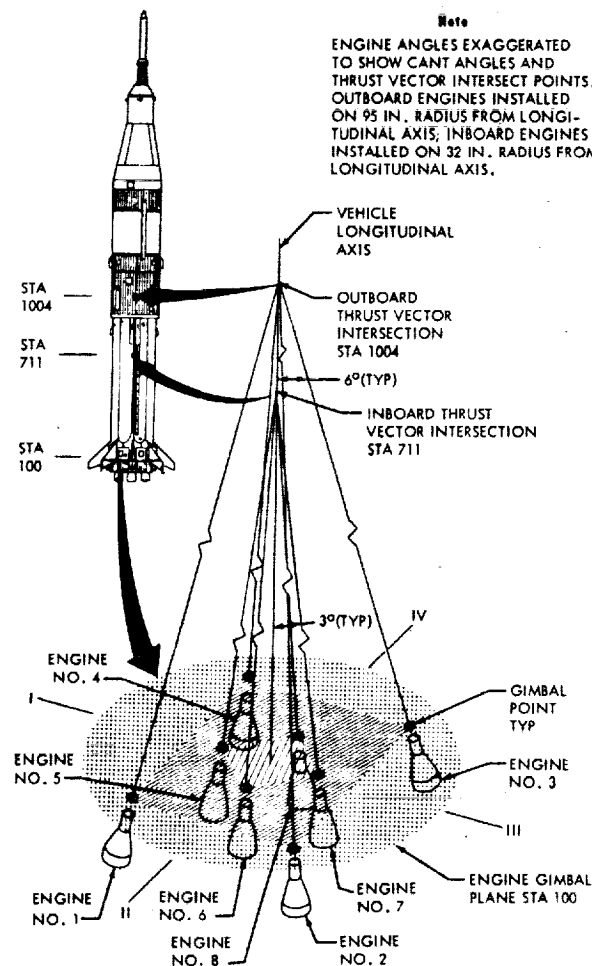


Figure A-5. Engine Thrust Vectors

Table A-2. S-IB Configuration Changes

SYSTEM	CHANGE	REASON
Structures	<ul style="list-style-type: none"> Repair of crack in channel, upper outrigger assembly, fin position 4. Remove 1-in. x 3-3/4-in. coupon containing crack and install spacer and splice plate. 	<ul style="list-style-type: none"> Crack detected on the stage at KSC during special inspection conducted after imperfection noticed in surface of same channel on stage S-IB-9. Channel is made from stress corrosion susceptible material 7178-T6 AL alloy forging. Removed cracked area to preclude propagation.
	<ul style="list-style-type: none"> Add reinforcing blocks at fin rear spar attachment fittings. Shim mating surfaces between fin and outrigger as required. 	<ul style="list-style-type: none"> Cracks detected in rear spar attachment fittings of all eight fins during post CDDT inspection. All eight fins replaced; reinforcing blocks added to provide fail-safe (i.e. alternate loads path) feature in event cracks occur after last preflight inspection.
	<ul style="list-style-type: none"> Rework of fuel tanks F3 and F4 	<ul style="list-style-type: none"> Upper bulkheads of fuel tanks F3 and F4 were reformed pneumatically to original contour following accidental damage during launch operation.
Propulsion and Mechanical	<ul style="list-style-type: none"> Reduction in fuel vent valve relief pressure and prepressurization pressure. 	<ul style="list-style-type: none"> Accidental damage to upper bulkheads on fuel tanks F3 and F4 necessitated lowering relief setting from 21.0-21.5 psig to 19.0-19.1 psig to maintain an adequate structural margin. Maximum prepressurization pressure reduced from 18.5 psig to 18 psig.
	<ul style="list-style-type: none"> Addition of expansion loop in fuel vent sensing lines. 	<ul style="list-style-type: none"> Accidental damage to upper bulkheads on fuel tanks F3 and F4 caused the bulkheads to have more deflection than normal causing a strain on the fuel vent sensing system.

Table A-2. S-IB Configuration Changes (Continued)

SYSTEM	CHANGE	REASON
Instrumentation	<ul style="list-style-type: none"> Modification of multiplexer 270 DC-DC converter. Changes include: <ul style="list-style-type: none"> - Removing capacitor C-15 from the circuit - Removing capacitor C-2 from the circuit - Changing Q3 from 2N2218 to JAN2N2218A. 	<ul style="list-style-type: none"> To improve the reliability of the DC-DC converter in the 270 multiplexer.
Electrical	<ul style="list-style-type: none"> Two plug-in type J-boxes, 9A10 and 9A11, used for interconnection of the four groups of temperature sensors, have been deleted. 	<ul style="list-style-type: none"> Circuitry of the fire detection system has been simplified. Interconnection is accomplished in cable 9W146.
	<ul style="list-style-type: none"> IN2150A diodes replaced in propulsion system distributor 9A1 by SIN1204A diodes. 	<ul style="list-style-type: none"> The approved vendor for IN2150A diodes has closed operations and the diodes are unavailable. SIN1204A diodes are used in other Saturn stages and electrical characteristics equal or exceed those of the IN2150A.

REFERENCES

- A. CCSD Technical Bulletin TB-P&VE-70-316 (Revision D), "S-IB Stage Propellant Criteria for Skylab 2, 3, and 4," CCSD New Orleans, La., dated July 11, 1972.
- B. CCSD Technical Report TR-P&VE-73-153, "Final Launch Vehicle Propulsion Systems Flight Performance Prediction for SA-208 (Third Skylab Mission, SL-3 Launch), " CCSD New Orleans, La., dated June 20, 1973.
- C. CCSD Report HSM-R19-73, "Saturn IB Vehicle Propellant Loading for Vehicle SA-208," CCSD Huntsville, Alabama, dated August 24, 1973.
- D. "Saturn S-IB Stage Final Static Test Report, Stage S-IB-8," CCSD Huntsville, Alabama, dated January 4, 1967.
- E. CCSD Technical Report TR-P&VE -67-44, "Saturn S-IB-8 Stage Static Test Analysis Report (SA-40 and SA-41), " CCSD New Orleans, La., dated March 6, 1967.
- F. Rocketdyne Report SSM 7114-4001, "Effects of Fuel Inlet Temperature Upon Engine Performance, H-1 Engine System" Rocketdyne Division - Rockwell International, Canoga Park, California, dated March 8, 1967.
- G. Rocketdyne Letter POL 166, "Transmittal of Revised H-1 200K and 205K Influence Coefficients," Rocketdyne-Rockwell International, Canoga Park, California, dated June 2, 1967.
- H. Rocketdyne Report R-6539-1, "Presentation of 200K and 205K H-1 Acceptance Data and Statistical Summaries (Supplement 1), " Rocketdyne Division - Rockwell International, Canoga Park, California, dated June 30, 1967.
- I. CCSD Report, "Sea Level Reduction of Engine Data for Static Tests of Saturn S-IB Stages," CCSD New Orleans, La. by J. K. Patterson, dated January 24, 1969.
- J. CCSD Technical Report TD-R-P&VE-XSB-4, "Launch-and-Launch Vehicle Systems Dispersions Analysis for Saturn IB Vehicles SA-201, -202, -203, -204, -205," CCSD Huntsville, Alabama, dated March 15, 1969.

REFERENCES (Continued)

- K. CCSD Technical Report TR-P&VE-70-83, "Evaluation of Propulsion System Performance Differences Between Flight and Ground Tests for S-IB Stage," CCSD New Orleans, La., dated February 20, 1970.
- L. CCSD Technical Report TR-P&VE-70-85, "Analysis of Saturn IB Propulsion System Performance Dispersions," CCSD New Orleans, La., dated April 20, 1970.
- M. CCSD Technical Report TR-P&VE-70-88, "S-IB Propulsion System Static Test Summary," CCSD New Orleans, La., dated October 8, 1970.
- N. CCSD Technical Bulletin TB-P &VE-72-338, "S-IB-7 Stage Long Duration Static Test (SA-41) Reconstruction," CCSD New Orleans, La., dated February 8, 1972.
- O. Rocketdyne Letter 72RC-8343, "Launch and Flight Operational Predictions, AS-208," Rocketdyne Division - Rockwell International, Canoga Park, California, dated November 14, 1972.
- P. CCSD Technical Report TR-P&VE-72-123, "Evaluation of the Effects of Fuel (RP-1) Characteristics on Saturn S-IB Stage Performance," CCSD New Orleans, La., dated June 30, 1972.
- Q. Rocketdyne Letter 73RC-2834, "AS-208 Static Performance (Task A2100)," Rocketdyne Division - Rockwell International, Canoga Park, California, dated April 19, 1973.
- R. CCSD Report SDES-73-418, "Saturn S-IB Stage Final Flight Report S-IB-6 (Applicable to Skylab-2, AS-206)," CCSD New Orleans, La., dated July 16, 1973.
- S. CCSD Report TR-P&VE-73-157, "Vehicle Propulsion Performance Reconstruction SA-206," CCSD New Orleans, La., dated September 17, 1973.
- T. CCSD Report SDES-73-421, "Saturn S-IB Stage Final Flight Report S-IB-7 (Applicable to Skylab-3, SA-207)," CCSD New Orleans, La., dated October 5, 1973.
- U. CCSD Report TR-P&VE-73-160, "Vehicle Propulsion Performance Reconstruction SA-207," CCSD New Orleans, La., dated October 25, 1973.

DISTRIBUTION

NASA

J. I. Kistle	Hdqs. - MAE	1
G. H. McKay, Jr.	SAT-E	5
R. J. Nuber	SAT-MA-S	1
J. C. Rains	SAT-C	6
M. Savage	Hdqs. - MLE	1
A. C. String	Hdqs. - KSS - 10	1

CCSD

W. C. Beamer	1
C. A. Brakebill	1
A. F. Carlson, Jr.	1
T. R. Cotter	1
E. J. Dofter	1
M. A. Donovan, Jr.	1
B. D. Emerick	1
H. B. England	1
H. P. Estes	2
H. V. Green	3
L. L. Hartley	2
B. F. Heinrich	1
W. S. Johnson	4
W. H. Juengling	1
J. M. Landon	1
D. R. Lewis	1
W. H. McCarter, Sr.	1
R. Muir	1
W. S. Parker, Jr.	5
J. F. Patrick	1
R. H. Ross	1
G. Salvador	3
A. R. Trahern	1
H. J. Tymkiw	1
V. J. Vehko	1
J. H. Wood	1
Technical Files	2

